ДОКЛАДЫ
АКАДЕМИИ НАУК СССР

Volume 141, Numbers 1-6
November-December, 1961

PROCEEDINGS OF THE ACADEMY OF SCIENCES

OF THE USSR

(DOKLADY AKADEMII NAUK SSSR)

Physical Chemistry Section

IN ENGLISH TRANSLATION

c/b

CONSULTANTS BUREAU

Volume 141, Numbers 1-6

November-December, 1961

PROCEEDINGS OF THE ACADEMY OF SCIENCES

OF THE USSR

(DOKLADY AKADEMII NAUK SSSR)

Physical Chemistry Section

A publication of the Academy of Sciences of the USSR

IN ENGLISH TRANSLATION

Year and issue of first translation:
Vol. 112, Nos. 1-6 Jan.-Feb. 1957

Annual subscription *$160.00*
Single issue *35.00*

Printed in the United States of America

PROCEEDINGS OF THE ACADEMY OF SCIENCES OF THE USSR
Physical Chemistry Section

Volume 141, Numbers 1-6 November-December, 1961

CONTENTS

CONTENTS (continued)

CONTENTS (continued)

DETECTION OF OXYGEN ATOMS IN A RAREFIED FLAME OF CARBON MONOXIDE WITH OXYGEN WHEN SMALL AMOUNTS OF HYDROGEN ARE ADDED

V. V. Azatyan, L. A. Akopyan, A. B. Nalbandyan, and B. V. Ozherel'ev

Institute of Chemical Physics, Academy of Sciences, USSR
(Presented by Academician V. N. Kondrat'ev, May 31, 1961)
Translated from Doklady Akademii Nauk SSSR, Vol. 141, No. 1, pp. 129-130, November, 1961
Original article submitted May 24, 1961

The low-temperature combustion of carbon monoxide catalyzed by small additions of molecular oxygen in the vicinity of the first limit of self-ignition is explained by the following set of elementary reactions [1-4]:

$$OH + CO = CO_2 + H; \quad H + O_2 = OH + O; \quad O + H_2 = OH + H; \quad H + \text{wall} \rightarrow \text{chain destruction}; \quad O + \text{wall} \rightarrow \text{chain destruction}.$$

From the chain mechanism of the reactions it follows that very high concentrations (many times exceeding the equilibrium values) of hydrogen atoms, oxygen atoms and hydroxyl radicals must be built up in the combustion zone. From the given scheme, when one takes into account the rate constants of the elementary reactions [4-6], it also follows that in flames of these mixtures the concentrations of hydrogen- and oxygen atoms must be commensurate and many times higher than that of the OH radicals.

In moist flames of CO and O_2 mixtures where the catalytic action of water is analogous to that of hydrogen [2] V. N. Kondrat'ev, in fact, detected hydroxyl concentrations by far exceeding the equilibrium value [2]. By the method of the thermoelectric probe [7] it was established that in flames of these mixtures there exist high concentrations of active particles recombining on the specially treated surface of the probe. When taking into account that the hydroxyl radical concentration is much less than that of the H and O atoms and that the diffusion coefficient of O is smaller than that of H the authors think that the recombining particles are H atoms.

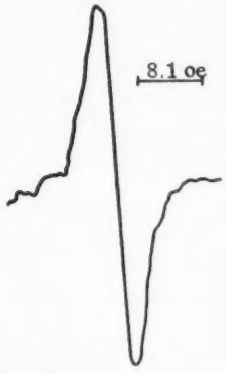

Until recently, straightforward experiments for the direct detection of H and O atoms and for measuring their concentrations in flames of CO and O_2 with small additions of H_2 did not exist. Of late we succeeded to detect by means of the EPR method in these mixtures hydrogen atoms in concentrations several orders of magnitude exceeding the equilibrium values [8].

The present study was devoted to detecting O atoms in rarefied flames of CO and O_2 mixtures containing small additions of molecular hydrogen. For this purpose we used the EPR method. The experimental procedure has been described in a paper by V. N. Panfilov, Yu. D. Tsvetkov, and V. V. Voevodskii [9]. In order to obtain the smallest possible effectivity of atomic recombination on the surface of the reaction tube the latter was rinsed consecutively with hydrofluoric acid, distilled water and coated with potassium tetraborate. Then the tube was treated several days by a stationary flame in a current of a CO and O_2 mixture containing added H_2. Such a treatment allowed us to obtain flames of these mixtures at pressures not exceeding 1.5-2 mm Hg in the temperature range 600-650°.

The experiments were done with a stoichiometric mixture of CO and O_2 containing up to 7% H_2 at a flow rate equal to 82 cm^3/min (linear velocity 18 m/sec) and a pressure of the mixture equal to 5.5 mm Hg. The temperature was varied between 607 and 650°.

H_2 content in the mixture, %	$[H]\cdot10^{-14}$ particles/cm^3	$[O]\cdot10^{-14}$ particles/cm^3	[O]/[H]
1,1	0,3	1,5	4,5
1,7	1,3	4,1	3,2
2,4	2,1	5,9	2.8
2,7	2,4	6,4	2.7
3,1	3,4	5,9	1,7
4,4	4,1	6,0	1,4
5,1	5,2	5,9	1,1
6,1	5,6	6,0	1,1
6,9	6,8	6,4	0,9

Under these conditions an EPR signal of atomic oxygen having a g factor equal to 1.5 and consisting of one component was recorded.

The spectrum of atomic oxygen, as was obtained at 645° with a mixture containing 2.7% hydrogen. The value which we found for the g factor coincides with that known in the literature for atomic oxygen obtained in a discharge [10-12]. As has been shown by Ultee [12], the shape of the spectrum in an essential way depends on pressure and at pressures exceeding 0.02 mm Hg the four components resulting from the $^3P_2$ state merge into one line.

Together with the determination of the concentrations of O atoms we did parallel measurements of those of H atoms.

In a stoichiometric mixture of CO and O_2 at 610° we studied the relation between the H_2 content and the concentrations of H and O atoms. From the results of the measurements which are given in table it follows that, in fact, the concentrations of O atoms are commensurate with those of the H atoms and that both concentrations increase, when the H_2 content in the mixture is raised. But the (O)/(H) ratio decreases from 4.5 to 0.9, when the H_2 content is raised from 1.1 to 6.9%.

When the temperature is raised from 607 to 650°, then in the mixture containing 3.8% H_2 the concentration of H and O atoms increases from $2.9 \cdot 10^{14}$ to $4.1 \cdot 10^{14}$ particles/cm^3 and from $4.6 \cdot 10^{14}$ to $7.8 \cdot 10^{14}$ particles/cm^3, respectively.

From the values found for the concentration of H and O atoms it follows that the sum of their partial pressures may attain 2% of the total pressure.

It should be noted that the very high concentrations of oxygen and hydrogen atoms which we have found do not completely give the actual concentrations of these particles in the flame, where, evidently, their concentrations are still higher. The method which we have used allowed us to measure the concentrations of atoms not in the flame itself but only at a distance of about 10 mm from it.

We have undertaken more detailed investigations of the O and H concentrations as a function of the various parameters and this study will allow as in the fugure to come to a more accurate determination of the relation between the concentrations which we measure and those existing in the flame itself. This will also allow us to come nearer to the complete clarification of the oxidation mechanism of CO.

LITERATURE CITED

1. E. J. Buckler and R. G. W. Norrish, Proc. Roy. Soc. 167, 318 (1938).
2. V. N. Kondrat'ev, Spectroscopic Studies of Chemical Reactions [in Russian] (Acad. Sci. USSR Press, 1944).
3. N. S. Enikolopyan and A. B. Nalbandyan, The Kinetics of Oxidative Chain Reactions [in Russian] (Acad. Sci. USSR Press, 1950).
4. V. V. Azatyan, V. V. Voevodskii and A. B. Nalbandyan, Kinetika i Kataliz, 2, 3 (1961).
5. L. I. Avramenko and R. V. Lorentso, ZhFKh, 24, 207 (1950).
6. L. V. Karmilova, A. B. Nalbandyan, and N. N. Semenov, ZhFKh, 32, 1193 (1957).
7. E. I. Kondrat'eva and V. N. Kondrat'ev, ZhFKh, 21, 7, 769 (1947).
8. V. V. Azatyan, V. N. Panfilov, and A. B. Nalbandyan, Kinetika i Kataliz, 2, 2 (1961).
9. V. N. Panfilov, Yu. D. Tsvetkov, and V. V. Voevodskii, Kinetika i Kataliz, 1, 2, 333 (1960).
10. E. R. Rawson and R. Beringer, Phys. Rev. 88, 677 (1952).
11. S. Krongelb and M. W. P. Strandberg, J. Chem. Phys. 31, 5, 1196 (1956).
12. C. J. Ultee, J. Phys. Chem. 64, 12, 1873 (1960).

THE MECHANISM OF CHAIN INITIATION WHEN CYCLOHEXANOL IS OXIDIZED

E. T. Denisov

Institute of Chemical Physics, Academy of Sciences, USSR
(Presented by Academician V. N. Kondrat'ev, May 31, 1961)
Translated from Doklady Akademii Nauk SSSR, Vol. 141, No. 1,
pp. 131-134, November, 1961
Original article submitted May 24, 1961

Since oxidation in liquid phase is a chain reaction, it starts with the formation of free radicals in the original substance containing dissolved oxygen. As yet the mechanism of this type of reaction has not been studied, although an investigation of such reactions is of considerable scientific interest. In the literature on hydrocarbon oxidation the prevailing opinion is that at the start of oxidation the free radicals are formed by the reaction

$$RH + O_2 \rightarrow \dot{R} + HO_2^{\cdot}. \quad (1)$$

However, a calculation showed that this reaction would give a formation rate of free radicals which is much smaller than that found in the experiment [1]. For this reason for oxidation in liquid phase a trimolecular reaction of free radical formation was proposed as an energetically more efficient one [1]:

$$RH + O_2 + RH \rightarrow 2R^{\cdot} + H_2O_2. \quad (2)$$

Besides the original substance and dissolved oxygen, various contaminations, in particular, the peroxide which is slowly formed at room temperature may participate in the formation of free radicals. Only the experiment can give the definitive answer to the question by which mechanism free radicals are formed in the original substance when it is oxidized.

In the present investigation the mechanism of free radical formation in cyclohexanol in the presence of oxygen was studied by means of an inhibitor (α-naphthol). The inhibitor was only consumed in the reaction with the free radicals and thus the rate at which it was used up specified the rate of free radical formation. Per one inhibitor(naphthol)molecule two peroxide radicals go lost [2]:

$$InH + RO_2^{\cdot} \rightarrow In^{\cdot} + ROOH,$$
$$In^{\cdot} + RO_2^{\cdot} \rightarrow InOOR.$$

Therefore, the rate of radical formation $W_0 = 2\,(-d[InH]/dt)$. The presence of the inhibitor retarded the accumulation of peroxide decomposing to free radicals and in experiments with the inhibitor we succeeded to follow during a quite long time the formation of radicals resulting exclusively from the reaction between the original cyclohexanol and the dissolved oxygen.

Cyclohexanol was chosen as the object of the investigation, because at present a systematical study of its oxidation mechanism is being carried out[3]. The experiments were done in a cylindrical quartz reactor provided by a reflux cooler and a capillary tube via which oxygen was admitted to the reactor. The reactor was heated to the assigned temperature, the cyclohexanol (20 ml) containing the dissolved α-naphthol(10^{-3}-$1.5 \cdot 10^{-4}$ mole / liter) was poured in and after heating during five minutes the current of oxygen with a rate of 0.2 cm^3/sec was switched on. In the course of the experiment cyclohexanol samples were taken from the reactor and their α-naphthol content was analyzed by the procedure worked out in the paper [4]. To the sample containing α-naphthol we added a solution of parasulfophenyldiazonium sulfate and a small amount of alcoholic alkali; the amount of isodye formed was determined colorimetrically with a green light filter. The inhibitor concentration was determined with an accuracy of $\pm 0.7\%$.

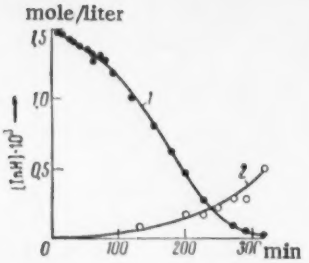

Fig. 1. Kinetics of α-naphthol consumption in cyclohexanol at 121° (1) and those of peroxide accumulation in the presence of the inhibitor (2) (for the peroxide concentration the scale was reduced by 100 times)

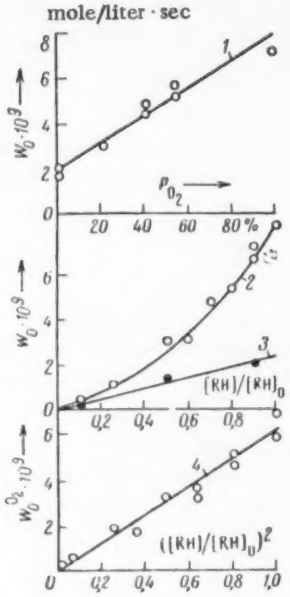

Fig. 2. 1) The rate of free radical formation in cyclohexanol plotted versus oxygen partial pressure at 111°; 2) this same rate as a function of cyclohexanol concentration at 121° in the presence of oxygen; the said rate in nitrogen atmosphere; 4) the rate at which radicals are formed by the interaction between cyclohexanol and oxygen plotted versus the square of the cyclohexanol concentration.

Experimental conditions			W_0	W'_0	$W_0^{O_2}$
t, °C	O_2 concentration in the mixture	cyclohexanol content, mole, %	mole % · liter^{-1} · sec^{-1} · 10^9		
111	1	100	2,0		
111	1	100	1,7		
111	21	100	3,0		
111	41	100	4,4		
111	41	100	4,8		
111	55	100	5,1		
111	100	100	7,1	2,0	5,1
121	100	100	8,2	2,3	5,9
121	100	90	7,2	2,1	5,1
121	100	90	6,7	2,1	4,6
121	100	80	5,4	1,8	3,6
121	100	80			3,2
121	100	70	4,8	1,4	3,2
121	100	60	3,1	1,4	1,7
121	100	50	3,1	1,2	1,9
121	100	25	1,2	0,6	0,6
121	100	10	0,5	0,2	0,3
121	100	0,0	0,0	0,0	0,0
121	1	90		2,1	
121	1	50		1,4	
121	1	10		0,2	
111	100	100			4,3
121	100	100	15,7	8,8	6,9
130,5	100	100	20	10	10

A kinetic curve of inhibitor consumption in cyclohexanol at 121° is shown in Fig. 1. During the first 100 minutes the inhibitor is consumed at a constant rate, later on the rate rises and this is connected with the accumulation of peroxide. α-Naphthol is a reducing agent and one may expect that it reacts not only with free radicals but also with dissolved oxygen. Special experiments showed that in chlorobenzene in the presence of oxygen at 121° no α-naphthol is consumed. Consequently, under the condition at which our experiments were carried out the consumption of inhibitor takes place only by the reaction with free radicals. The formation rate of free radicals in cyclohexanol oxidation, as was found from the initial slope of the curve for inhibitor consumption, was equal to $8.3 \cdot 10^{-9}$ mole/liter · sec (at 121°). From Fig. 1 it is evident that measuring the consumption of inhibitor in the substance oxidized gives W_0 values which are more reliable than those determined from $W_0 = 2\,[InH]_0 / t_{inh}$ where t_{inh} is the induction period caused by the initial concentration $[InH]_0$ of the inhibitor. In the latter case the value of W_0 is more or less too high because peroxide accumulates during the induction period. By measuring the initial rate of inhibitor consumption we were able to determine W_0 with an accuracy of $\pm\ 0.5 \cdot 10^{-9}$ mole/liter · sec.

In order to clarify the mechanism of radical formation in the system cyclohexanol plus oxygen it is necessary to establish the relations between W_0 and the following parameters: the oxygen concentration (or its partial pressure), the cyclohexanol concentration and temperature. The relation between W_0 and the concentration of dissolved oxygen was determined in experiments at 111° with an α-naphthol concentration of $2.5 \cdot 10^{-4}$ mole/liter, whereas from experiment to experiment the partial oxygen pressure was varied by diluting it with nitrogen while the total pressure was maintained at 1 atm. When the partial

oxygen pressure was raised, W_0 increased linearly: $W_0 = W'_0 + \underline{a}\ P_{O_2}$ (Fig. 2). The fact that in the absence of dissolved oxygen W_0 is not equal to zero indicates that there are formed radicals in reactions without participation of oxygen (evidently, because contaminations present in the cyclohexanol decompose under formation of free radicals). The linear increase of W_0 with raised P_{O_2} points out that the free radicals are formed in reactions in which one oxygen molecule participates. It may be supposed that the finite value of W'_0 results from traces of peroxide formed in cyclohexanol during storage. An iodometric analysis showed that the original cyclohexanol contained $1.6 \cdot 10^{-4}$ mole/liter peroxide. For the peroxide formed in the oxidation of cyclohexanol the rate constant of the decomposition into free radicals at 111° was about $6 \cdot 10^{-7}$ sec^{-1} [3]. Consequently, the peroxide may secure a free radical formation rate of 10^{-10} mole/liter sec, which amounts to not more than 5% of W'_0 and 1.4% of W_0 at P_{O_2} equal to 1 atm. When the reactor made from quartz glass was replaced by one made from pyrex glass, the formation rate of free radicals did not change and this proves the homogeneous character of the said formation. Further experiments showed that W'_0 varies from one series of experiments to another (each series was done with one and the same solution of α-naphthol in cyclohexanol) and is connected with accidental contaminations getting into the cyclohexanol.

The relation between the formation rate of free radicals and the cyclohexanol concentration was investigated at 121° and a α-naphthol concentration of $1.5 \cdot 10^{-4}$ mole/liter in experiments where cyclohexanol was diluted by chlorobenzene. The experimental results are given in table and Fig. 2. As is evident from Fig. 2, W_0 decreases, when the cyclohexanol concentration is lowered and in pure chlorobenzene it is equal to zero.

From Fig. 2 it is evident that W'_0 is proportional to [RH] and $W_0^{O_2}$ to $[RH]^2$. In order to establish more exactly which is the reaction order with respect to cyclohexanol one must plot log $W_0^{O_2}$ as a function of log [RH], determine from the slope of the straight line the reaction order with respect to cyclohexanol and apply a correction for the fact that the concentration of dissolved oxygen changes when cyclohexanol is diluted by chlorobenzene. For [RH] varying between 9.6 and 5.8 mole/liter $\Delta \log W_0^{O_2} / \Delta \log [RH] = 2.3 \pm 0.2$. When cyclohexanol is diluted by chlorobenzene, the partial oxygen pressure is lowered, because the vapor pressure of chlorobenzene is higher than that of cyclohexanol. The concentration of oxygen dissolved in heated cyclohexanol was determined in autoclave equipment at 110° and an oxygen pressure of 10 atm. Under these conditions one liter of cyclohexanol dissolves 0.095 ± 0.010 mole O_2. Therefore, one must take into account the change in concentration of dissolved oxygen just resulting from the changed partial oxygen pressure

$$W_0^{O_2} = k\,[RH]^n P_{O_2}; \quad \Delta \lg W_0^{O_2} = n\,\Delta \lg [RH] + \Delta \lg P_{O_2},$$

hence

$$n = \frac{\Delta \log w_0^{O_2}}{\Delta \log [RH]} - \frac{\Delta \log P_{O_2}}{\Delta \log [RH]} = 2{,}3 - \frac{\Delta \log P_{O_2}}{\Delta \log [RH]}.$$

At 120° for pure cyclohexanol P_{O_2} = 560 mm Hg, for pure chlorobenzene P_{O_2} = 225 mm Hg, for a 1 : 1 mixture of cyclohexanol and chlorobenzene one may take P_{O_2} = 393 mm Hg, hence

$$\Delta \lg P_{O_2} / \Delta \lg [RH] = 0{,}15/0{,}30 = 0{,}5, \quad n = 2{,}3 - 0{,}5 = 1{,}8 \pm 0{,}3,$$

that is, practically n = 2. This proves that in cyclohexanol the free radicals are formed in a reaction between one oxygen molecule and two cyclohexanol molecules, that is, in the case of cyclohexanol the trimolecular mechanism of chain initiation proposed in the paper [1] is realized.

Since we know the solubility of oxygen in cyclohexanol, we are able to determine the absolute value of the rate constant for reaction (2). At 111° and a total pressure of 1 atm P_{O_2} = 630 mm Hg, then the concentration of dissolved oxygen is $7.9 \cdot 10^{-3}$ mole/liter, the cyclohexanol concentration in the liquid phase is 9.6 mole/liter. $W_0^{O_2} = 5.1 \cdot 10^{-9}$ mole/liter sec, hence $k = 0.7 \cdot 10^{-8}$ $liter^2/mole^2 \cdot sec$. Experiments at various temperatures enables us to find the activation energy; it is equal to 12 ± 2 kcal/mole. However, the actual activation energy is somewhat higher, because, as temperature is raised, the cyclohexanol vapor pressure increases and the partial oxygen pressure and the oxygen concentration in the liquid phase are lowered. At 111° P_{O_2} = 630 mm Hg, at 130° it is 490 mm Hg. This lowering of the oxygen concentration decrease the activation energy by 4 kcal/mole. Consequently, the actual activation energy for the trimolecular formation of free radicals is equal to 16 kcal/mole. The rate constant of this reaction is expressed by the relation

$$k = 8{,}3 \exp(-16000/RT)\ liter^2/mole^2 \cdot sec.$$

LITERATURE CITED

1. E. T. Denisov, DAN, 130, 1055 (1960).
2. C. E. Boozer, G. S. Hammond, C. E. Hamilton, and J. N. Sen, J. Am. Chem. Soc. 77, 3233 (1955).
3. E. T. Denisov and V. V. Kharitonov, ZhFKh, 35, 444 (1961).
4. D. G. Knorre, Z. K. Maizus, and M. Émanuél', DAN, 123, 123 (1958).

All abbreviations of periodicals in the above bibliography are letter-by-letter transliterations of the abbreviations as given in the original Russian journal. *Some or all of this periodical literature may well be available in English translation.* A complete list of the cover-to-cover English translations appears at the back of this issue.

DIFFERENT RATES OF FILTRATION OF ANIONS AND CATIONS THROUGH FINE-PORED FILTERS

V. A. Zharikov, T. N. Dyuzhikova, and E. M. Maksakova

Institute of Geology of Ore Deposits, Petrography,
Mineralogy and Geochemistry
(Presented by Academician D. S. Korzhinskii, June 6, 1961)
Translated from Doklady Akademii Nauk SSSR, Vol. 141, No. 1,
pp. 135-138, November, 1961

In geochemistry at present attention is being paid to the hypothesis of acid-base hydrothermal differentiation, put forward by D. S. Korzhinskii [2]. According to this hypothesis the change in the acidity of solutions, which is a determinative factor in the evolution of postmagmatic solutions, occurs as a consequence of a difference in the rates of filtration of anions and cations during percolation of hydrothermal solutions through fine-pored rock, i.e., as a consequence of an acid-base filtration effect.

We have conducted an experimental investigation of the acid-base filtration effect with 0.1-0.001 N solutions of the chlorides and sulfates of copper and iron. Preceding experimental investigations of the filtration effect [3-5] could not be utilized in our work since the change in concentration of the solutions during filtration was estimated by indirect methods (by change of electroconductivity).

In studying the filtration effect, first of all the effects of sorption of the components of the solution by the filter material must be excluded and estimated. Therefore we chose carefully purified quartz as the filter material and carried out experiments to determine the adsorption of the solution components on the ground quartz. The adsorption experiments gave a negative result. They showed that within the sensitivity and accuracy of the methods we employed, adsorption of copper ion, chloride and sulfate from dilute solutions (0.1-0.001 N) onto quartz did not occur.

We carried out more than 100 experiments on the filtration of 0.1-0.001 N solutions of the chlorides and sulfates of copper and iron through fine-pored filters of ground quartz, at room temperature (18-22°) and normal pressure. A quartz tube filled with quartz powder was used for the filtration. The conditions of a standard experiment were as follows. Dimensions of tube: D = 22-33 mm, l = 280-300 mm. Filter: quartz powder of particle sizes: 1) 0.020-0.025 mm; 2) 0.015-0.019 mm; 3) 0.009-0.014 mm. Height of filter column 160 mm. Height of solution column above the filter was kept constant and equal to 110-120 mm. The solution above the filter was stirred.

A test sample of the total volume of filtrate was withdrawn after definite time intervals. The size of the test sample was from 0.5 to 3.5 ml. Depending on the composition and concentration of the solution the following analytical methods were used: 1) the diethylthiocarbamate colorimetric method for the determination of copper; 2) the thiocyanate (in absence of copper) and salicylate (in presence of copper) colorimetric methods for the determination of iron; 3) the barium chromate and diphenylcarbazide colorimetric method for the determination of sulfate ion; 4) the mercurimetric volumetric method for the determination of chloride ion. Errors of determination did not exceed 2-3% with a test sample of 0.3-1.0 g for a single determination.

Two series of experiments were carried out. In the first series filtration of solutions was made through a filter which was initially dry.

In all experiments a well defined change of concentration was observed according to the degree of filtration of the solution: a) the concentration of cations (Cu^{++}, Fe^{+++}) in the first test samples was less than in the original solution; b) the concentration of anions (Cl^-, SO_4^{--}) in the first test samples was greater or equal to their concentration in the original solution; c) according to the degree of filtration of the solutions the concentration of cations increased and of the anions decreased or remained equal to the concentration of the original solution; the initial part of the plots of C against v or C against t shows the presence of diffusion; d) the effect of the concentration change in the first test samples was more evident in the more dilute solutions and varied for different components. In Fig. 1 are shown for example, the results of some experiments on the filtration of 0.001 N solutions.

The concentration changes observed in the filtrate are due to different rates of filtration (filtration effect) of the cations and anions, which in turn differ from the filtration rate of the solvent. On passage of the solution into the fine-pored filter medium the initially unified stream of solution is broken up, differential movement of the so-

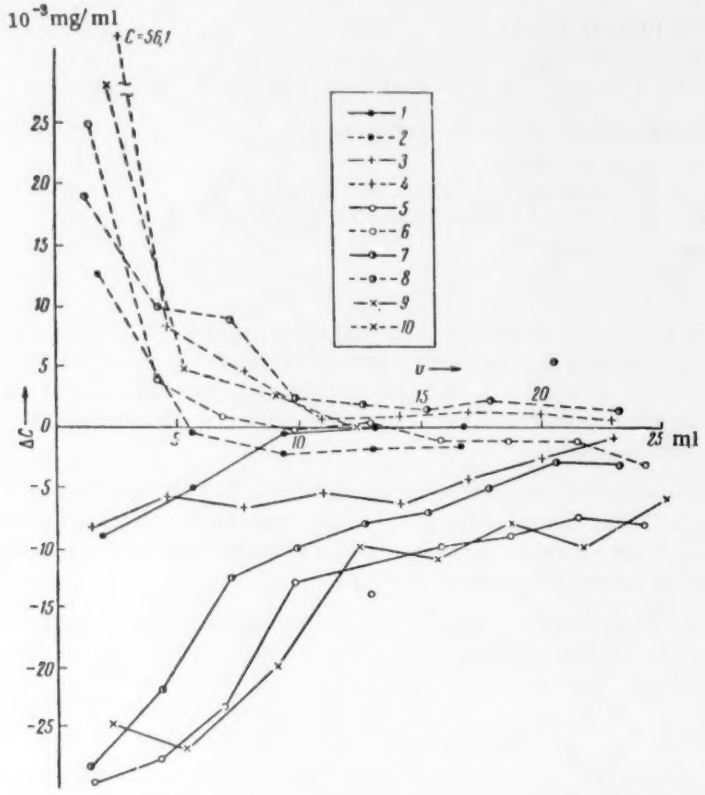

Fig. 1. ΔC, v experimental curves for experiments in which 0.001 N $CuCl_2$ and $FeCl_3$ solutions were filtered through a dry filter.

No. of experiment	Solution	Ion	Size of filter particles, mm	Porosity, %	Initial concentration 10^3 mg/ml	φ_i	Point
21	0.001 *N* $FeCl_3$	Fe^{+++}	0.015—0.019	41.6	15.9	0.90	*1*
		Cl^-			38.2	1.04	*2*
22	0.001 *N* $FeCl_3$	Fe^{+++}	0.015—0.019	45.6	15.6	0.78	*3*
		Cl^-			38.3	1.23	*4*
124	0.001 *N* $CuCl_2$	Cu^{++}	0.015—0.019	39.3	35.1	0.73	*5*
		Cl^-			39.5	1.07	*6*
125	0.001 *N* $CuCl_2$	Cu^{++}	0.015—0.019	43.4	35.9	0.81	*7*
		Cl^-			38.8	1.11	*8*
128	0.001 *N* $CuCl_2$	Cu^{++}	0.020—0.025	38.9	32.0	0.69	*9*
		Cl^-			40.9	1.30	*10*

lution occurs while the solvent and each dissolved component move at different rates. The cations progress more slowly than the solvent which leads to reduction of their concentration in the first test samples. The anions move simultaneously with or rather more rapidly than the solvent, and consequently the anion concentration in the first test samples is equal to or more than the concentration in the original solution.

The different rates of movement of the anions and cations showed up particularly well in a second series of experiments, in which filtration of the solution was made through a filter previously saturated with water. The results of these experiments are shown in Fig. 2. It is readily seen that the greater rate of movement of the anions leads to their outstripping the cations during filtration.

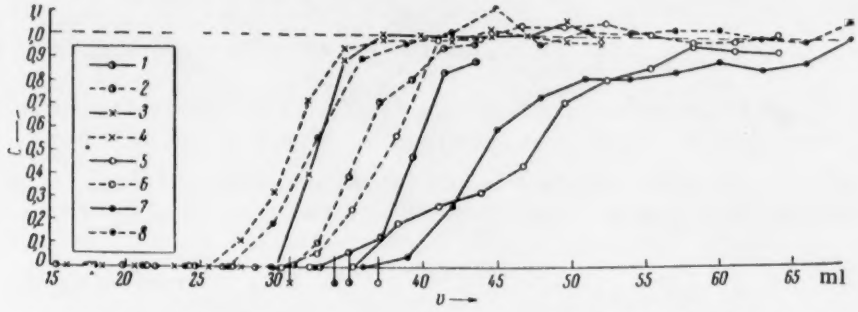

Fig. 2. C versus v experimental curves for experiments in which 0.01 and 0.001 N $CuCl_2$ and $FeCl_3$ solutions were filtered through a filter saturated with water. Concentration in hundredths and thousandths of a gram-equivalent. 10^{-2} and 10^{-3} g-equiv.

No. of experiment	Solution	Ion	Size of filter particles, mm	Porosity, %	Initial concentration, g-equiv.	φ_i	Point
25	0,01 *N* $FeCl_3$	Fe^{+++}	0,015—0,019	46.7	10^{-2}	0,89	*1*
		Cl^-				0,91	*2*
26	0,01 *N* $FeCl_3$	Fe^{+++}	0,015—0,019	47,2	10^{-2}	0,94	*3*
		Cl^-				1,00	*4*
27	0,001 *N* $FeCl_3$	Fe^{+++}	0,015—0,019	54,0	10^{-3}	0,80	*5*
		Cl^-				1,02	*6*
129	0,001 *N* $CuCl_2$	Cu^{++}	0,015—0,019	45,0	10^{-3}	0,78	*7*
		Cl^-				1,30	*8*

The experimentally observed concentration change in the filtrate is not only due to a difference in the rate of filtration of the ions, but is complicated by associated diffusion effects. The combination of the processes, occurring during filtration of a solution through a fine-pored inert filter, is described by the equation:

$$\partial C_i/\partial t + w_0 \varphi_i \partial C_i/\partial x + w_0 C_i \partial \varphi_i/\partial x - D_i \partial^2 C_i/\partial x^2 = 0,$$

where C_i is the concentration of any component i in the solution; w_0 is the filtration rate of the solvent; x is distance; t is time; D_i is the diffusion coefficient; φ_i is the filtration effect coefficient, equal to $\varphi_i = w_i/w_0$, as shown by D. S. Korzhinskii [1]; w_i is the filtration rate of a component.

Study of this equation shows that on passage of a solution into a medium with differing φ_i there first occurs a general non-stationary flow of solution by which C_i varies in each section. Since the filtration will tend towards a stationary state, which is characterized by $C_i = C^0/\varphi_i$, $(\partial x/\partial t)\, c_i = w_i$ and $w_i = \varphi_i w_0$, the non-stationary flow will be localized in the leading zone of the solution, where, owing to the difference of w_i and w_0, a concentration gradient will arise and diffusion will occur. The diffusion will oppose the differentiation of the substance which arises owing to the different rates of filtration. Thus it is evident that the lower the diffusion rate the better will be the filtration effect.

It is always better to estimate the different filtration rates of cations and anions from φ_i, the filtration effect coefficient. Experimentally the following equivalent expressions are applicable for $\varphi_i = w_i/w_0 = t_0/t_i = v_0/v_i$, where w_0, w_i are the filtration rates of solvent and component i; t_0, t_i are the times of filtration of solvent and com-

ponent i through the given filter; v_i is the volume filtering through before appearance of the dissolved component; v_0 is the volume of solvent in the filter (equal to the volume of the filter pores).

The values of t_i and v_i can be obtained from the experimental curves, provided that the effect of diffusion is excluded.

Then $v_i = v_0 - \left(\sum_1^n \Delta C_n \Delta v_n\right) / C_0$, where $\Delta C_n = (C_n - C^0)$ is the concentration difference between the test sample (C_n) and the original solution (C^0), and $\Delta v_n = v_n - v_{n-1}$ is the size of the test sample up to C_n, v_n the concentration and volume in the last test sample which is different from the original solution.

The value of φ_i can also be calculated from the material balance during filtration, i.e., by assuming that a deficiency (excess of substance in the first test samples is compensated by an equal and opposite concentration change in the solution in the filter. Then $\varphi_i = C^0 v_0 / \left(C^0 v_0 - \sum_1^n \Delta C_n \Delta v_n\right)$. The results of the calculated and corresponding experimental values of φ_i carried out by the two methods, with complete convergence of the results, are given in the tables with the figures.

The experimental studies carried out show that during passage of a solution through a fine-pored filter a filtration effect occurs, i.e., a differential flow of solution results during which each dissolved component has its own rate of filtration. Cations (Cu^{++}, Fe^{+++}) move more slowly than the solvent, the value of φ_i is different for different cations: $\varphi_{Cu^{+++}} = 0.70\text{-}0.96$, $\varphi_{Fe^{+++}} = 0.80\text{-}0.96$. Anions move at the same rate or somewhat more rapidly than the solvent, with the chloride ion moving more rapidly than the sulfate ion: $\varphi_{Cl^-} = 1.00\text{-}1.30$, $\varphi_{SO_4} = 1.00\text{-}1.04$. The value of φ_i depends on the concentration of the solution and the characteristics of the filter (density, pore size, etc.).

Of special interest is the difference in the filtration rates of anions and cations; the difference $\Delta\varphi = \varphi_a - \varphi_k = (w_a - w_k)/w_0$ is 0.4-0.6 in 0.001 N solutions. This shows that during filtration of solutions through fine pored media an acid-base filtration effect occurs, in which the more rapid filtration of the anions causes a corresponding migration (change in concentration) of hydrogen ions, leading to an increase in the acidity of the leading flow of solution.

The investigation reported here gives experimental confirmation of D. S. Korzhinskii's hypothesis of acid-base hydrothermal differentiation.

LITERATURE CITED

1. D. S. Korzhinskii, Izv. AN SSSR, Ser. Geol. 2, 35 (1947).
2. D. S. Korzhinskii, Izv. AN SSSR, Ser. Geol. 12, 3 (1957).
3. L. N. Ovchinnikov and V. G. Maksenkov, Izv. AN SSSR, Ser. Geol. 3, 82 (1949).
4. L. N. Ovchinnikov and A. S. Shur, Transacts of the IV Conf. on Experimental Mineralogy and Petrography [in Russian] (1953), No. 2, 163, (1953).
5. W. Hakker, Koll. Zs. 94, H. 1, 11 (1941).

All abbreviations of periodicals in the above bibliography are letter-by-letter transliterations of the abbreviations as given in the original Russian journal. *Some or all of this periodical literature may well be available in English translation.* A complete list of the cover-to-cover English translations appears at the back of this issue.

THE EMISSION OF POSITIVE MOLECULAR IONS FROM HEATED SURFACE IN VACUO

E. Ya. Zandberg and N. I. Ionov

A. F. Ioffe Physicotechnical Institute, Academy of Sciences, USSR
(Presented by Academician B. P. Konstantinov, June 14, 1961)
Translated from Doklady Akademii Nauk SSSR, Vol. 141, No. 1, pp. 139-142, November, 1961
Original article submitted May 20, 1961

In order to study the surface ionization in strong electrical fields of atoms with high values for the ionization potentials, the sensitivity of the ion detector of the mass-spectrometric assembly previously used [1] was increased to $\sim 10^{-18}$ amp/division by the introduction of a secondary-electron multiplier before the EMU-3 electrometric amplifier.

A study was made beforehand of the mass spectrum of the background of positive thermionic emission from tungsten filaments over a wide range of temperatures T, including low values of T at which a fairly intense nonstationary emission of positive ions with mass number 101 was previously observed [2]. The present communication gives further data on the emission of molecular positive ions from filaments of tungsten and other materials.

Figure 1 gives a diagram illustrating the ion source. As usual, in order to obtain strong electric fields, the ion source was constructed in the form of a cylindrical condenser with a fine filament F extending along the axis of the cylinder [1, 3]. The diameter of the filaments varied between 18 and 50 μ. The power liberated when these filaments are heated is insufficient to heat the armature of the source, which is important in this case. The cylinder C_2 and the mass-analyzer tube M-A were earthed, the filament F was kept at a potential of +1300 v, and it was possible to apply potentials of different magnitude and sign to the cylinder C_1. Some of the ions formed on the filament entered the mass-analyzer through the slits S_1, S_2 and S_3. In order to interpret the mass spectra it was possible to obtain reference lines by the surface ionization, on the filament, of molecules of alkali halides directed by the vaporizers V_1 and V_2. The resolving power of the mass-analyzer amounted to ~100.

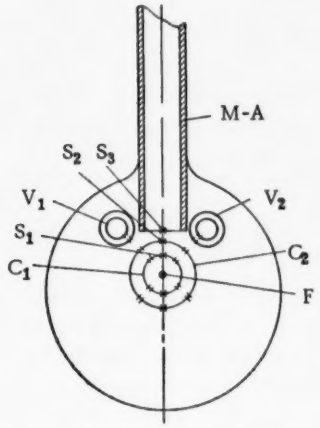

Fig. 1. Diagram of the ion source.

The apparatus was evacuated by means of a TsVL-100 vapor-oil pump (working oil D-1-A) and a VN-461 forevacuum pump (VM-4 oil). The TsVL-100 pump was connected to the apparatus via a trap containing liquid nitrogen. All the measurements were carried out at a residual gas pressure of $(1\text{-}2)\cdot 10^{-7}$ torr, with the trap filled with liquid nitrogen. The temperature T of the filaments in the range between room temperature and the temperatures measurable by a pyrometer were found from the values of the resistance R on the assumption that R is linearly dependent on T [4]. For filaments which had not undergone preliminary purification by thermal treatment, it was possible in this case to assume a systematic error of < 5%, towards increase in temperature, since it was impossible to know the exact value of the monochromatic blackness coefficient of the radiation for the surfaces.

With gradual increase in T for fresh unpurified tungsten filaments, the emission of positive ions with mass numbers 59, 85, 96, 101, 102 and 202, of which the line from m = 101 was the most intense, appeared at $T \approx 400$°K; this emission remained stable over a prolonged period of continuous observation for many hours. When the filament was heated at $T \approx 1100$°K, there was a subsequent increase in the intensity of all the mass lines by two or three orders of magnitude, i.e., activation of the surface took place. The current density for m = 101 reached 10^{-7} -10^{-8} amp/cm^2. Prolonged treatment of the cold activated filaments in forevacuum and in air did not reduce their

emission activity in high vacuum. The "built-up" noted in [2] was characteristic of ions of almost all masses: the instantaneous value of the ionic current when the filament heating is switched on increases with increase in the time for which the filament has been disconnected beforehand. In a vacuum of $(1\text{-}2) \cdot 10^{-7}$ torr, however, the build-up reaches saturation in a time of the order of several minutes, which is different for different mass lines (for example, 3 minutes for m = 101 and 10 minutes for m = 59).

With increase in the temperature of the trap containing liquid nitrogen and the continuous increase in the pressure in the apparatus, an increase in the intensity of the principal mass peaks is observed only in a certain range of trap temperatures, at which the volatilization of some organic substances apparently takes place.

Mechanical cleaning of the surface of fresh filaments with fine emery paper and subsequent thorough washing with solvents leads to a sharp decrease in the ionic emission. Activation at ~ 1100°K and a pressure of $\sim 2 \cdot 10^{-7}$ torr restores the emission, however. When the filaments are heated to T $\simeq$ 1500-1600°K, there is an irreversible loss of emission not only for the line for m = 101 [2], but also for all the other lines. After deactivation of the surface in this way, only the characteristic emission of the atomic ions of the alkali metals present as impurities in the tungsten is observed. The deactivation of the filaments is always accompanied by an irreversible sudden change in the radiation properties of the surface, shown by a sharp change, at the temperature of the deactivation, in the curve obtained by plotting the resistance of the filament versus the power used up to heat the filament.

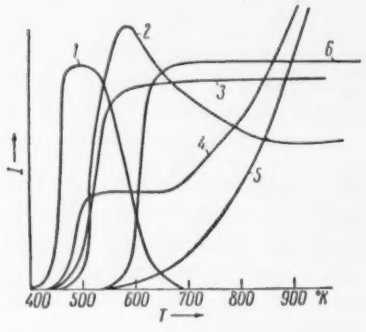

Fig. 2. Relationship between temperature and ionic current for different masses: 1) For m = 101 (102, 94, 96); 2) m = 59 (97, 83, 109); 3) m = 81 (84); 4) m = 73 (60); 5) m = 85 (86); 6) for CsCl.

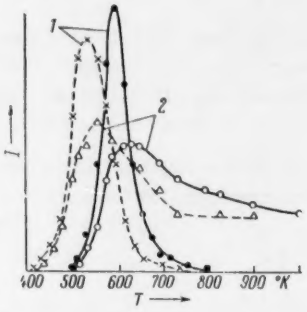

Fig. 3. Relationship between ionic current and temperature for two values of the electric field intensity: $E_1 = 2.3 \cdot 10^5$ v/cm – solid lines; $E_2 = 2.3 \cdot 10^6$ v/cm – broken lines. 1) m = 101; 2) m = 59.

The ionic emission of deactivated tungsten filaments can be restored by the oxidation resulting from ignition in forevacuum to a dark red heat. The spectrum of the ionic emission from tungsten surfaces prepared in this way is much richer than that from activated tungsten filaments and the intensity of many lines in the spectrum becomes very high (m = 59, 73, 81, 82, 83, 84, 85, 86, 94, 96, 97, 98, 101, 109, 116, 123, 125, and 137). The lines with mass numbers 84, 85, 101 (current density $j \simeq 10^{-7}$-10^{-8} amp/cm^2) and 59, 94, 109 and 123 ($j \simeq 10^{-8}$-10^{-9} amp/cm^2) are particularly intense.

Figure 2 gives typical curves showing the temperature dependence of the ionic currents from an oxidized tungsten filament for a number of mass lines. Some of the curves in Fig. 2 are similar to the analogous graphs for the currents for the surface ionization of atoms: for example, for m = 81 and 84, the relationships are the same as those for the surface ionization of atoms with ionization potentials Vi less than the work of removal for the surface φ. For m = 85 and 86, the relationships are similar to those for surface ionization for the case where Vi > φ [3]. For the majority of masses, however, the temperature dependence of the ionic currents is more complex in character, which is probably due to the fact that several competing processes take place simultaneously on the surface. It should be noted that the nonstationary character of the emission of ions with mass 101, observed in [2] by use of the flash method, is only apparent and is due to the nature of the temperature dependence of the ionic current for this mass.

Figure 2 gives for comparison the curve for the surface ionization of CsCl molecules on an oxidized tungsten filament. It can be seen that T for the appearance of organic molecules and radicals differs little from T for the

appearance of Cs^+ ions for the surface ionization of CsCl molecules. Measurable ionic currents for all the mass lines appear in the temperature range 400-600°K. The characteristic emission of the impurity ions of the alkali metals Na^+ and K^+ from the filaments was observed at much higher temperatures of ~800°K. All these experimental facts on the thermionic emission give grounds for assuming that on the surface of oxidized tungsten in the temperature range from ~400 to ~1500°K processes take place involving the catalytic dissociative ionization of the molecules of organic compounds, which are probably present in the pump oils or are products of their decomposition. The high values of the ionization coefficients observed in the experiments indicate that the values of the electron affinity of the observed positive ions are comparatively low.

If the theories of the surface ionization of atoms are applicable to this ionic emission, then, depending on the relationship between the work of removal for the surface and the electron affinity of the positive ion, increase in the intensity of the electric field at the surface will lead either to displacement of the temperature threshold of ionization without appreciable increase in the ionic current or to increase in the ionic current without significant displacement of the ionization thresholds [3].

Figure 3 gives the temperature dependence of the current for masses 59 and 101, for two values of the intensity of the electric field accelerating the ions at the surface: $E_1 = 2.3 \cdot 10^5$ v/cm and $E_2 = 2.3 \cdot 10^6$ v/cm. It can be seen that with increase in the intensity of the field, the temperature threshold of the ionization is displaced towards lower temperatures, whereas the value of the current remains practically unchanged.

We also studied the thermionic emission from nickel, iron, platinum and gold-plated tungsten filaments. Stable emission of ions with mass 101 was observed from nickel and iron, and no emission other than that due to the ions of impurity alkali metals was observed from platinum and gold-plated filaments. Analogous results for nickel and platinum were obtained in [2].

In conclusion we may point out fields in which the thermionic emission considered above may be of significance:

1) The initiation of the initial conductivity in the vacuum gaps between the electrodes vacuum break-down [5].

2) The break-down effect of ionic emission from the grids of electronic valves may act as a source of noise in valves (it is known that noise is reduced in valves with gold-plated grids).

3) The thermal emission of charged organic molecules and radicals may be of importance in the mass-spectrometry of organic compounds and the study of physicochemical processes at the surface of solids.

LITERATURE CITED

1. E. Ya. Zandberg, ZhTF, 30, 1215 (1960).
2. E. I. Agishev and Yu. I. Belyakov, ZhTF, 30, 223 (1960).
3. E. Ya. Zandberg and N. I. Ionov, UFN, 67, 581 (1959).
4. E. Ya. Zandberg, ZhTF, 27, 2583 (1957).
5. N. I. Ionov, ZhTF, 30, 561 (1960).

KINETICS OF THE DECOMPOSITION OF ALKALI METAL AMALGAMS IN ALKALINE SOLUTIONS OF ELECTROLYTES

V. N. Korshunov and Z. A. Iofa

M. V. Lomonosov Moscow State University
(Presented by Academician A. N. Frumkin, June 27, 1961)
Translated from Doklady Akademii Nauk SSSR, Vol. 141, No. 1,
pp. 143-146, November, 1961

Bronsted and Kane in 1931 [1] showed that the kinetics of the decomposition of dilute sodium amalgams in phosphate buffers (pH ~7-9) were described by the equation

$$i = kC_{am}^{0.5} \quad (1)$$

where i is the rate of decomposition of the amalgam, C_{am} is its concentration, k is a constant. The correctness of equation (1) for different amalgams and buffer solutions was confirmed in a number of papers [2-5] and its theoretical interpretation was given by A. N. Frumkin [6] and Hammet and Lorch [7] who suggested that the decomposition of the amalgam be considered as an electrochemical process in which the discharge of hydrogen ions is the slow stage determining the rate of the whole process.

The data on decomposition of alkali metal amalgams with solutions of high pH value (>10) obtained by various authors [1-4, 8-10] differ greatly among themselves and therefore there is also unequal interpretation of the experimental results. In reference [8] the electrochemical theory already mentioned was applied to the decomposition of amalgams in a strongly alkaline medium. It was found that on calculating the dependence of the activity of the amalgam on the concentration the power index for C_{am} in equation (1) must exceed 0.5 in value. Bockris and Watson [9] in order to explain variations in the regular decomposition of alkali and alkaline-earth metal amalgams proposed a chemical reaction of the surface atoms of the metal amalgam with water molecules, but in deducing kinetic relationships they started from equation (1) which is derived from the electrochemical theory. Volkov [10] showed, from a study of the decomposition kinetics of amalgams,that the removal of surface impurities plays an important part, resulting in a sharp decrease in the decomposition rate.

Thus, from the results obtained there is no doubt that the decomposition kinetics of alkali metal amalgams in buffer solutions of pH ~7-9, follows the electrochemical theory and obeys the kinetic equation (1). However in the case of strongly alkaline solutions (pH > 10) deviation of the results does not allow simple determination of the kinetics and mechanism of the process.

The present work is concerned with the study of the decomposition kinetics of alkali metal amalgams by aqueous solutions of electrolytes under conditions of maximum purity of reagents and apparatus.

The decomposition rate was determined by a gasometric method. The concentration of amalgam prepared by electrolysis, was found by titration of excess acid added to the amalgam. To prevent introduction of impurities from glass, the experiments were carried out in a polystyrene apparatus. Organic impurities which might be transferred from polystyrene into solution must be desorbed from the electrode surface at the high negative potentials which are inherent with alkali metal amalgams and cannot influence the decomposition kinetics. Solutions from which the amalgams were obtained and in which they were decomposed were subjected to lengthy cathodic purification. The platinum electrodes were removed and the potentials of the amalgams were found by calculation or by measurement in a separate cell. The system was not stirred since under our experimental conditions it had no effect on the decomposition kinetics.

The apparatus in which the measurements were carried out, shown in Fig. 1. was made of clear polystyrene with a screw-on cover. It was filled with the solution under study and hydrogen was blown through. The amalgam from vessel A was transferred through a three-way tap into the dish B. The hydrogen liberated passed into the col-

lecting funnel and then into the gas buret C. The collecting funnel and buret were of glass, since the adherence of small bubbles of hydrogen to polystyrene made it difficult to record the volume of gas. As seen in Fig. 1, the

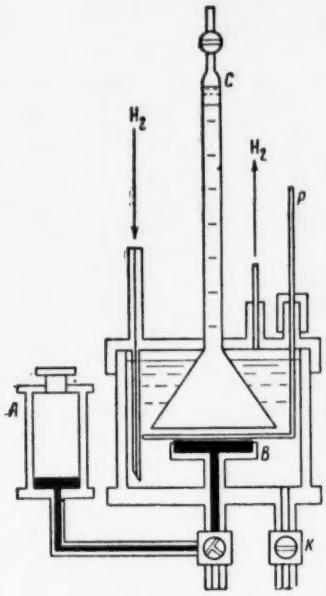

Fig. 1

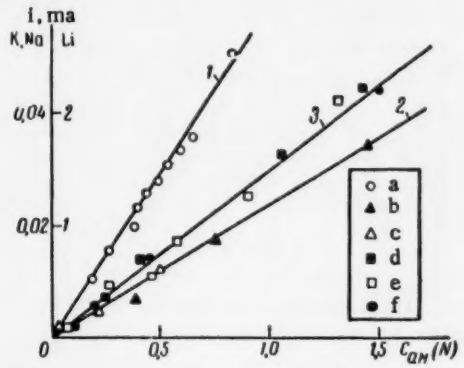

Fig. 2. Dependence of the rate of decomposition of Li (1), Na (2) and K (3) amalgams on their concentration, in aqueous electrolyte solutions: a) Li amalgam in 0.1 N LiOH solution; b) Na amalgam in 0.1 N NaOH solution; c) K amalgam in 0.1 N KOH solution; d) the same in 0.1 N KOH + KH_2PO_4 solution with pH 10.6; e) the same in 0.1 N KOH + KH_2PO_4 solution with pH 11.4; f) the same in 1 N KOH solution.

amalgam does not come into contact with glass, which as the experiment showed, accelerates the decomposition process. However contact of the solution with glass did not have any appreciable effect on this process within the time of the experiment.

The surface of the amalgam was rendered clean by discarding, with the aid of the arm P, the layer of amalgam with centers of intense liberation of hydrogen. The discarded layer was removed from the apparatus through tap K. Before recording the volume of hydrogen liberated, small bubbles of the gas present on the surface of the amalgam were transferred into the gas buret by means of the arm P. The experimental temperature was 20 ± 1°. Volume of solution 500 ml. Area of the amalgam mirror 20 cm^2. Since, because of the high negative potential of the amalgam there occurs a drawing in of the solution between the walls of the apparatus and the amalgam, the true surface of contact of the latter with the solution exceeds the apparent surface and therefore values of the current densities for the decomposition of the amalgams may be considered somewhat overestimated.

In Fig. 2 is shown the dependence of the decomposition rate of Li, Na and K amalgams on their concentration in different solutions obtained by the method described above. As can be seen, there is a straight line proportionality between the amalgam concentrations and their rate of decomposition which corresponds to the kinetic equation

$$i = kC_{am} \qquad (2)$$

(i expressed in a/cm^2, C_{am} in g. equiv./l). Below are given the values of the constant k:

Amalgam	Li	Na	K
k, $a/cm^2 \cdot 1/g.\ equiv.$	$3 \cdot 10^{-3}$	$2.4 \cdot 10^{-5}$	$3 \cdot 10^{-5}$

In Fig. 3 are shown the results for the decomposition of Li, Na and K amalgams in 0.1 N solutions of electrolytes with the coordinates – potential, and logarithm of the decomposition current density. For small concentrations of the Na and K amalgams there is a linear dependence of φ on log i with a coefficient of slope 0.06-0.07 v. On transition to concentrated amalgams, the activity coefficient of which rises, an increase in the slope is observed. In the case of Li amalgam, for which the relationship between the logarithm of the activity coefficient and the amalgam concentration in the range of concentration examined is linear [11] the plot of φ against log i is obtained with a coefficient of slope 0.073-0.75 v.

TABLE 1

C_{am}(N)	Composition and concentration of electrolyte	i, a/cm²	φ, v, N.C.E.
0,54	0,1 *N* LiCl	$1,8 \cdot 10^{-3}$	2,413
0,51	0,55 *N* LiCl	$1,6 \cdot 10^{-3}$	2,374
0,47	2,0 *N* LiCl	$1,5 \cdot 10^{-3}$	2,313
0,45	10,8 *N* LiCl	$2,0 \cdot 10^{-3}$	2,111
0,50	0,63 *N* LiOH	$1,6 \cdot 10^{-3}$	2,352
0,50	2,20 *N* LiOH	$1,6 \cdot 10^{-3}$	2,325
0,50	5,0 *N* LiOH	$1,5 \cdot 10^{-3}$	2,307

TABLE 2

Current density for decomposition of 0.55 N amalgam		Source
Li	K	
$15 \cdot 10^{-3}$	$6 \cdot 10^{-3}$	(4)
$6 \cdot 10^{-3}$	$1 \cdot 10^{-4}$	(8)
$5 \cdot 10^{-3}$	$1 \cdot 10^{-3}$	(9)
$1.6 \cdot 10^{-3}$	$1.6 \cdot 10^{-5}$	Our results

In table 1 are set out the experimental results for the decomposition of Li amalgam of approximately constant concentration in different solutions.

From the data of Fig. 2 and Table 1 it is seen that the rate of decomposition of the Li and K amalgams does not depend on the composition, concentration or pH of the solution. The only factor determining the rate of decomposition of the amalgams under the given conditions is their concentration.

In order to compare our results with those of previous investigations the decomposition current densities for 0.55 N Li and K amalgams in electrolyte solution (pH ~ 12-13) taken from the data of different authors * are collected together in Table 2. Since the experimental results in the series of papers were expressed in different ways, we have made an appropriate calculation.

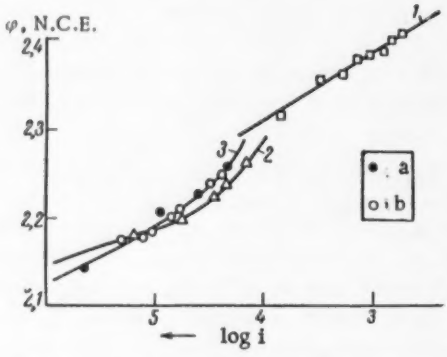

Fig. 3. φ, log i curves for: 1) Li amalgam in 0.1 N LiOH; 2) Na amalgam in 0.1 N NaOH; 3) K amalgam in 0.1 N KOH (a) and in 0.1 N KOH + KH_2PO_4 (b) solution.

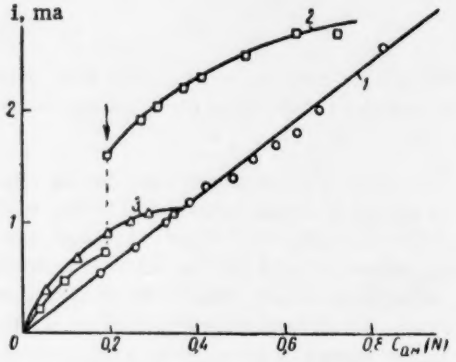

Fig. 4. Dependence of the rate of decomposition of Li amalgam on its concentration in 0.1 N LiOH for various conditions of purity.

The impurities on an amalgam surface which get into it, for example, from glass, not only alter the value of the decomposition rate, but also the character of the kinetic relationship. In Fig. 4 are reported experiments on the decomposition of Li amalgam in 0.1 N LiOH. By careful removal of contamined sections from the amalgam surface (curve 1) the decomposition rate became minimized and was proportional to the amalgam concentration. Curve 2 relates to the case where the contaminated sections are not removed. After their instant removal with the arm mentioned, the decomposition rate falls sharply and approximates to the rate expressed by the straight line 1. After introduction of glass splinters onto the pure surface of the amalgam (curve 3) the decomposition rate somewhat increased and was now not proportional to the amalgam concentration. In this case, as in the case of curve 2, the decomposition process is more satisfactorily described by equation (1).

* In reference [10] for the case of the decomposition of a ~0.2 N Na amalgam in saturated NaCl solution there was obtained $i = 3.47 \cdot 10^{-7}$ a/cm². The experiments were carried out under conditions in which complete harmonicity was not secured.

Experiments which we carried out showed that cathodic polarization of Li amalgams in a $N(CH_3)_4I$ solution up to a potential of 2.73 v N. C. E. did not affect their rate of decomposition.

It was also found that a mixed Li and Na amalgam decomposed in LiOH + KOH solution at a rate which was the sum of the decomposition rates of Li and K amalgams separately.

From the results we obtained it can be concluded that the decomposition of alkali metal amalgams in solutions of high pH carried out experimentally under sufficiently pure conditions occurs by a direct reaction of the surface atoms of the metal amalgam with water molecules, according to the simplified scheme (3), without any demarcation of the cathodic and anodic processes:

$$Me\,(Hg) + H_2O \rightarrow Me^+ + {}^1/_2H_2 + OH^- + Hg. \qquad (3)$$

This conclusion is in agreement with the ideas expressed by Bockris and Watson, although under their experimental conditions reaction (3) cannot be observed since (see Table 2) the rates of decomposition of the amalgams obtained by these authors are considerably higher than those found by us, i.e., the amalgam surface in Bockris and Watson's experiments was contaminated. However in contradiction to the kinetics which the authors of paper [9] proposed, the kinetics of the decomposition of amalgams in a strongly alkaline medium is expressed by equation (2) of the first order. Introduction of impurities on to the amalgam surface, the hydrogen overvoltage on which is lowered, leads to a separation of the cathodic and anodic processes. The kinetics of decomposition of amalgams under these conditions is very close to the relationship expressed by equation (1) derived from the electrochemical theory. As will be shown in the following paper, the decomposition kinetics of amalgams in phosphate buffer solutions with ph < 10 obeys equation (1) and conforms with the electrochemical mechanism under conditions of maximum purity.

We convey our deep appreciation to Academician A. N. Frumkin for advice and consideration shown during the execution of this work.

LITERATURE CITED

1. J. Brönsted and N. Kane, J. Am. Chem. Soc. 53, 3624 (1931).
2. F. Fletcher and M. Kilpatrick, J. Phys. Chem. 42, 113 (1938).
3. W. Dunning and M. Kilpatrick, J. Phys. Chem. 42, 215 (1938).
4. S. I. Sklyarenko and B. A. Sakharov, ZhFKh, 21, 97 (1947); ZhPKh, 20, 406 (1947); ZhOKh, 17, 1385 (1947).
5. G. Trümpler and K. Gut, Helv. Chim. Acta. 33, 1922 (1950); 34, 2044 (1951).
6. A. N. Frumkin, Zs. Phys. Chem. A160, 116 (1932).
7. L. Hammet and A. Lorch, J. Am. Chem. Soc. 54, 2128 (1932).
8. O. L. Kaptsan and Z. A. Iofa, ZhFKh, 26, 193, 201 (1952).
9. J. O'M. Bockris and R. Watson, J. Chim. Phys. 49, 70 (1952).
10. G. I. Volkov, ZhFKh, 27, 194 (1953); 29, 390 (1955).
11. I. Ueda, Sci. Rep. Tohoku Imp. Univ. 22, 448 (1933).

All abbreviations of periodicals in the above bibliography are letter-by-letter transliterations of the abbreviations as given in the original Russian journal. *Some or all of this periodical literature may well be available in English translation.* A complete list of the cover-to-cover English translations appears at the back of this issue.

THE INFLUENCE OF THE STRUCTURE OF THE DOUBLE LAYER ON THE POLAROGRAPHIC SURFACE OF CATALYTIC WAVES OF HYDROGEN

S. G. Mairanovskii, L. D. Klyukina, and Academician A. N. Frumkin

Electrochemistry Institute, Academy of Sciences, USSR
Translated from Doklady Akademii Nauk SSSR, Vol. 141, No. 1, pp. 147-150, November, 1961
Original article submitted July 1, 1961

In buffer solutions the charge of the proton donors (the acidic components) is always one unit higher than the charge of their conjugate bases, so that close to a negatively charged electrode surface the ratio of the concentration of acids to the concentration of the conjugate bases should be greater than the corresponding ratio in the mass of the solution [1]. Acids and bases in solution are present in protolytic equilibrium with one another, and the ratio between the concentrations of an acid and its conjugate base, outside the dependence on the presence of other acids and bases in solution, is determined by the magnitude of the dissociation constant of the given acid and the hydrogen ion concentration. An increase in the ratio of the concentrations of acid and base close to the cathode, corresponding to a shift in the protolytic equilibrium, may therefore be reflected in a decrease in the pH in the region next to the cathode, compared with the bulk of the solution.

The magnitude of the displacement of the pH under the influence of the electrode field reaches a maximum value at the surface of the electrode and decreases rapidly on going away from the electrode into the solution. Thus if we consider electrode processes with preceding chemical protonization of the depolarizer, it can readily be seen that the thinner the reaction layer in which the preceding protonization reaction takes place, the more strongly it is influenced by the field of the electrode [2]. The maximum action of the field should evidently be shown for protonization processes taking place at the electrode surface itself, with the participation of adsorbed substances, i.e., in the case of preceding "surface" reactions [3]. The increase in the hydrogen ion concentration at the electrode surface compared with that in the bulk of the solution depends on the magnitude of the potential drop in the diffusion section of the electrical double layer, usually described as the ψ_1-potential, and is determined by the expression [4]:

$$[H^+]_s = [H^+]_0 e^{-\psi_1 F/RT}, \quad (1)$$

where $[H^+]_s$ and $[H^+]_0$ are the concentrations of hydrogen ions at the electrode surface and in the bulk of the solution respectively.

In the present work we studied the influence of the concentration and nature of indifferent electrolytes, which change the magnitude of the ψ_1-potential, on the "surface" catalytic waves of hydrogen. The object of study was the second wave produced by quinine (or, more correctly, by its hydrogenated derivative [5]) in borate solutions with constant analytical boric acid concentration (0.04 M) at a constant pH of 9.5 (with the addition of LiOH, NaOH or KOH respectively) in the presence of different quantities of the chlorides of the alkali metals: Li, Na, K, Rb and Cs. The polarograms were recorded on a PE-312 recording polarograph in a cell with removable anode at 25° in a thermostat. The dropping electrode with forced removal of the drops had the following characteristics: m = 1.98 mg/sec, t = 0.28 sec. The curve for the supporting electrolyte was recorded for all the solutions studied, in order to introduce a correction for the residual current. Nitrogen was blown through the solutions to remove atmospheric oxygen. The experimental conditions in the present work, compared with those of [3], were chosen with the aim of increasing the proportion of the surface term in the over-all value of the catalytic current (higher pH values, lower concentrations of catalyst and electrolyte). The almost complete disappearance of the catalytic wave when the salt concentration was increased sufficiently indicates that the value of the exchange current is low under the experimental conditions used in this work.

The form of the surface catalytic waves can be expressed approximately by the combination of equations [6]:

$$E = E^{\circ}_{1/2} - \frac{RT}{\alpha F} \ln \frac{i^0}{i^0_{\lim} - i^0}; \quad (2)$$

$$i/i^0 = e^{-a\varphi}, \quad (3)$$

where Eq. (2) shows the relationship between the current i^0 which would pass if no catalyst desorption took place and the potential, while Eq. (3) takes account of the change in the current taking place as a result of the decrease in the quantity of adsorbed catalyst with increase in potential [7]. According to A. N. Frumkin [7], $a = (c - c') : 2RTT_{\infty}$, where c and c' are the integral capacities of the double layer in the absence of surface-active substance and with complete covering of the electrode surface by surface-active substance, respectively, and φ is the potential measured relative to the potential of maximum adsorption.

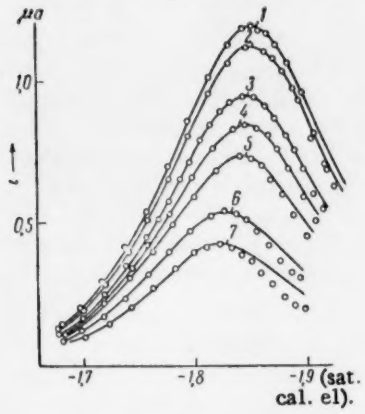

Fig. 1. Catalytic waves for quinine in borate buffer solution (pH 9.5) containing $3 \cdot 10^{-6}$ M quinine at different Na^+ concentrations: 1) 0.040; 2) 0.045; 3) 0.05; 4) 0.055; 5) 0.060; 6) 0.070; 7) 0.080 M.

Figure 1 gives as an example (the points) the values of the catalytic currents in $3 \cdot 10^{-6}$ M quinine solution in the presence of different quantities of sodium chloride; the curves were constructed from Eqs. (2) and (3). The data used in the construction of these curves are given in Table 1. The values of c for solutions of the salts NaCl and KCl were found by graphical integration of the differential capacity curves [8] with subsequent interpolation of the values obtained for the appropriate salt concentrations. All the values of c were taken for E = −1.85 v (sat. cal. el.) and in all cases the value of c' was taken as 5.0 $\mu f/cm^2$. Since the "surface" catalytic wave is irreversible [9], the values of $E^0_{1/2}$ became more positive by an amount equal to the change in the ψ_1-potential with increase in the concentration (see Table 1) [4].

Figure 1 shows that the height of the catalytic wave decreases with increase in the sodium ion concentration. For surface currents close to the limiting value we can write [6]

$$i^0_{\lim} = sF\rho_s\Gamma^0 \text{ and } i_{\lim} = sF\rho_s\Gamma, \quad (4)$$

where Γ^0 and Γ are the surface concentrations of adsorbed catalyst in the given solution at the potential of maximum adsorption and at the given potential respectively, and $\rho_s = k_1 [DH_1^+]_s + k_2 [DH_2^+]_s + \ldots$ is the overall rate constant for the protonization of the catalyst under the influence of different acids $[DH^+]$ in the solution.

TABLE 1. The Influence of the Concentration of NaCl and KCl on the Catalytic Waves in Quinine Solution

Total M + concn	NaCl					KCl			
	$-\psi_1$, mv, calc.	$i^0_{\lim}$, μa	i_{max}, μa	$E^0_{1/2}$ exp, v	a, v^{-2}	$i^0_{\lim}$, μa	i_{max}, μa	$E^0_{1/2}$ exp, v	a v^{-2}
0,040	157,6	106,0	1,18	1,85	8,5	154,0	1,52	1,81	9
0,045	154,4	92,8	1,10	1,845	8,5	121,5	1,38	1,80	9
0,050	151,8	76,8	0,93	1,84	8,55	107,5	1,22	1,80	9
0,055	149,3	69,7	0,83	1,84	8,6	—	—	—	—
0,060	147,2	61,3	0,73	1,835	8,6	70,0	0,88	1,79	9
0,070	142,7	42,5	0,535	1,83	8,7	50,2	0,608	1,79	9,1
0,080	139,5	35,1	0,43	1,83	8,8	—	—	—	—

Neglecting the proton-donating action of water compared with the action of H^+ and H_3BO_3, we can write:

$$\rho_s = k_{H^+} [H^+]_s + k_{BA} [H_3BO_3]_s = k [H^+]_s, \quad (5)$$

since the change in the effective $[H_3BO_3]_s$ is proportional to $[H^+]_s$ [10].

In the subsequent discussion we shall assume that k = const, neglecting the small salt effect (the change in the dissociation constants and reaction rate with change in the ionic strength of the solution).

From Eq. (4), taking account of Eqs. (1) and (5), we obtain

$$i^0_{\lim} \approx sFk\Gamma^0 [H^+]_0 e^{-\psi_1 F/RT}. \qquad (6)$$

Figure 2 gives the relationship between $i^0_{\lim}$ and $e^{-\psi_1 F/RT}$ for solutions containing Na^+ (1) and K^+ (2). The values of ψ_1 were calculated from the theory of the diffusion double layer with the assumption that the capacity of the Helmholtz layer is constant and equal to c = 18 $\mu f/cm^2$ [11].

The fact that the curve giving the relationship between $i^0_{\lim}$ and $e^{-\psi_1 F/RT}$ is linear (the straight lines 1 and 2) indicates that Eq. (6) is correct. The curves 1' and 2' in Fig. 2 show the change in the observed catalytic current at the maximum of the wave, i_{max}, as a function of $e^{-\psi_1 F/RT}$. It can be seen from Fig. 2 that i_{max} is not proportional to $e^{-\psi_1 F/RT}$. This was expected, since with increase in the concentration of the salts, as a result of the increase in the capacity c, there is an increase in the value of the coefficient a in Eq. (3), which indicates a more rapid decrease in the adsorbability of the catalyst with increase in the negative potential [7].

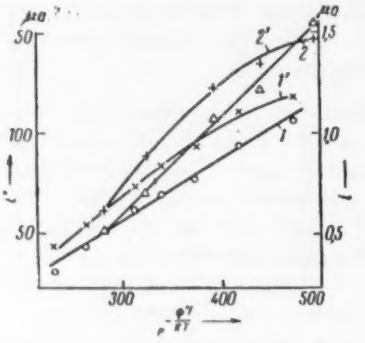

Fig. 2. Relationship between $i^0_{\lim}$ and $e^{-F\psi_1/RT}$ for the catalytic waves in solutions with different concentrations of: 1) Na^+ ($C_{quin} = 3 \cdot 10^{-6}$ M), 2) K^+ ($C_{quin} = 6 \cdot 10^{-6}$ M); 1', 2') the same for i_{max}.

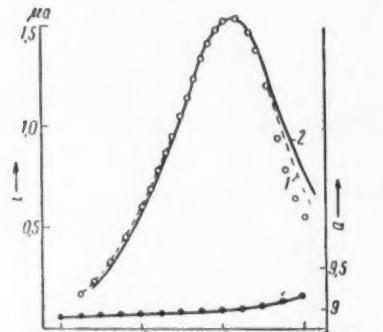

Fig. 3. Catalytic wave constructed with allowance for the change in a with potential. 2) Constructed on the assumption that a = const; the points mark the experimental values of the currents for $6 \cdot 10^{-6}$ M quinine solution in 0.04 N $K_2B_4O_7$. The lower curve gives the relationship between a and E.

The estimation of the influence of different factors on the change in i_{max} is only approximate, since i_{max} corresponds not to the limiting current $i^0_{\lim}$ but to the current on the rising section of the wave [3]. The current i_{max} is thus influenced not only by the rate of the forward reaction $\rho_s \Gamma$, but also to some extent by the rate of the back reaction $\rho_s \sigma_s \Gamma^+$ leading to deprotonization of the catalyst. With increase in the ionic strength of the solution, the constant for the equilibrium at the surface $\sigma_s = [BH]_s/[BH^+]_s = K_A/[H^+]_s$ increases, so that at potentials before $i^0_{\lim}$ has been reached (particularly in the region of i_{max}) there is an increase in the influence of the back reaction, leading to a greater decrease in i_{max} than in $i^0_{\lim}$. Thus the observed catalytic waves decrease with increase in the ionic strength of the solution both as a result of a decrease in the negative ψ_1-potential, leading to a decrease in the concentration of proton donors at the electrode, and also as a result of a decrease in the adsorbability of the catalyst.

A marked influence on the surface waves is also shown by the nature of the cation of the indifferent electrolyte. It has recently been shown [8, 12, 13] that the cations of alkali metals with large radii exhibit superequivalent adsorption on an electrode surface. This results in a decrease in the absolute magnitude of the ψ_1-potential and an increase in the capacity of the double layer in solutions of salts of the alkali metals from lithium to cesium [12, 13].

The influence of the nature of the cations can be seen from the data in Table 2. The change in the ψ_1-potential on going from Li^+ to K^+, in accordance with Eq. (6), leads to a decrease in $i^0_{\lim}$. On the other hand, increase in c and hence in a increases the curvature of the drop on the observed waves and decreases the value of their i_{max}. An even more marked decrease in the catalytic currents is shown when salts of Rb^+ and Cs^+ are introduced into the solution. Table 2 gives the results of experiments in which additional alkali metal salts were introduced into a 0.04 M solution of lithium borate (pH 9.5) at constant quinine concentration ($3 \cdot 10^{-6}$ M). The data in Table 2 show that the action of the salts on $i^0_{\lim}$ and i_{max} for the catalytic waves increases con-

TABLE 2. Comparison of the Influence of the Nature of the Cation of the Indifferent Electrolytic Waves for Quinine in 0.04 N $Li_2B_4O_7$

Added salt	Concn. of salt	$i^0_{lim.}$ μa	$i_{max.}$ μa, obs.	$E^0_{1/2}$, exp. v	$\overline{C}$, μf/cm²	a, v^{-2}
—	—	300	2,8	1,9	18,00	8,35
LiCl	$5 \cdot 10^{-3}$	278	2,6	1,9	18,00	8,35
LiCl	$1 \cdot 10^{-2}$	242	2,5	1,89	18,10	8,40
NaCl	$5 \cdot 10^{-3}$	248	2,55	1,87	18,25	8,50
NaCl	$1 \cdot 10^{-2}$	196	2,40	1,87	18,25	8,50
KCl	$5 \cdot 10^{-3}$	222	2,2	1,87	19,00	9,00
KCl	$1 \cdot 10^{-2}$	172	1,7	1,87	19,00	9,00
RbCl	$5 \cdot 10^{-3}$	183	1,64	1,86	19,8	9,5
CsCl	$1 \cdot 10^{-3}$	182	1,86	1,85	20,02	9,6
CsCl	$5 \cdot 10^{-3}$	27,7	0,4	1,80	20,02	9,6

siderably on going from Li^+ to Cs^+. Thus when the solution is brought to $1 \cdot 10^{-3}$ M with respect to CsCl the effect is greater than that for $1 \cdot 10^{-2}$ NaCl solution, and $5 \cdot 10^{-3}$ M RbCl solution has a much greater influence than $1 \cdot 10^{-2}$ M LiCl.

In the construction of the theoretical curves from Eqs. (2) and (3) (for example the curves in Fig. 1), since the calculations are tedious, it was assumed that a = const. In fact, as a result of the increase in c, particularly at potentials close to the range between − 1.9 and −2.0 v (sat. cal. el.), the value of a increases slightly with increase in the cathode potential (as a result of the increase in c). If account is taken of the change in a with potential (Curve 3 in Fig. 3), the theoretical curve shows better agreement with the experimental curve (see Fig. 3).

LITERATURE CITED

1. A. N. Frumkin, Zs. Phys. Chem. (A), 164, 121 (1933).
2. M. Breiter, M. Kleinerman, and P. Delahay, J. Am. Chem. Soc. 80, 5111 (1958); L. Gierst and H. Hurwitz, Zs. Elektrochem. 64, 36 (1960); Z. Grabowski and E. Bartel, Roczn. Chem. 34, 611 (1960); S. G. Mairanovskii, Ya. Koutetskii, and V. Ganush, ZhFKh (in the press).
3. S. G. Mairanovskii, DAN, 132, 1352 (1960).
4. A. N. Frumkin, V. S. Bagotskii, Z. A. Iofa, and B. N. Kabanov, The Kinetics of Electrode Process [in Russian] (Moscow, 1952), p. 176.
5. J. Bartek, M. Cernoch, and F. Sontavy, Coll. 19, 605 (1954).
6. S. G. Mairanovskii, DAN, 133, 162 (1960).
7. A. N. Frumkin, Tr. Fiz.-Khimich. Inst. im. Karpova, 5, 3 (1926).
8. B. B. Damaskin, Candidate's Thesis [in Russian] (Moscow, 1959); D. Grahame, J. Electrochem. Soc. 98, 344 (1951).
9. S. G. Mairanovskii, DAN, 120, 1294 (1958).
10. S. G. Mairanovskii, DAN (in the press).
11. V. S. Bagotskii, DAN, 58, 1387 (1947).
12. A. N. Frumkin, B. B. Damaskin, and N. V. Nikolaeva-Fedorovich, DAN, 115, 751 (1957).
13. B. B. Damaskin, N. V. Nikolaeva-Fedorovich, and A. N. Frumkin, DAN, 121, 129 (1958).

All abbreviations of periodicals in the above bibliography are letter-by-letter transliterations of the abbreviations as given in the original Russian journal. *Some or all of this periodical literature may well be available in English translation.* A complete list of the cover-to-cover English translations appears at the back of this issue.

THE RATE OF PROPAGATION OF THE FRONT OF AN EXOTHERMIC REACTION IN A CONDENSED PHASE

B. V. Novozhilov

Chemical Physics Institute, Academy of Sciences, USSR
(Presented by Academician V. N. Kondrat'ev, June 7, 1961)
Translated from Doklady Akademii Nauk SSSR, Vol. 141, No. 1,
pp. 151-153, November, 1961
Original article submitted June 1, 1961

Ya. B. Zel'dovich and D. A. Frank-Kamenetskii [1] have developed a theory for the thermal propagation of flame in gases. In the derivation of the approximate analytical formulae for the rate of propagation of the flame front, they made use of the similarity between diffusion and heat-transfer, i.e., the equality of the diffusion and temperature-conductivity coefficients. This condition made it possible to relate the concentration to the temperature and to reduce the system of two equations (diffusion and heat-conductivity) to one equation containing only temperature.

An analogous problem may arise in the examination of exothermic reactions in a condensed phase (for example polymerization reactions). Thus it is possible to formulate the problem of the stationary rate of the propagation front of an exothermic reaction in a condensed medium. In this case it is impossible to take the diffusion and temperature-conductivity coefficients as equal to one another, since they may differ from one another by several orders of magnitude. In the present work we will assume that the diffusion coefficient is equal to zero. We should emphasize that this case is not a particular case of the theory of Zel'dovich and Frank-Kamenetskii, for the equality of the diffusion and temperature-conductivity coefficients is an essential feature of their theory.

Let us consider the one-dimensional case. Let us assume that a substance with density ρ = const has a temperature T_0 at $x = -\infty$ and a temperature $T_1 = L/c + T_0$ at $x = \infty$, where L is the thermal effect of the reaction and c is the heat capacity. Let us solve this problem in a system of coordinates in which the reaction front is at rest. In this system the substance moves with a rate u, which we have to determine. In addition, let us introduce the symbols: $\varkappa = \lambda/\rho c$, the temperature-conductivity coefficient (λ is the thermal-conductivity coefficient); ρ_1 and ρ_2 are the densities of the original substance and the product ($\rho = \rho_1 + \rho_2$); $\eta = \rho_2/\rho$ is the relative concentration of the final product; and $f(T, \eta) = \partial\eta/\partial t$ is the rate of the chemical reaction.

The equations for the conservation of mass and energy have the form

$$\varkappa \frac{d^2T}{dx^2} - u\frac{dT}{dx} + \frac{L}{c} f = 0; \tag{1}$$

$$-u\frac{\partial\eta}{\partial x} + f = 0 \tag{2}$$

with boundary conditions $T(-\infty) = T_0$, $\eta(-\infty) = 0$, $T(\infty) = T_1$ and $\eta(\infty) = 1$.

Eliminating the rate of reaction from these equations and taking account of the boundary conditions for $x = -\infty$, we find

$$\varkappa \frac{dT}{dx} - u(T - T_0) + \frac{uL}{c}\eta = 0. \tag{3}$$

Since the rate of the reaction depends to a considerable extent on the temperature, the whole reaction will take place at temperatures close to T_1. Let us therefore put $T = T_1$ in the reaction zone, so that in this zone

$$\varkappa \frac{dT}{dx} = u\frac{L}{c}(1 - \eta). \tag{4}$$

This relationship replaces in our case the relationship between T and η in Zel'dovich and Frank-Kamenetskii's work. At one boundary of the reaction zone $dT/dx = 0$ and at the other

$$\left(\frac{dT}{dx}\right)^* = \frac{uL}{c\varkappa}. \tag{5}$$

By making use of Eq. (4), it is possible to express the concentration appearing in the reaction rate f in terms of the temperature gradient and to reduce the problem to one heat-conductivity equation. As in [1], the second term in this equation can be neglected, since the temperature changes only slightly in the reaction zone. Introducing the new variable $p(T) = dT/dx$, we reduce it to the first order equation

$$pp' + \frac{L}{c\varkappa} f(T, p) = 0. \tag{6}$$

Let us consider some particular cases.

1. A zero-order reaction: $f_0 = Z_0 \exp(-E/RT)$. Equation (6) has the solution

$$p^{*2} = -\frac{2LZ_0}{c\varkappa}\int_{T^*}^{T^*} \exp\left(-\frac{E}{RT}\right)dT,$$

where the quantities marked with an asterisk refer to the zone boundary. Usually $E \gg RT_1$, so that the integral is equal to $e^{-E/RT_1}RT_1^2/E$ (T^* can be put equal to zero). Substituting p^* from Eq. (5), we find the rate of the reaction front for the case of a zero-order chemical reaction to be

$$u_0 = \sqrt{\frac{2Z_0\varkappa c \exp(-E/RT_1)\, RT_1^2}{LE}} \tag{7}$$

which agrees with the rate of flame propagation found in [1]. This is understandable, since the presence or absence of diffusion should have no influence on the rate of a zero-order reaction.

2. A first-order reaction: $f_1 = Z_1 e^{-E/RT}(1 - \eta)$. Equation (6) is readily integrated and with account taken of Eq. (5) gives for the velocity of the front

$$u_1 = \sqrt{\frac{Z_1\varkappa c e^{-E/RT_1} RT_1^2}{LE}}, \tag{8}$$

which differs from u_0 only by a factor of $1/\sqrt{2}$.

3. Let us consider finally the case of an autocatalytic reaction:

$$f = Z_1 e^{-E_1/RT}(1 - \eta) + Z_2 e^{-E_2/RT}\eta\,(1 - \eta). \tag{9}$$

The first term in this expression corresponds to the "initiating" reaction, so that the most interesting case is that where $Z_1 e^{-E_1/RT} \ll Z_2 e^{-E_2/RT}$. Equation (6) reduces to the linear equation

$$p' - \frac{\varkappa c}{Lu^2} Z_2 \exp(-E_2/RT)\, p = -\frac{1}{u}\left[Z_1 \exp(-E_1/RT) + Z_2 \exp(-E_2/RT)\right],$$

solution of which gives

$$p^* = \frac{Z_2}{u}\exp\left[-\frac{\varkappa c Z_2}{Lu^2}\int_{T^*}^{T} \exp\left(-\frac{E_2}{RT}\right)dT\right] \times$$

$$\times \int_{T^*}^{T}\left[1 + \frac{Z_1}{Z_2}\exp\left(-\frac{E_1 - E_2}{RT}\right)\right]\exp\left(-\frac{E_2}{RT}\right)\exp\left[\frac{\varkappa c Z_2}{Lu^2}\int_{T}^{T_1}\exp\left(-\frac{E_2}{RT'}\right)dT'\right]dT. \tag{10}$$

Since two exponents are present ($\exp(-E_2/RT)$ increasing and $\exp\left[\frac{\varkappa c Z_2}{Lu^2}\int_T^{T_1}\exp\left(-\frac{E_2}{RT'}dT'\right)\right]$ decreasing with increase in T), the function under the integral will have a sharp maximum at a certain temperature T_m (which may coincide with T_1). Let us therefore remove the factor $1+\frac{Z_1}{Z_2}\exp\left(-\frac{E_1-E_2}{RT}\right)$ at the maximum point from under the integral sign. The remaining integral can then readily be calculated and after substitution of p^* we obtain a value for the velocity of the front:

$$u=\sqrt{\frac{Z_2\varkappa c\exp(-E_2/RT_1)RT_1^2}{LE\ln\left[1+\frac{Z_2}{Z_1}\exp\left(-\frac{E_2-E_1}{RT_m}\right)\right]}}. \tag{11}$$

Let us now find T_m. The maximum of the function under the integral is reached at the point where the quantity

$$-\frac{E_2}{RT}+\frac{Z_2\varkappa c}{Lu^2}\int_T^{T_1}\exp\left(-\frac{E_2}{RT'}\right)dT'.$$

is a maximum.

Equating the derivative of this to zero and substituting u from Eq. (11), we obtain an equation for T_m:

$$\frac{1}{T_m^2}=\frac{1}{T_1^2}\frac{\exp(-E_2/RT_m)}{\exp(-E_2/RT_1)}\ln\left[1+\frac{Z_2}{Z_1}\exp\left(-\frac{E_2-E_1}{RT_m}\right)\right].$$

Assuming $T_m=T_1$ everywhere, except in the exponent, we find

$$\frac{1}{T_m}=\frac{1}{T_1}+\frac{R}{E_2}\ln\ln\left[1+\frac{Z_2}{Z_1}\exp\left(-\frac{E_2-E_1}{RT_1}\right)\right].$$

Assuming that everywhere, except the exponent, $T_m<T_1$, i.e., when $1+\frac{Z_2}{Z_1}\exp\left(-\frac{E_2-E_1}{RT}\right)\geqslant e$. After substituting T_m in Eq. (11), we obtain finally

$$u=\left\{\frac{Z_2\varkappa c\exp(-E_2/RT_1)RT_1^2}{LE\ln\left\{1+\frac{Z_2}{Z_1}\exp\left(-\frac{E_2-E_1}{RT_1}\right)\left[\ln\left(1+\frac{Z_2}{Z_1}\exp\left(-\frac{E_2-E_1}{RT_1}\right)\right)\right]^{\frac{E_1}{E_2}-1}\right\}}\right\}^{1/2} \tag{13}$$

when $1+\frac{Z_2}{Z_1}\exp\left(-\frac{E_2-E_1}{RT_1}\right)\gg e$ and

$$u=\left\{\frac{Z_2\varkappa ce^{-E_2/RT_1}RT_1^2}{LE\ln\left[1+\frac{Z_2}{Z_1}\exp\left(-\frac{E_2-E_1}{RT_1}\right)\right]}\right\}^{1/2} \tag{14}$$

when $1+\frac{Z_2}{Z_1}\exp\left(-\frac{E_2-E_1}{RT_1}\right)\leqslant e$.

The expression (13) becomes zero as $Z_1\to 0$, as should in fact be the case, for without the "initiating" reaction the rate of the autocatalytic reaction is equal to zero. As $Z_2\to 0$, formula (14) becomes the expression for the velocity of the front for the case of a first-order reaction u_1.

I wish to thank G. B. Manelis for bringing this problem to our attention, and also A. S. Kompaneits and E. I. Andriankin for discussion of the work.

LITERATURE CITED

1. Ya. B. Zel'dovich and D. A. Frank-Kamenetskii, ZhFKh, 12, 100 (1938).

A STUDY OF THE THERMODYNAMIC PROPERTIES OF PLATINUM – LEAD ALLOYS

P. P. Otopkov, Corresponding Member, Academy of Sciences, USSR, Ya. I. Gerasimov, and A. M. Evseev

M. V. Lomonosov Moscow State University
Translated from Doklady Akademii Nauk SSSR, Vol. 141, No. 1, pp. 154-156, November, 1961
Original article submitted June 21, 1961

The thermodynamic functions of the Pt – Pb system have been studied in the range 700-875°. In this temperature range the phase diagram of the Pt – Pb system includes two intermetallic compounds PtPb and Pt_3Pb, a region of liquid solutions (L) in the lead concentration range from 1.0 to 0.65-0.47, and four heterogeneous regions: L + + PtPb, L + Pt_3Pb, Pt_3Pb + PtPb and Pt + Pt_3Pb [1]. We have determined the activity of lead in lead – platinum alloys by measuring the saturated vapor pressure (by Knudsen's effusion method). The apparatus and experimental procedure have been described in [2].

The alloys were prepared from 99.9% pure platinum and spectrally pure lead.

The activity a_i, determined by measuring the vapor pressure of one of the components of the alloy – lead, is related to the change in chemical potential by the equation:

$$\Delta\mu_i = RT \ln a_i = RT \ln \frac{p_i}{p_i^0},$$

where a_i is the activity of lead in the alloy, p_i the saturated vapor pressure of lead above the alloy, and p^0_i the saturated vapor pressure of pure lead at the same temperature.

TABLE 1. The Activity of Lead in Lead – Platinum Alloys

Atomic fraction of lead in the alloy, N_{Pb}	Activity of lead a_i	
	T = 973°K	T = 1063°K
1.0	1.0	1.0
0.921	0.891	0.891
0.832	0.776	0.741
0.734	0.550	0.389
0.545	0.347	0.148
0.514	0.347	0.148
0.385	0.049	0.135
0.193	0.006	0.016
0.113	0.006	0.016

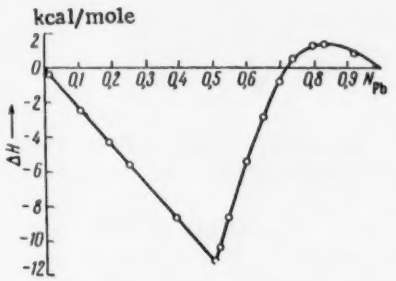

Fig. 1. The integral enthalpy of formation of lead – platinum alloys.

The rate of volatilization of lead from the alloy (the rate of volatilization, in accordance with the procedure which we have used, is proportional to the vapor pressure) was measured in the temperature range 700-875°; the activity of the lead in the alloys was calculated for the temperature range 700-790°. The data are given in Table 1.

The partial enthalpies and entropies of formation of the alloys were then found from the usual formulae and the integral enthalpies and entropies of formation of the alloys from the pure metals were found by graphical integration of the Duhem-Margules equation. The data on the integral values of the enthalpy and entropy for the central temperature of the range 700-790° were used to calculate the change in the free energy.

TABLE 2. Partial and Integral Thermodynamic Functions for Alloys of the Lead – Platinum System (in the range 973-1063°K)

Atomic fraction of lead in alloy, N_{Pb}	$\Delta\bar{H}_{Pb}$ kcal / mole	$\Delta\bar{S}_{Pb}$ cal / mole · deg	ΔH kcal / mole	ΔS cal / mole · deg	ΔG kcal / mole
1,00	0,00	0,00	0,00	0,00	0,00
0,921	0,20	0,22	1,00	1,60	—0,63
0,832	1,06	1,56	1,40	3,28	—1,94
0,800	2,02	2,71	1,36	3,50	—2,20
0,734	7,90	9,10	0,70	2,90	—2,25
0,700	9,73	11,30	— 0,90	2,10	—3,04
0,650	12,60	14,83	— 2,94	0,26	—3,20
0,600	16,28	18,55	— 5,36	—2,00	—3,32
0,545	19,48	21,70	— 8,53	—5,20	—3,23
0,514	19,48	21,70	—10,43	—7,03	—3,27
0,500	19,48	21,70	—11,30	—7,85	—3,31
0,385	—23,11	—17,50	— 8,67	—5,64	—2,93
0,250	—21,81	—12,06	— 5,47	—3,00	—2,41
0,193	—21,81	—12,06	— 4,20	—2,31	—1,85
0,113	—21,81	—12,06	— 2,40	—1,35	—1,03

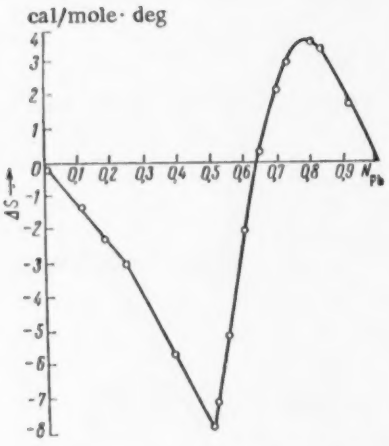

Fig. 2. The integral entropy of formation of lead – platinum alloys.

The temperature range 700-790° was chosen for the calculation of the thermodynamic properties because here it is convenient to calculate the heats and free energies of the reactions 3Pt + Pb = Pt_3Pb and Pt_3Pb + 2Pb = 3PtPb and hence the values for the formation of Pt_3Pb and PtPb from the metals in the ranges N_{Pb} = 0.00-0.25 and 0.25-0.50. The partial heats of dissolution of liquid lead in the melt are calculated in the same temperature range at N_{Pb} > 0.65. The values for melts in the concentration range N_{Pb} = 0.65-0.55 are not accurate, since here the temperature range studied includes the liquid curve.

The partial and integral thermodynamic functions are given in Table 2. The error in the determination of the activity of lead is approximately 1%, the error in the calculation of the enthalpy of formation of the alloys is ~ 20%, and the error for the entropy ~ 25%.

An interesting feature is that the integral enthalpies and entropies of formation of the alloy change sign at N_{Pb} = 0.65-0.70 (Figs. 1 and 2). This is evidently due to transition from the region of liquid solutions to the heterogeneous regions.

The more accurate calculation of the thermodynamic functions of the melt, particularly in the range from ~ 0.65 to 0.545 (atomic fractions of lead), more detailed study of melts in thse concentration ranges would be necessary. It might then be possible to extrapolate ΔH_{Pb} from the homogeneous region into the heterogeneous region and to establish these quantities close to the liquids curves.

It should however be emphasized that the aim of this work was to find ΔH and ΔS for the solid lead–platinum compounds.

LITERATURE CITED

1. M. Hansen and K. Anderko, Constitution of Binary Alloys, 4 (1958).
2. G. F. Voronin and A. M. Evseev, ZhFKh, 33, 2245 (1959).

STUDY OF THE SECONDARY STRUCTURES FORMED IN CAPRON FIBERS

K. Kh. Razikov, G. S. Markova, and Academician V. A. Kargin

L. Ya. Karpov Institute of Physical Chemistry
Translated from Doklady Akademii Nauk SSSR, Vol. 141, No. 1, pp. 157-160, November, 1961
Original article submitted June 12, 1961

It is known that the properties of fibers and of articles made from them can change substantially when put into use as the result of a number of processes taking place in the polymers themselves. One of these processes, leading to an impairment of the physicomechanical properties of fibers, is the formation of secondary structures. It is natural that in order to prevent or reduce the intensity of the progress of such phenomena it is necessary to know the mechanism of such processes. Despite the importance of this problem, the formation of secondary structures has received little study.

In the literature the processes of the crystallization of various polyamides from dilute solutions have been studied in the greatest detail and the formation of secondary structures was established [1, 2]. Various forms of secondary structures ranging from spherulitic formations to single crystals were formed when the crystallization was run slowly. It seems of great interest to study the conditions for the formation of secondary structures when the crystallization of polyamides is run in the condensed phase. The present paper is devoted to this problem.

Study Objects and Experimental Procedure

As study objects we took Capron monofilament (approximately 1 mm thick), stretched 5 fold. The use of such monofilament is convenient for the reason that the secondary structures, arising in various layers of the fiber, ranging from the surface to its center, can be followed in the transverse direction.

The annealing technique was used to effect the process of recrystallization in the fiber, in which connection measures were taken in advance to prevent shrinkage of the fiber and oxidation of the object during the heat treatment. The annealing was run at 205° (the melting point of Capron is 215°). The specimens were held at this temperature for 1-1.5 hr, and then cooled slowly to room temperature. The entire recrystallization process was accomplished in a matter of 10 hr.

The method of ultrathin sections was used to study the secondary structures formed in the recrystallization of the fiber. Sections from different regions of the fiber were obtained by the method developed by us, employing an ultramicrotome of the Sostrand Ultra-microtome LKB-Producter type. Sections were obtained from the recrystallized oriented Capron fibers, as well as from the starting unrecrystallized, but oriented monofilaments. In order to make sure that the structure of the cut specimens is not altered significantly in the cutting process, cuts were made with the cutting edge of the knife in different positions relative to the fiber axis. For example, the longitudinal sections were obtained in two ways: 1) the fiber axis was placed perpendicular to the knife edge, and here the knife moved parallel to the fiber axis; 2) the fiber axis was placed parallel to the knife edge, and here the knife cut the sample as from the side.

The ultrathin sections, having a thickness of about 200 A, were studied using a UEMB-100 electron microscope. From the obtained microphotographs it was established that the picture of the longitudinal sections, obtained by the two methods indicated above, was the same.

Experimental Data and Their Evaluation

In studying the sections of the starting oriented Capron fiber we found that apparently only small secondary structure formations are present in the oriented fiber. The coarse structure formations present in the Capron fiber are destroyed in the orientation of the latter.

The microphotograph of a longitudinal section from the surface layer of the fiber is shown in Fig 1a. Coarse spherulitic formations are formed during recrystallization; they do not have a spherical shape. In studying the cross sections of the surface layer of the fiber individual sheaves were found. This can serve as proof that flatter spherulites are formed in the surface layers of the recrystallized fiber. On the sections, obtained from the internal layers of the fiber, both longitudinally and in the transverse direction, more perfect crystalline formations can be seen. Micro-

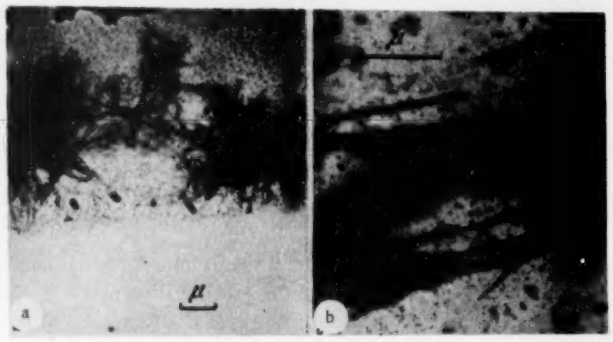

Fig. 1. a) Large flat spherulites of Capron from the longitudinal sections; b) elementary microfibrils, meeting in the cross sections of the fiber.

photographs of sections of recrystallized Capron fiber are shown in Figs. 1b, 2 and 3, from which it can be seen that various shapes of the secondary structures are formed via the elementary microfibrils. The microdiffraction data, obtained by us on these specimens, make it possible to postulate the following process: at first crystalline microfibrils are formed, the minimum dimensions of which reach about 100 A in width and several microns in length. Then a branching of the elementary microfibrils is observed, with the formation of individual sheaves and complex spherulitic structures clear down to the formation of individual, well-defined crystals. The dimensions of these secondary structures, even for the same shapes of the structure formations, can be different. The reactions, taking place between several growing crystalline centers, and the presence of all types of structure defects in the solid polymer specimen are probably the main reasons for the fact that the secondary structures, even for the same shape, have different dimensions.

In the recrystallization of the specimens we were also able to observe the formation of more complex structure formations, which have dimensions of tens of microns. Evidently, these secondary structures are formed as a result of the packing of the elementary crystalline microfibrils in a definite order. Microphotographs of the cross sections of such structure formations are shown in Fig. 2. Frequently lamellar crystals are observed in the cross sections of the recrystallized Capron fiber specimens (Fig. 3a), and at times these lamellar crystals combine with each other to form large crystalline aggregates. We believe that lamellar crystals are also formed via the crystalline microfibrils. In some cases we observed that disorderly arranged microfibrils are also found along with the lamellar crystals. Apparently, they are formed in the destruction of the lamellar crystals under the action of the knife in the cutting process. Clearly defined single crystals can be seen on the sections, obtained both in the longitudinal and the transverse directions of the oriented recrystallized fibers. In some cases we were able to discern aggregates composed of such crystals (Fig. 3b).

The fact that protruding microfibrils can be seen on many of the crystalline formations observed by us causes us to postulate that these crystals have a microfibrillar structure.

On the basis of a careful study of the section microphotographs of the oriented recrystallized fiber it was established by us that in the recrystallization there first occurs a very marked coarsening of the secondary structures when compared with those observed in the starting oriented fiber. Such a coarsening of the secondary structure formations is excellently confirmed by the literature data [3]. Second, new secondary structures of various shape are formed in the recrystallization of Capron fiber. Apparently, this is associated with the fact that they originate under different conditions than in solution, and specifically, in the condensed state. It is quite evident from the microphotographs that all of the shapes of the secondary structure formations have sharp boundaries, similar to the situation that exists for metal crystals. It is possible to assume that in the polymer disorderly, more friable regions are

distributed between the well-ordered crystalline formations. We were unable to detect a continuous transition of the crystalline formations to a friable disorderly region.

In our electron-microscope study of the shape of the secondary structures arising in the recrystallization of oriented Capron fiber, we established that all of the secondary structure formations are found in the crystalline regions of the investigated polymer. These regions have anisodiametric shapes, the diameters of which range from 1 to 10 μ.

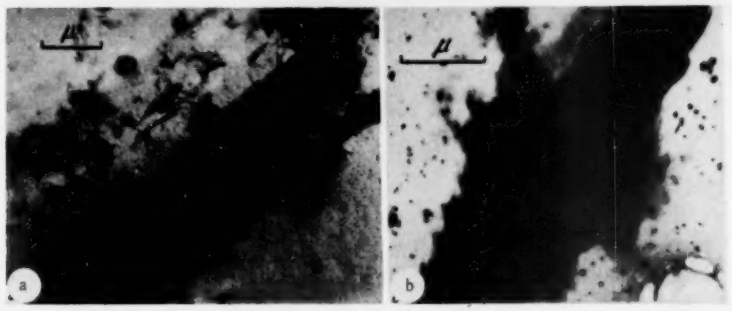

Fig. 2. Cross sections of Capron secondary structures, composed of microfibrils.

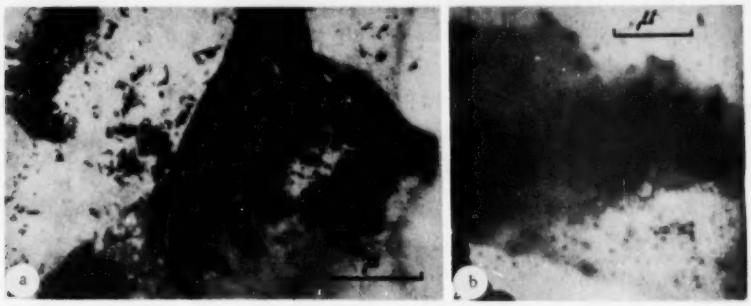

Fig. 3. Crystalline Capron formations from the cross sections. a) Lamellar crystals; b) aggregates of crystals.

The boundaries of these anisodiametric regions are clearly seen in the microphotographs. Evidently, the partially crystalline polymeric Capron fiber is composed of these regions of "macrofibrils." In the spaces between these crystalline macrofibrils are found friable disorderly regions – the amorphous phase of the polymer. These amorphous regions act like a binding – holding medium for the crystalline macrofibrils.

LITERATURE CITED

1. A. Keller, J. Polymers Sci. 36, 361 (1959).
2. P. H. Geil, J. Polymer. Sci. 44, 449 (1960).
3. W. O. Statton and P. H. Geil, J. Appl. Polymer Sci. 3, 9, 357 (1960).

ISOTOPE EFFECT IN THE RADIOLYSIS OF POLYETHYLENE

V. E. Skurat

Institute of Physical Chemistry, Academy of Sciences, USSR
(Presented by Academician V. N. Kondrat'ev, June 12, 1961)
Translated from Doklady Akademii Nauk SSSR, Vol. 141, No. 1,
pp. 161-164, November, 1961
Original article submitted June 6, 1961

As is known hydrogen is the principal gaseous product of the radiolysis of solid saturated hydrocarbons. For instance, when polyethylene is radiolyzed at dosages of 10-200 Mrad hydrogen constitutes 85-98% of the gaseous products [1]. A very large amount of work dealing with the radiochemical reactions of alkanes has been devoted to the study of the mechanism of hydrogen formation. From the comparison of the radiation yield of radicals (determined by the addition of I_2) with the radiation yield of hydrogen it was deduced that hydrogen is formed by two routes: a free radical and a molecular route, each one accounting for about half the generated hydrogen (see [2]). This was further confirmed in experiments where the yield of radicals produced by the stripping of hydrogen atoms from polyethylene [3] was determined together with the number of double bonds [1] formed by the elimination of a hydrogen molecule. Dorfman [4] was the first one to determine the yield of hydrogen formed by a molecular route in the radiolysis of $C_2H_6 + C_2D_6$ mixtures. Isotopic methods were also used by Newitt and Remsberg [5] and Dyne and Jenkinson [6] in the investigation of the liquid phase radiolysis of cyclohexane.

It was previously been assumed [4, 5] that the radiation yield of the H_2 formed by the molecular route from normal hydrocarbons differs very little from the yield of the D_2 formed in the radiolysis of deuterated hydrocarbons.

In the present work we measured the amount of H_2 and D_2 formed by the molecular route from polyethylene and deuteropolyethylene respectively.

The materials used in our work were: a high pressure form of polyethylene and deuteropolyethylene with a softening point of 126-127° and a 98 mole % D content. Mixtures of $(C_2H_4)_n$ and $(C_2D_4)_n$ were prepared by dissolving known amounts of each component in chemically pure toluene at temperatures near the boiling point and then precipitating the product by the addition of methyl alcohol to the solution. The precipitate was filtered out and thoroughly washed with methyl alcohol. It was then dried to a constant weight. Samples of the resulting loose white powder weighing 0.05-0.1 g were melted into copper crucibles 8 mm in diameter and placed into a segmented metal tube in which the mixture was exposed to 1.6 Mev electrons. The absorbed dosage was calculated from the electron current and the stopping power of polyethylene which is 1.92 Mev/g · cm^2 for $(C_2H_4)_n$ and 1.68 Mev/g · cm^2 for $(C_2D_4)_n$. We assumed that the fraction of energy absorbed by either $(C_2H_4)_n$ or $(C_2D_4)_n$ in the mixture is proportional to the respective fraction of electrons. The amount of gas formed in the radiolysis was measured by means of a U-shaped manometer filled with D-4 oil. The manometer was calibrated with a mercury manometer. At different instants in the course of radiolysis gas samples were removed and analyzed on a model MKh-1302 mass spectrometer. We used in our calculations the mass spectra of D_2 and HD reported in [7]. The concentration of HD in the samples tested was so large that we could neglect the H_3^+ ions formed in the mass spectrometer. Control experiments showed that as far as our work was concerned the isotopic exchange in the mass spectrometer was negligible.

In principle our method differed very little from that used by Dyne and Jenkinson. When mixtures of $(C_2H_4)_n$ and $(C_2D_4)_n$ are radiolyzed the amount of H_2 and D_2 formed by the molecular route is a linear function of the $(C_2H_4)_n$ and $(C_2D_4)_n$ concentrations (from now on we will denote these concentrations by C_H and C_D respectively.) On the other hand amounts of H_2 and D_2 formed by the radical route vary as the fourth power of C_H and C_D respectively. Hydrogen can be formed by the following reactions:

$$(C_2H_4)_n \rightsquigarrow H_2 + M_1 \quad G_1(H)$$
$$(C_2D_4)_n \rightsquigarrow D_2 + M_2 \quad G_1(D)$$
$$(C_2H_4)_n \rightsquigarrow H + R_1 \quad G_2(H)$$

$$H + (C_2H_4)_n \rightarrow H_2 + R_2 \quad k_1$$
$$(C_2D_4)_n \rightsquigarrow D + R_3 \quad G_2(D)$$
$$D + (C_2H_4)_n \rightarrow D_2 + R_4 \quad k_2$$
$$D + (C_2H_4)_n \rightarrow HD + R_5 \quad k_3$$
$$H + (C_2D_4)_n \rightarrow HD + R_6 \quad k_4$$

$G_1(H)$ and $G_1(D)$ are the radiation yields of the H_2 and D_2 formed by the molecular route; $G_2(H)$ and $G_2(D)$ are the radiation yields of H and D atoms; k_1, k_2, k_3, and k_4 are the rate constants for the reactions of hydrogen atoms with polyethylene in which hydrogen atoms are stripped. One can now determine the radiation yields of H_2, $G(H)_2$, and of D_2, $G(D_2)$, as a function of the $(C_2H_4)n$ and $(C_2D_4)n$ concentrations in the mixture. For a dilute solution of $(C_2H_4)n$ in $(C_2D_4)n$ we get

$$\frac{G(H_2)}{F_1} = G_1(H) + \frac{k_1}{k_4} G_2(H) F_1, \quad F_1 = \frac{C_H}{C_D}, \tag{A}$$

while for a similar solution of $(C_2D_4)n$ in $(C_2H_4)n$ we have

$$\frac{G(D_2)}{F_2} = G_1(D) + \frac{k_3}{k_3} G_2(D) F_2, \quad F_2 = \frac{C_D}{C_H}. \tag{B}$$

By setting up $G(H_2)/F_1$ as a function of F_1 and $G(D_2)/F_2$ as a function of F_2 in the radiolysis of solutions of the appropriate composition we will get $G_1(H)$ and $G_1(D)$.

In experiments where the molecular yields of H_2 and D_2 were determined at 30° mixtures were used in which $F_1 = 3.76$, 5.65, 8.86, 9.35, and $11.5 \cdot 10^{-2}$, and $F_2 = 1.58$, 5.97, 9.60, and $14.7 \cdot 10^{-2}$. In Fig. 1 we have plotted

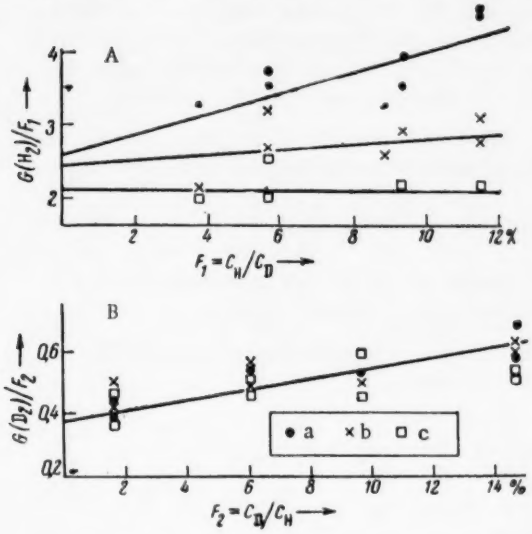

Fig. 1. A) $G(H_2)/F_1$ as a function of F_1 in a mixture of $(C_2H_4)n$ and $(C_2D_4)n$; B) $G(D_2)/F_2$ as a function of F_2 in a mixture of $(C_2H_4)n$ and $(C_2D_4)n$. a) $G(H_2)/F_1$ at a radiation dosage of 10 Mrad; b) 20 Mrad; c) 50 Mrad. G gives the number of molecules formed per 100 ev of energy absorbed.

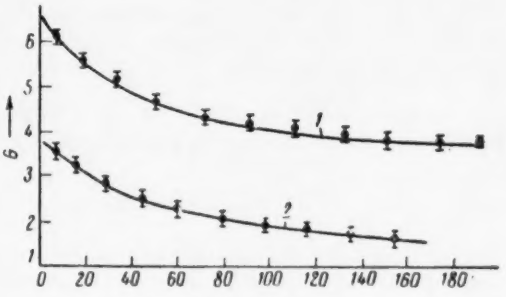

Fig. 2. The radiation yields $G(H_2)$ (1) and $G(D_2)$ (2) as a function of radiation dosage (in Mrad) in the radiolysis of pure polyethylene and deuteropolyethylene.

$G(H_2)/F_1$ versus F_1 and $G(D_2)/F_2$ versus F_2 for these mixtures. The plots show that $G_1(D) = 0.37 \pm 0.05$ and within the limits of experimental errors it is independent of the dosage in the range from 10-60 Mrad; $G_1(H) = 2.6 \pm 0.4$ at a dosage of 10 Mrad, $2.3 \pm \pm 0.4$ when the preliminary radiation dosage is 20 Mrad, and 2.1 ± 0.4 in cases where the sample was preexposed to 50 Mrad.

The values of $G_1(H)$ may turn out to be even smaller than the ones given above by about 10%, since the deuteropolyethylene used by us contained about 2 mole % H. The ratio of HD/D_2 in the hydrogen generated during the radiolysis of pure $(C_2D_4)n$ was 0.10. The radiation yields of H_2 and D_2 from pure $(C_2H_4)n$ and $(C_2D_4)n$ were 6.0 and 3.8 respectively so that one can calculate the frac-

tion formed by the molecular route. It turns out to be $10 \pm 1.5\%$ in the case of D_2 and $38 \pm 10\%$ in the case of H_2. The different slopes seen in Fig. 1 for different preliminary exposure to radiation can be attributed to the fact that groups able to act as a hydrogen trap (free radicals and olefins [1, 3]) accumulate in the polyethylene during the exposure then capture the subsequently generated hydrogen atoms and interfere with the formation of hydrogen gas. This is further confirmed by the fact that the yield of hydrogen produced by the radiolysis of pure polyethylene and deuteropolyethylene decreases with increasing radiation dosage (Fig. 2).

If we take into consideration the reactions of atomic hydrogen with free radicals and olefins the second term in Equations (A) and (B) will be changed to

$$G_2(H)F_1 \frac{k_1}{k_4 + k_r \frac{C_R}{C_D} + k_o \frac{C_o}{C_D}}$$

$$G_2(D)F_2 \frac{k_2}{k_3 + k'_r \frac{C_R}{C_H} + k'_o \frac{C_o}{C_H}}$$

where k_r, k_o, k'_r and k'_o are the respective rate constants for the reactions

$$H + R \rightarrow RH \quad k_r$$

$$H + \text{olefin} \rightarrow R \quad k_o$$

$$D + R \rightarrow RD \quad k'_r$$

$$D + \text{olefin} \rightarrow R' \quad k'_o$$

C_R and C_o are the concentrations of free radicals and olefins respectively. Hence as the dosage increases and the concentration of olefins and free radicals increases too the slopes of $G(H_2)/F_1 = f(F_1)$ and $G(D_2)/F_2 = f(F_2)$ should decline. One can see readily in Fig. 1 that the slope does indeed decline in the case of polyethylene when the radiation dosage is increased. In the case of deuteropolyethylene this relationship seems to be less evident.

If we know $G_1(H)$ and $G_1(D)$ and the radiation yields of H_2 and D_2 from pure $(C_2H_4)_n$ and $(C_2D_4)_n$ we can calculate the radiation yields of H_2 and D_2 formed by the radical route. At a radiation dosage of 10 Mrad these yields are

$$G_2(H) = 6{,}0 - 2{,}6 = 3{,}4, \quad G_2(D) = 3{,}8 - 0{,}37 = 3{,}43.$$

The values of $G_2(H)$ and $G_2(D)$ are in good agreement. Thus the isotopic effect observed in the formation of hydrogen by the radiolysis of polyethylene comes entirely from the molecular elimination reaction.

The author would like to thank V. L. Tal'roze for his valuable advice and discussion of results and N. Ya. Buben for several useful comments made during the reading of the manuscript.

LITERATURE CITED

1. A. A. Miller, E. J. Lawton, and J. S. Balwit, J. Phys. Chem. 60, 599 (1956).
2. M. Burton and J. Chang et al., Radiation Res. 8, 203 (1958).
3. A. T. Koritskii, Ya. N. Molin, et al. Vysokomol. Soed. 1, 8, 1182 (1959).
4. L. M. Dorfman, J. Phys. Chem. 60, 826 (1956); 62, 29 (1958).
5. T. D. Newitt and L. P. Rembsberg, J. Phys. Chem. 64, 969 (1960).
6. P. J. Dyne and W. M. Jenkinson, Canad. J. Chem. 38, 539 (1960).
7. F. L. Mohler and V. H. Dibeler et al., Phys. Rev. 79, 223 (1950).

METASTABLE SOLUTIONS OF CALCIUM SILICATES

Chou P'ing-i, O. I. Luk'yanova, and E. E. Segalova

M. V. Lomonosov Moscow State University
(Presented by Academician P. A. Rebinder, June 1, 1961)
Translated from Doklady Akademii Nauk SSSR, Vol. 141, No. 1,
pp. 165-167, November, 1961
Original article submitted May 20, 1961

Classical physico-chemical investigations of the $CaO + SiO_2 + H_2O$ system and the anhydrous calcium silicates β-Ca_2SiO_4(β-C_2S) and Ca_3SiO_5(C_3S)[1-5] have left unexplained the formation and properties of the metastable solutions formed as intermediates in the reaction of these compounds with water.

Work done by P. A. Rebinder and co-workers [6-9] revealed that the hardening of inorganic cements is proceeded by the formation of a crystalline dispersion which forms and grows in a medium supersaturated with respect to the hydrated derivatives of the anhydrous cement. These processes will greatly depend on how much and how fast do the concentrations of the supersaturated solutions change. In this work we have investigated the formation of supersaturated solutions during the hydration of β-C_2S and C_3S and determined the connection between the metastable solubility of these silicates and the concentration of $Ca(OH)_2$, which precipitates during the hydration. Concentration changes in the aqueous phase were followed during the hydration of silicates by measuring the concentration of Ca^{++} and silicate ions (expressed as SiO_2 by convention) directly in vigorously stirred dilute suspensions (0.04-2.0% silicate) free of atmospheric CO_2. Anhydrous silicates were prepared at 1500° from chemically pure oxides; the two subsilicates contained 96° β-C_2S and 90% C_3S respectively plus other lower subsilicates while free CaO was absent entirely. SiO_2 was determined colorimetrically in the form of the blue silico-molybdate complex while Ca was determined complexometrically.

By following changes in the composition of the aqueous phase during the hydration of calcium silicates at 20 and 30° (β-C_2S in Fig. 1a, and C_3S in Fig. 1b) we found that the silicate ion concentration passes through a maximum; the more concentrated the suspension and the more disperse the original anhydrous silicate the sooner is the maximum attained, and other conditions being equal it is also observed sooner in C_3S solutions than in solutions of β-C_2S. The concentration of SiO_2 declines to practically zero in the same order. At the same time Ca^{++} concentration keeps increasing reaching a value of 8-10 mmoles/liter after SiO_2 has almost completely disappeared from solution.

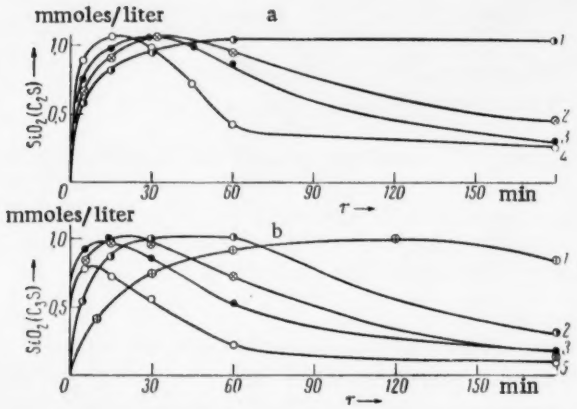

Fig. 1. The rate of formation of supersaturated solutions of calcium silicates. a) β-C_2S (30°): 1) 0.08; 2) 0.2; 3) 0.4; 4) 0.8 % silicate. b) C_3S (20°): 1) 0.04; 2) 0.08; 3) 0.2; 4) 0.4% silicate.

The maximum concentration of SiO_2 (C_m) or the equivalent silicate concentration in solution can be considered invariant only as a first approximation, and in contrast with the nonhydrolyzable cements, particularly gypsum, the suspensions last for very brief periods of time. The apparent inability to sustain a highly supersaturated solution for any appreciable length of time particularly noticeable, even in dilute suspensions, when the concentration of anhydrous silicate is increased may lead to an erroneous conclusion that supersaturation does not play an important role in the structure formation in calcium silicates. As we are about to demonstrate, the unusual behavior can be explained by examining the relationship between the solubility of silicates and the concentration of $Ca(OH)_2$, which is formed during the hydrolysis. For the same reason the indirectly determined solubility of β-C_2S and C_3S in water [10] can not be achieved

under the conditions normally prevailing during the hardening of silicates. One can safely assume that the solubility, just like the equilibrium solubility of hydrosilicates, decreases with increasing concentration of the $Ca(OH)_2$ (which eventually precipitates) formed when anhydrous silicates are hydrolyzed.

A comparison of the Ca and SiO_2 concentrations in the aqueous phase of the β-C_2S and C_3S suspensions reveals that when C_{max} is attained the solution already contains $Ca(OH)_2$ in excess of the stoichiometric concentration. Thus by the time we reach C_{max} = 1.05 mmoles/liter in the β-C_2S system at 30° and 1.07 mmoles/liter in the C_3S system the CaO/SiO_2 ratio in solution has increased from 2 to 3 and from 3 to 3.8 respectively.

Hence the C_{max} concentrations determined by us represent $Ca(OH)_2$ solutions of a certain concentration different in the case of β-C_2S and C_3S. It would consequently be interesting to represent the results obtained in the form $SiO_2 = f(CaO)$ which was used in the investigation of the $CaO + SiO_2 + H_2O$ system. In Fig. 2 where we have plotted this function for β-C_2S at 30° we can distinguish three sections representing the three stages in the formation of supersaturated calcium silicate solutions. The left side of the graph represents the solution of anhydrous silicates, and since the crystal dissolving is ionic the process simply involves a transfer of the constituent ions into solution in the stoichiometric ratio, but as the compounds are unstable in the presence of water a supersaturated solution results. The dotted line gives the molar ratio in solution corresponding to the composition of the anhydrous silicate.

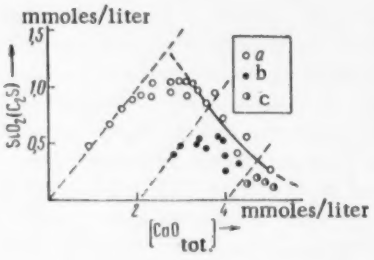

Fig. 2. A phase diagram representing the formation of a supersaturated solution of β-C_2S: a) Water suspension; b) in a solution containing 2 mmoles/liter of $Ca(OH)_2$; c) similar solution but with a concentration of 4 mmoles/liter.

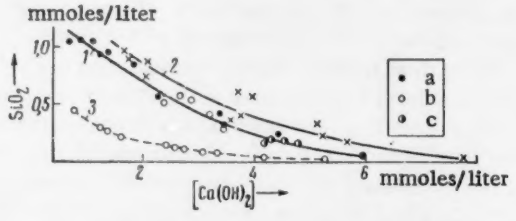

Fig. 3. The metastable solubility of calcium silicates as a function of the $Ca(OH)_2$ concentration in solution when either the latter is precipitated during hydrolysis or is introduced as a suspension (30°). 1) β-C_2S: a) hydrolysis accompanied by precipitation of $Ca(OH)_2$; b) 2 mmoles/liter; c) 4 mmoles/liter of additional $Ca(OH)_2$ introduced into the suspension. 2) C_3S: 3) equilibrium solubility of the hydrosilicate [11].

Superimposed on the solution process is the crystallization of low subsilicates which shows up in the deviation of experimental points from a straight line due to a change in the molar ratio of CaO/SiO_2 in solution. When SiO_4^{4-} goes into solution and is hydrolyzed it reduces the CaO/SiO_2 ratio in the hydroxysilicate precipitate below the ratio in the original anhydrous silicate leaving behind (in the solution) an excess of $Ca(OH)_2$. The same solid hydrate, monocalcium hydrosilicate, forms in both the β-C_2S and the C_3S system; this is in full accord with the literature data.

On the right side of Fig. 2 we can see how the SiO_2 concentration (silicates) decreases when the total CaO concentration in solution is increased. This portion of the curve is independent of the suspension concentration. But the addition of more $Ca(OH)_2$ to the suspension reduces C_{max} and subsequent SiO_2 concentrations to a greater extent than would be expected from the established relationship between the SiO_2 concentration and the total calcium concentration in solution.

The relationship between the excess Ca and the SiO_2 concentration can be conveniently represented with reference to the stoichiometric ratio for a given silicate, or, which amounts to the same thing, with reference to the amount of $Ca(OH)_2$ which had precipitated as a result of hydrolysis. When plotted in this form (Fig. 3) the curves are independent of the β-C_2S and C_3S concentrations in suspension (within the limits of experimental errors) and of the initial $Ca(OH)_2$ concentration in solution (curve 1): they express the effect of the $Ca(OH)_2$ concentration on

the concentration of the metastable solutions of anhydrous silicates which are formed during the hydrolysis after the C_{max} has been passed. Hydrolysis of silicates with the resulting precipitation of monocalcium hydrosilicate and accumulation of $Ca(OH)_2$ begins before the metastable solution is achieved. Therefore under normal conditions of calcium silicate hydrolysis the metastable solubility is always smaller than solubility in pure water.

When the metastable solubility of the silicates (C) is compared with the equilibrium solubility (C_0) at the same $Ca(OH)_2$ concentration (Fig. 3, 3 based on the data of Roller and Ervin [11]) the ratio of C/C_0 remains constant to a first approximation; this is particularly evident in the case of β-C_2S over the entire range of $Ca(OH)_2$ concentrations at which the SiO_2 concentrations could be determined. This ratio (4.4 in β-C_2S) can be regarded as a measure of the relative supersaturation, which remains constant due to the fact that the metastable and the equilibrium solubilities of SiO_2 (silicates) seem to depend in the same way on the excess $Ca(OH)_2$.

Thus the experimentally observed decline in the concentration of the supersaturated solutions of β-C_2S and C_3S after C_{max} is passed (in the course of hydrolysis) is still no indication that the relative supersaturation in the aqueous phase of the suspension has decreased, but simply reflects the dependence of metastable solubility on the $Ca(OH)_2$ concentration.

The discovery that the concentration of supersaturated solutions is independent of the suspension concentration as well as the fact that monocalcium hydrosilicate is isomorphous with the lower subsilicates formed in the hydrolysis of concentrated suspensions (gels) would indicate that the laws found to operate in our experiments should also hold in concentrated suspensions.

LITERATURE CITED

1. H. Steinour, Chem. Rev. 40, 391 (1947).
2. E. Flint and L. Wells, J. Res. Nat. Bur. Stand. 12, 751 (1934).
3. K. G. Krasil'nikov, Trans. Confer. on the Chemistry of Cement [in Russian] (Moscow, 1956).
4. T. Torvaldson and V. Vigfusson, Trans. Roy. Soc. Canad. 22, 3, 423 (1928).
5. H. F. W. Taylor, J. Chem. Soc. 12, 3682 (1950).
6. P. A. Rebinder, E. E. Segalova, and V. N. Izmailova, DAN, 110, 5 (1956).
7. P. A. Rebinder and E. E. Segalova, Stroit. Mater. 1 (1960).
8. E. S. Solov'eva and E. E. Segalova, Coll. Zhurn. 20, 5 (1958).
9. E. E. Segalova, Z. N. Markina, and P. A. Rebinder, DAN, 133, 3 (1960).
10. B. V. Ratinov, DAN, 136, 4 (1961).
11. P. S. Roller and G. Ervin, J. Am. Chem. Soc. 62, 461 (1940).

All abbreviations of periodicals in the above bibliography are letter-by-letter transliterations of the abbreviations as given in the original Russian journal. *Some or all of this periodical literature may well be available in English translation.* A complete list of the cover-to-cover English translations appears at the back of this issue.

THE VIBRATION SPECTRA OF CERTAIN ALKYL- AND ALKYLALKENYL STANNANES (Sn^{IV})

N. A. Chumaevskii

Institute of Heteroorganic Compounds, Academy of Sciences, USSR
(Presented by Academician I. V. Obreimov, June 1, 1961)
Translated from Doklady Akademii Nauk SSSR, Vol. 141, No. 1, pp. 168-171, November, 1961
Original article submitted May 27, 1961

The work presented here deals with the vibration spectra of several alkyl- and alkylalkenyl derivatives of tin.

The infrared absorption spectra were recorded in the following manner. In the 3000 cm^{-1} region a VIKS M-3 infrared spectrophotometer with a LiF prism ($\Delta\nu$ = 6 cm^{-1}) was used. In the 700-2000 cm^{-1} region the same spectrophotometer was used but with a NaCl prism (in the 1000 cm^{-1} region $\Delta\nu$ = 10 cm^{-1}). In the 400-700 cm^{-1} region an IKS-14 infrared spectrophotometer with a KBr prism ($\Delta\nu$ = 4 cm^{-1}) was used. When LiF and NaCl optics were used the samples were placed in cells of a fixed size (0.05 mm thick) with NaCl windows; certain compounds were also examined in the form of thin layers of undetermined thickness between two tightly pressed NaCl windows. When KBr optics were used the compounds were contained in a cell with KBr windows (the layer was 0.020 mm thick).

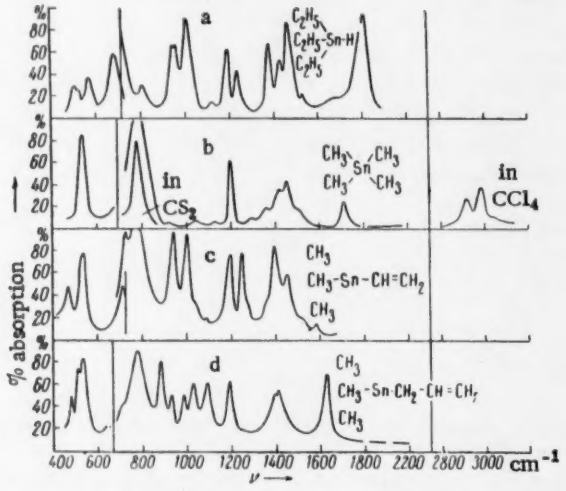

Fig. 1. The absorption spectra of: a) Triethylstannane; b) tetramethylstannane; c) trimethylvinylstannane; d) trimethylallylstannane. Each spectrum is subdivided into three parts: KBr optics on the left side, NaCl in the middle, and LiF on the right. All the spectra are represented on the same frequency scale.

The Raman spectra were recorded on a three-prism model ISP-51 glass spectrograph to which an FEP-1 photoelectric recorder was attached. The 4358.3 A line of Hg passed through a blue filter provided the excitation radiation.

It is already known that the stretching frequencies of the Si – H and Ge – H bonds lie at 2125 cm^{-1} and 2010 cm^{-1} respectively (in $(C_2H_5)_3SiH$ and $(C_2H_5)_3GeH$ [1,2]). The Sn – H stretching frequency in triethylstannane $(C_2H_5)_3SnH$ lies, however, at 1820 cm^{-1} (Fig. 1). Hence one can see that the frequency of the M – H stretching

The Stretching Frequencies for the Sn – Bonds

Td symmetry group		C_3v symmetry group			C_2v symmetry group
$(CH_3)_4Sn$	$(C_2H_5)_4Sn$	$(CH_3)_3Sn(CH{=}CH_2)$	$(CH_3)_3Sn(CH_2{-}CH{=}CH_2)$	$(C_2H_5)_3Sn(CH_2{-}CH{=}CH_2)$	$(C_2H_5)_2Sn(CH{=}CH_2)_2$
528 (I.R.) (F) 525 (Raman) (F)	503 (I. R.) (F) 500(Raman)(F)	527 (E) 512 ? (A) } $Sn(CH_3)_2$	527 (E) 512 (A) } $Sn(CH_3)_2$	517 (E) 495 (A) } $Sn(C_2H_5)_2$	518 (A) 495 (β) } $Sn(C_2H_5)_2$
500 (Raman) (A)	475(Raman)(A)	462 (A) { $Sn{-}CH{=}CH_2$	480 (A) { $Sn{-}CH_2{-}CH{=}CH_2$	478 (A) { $Sn{-}CH_2CH{=}CH_2$	476 (A) 462 (β) } $Sn(CH{=}CH_2)_2$

Note: F represents triply degenerate while E represents doubly degenerate frequencies; A represents symmetrical vibrations.

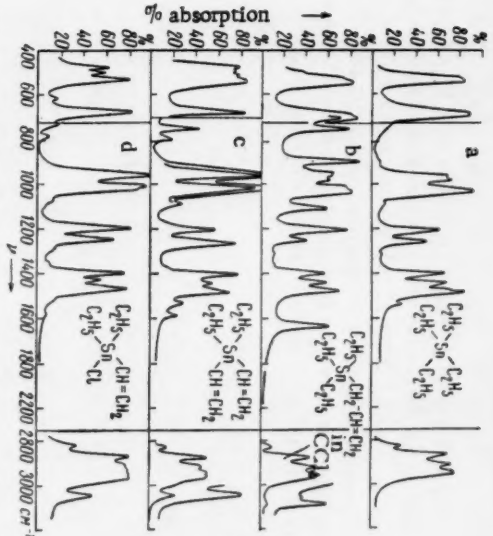

Fig. 2. The absorption spectra of: a) Tetraethylstannane; b) triethylallylstannane; c) diethyldivinylstannane; d) diethylvinylchlorostannane. The rest of the legeng is the same as in Fig. 1.

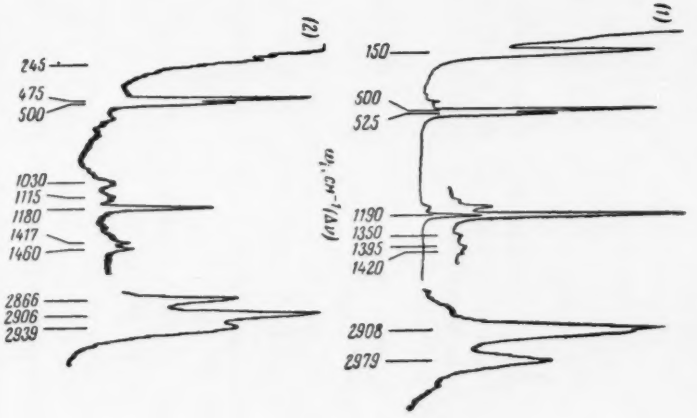

Fig. 3. The Raman spectra of: 1) Tetramethylstannane; 2) tetraethylstannane. The spectrum on the right (in the 3000 cm^{-1} region) was recorded at a slower rate than the one in the region below 1460 cm^{-1}.

vibration decreases from 2900 cm^{-1} (for a $-\overset{|}{\underset{|}{C}}-H$ group) to 1820 cm^{-1} in the order M = C, Si, Ge, Sn. The force constant of the M – H bond decreases as one proceeds from C to Sn (the effect of the atomic mass M is negligible). Thus for example the force constant in CH_4 (expressed in the usual units [3, 4]) $K_{q(C-H)}$) 8.34 · 10^6 cm^{-2} [3] while in SiH_4 $K_{q(Si-H)} = 4.67 \cdot 10^6$ cm^{-2} [4]; as one can see K_q in silane is half as large as in methane. Using standard equations [3] and assuming that the angular coefficients and interaction coefficients for the Ge – H and Sn – H bonds are not very different from what they are in the case of Si – H we find that $K_{q(Ge-H)} \approx 4.3 \cdot 10^6$ cm^{-2} while $K_{q(Sn-H)} \approx 3.8 \cdot 10^6$ cm^{-2} (in molecules of the type MH_4).

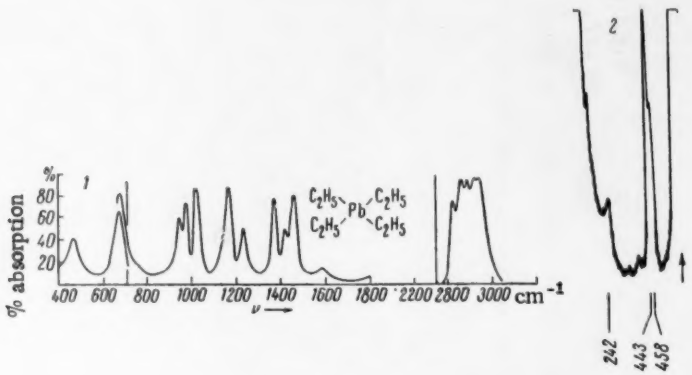

Fig. 4. 1) The absorption spectrum of tetraethyllead (the legend is otherwise the same as in Fig. 1); 2) the Raman spectrum of $Pb(C_2H_5)_4$. The sharp rise on the curve indicated by the arrow shows where the compound begins to decompose while the spectrum is being taken.

The absorption and scattering frequencies connected with the Sn – Alk groups (vibrations involving a change in the H – C – Sn bond angle) in Sn – CH_3 fall at 1190-1195 cm^{-1} (Fig. 1) and at 1183-1190 cm^{-1} in Sn-C_2H_5 (Fig. 2). The corresponding absorption band in $Pb(C_2H_5)_4$ falls at 1158 cm^{-1} (Fig. 4) (the Pb – CH_3 group in $Pb(CH_3)_4$ has the band at 1170 cm^{-1} [5]).

The C = C bonds in the vinyl and allyl derivatives absorb at 1580 cm^{-1} [in $(C_2H_5)_2Sn(CH=CH_2)_2$ for example] and 1628 cm^{-1} [in $(CH_3)_3SnCH_2 - CH = CH_2$ and $(C_2H_5)_3SnCH_2 - Ch = CH_2$] respectively (Figs. 1 and 2).

The absorption bands for the stretching vibrations of terminal methylene groups = CH_2 falls at ν_{as} = 3045-3050 cm^{-1} in the vinyl derivatives and ν_{as} = 3080 cm^{-1} in the allyl derivatives (Figs. 1 and 2).

The frequencies for the absorption and scattering of light by Sn – C bonds in individual molecules are listed in table (see also the figures).

The $Sn(C_2H_5)_2$ group in diethylvinylchlorostannane has a ν_{Sn-C} = 526 cm^{-1} and 495 cm^{-1} while the Sn – CH = = CH_2 has the band at 471 cm^{-1} (Fig. 2).

In the case of tetraethyllead the Raman spectrum yields bands at ν_{Pb-C} = 443 cm^{-1} (type A) and 458 cm^{-1} (type F) while the IR spectrum exhibits a band at 460 cm^{-1} (type F); or in other words the skeletal vibrations occur at lower frequencies than in the case of tetraethyltin (Figs. 2, 3, 4).

It is obvious that the IR absorption bands and Raman lines representing the Sn – C stretching vibrations generally fall in the 450-530 cm^{-1} region; in organic derivatives of germanium the stretching frequencies for the Ge – C bond lie in the 500-650 cm^{-1} region [2].

The author would like to express his gratitude to I. V. Obreimov for his interest in this work and valuable comments and also thank V. F. Mironov for kindly providing the compounds.

LITERATURE CITED

1. N. A. Chumaevskii, Optika i Spektroskopiya, 10, 69 (1961).

2. M. V. Volkenshtein, M. A. El'yashevich, and B. I. Stepanov, Molecular Vibrations [in Russian] (1949), Vol. 1.
3. I. F. Kovalev, Papers Delivered at the 10th All-Union Conference on Spectroscopy [in Russian] (Lvov, 1957), Vol. 1, 1957, p. 304.
4. C. W. Joung, J. S. Koehler, and D. S. McKinney, J. Am. Chem. Soc. 69, 1410 (1947).

All abbreviations of periodicals in the above bibliography are letter-by-letter transliterations of the abbreviations as given in the original Russian journal. *Some or all of this periodical literature may well be available in English translation.* A complete list of the cover-to-cover English translations appears at the back of this issue.

THERMODYNAMIC PROPERTIES OF Ag – Bi MELTS

A. A. Vecher and Corresponding Member of the Academy of Sciences, USSR, Ya. I Gerasimov

M. V. Lomonosov Moscow State University
Translated from Doklady Akademii Nauk SSSR, Vol. 141, No. 2, pp. 381-383, November, 1961
Original article submitted June 28, 1961

From a study of the electro-motive forces (EMF) of the galvanic elements:

$$Ag/Ag^{+} \text{ in melt AgI + NaI + KI } Ag-Bi \text{ alloy.}$$

As a function of the temperature (650-850°C) and the composition of the alloys, we determine the thermodynamic properties of the system Ag – Bi in the liquid state at 1000°K. The technique of conducting the experiment has been described previously [1]. The silver used to prepare the alloys was made from "pure" grade Ag_2O by thermal decomposition, and the bismuth was made from analytically pure Bi_2O_3 by hydrogen reduction. The majority of the alloys were analyzed after the experiments, and, as may be seen from Table 1, during the course of the experiment the composition of the alloys remain practically unchanged. We did not observe any indications of electro-

TABLE 1. Experimental Data on Ag – Bi Alloys at 1000°K

X_{Ag} assumed	X_{Ag} found	E, millivolts	dE/dT, millivolts/100°C	a^{*}_{Ag}	$\Delta\bar{H}^{*}_{Ag}$, kcal g·atom	$\Delta\bar{S}^{*}_{Ag}$, electropy units/g·atm	Temperature of liquid phase, °C		
							our data		refs [4, 5]
							neglecting solubility of Bi in Ag	including solubility of Bi in Ag	
0,097	0,092	135,9	36,5	0,207	5,28	8,42	355	357	293
0,207	—	93,2	28,6	0,339	4,59	6,60	401	405	359
0,323	0,309	66,2	22,8	0,464	3,74	5,26	437	443	388
0,454	—	47,8	18,2	0,574	3,09	4,20	464	473	423
0,564	0,558	35,5	16,0	0,662	2,86	3,69	505	518	450
0,682	0,679	20,3	12,7	0,790	2,47	2,93	567	586	521
0,781	—	6,4	11,2	0,928	2,44	2,58	670	689	669

* Standard state – solid silver.

chemical interaction between the alloy and the electrolyte, and the reproducibility of the EMF values was not less than 0.5%. Our experimental data is given in Table 1, and the thermodynamic quantities, calculated in the usual way, for the formation of alloys from liquid components are given in Table 2 and in Figs. 1 and 2.

The phase diagram of the system Ag – Bi is a simple eutectic with very narrow solid solution regions [3]. Over a wide range of compositions practically pure silver is deposited from the alloys on cooling, and this makes it possible to find the temperature of the liquid phase corresponding with the alloys immediately, by extrapolating the data on the EMF as a function of temperature to zero EMF. As may be seen from Table 1, good agreement with the data in the literature [4, 5] occurs only at high temperatures. If we take account of the fact that what is deposited is a

TABLE 2. Energy Changes of Two Liquid Ag – Bi Alloys at 1000°K*

x_{Ag}	a_{Ag}	a_{Bi}	ΔZ^{exc} cal g·at	ΔH kcal g·at	ΔS^{exc} entropy units g·at	x_{Ag}	a_{Ag}	a_{Bi}	ΔZ^{exc} cal g·at	ΔH kcal g·at	ΔS^{exc} entropy units g·at
0,1	0,164	0,909	+116	+0,30	+0,18	0,5	0,479	0,619	+168	+0,65	+0,47
0,2	0,258	0,844	+186	+0,52	+0,33	0,6	0,535	0,540	+101	+0,55	+0,44
0,3	0,341	0,769	+207	+0,65	+0,43	0,7	0,624	0,402	+15	+0,39	+0,35
0,4	0,417	0,691	+174	+0,69	+0,47	0,8	0,745	0,233	−52	+0,18	+0,22
						0,9	0,87	0,1	−20	+0,05	+0,1

* Standard state – liquid components; expressed in terms of [2] the values taken were melting point of silver 1234°K, heat of fusion 2.69 kcal/g-atom.

TABLE 3. Enthalpy of Formation (Fig. 2) [2] and Electrode Potential [8] of Halides of Bi and Ag

Cation	Cl^{1-}	Br^{1-}	I^{1-}
Ag^{1+}	30,5±0,1 +2,33	23,70±0,1 +2,11	15,34±0,1 +1,75
Bi^{3+}	30,2±0,7 +2,23	19,3+2,7 +2,15	8,0±1,75 +2,08

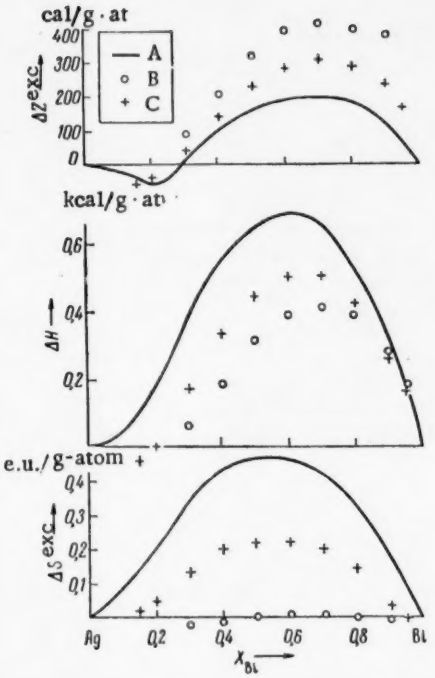

Fig. 1. Energy changes of the system Ag–Bi at 1000°K. A) Our data, obtained in iodide electrolyte; B) data of [6], obtained in chloride electrolyte; C) data of [7], obtained in bromide electrolyte.

solid solution of bismuth and silver, this does not help matters, since in this case (see Table 1), the calculated temperature of the liquid phase is even higher. The values of the solubility of Bi and solid Ag were taken from [3]). It is probable that at the lower temperature there is a change in the entropy of mixing of the alloys, from a change in coordination number, and the relation between EMF and temperature ceases to be linear. This phenomenon requires further study.

There is data in the literature on the EMF of Ag – Bi melts, but in contrast with our work, the electrolytes used were melts of chlorides of lithium and potassium [6] and bromides of lithium and potassium [7]. The data on the energy changes of the energy system Ag – Bi obtained by using all these electrolytes is given in Fig. 1. Comparing it with our data it can be said that in general they are all similar to one another, although it should be noted, that the data from the experiments with bromide electrolytes always lies between the data from the experiments with chlorides and iodides. In Table 3 we give data on the enthalpy of formation in kilocalories per gram – equivalent at 298°K to the salts of silver and bismuth [2] and question the values of the electrode potentials of these metals (in volts) in the salts in question with respect to sodium, as given by Delimarskii [8].

It is clear from Table 3 that if bromides and chlorides are used as electrolytes it is possible to have a distorting effect from the electrochemical interaction between the alloy and the electrolyte, which has small probability when iodides are used, because of the large difference between the enthalpys of formation and the electrode potentials, and therefore we are inclined to consider our data on the thermodynamic properties of Ag – Bi melts as more reliable.

We have pointed out previously [9] that there is a great similarity between the energy changes of the system Cu – Sb and the system Ag – Sb; no such similarity exists between the system Cu – Bi and the system Ag – Bi. More than this, in contrast with the Cu – Bi alloys where there are large positive deviations from Raoult's law [10], in the system Ag – Bi the positive deviations from Raoult's law with small concentrations of silver in the alloys, become negative at a concentration of silver greater than 45 atom % (see Fig. 2). We also note, that while in the series Cu – Sb, Ag – Sb, and Au – Sb the complexity of the phase diagrams becomes less (see [3], in the series Cu – Bi, Ag Bi, and Au – Bi the reverse effect is observed. It is probable that in all these alloys a very great role is played by interaction between the electronic shells of the atoms, and their behavior can be understood only after investigating this interaction.

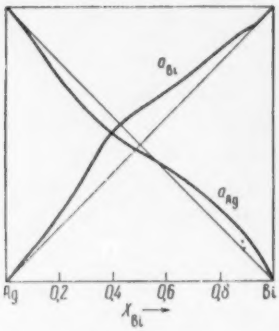

Fig. 2. Activity of the components in the system Ag – Bi at 1000°K.

LITERATURE CITED

1. A. A. Vecher, V. A. Geiderikh, and Ya. I. Gerasimov, ZhFKh, 35, 7 (1961).
2. O. Kubashevsky and E.Evans, Thermochemistry in Metallurgy [Russian translation] (IL, 1954).
3. M. Hansen and K. Anderko, Constitution of Binary Alloys, New York (1958).
4. C. T. Heycock and F. H. Neville, Phil. Trans. Roy. Soc. Lond., A 189, 67 (1897).
5. G. I. Petrenko, Zs. anorg. u. allgem. Chem. 50, 136 (1906).
6. Z. Gregorczyk, Roczniki Chem. 34, 621 (1960).
7. Z. Gregorczyk, Roczniki Chem. 35, 307 (1961).
8. Yu. K. Delimarskii, Fused Electrolytes, in the Book Work on the Chemistry of Solutions and Complex Compounds [in Russian] (Kiev, 1954).
9. Ya. I. Gerasimov and A. A. Vecher, DAN, 139, 4 (1961).
10. A. V. Nikol'skaya, A. L. Lomov, and Ya. I. Gerasimov, ZhFKh, 33, 1134 (1959).

All abbreviations of periodicals in the above bibliography are letter-by-letter transliterations of the abbreviations as given in the original Russian journal. *Some or all of this periodical literature may well be available in English translation.* A complete list of the cover-to-cover English translations appears at the back of this issue.

THE THEORY OF THE SLIP OF A GAS ALONG A SOLID SURFACE UNDER THE INFLUENCE OF A TEMPERATURE DROP

Corresponding Member of the Academy of Sciences, USSR

B. V. Deryagin and S. P. Bakanov

Translated from Doklady Akademii Nauk SSSR, Vol. 141, No. 2,
pp. 384-386, November, 1961
Original article submitted July 26, 1961

The question of the "thermal" slip of a gas along a solid surface was first treated theoretically at the end of the last century by Maxwell [1]. He showed that if there is a tangential temperature gradient, grad T, the gas begins to move along the wall, and he obtained the equation for the rate of slip as a function of grad T, the viscosity of the gas η, the density ρ and the temperature. However, as we have shown previously [2], Maxwell's approach to the solution of the problem was extremely unrigorous. Consequently, the value of the numerical coefficient in the equation which he derived has raised considerable doubt. Nevertheless, all the people who have investigated this problem, both theoreticians and experimenters, right up to the present time, have used precisely Maxwell's formula for lack of anything better. A thermal slip has been used, and at the present time is still being used to explain the thermophoretic motion of large aerosol particles with dimensions greater than the mean free path of the molecules in the surrounding gas. However, a number of experiments show that the theory of this phenomenon, based on Maxwell's formula [3], fails to give results that are in agreement with experiment, in particular, with respect to the relation between the rate of motion of the particle and the thermal conductivity of the material that it is made of. In what follows we shall try to show how to obtain a more rigorous expression for the rate of thermal slip, using Onsager's principle of the thermodynamics of irreversible processes for the purpose.

1. We shall consider the problem of the motion of a gas in a quasi plane slot formed by the lateral surface of a cylinder of fairly large radius r, capable of rotation, with a fixed curving surface. The width of the slot $h \ll r$. Assume that a temperature gradient may be established in the gas contained in this slot. Then, if the cylinder is rotated under the action of a moment M, with the temperature drop ΔT between the ends of the slot, there will be a change in the entropy S of the system according to the law:

$$\frac{dS}{dt} = v\frac{M}{rT} + \frac{I_Q \Delta T}{T^2},$$

where v is the velocity of the cylindrical surface, and I_Q is the heat flux through the cross section of the slot. In accordance with the methods of the thermodynamics of irreversible processes, we may write the thermodynamic equations of the motion in the form:

$$v = L_{11}\frac{M}{rT} + L_{12}\frac{\Delta T}{T^2},$$
$$I_Q = L_{21}\frac{M}{rT} + L_{22}\frac{\Delta T}{T^2},$$

where from Onsager's theorum L_{21} as equal to L_{12}.

We shall consider isothermal motion ($\Delta T = 0$). The heat flux at constant temperature will be expressed in the form $I_Q = L_{21} M/rT$. On the other hand, at $M = 0$

$$v\big|_{M=0} = L_{12}\frac{\Delta T}{T^2} = \frac{I_Q\big|_{T^r}}{M}\frac{\Delta T}{T}.$$

Thus, having calculated the heat flux in the gas when the cylinder is rotating under the influence of the moment M at constant temperature, we can find the rate of motion of the cylinder v under the influence of the temperature drop ΔT. For nonturbulent gas flow in the plane slot at constant temperature we have:

$$\frac{M}{r} = \eta \frac{dv}{dx},$$

where η is the coefficient of viscosity of the gas, and dv/dx is the velocity gradient in the gas at a sufficiently great distance from the walls (the x axis is directed along the normal to the cylinder inside the slot). Thus, the rate of thermal motion of the cylinder may be expressed in the form:

$$v\,|_{M=0} = \frac{I_Q|_T}{dv/dx} \frac{\Delta \ln T}{\eta}.$$

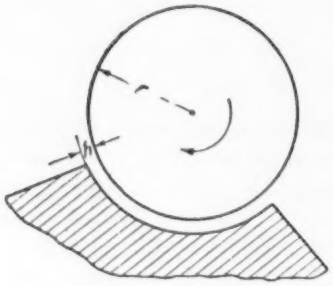

Fig. 1.

2. Let the surface of the cylinder be such that fraction ε_1 of the gas molecules striking it is reflected diffusely, while the fraction $1 - \varepsilon_1$ is reflected specularly. Correspondingly, let the coefficient of diffused reflection on the surface of the wall be ε_2. Further, let the volume of gas in the slot far from the walls (we assume that the thickness of the slot $L \gg \lambda$, the mean free path of the gas molecules) establish under the influence of the rotation of the cylinder a velocity gradient

$$\frac{dv}{dx} = \left(\frac{2kT}{m}\right)^{1/2} \frac{du}{dx},$$

where k is Boltzmann's constant, m is the mass of a molecule, and u is a dimensionless velocity.

Using the results of our work [2], it may be shown that the gas in the slot can be described in the region near the wall by the distribution function

$$f = f^{(0)}\left[1 + \left(\frac{a_0^+ + a_0^-}{2} + \frac{a_1^+ + a_1^-}{2} c_x\right) c_z + \right.$$
$$\left. + \left(\frac{a_0^+ - a_0^-}{2} + \frac{a_1^+ - a_1^-}{2} c_x\right) c_z \operatorname{sign} c_x\right]$$

(where the symbols have the same meaning as in [2]).

In the region near the surface of the cylinder we have:

$$a_0^+ = \left[-\frac{B}{C} + 2\frac{x}{l} + \frac{B\varepsilon_1}{(1-\varepsilon_1)D + C} e^{-\alpha x}\right] l \frac{du}{dx},$$
$$a_0^- = \left[-\frac{B}{C} + 2\frac{x}{l} + \frac{A\varepsilon_1}{(1-\varepsilon_1)D + C} e^{-\alpha x}\right] l \frac{du}{dx},$$
$$a_1^+ = \left[-1 + \frac{C\varepsilon_1}{(1-\varepsilon_1)D + C} e^{-\alpha x}\right] l \frac{du}{dx},$$
$$a_1^- = \left[-1 + \frac{D\varepsilon_1}{(1-\varepsilon_1)D + C} e^{-\alpha x}\right] l \frac{du}{dx}.$$

Near the fixed wall the state of the gas is described by a similar distribution function containing the coefficient ε_2. With the aid of the distribution function it is an easy matter to calculate the heat flux $I_Q|T$ from the usual formulas (the energy flux minus the enthalpy flux). We have

$$dI_Q^{(1)}|_T = n\left(\frac{2kT}{\Pi m}\right)^{1/2} \frac{kT}{8} \frac{\varepsilon_1 (C + D)}{(1-\varepsilon_1)D + C} l \frac{du}{dx} e^{-\alpha x} dx$$

at the surface of the cylinder. Integrating with respect to x from 0 to ∞ gives

$$I_Q^{(1)}|_T = n\left(\frac{2kT}{\pi m}\right)^{1/2} \frac{kT}{8\alpha} \frac{\varepsilon_1 (C+D)}{(1-\varepsilon_1) D + C} l \frac{du}{dx}.$$

At the wall, using the opposite sign of du/dx, we have

$$I_Q^{(2)}|_T = -n\left(\frac{2kT}{\pi m}\right)^{1/2} \frac{kT}{8\alpha} \frac{\varepsilon_2 (C+D)}{(1-\varepsilon_2) D + C} l \frac{du}{dx}.$$

The total heat flux per unit length of the cylinder will be:

$$I_Q|_T = I_Q^{(1)}|_T + I_Q^{(2)}|_T =$$
$$= \frac{nkT}{8}\left(\frac{2kT}{\pi m}\right)^{1/2} (C+D) \frac{l}{\alpha} \frac{du}{dx}\left[\frac{\varepsilon_1}{(1-\varepsilon_1) D + C} - \frac{\varepsilon_2}{(1-\varepsilon_2) D + C}\right].$$

Thus, for the rate of rotation of the cylinder under the influence of a temperature drop we have (setting $\alpha = 7.56/\lambda$)

$$v = \frac{\eta}{\rho} \Delta \ln T \frac{4 (C+D)}{5\pi \cdot 7{,}56}\left[\frac{\varepsilon_1}{(1-\varepsilon_1) D + C} - \frac{\varepsilon_2}{(1-\varepsilon_2) D + C}\right].$$

It is clear from the resulting formula that the rate of rotation of the cylinder is the difference between two quantities, each of which depends only on the properties (ε_1, ε_2) of one of the two surfaces (the cylinder and the fixed curved surface), and is independent of the distance between them. This is physically possible only in the case where v is the difference of two velocity discontinuities, i.e., of the two thermal slip velocities of the gas, relative to the solid surfaces. Here the thermal slip velocity of the gas along the surface must have the form:

$$v_c = \frac{\eta}{\rho} \Delta \ln T \frac{4}{5\pi \cdot 7{,}56} \frac{\varepsilon_1 (C+D)}{(1-\varepsilon_1) D + C},$$

or for $\varepsilon_1 = 1$

$$v_c = \frac{\eta}{\rho} \Delta \ln T \frac{4}{5\pi \cdot 7{,}56}\left(1 + \frac{D}{C}\right).$$

Substituting the values of D and C calculated in [2], we obtain

$$v_c = 0{,}0218 \frac{\eta}{\rho} \Delta \ln T.$$

Comparing the resulting expression with Maxwell's formula for this case shows that they differ only in the coefficients, the coefficient in our formula being approximately 35 times smaller.

The calculation which has been made, makes it possible to conclude that the motion of aerosol particles in a temperature field is determined, basically, not by the effective slip, but by some other mechanism

Another indication of this is given by the fact that the thermophoresis rate of small aerosol particles, which we calculated [4] for the case of specular reflection, obviously bears no relation to the thermal slip at the macrosurfaces, and agrees with Maxwell's values for the velocity of "thermal slip."

LITERATURE CITED

1. J. C. Maxwell, The Scientific Papers of James Clark Maxwell, Cambridge (1890)
2. S. P. Bakanov and B. V. Deryagin, DAN, 139, 1 (1961).
3. P. S. Epstein, Zs. Phys. 54, 537 (1929).
4. S. P. Bakanov and B. V. Deryagin, Koll Zhurn. 21, 377 (1959).

EFFECT OF SOLUTION CONCENTRATION ON THE CONFORMATION OF A POLYMER CHAIN IN SOLUTION

P. I. Zubov, Yu. S. Lipatov, and E. A. Kanevskaya

Institute of Physical Chemistry, Academy of Sciences, USSR
(Presented by Academician V. A. Kargin June 20, 1961)
Translated from Doklady Akademii Nauk SSSR, Vol. 141, No. 2,
pp. 387-388, November, 1961
Original article submitted April 12, 1961

From a study of the properties of solutions of polymethacrylic acid over a wide range of temperatures and concentrations we have established the fact that on going from dilute to concentrated solutions a change in sign of the temperature dependence of viscosity occurs [1, 2]. The mechanism of this phenomenon, which has to do with a change in conformation of the chain, is discussed in the present paper.

We have used a rotational viscosimeter of Shvedov type to study the variation of the dynamic viscosity of aqueous solutions of polymethacrylic acid (viscosimetric molecular weight 330,000) concentrations of 6, 9, and 12% at temperatures of 20-65°. The most important results are given in figure. The data obtained testified to the fact that over a wide range of displacement velocities the viscosities of 6% solutions are higher at 20° than at 50°, and at the same time that, beginning with a concentration of 9%, the higher the viscosity value, the higher the temperature. A similar increase in the viscosity of solutions on heating of polymers in pure solvents has been observed previously with water solutions of gelatin [3, 4] and benzene solutions of butyl rubber [5, 6], and has been explained by the occurrence during heating of unwinding of the macromolecular chains. It is natural to assume that in the case of polymethacrylic acid, the viscosity increase on heating in concentrated solution is also a matter of chain unwinding caused by the decomposition of intermolecular bonds, accompanied by strengthening of the interaction of the unwound chains with one another. This assumption is also supported by the data given in figure on the sharp increase in viscosity on reaching some value of displacement velocity. For a 9% solution, the sharp increase in viscosity occurs at a displacement rate of 6.3 sec^{-1} at a temperature 50°, and for a 12% solution, it occurs at a lower displacement rate at as low a temperature as 20°. This phenomenon, observed by Kachal'skii [9] and called negative thixotropy, is to be explained only by chain unwinding under the influence of displacement stresses. It is an essential fact, as we have shown, that the phenomenon of negative thixotropy has both a lower and an upper temperature limit within which it appears. For a 9% solution the phenomenon of negative thixotropy does not appear at temperatures above 60°, for a 12% solution it is not observed even at 50°. Apparently, the upper limit of temperatures at which it is possible for negative thixotropy to occur is fixed by the temperature of gel formation [6]. It is obvious that at that gel formation temperature the chains are already sufficiently unwound so that no additional unwinding occurs under the influence of displacement stresses.

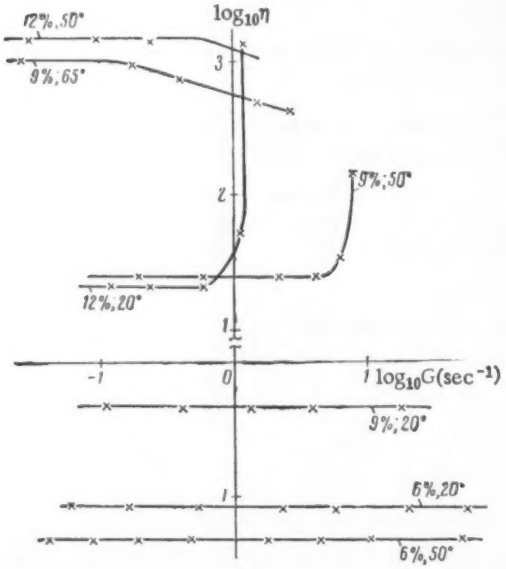

In our previous study [1, 2] of gel formation in polymethacrylic acid solutions, we started from the point of view that the increase in viscosity and the structuration occurring from reduced solubility on heating is a matter of additional winding up of the macromolecules and strengthening of the interaction between them. In the light of the data which we have now obtained, we feel that the gel formation is determined rather by the chains unwinding during heating. Actually,

going to a concentrated solution changes the ratio between the number of intra- and intermolecular bonds, as a result of which going over to a more unwound confirmation with poorer solubility can be thermodynamically more favorable. Although straightening out the chains causes a reduction in entropy, it can be compensated for by a considerable change in heat content on account of the fact, that with unwound chains, a considerably larger number of carboxyl groups can take part in the interaction.

The ideas presented here are in agreement with the data of Harmann and Patat [7], who observed a sharp reduction in the solubility of dextrane in water under a prolonged application of displacements stresses associated with chain unwinding and strengthening of intermolecular interaction between the chains. Transition to a more unwound conformation of the molecules of polyacrylic acid on increasing the concentration of the solution was observed in the paper by Kargin, Bakeev, and Pshezhetskii [10], which also supports our point of view as regards chain unwinding in more concentrated solutions.

Thus, it follows from what has been presented that the conformation of a polymer molecule in solution depends not only on the nature of the polymer, the solvent, and the temperature, but on the concentration of the solution as well.

LITERATURE CITED

1. Yu. S. Lipatov and P. I. Zubov, Vysokomol Soed. 1, 432 (1959).
2. Yu. S. Lipatov, P. I. Zubov, and E. A. Andryushchenko, Koll. Zhurn. 21, 598 (1960).
3. P. I. Zubov, Doctor's Dissertation [in Russian] (Moscow, 1949).
4. P. I. Zubov, Z. N. Zhurkina, and V. A. Kargin, DAN, 67, 659 (1949).
5. A. S. Novikov, T. V. Dorokhina, and P. I. Zubov, DAN, 105, 514 (1955).
6. T. V. Dorokhina, P. I. Zubov, and A. S. Novikov, Vysokomol Soed. 1, 36 (1959).
7. J. Harmann and F. Patat, Macromol. Chem. 176, 1119 (1955).
8. Yu. S. Lipatov, P. I. Zubov, and E. A. Andryushchenko, Vysokomol Soed. 1, 425 (1959).
9. J. Elliassaf, A. Silberberg, and A. Katchalsky, Nature, 25, 53 (1959).
10. N. F. Bakeev, V. S. Pshezhetskii, and V. A. Kargin, Vysokomol Soed. 1, 1812 (1959).

All abbreviations of periodicals in the above bibliography are letter-by-letter transliterations of the abbreviations as given in the original Russian journal. *Some or all of this periodical literature may well be available in English translation.* A complete list of the cover-to-cover English translations appears at the back of this issue.

THE ROLE OF PHASE TRANSFORMATIONS IN THE POLYMERIZATION OF MONOMERS IN THE SOLID STATE

Academician V. A. Kargin, V. A. Kabanov,

I. M. Papisov, and V. P Zubov

M. V. Lomonosov Moscow State University
Translated from Doklady Akademii Nauk SSSR, Vol. 141, No. 2,
pp. 389-392, November, 1961
Original article submitted June 19, 1961

It follows from a number of papers published in recent years, that the polymerization reactions of monomers in the solid state may be divided into two groups: fast (explosive in the extreme case) [1-6], and slow [7-9]. Explosive polymerization reactions are induced both by chemical means (in the simultaneous condensation of vapors of monomers and various initiators on a strongly cooled wall [1-4, 6]), and by the action of high energy radiation [5]. Therefore it is to be assumed, that the explosive character of the reaction is not so much a matter of the nature of the particles produced in the polymerization, as of the special conditions arising in the system of ordered monomer molecules.

It follows from the data to be found in the literature that slow polymerization of crystalline monomers proceeds at rates which are considerably less and are characterized by considerably larger activation energies of the chain growth reaction, than the polymerization of these same monomers in the liquid phase (in the case of acrylamide, for example, 25 kcal/mole in the solid phase, as contrasted with 7-10 kcal/mole in the liquid phase [9]). Along with this, the very fact that there is such a thing as fast polymerization at very low temperatures causes one to suspect that under the proper conditions the formation of polymer chains in the solid phase can occur with very small, practically zero, activation energies. It has been possible to show that explosive polymerization of a number of monomers (acrylonitrile, methacrylonitrile, acrylamide, methacrylamide, methylmethacrylate, etc., [3, 4, 6]) may be brought about at considerably lower temperatures than the temperatures at which slow polymerization has been repeatedly observed when the crystals are irradiated.

In order to elucidate the mechanism of fast polymerization in the solid phase, we have studied the conditions required for the existence of explosive polymerization in frozen molecular mixtures of monomers and active particles, using as an example the system: acrylonitrile (m.p. – 83°) – magnesium, and the system methylmethacrylate (m.p. – 50°) – magnesium, using for this purpose the method of thermal analysis and observation of the frozen molecular mixtures in polarized light. To prepare the molecular mixtures we used a modified form of the apparatus described previously [1, 4] (Fig. 1). Simultaneous vacuum condensation of the vapors of the monomer in the metal was effected on the glass plate 1, ground onto the end of the copper cylinder 2, which was cooled with liquid nitrogen. The temperature change in the condensate layer was measured by means of a thin (0.1 mm) copper-constantin thermocouple 3, one of the junctions of which was fastened directly to the surface of the glass plate, while the other was fastened to the body of the cylinder being cooled. The indications of the differential thermocouple were recorded on a sensitive EPP-09 electronic potentiometer. In making measurements on the surface of the glass plate a thin (0.03 mm) layer of molecular mixture of monomer and initiator in the approximate ratio of 100 : 1 was solely deposited. The condensation was carried out at such a rate, that the temperature in the layer did not exceed – 160°. At the end of condensation, the layer of condensate appeared as a glassified homogeneous transparent film, containing, according to [2], magnesium-organic radicals "stuck" in the monomeric glass. Then the liquid nitrogen was removed from the copper cylinder, after which the cylinder was slowly heated (at a rate of 2°/min). The temperature of the cylinder was measured with the copper-constantin thermocouple 4, one of the junctions of which was placed in the body of the cylinder, while the other was placed in liquid nitrogen. Figure 2 shows typical curves of temperature against time. It is obvious that explosive polymerization, accompanied by considerable liberation of heat, occurs either at –160° (curve 1), or at –135° (curve 2). Here the degree of conversion reaches 100%. The temperature time curves of a condensate which does not contain any active centers, taken under similar con-

ditions show that at these temperatures 2 exothermic transitions occur in frozen acrylonitrile (curve 3). The first transition can be observed visually from the clouding of the transparent condensate layer. It comes from crystallization of the monomeric glass when it reaches the Tamman temperature. The nature of the second transition is less clear. It is probable that it comes from additional ordering processes in the microcrystalline mass formed as a result of the first transition. Both transitions are irreversible and are not reproducible on repeated cooling and heating of the condensate.*

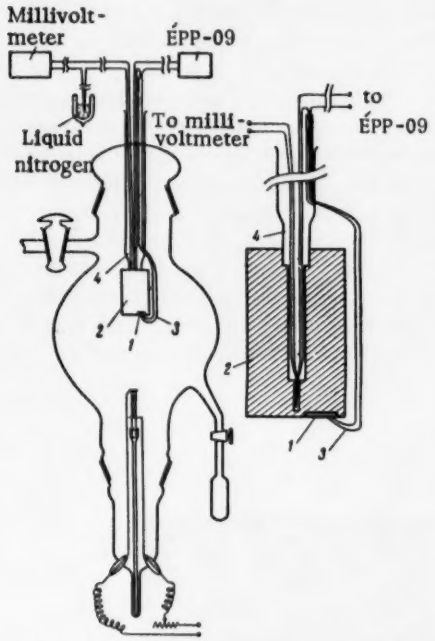

Fig. 1. Diagram of apparatus (Left: general view. Right: cooled cylinder and thermocouples.)

Thus, the experiments described show that fast polymerization of acrylonitrile at temperatures considerably below the melting point is intimately bound up with the molecular mobility, which can be achieved in phase transformations in the solid state in the present case with the transition of the glass crystals. A transition of this sort is always "held in reserve" if the monomer is in the glassy state. This condition is fulfilled in the condensation of vapors on a surface cooled to a temperature at which the monomer molecules experience inelastic collisions with the surface.

It should be noted that for explosive polymerization to exist it is not necessary for the whole volume of the solid monomer to take on a temperature at which molecular mobility appears. It is often sufficient to heat, for example, only the surface layer. In this case, the heat, developed by the polymerization, heats the adjoining layers, and the process goes like a thermal explosion. Analogous phenomena are observed in the thickening of layers (appearance of a temperature gradient) of molecular mixtures of monomers and initiators in the condensation reaction on a surface cooled to liquid nitrogen temperature.

If the surface, on which the condensation is being carried out, is at a higher temperature, the molecules and radicals being condensed are able to migrate over the surface, trying to produce crystallization nuclei. In this case, instead of a uniformly amorphous layer, growths of well formed crystals occur at various parts of the surface, which show characteristic birefringence. We have observed this phenomenon in the vacuum

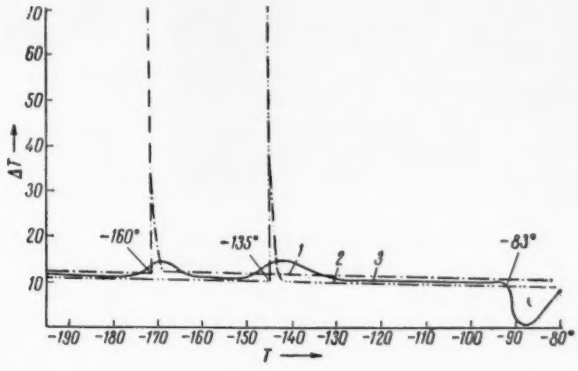

Fig. 2. Temperature - time curves of acrylonitrile – magnesium molecular mixtures (1, 2) and pure acrylonitrile (3). T) Temperature of copper cylinder; ΔT) temperature difference between copper cylinder and condensate.

* The question of why in some experiments the polymerization occurs at the first transition, and in other experiments occurs at the second transition requires additional investigation.

condensation of vapors of methylmethacrylate and magnesium on a glass sphere, cooled to −75°, in an apparatus, described previously [1, 4]. Figure 3a shows a typical photograph of a radial growth of crystals (spherolite) of methylmethacrylate on the surface of the sphere taken in polarized light. The characteristic Maltese Cross is clearly visible. Polymerization goes very slowly in such a system at −75°, and is accelerated by gradually raising the temperature. The polymerization reaction may be observed in polarized light from the disappearance of the birefringence. By examining the surface of the sphere between crossed polarizers with a long-focus microscope, we convinced ourselves that the polymer begins to form on the edges of the spherolites, on the boundaries between separate crystallites, and at the places where flaws occur. Later on, the reaction always occurs under heterogeneous conditions at the crystal − polymer boundary. The shifting of this boundary right up to the end of polymerization can be clearly observed in polarized light. Figure 3b shows a portion of spherolite, in which the polymerization is already over (the birefringence has disappeared), along with the boundary, separating this portion from a portion which has not yet started polymerizing enough shows birefringence. If the surface temperature of the sphere is raised at a rate of 0.3°/min, the polymerization is completely finished 3-4° below the melting point of methylmethacrylate. Here the birefringence disappears completely. Figure 3c shows a photograph of the same spherolite as in Fig. 3a, after the polymerization is completelv finished. The picture was taken with the polarizers removed. The growth of monomer crystals has been converted into an isotropic piece of polymethylmethacrylate, which maintains its original form, but with a considerably larger number of flaws.

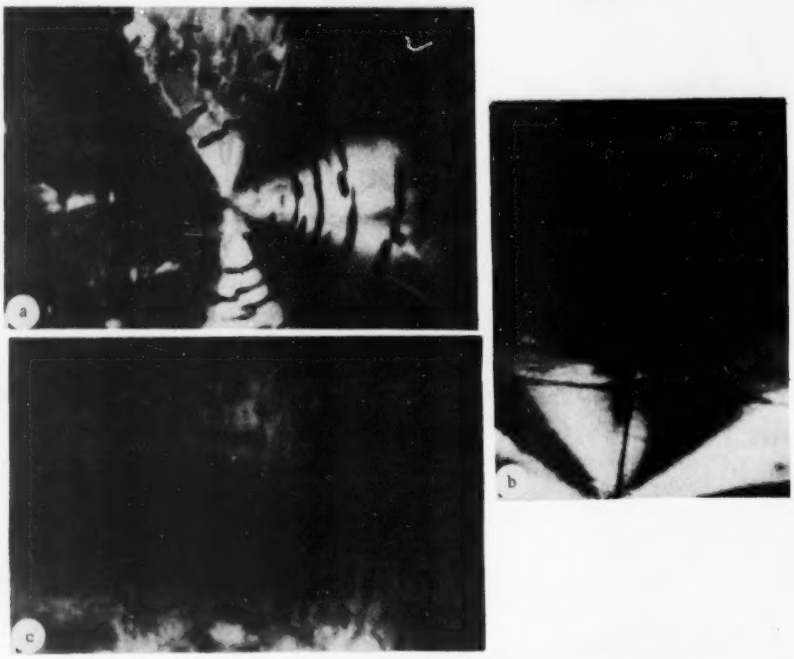

Fig. 3. Photomicrographs of methylmethacrylate crystalline growths in the course of polymerization. a) Spherolite before the start of polymerization; b) boundary between polymerized and unpolymerized parts of the crystalline growth; c) same spherolite as in a, after polymerization is complete. Magnification 70 ×.

Thus, by using the optical method, we were able to observe the typical picture of "slow" polymerization in the crystalline state, which is completely similar to the one which was observed by Adler et al [10] during irradiation of acrylamide crystals. It should be emphasized, that simultaneous condensation of methylmethacrylate and magnesium vapors on a surface, cooled by liquid nitrogen, accompanied by the formation of an amorphous layer, leads to explosive polymerization at considerably lower temperatures. Discussing the question of polymerization in the solid phase, N. N. Semenov [11] made the proposal that, because of the collectivation of electronic levels in the region where the crystal is ideal, the formation of the polymer chain from the ordered molecular substrate goes as one reaction act and does not require any activation energy. A concrete scheme of formation of a polymer

chain in an ideal monomer crystal under the influence of an exciting agent has been discussed recently by E. I. Adirovich [12]. N. N. Semenov's hypothesis is very attractive, since it enables us to explain the fast low temperature polymerization of solid monomers. However, examination of the experimental data on the polymerization of crystalline monomers shows that in equilibrium ("ideal") monomer crystals, far removed from their melting point, high transformation rates are not usually observed. They show typical "slow" polymerization. More than that, the polymerization reaction is found to be accelerated under precisely those conditions in which the crystals begin to show defects (for example, in the solidification of melts [9] or in the vicinity of the melting point).

In all probability, fast low temperature polymerization reactions in the solid phase can be brought about only in case the ordering of the reacting molecules is found to be associated with a sufficient degree of mobility. The fact of the matter is that if a polymer chain is formed in an ideal crystal, it must immediately produce a defect, on account of the change in the interatomic distances. As the chain becomes longer, the defect becomes bigger, which inevitably stops the growth of the chain, and causes "freezing" of the active center. If the active center is going to enter into the reaction again and continue the growth of the chain, there must be some local thermal reconstruction of the crystal ("healing of the defect"), i.e., relaxation of the stress caused by the irreversible displacement of the molecules taking part in the reaction. The observed high activation energies of the chain growth reaction (in particular in the postpolymerization stage) probably come from just this kind of reconstruction, which limits the polymerization rate. Reconstruction of this sort occurs most easily on the surface of crystals, or at the places where flaws and dislocations occur. Therefore these are precisely the places where polymerization of crystalline monomers starts, and it goes on principally at the crystal – polymer interface [10]. Factors which facilitate molecular regrouping of the monomer at an interface, e.g., adsorbed solvent layers [9, 13, 14], lead to a marked acceleration of the polymerization.

It is a different state of affairs if the conditions in the solid monomer are such as to allow fast migration of defects (appearance and "healing"). This removes the fundamental limitation on the instantaneous, activationless (Semenov) growth of chains in an ordered solid phase. Conditions of this sort can arise in a solid, for example, during phase transitions near the melting point. If the concentration of active centers in a frozen monomer is high enough, the sudden appearance of molecular mobility with the orderedness still maintained, will lead to practically instantaneous polymerization.

LITERATURE CITED

1. V. A. Kargin, V. A. Kabanov, and V. P. Zubov, Vysokomolek. Soed. 1, 265 (1959).
2. V. A. Kabanov, G. B. Sergeev, V. P. Zubov, and V. A. Kargin, Vysokomolek. Soed. 1, 1859 (1959).
3. V. A. Kabanov, Dissertation [in Russian] (Moscow, 1960).
4. V. A. Kargin and V. A. Kabanov, International Symposium on Macromolecular Chemistry, Section II [in Russian] (Moscow, 1960), p. 453.
5. M. Maga, Chemistry and Technology of Polymers, No. 7-8 [in Russian] (1960).
6. V. A. Kargin, V. A. Kabanov, V. P. Zubov, and I. M. Papisov, Vysokomolek. Soed. 3, 426 (1961).
7. R. B. Mesrobian and P. Ander et al., J. Chem. Phys. 22, 565 (1954).
8. A. J. Restaino and R. B. Mesrobian et al., J. Am. Chem. Soc. 78, 2939 (1956).
9. T. A. Fadner and H. Morawetz, J. Polymer Sci. 45, 475 (1960).
10. D. Adler, D. Ballantain, and B. Beizal, International Symposium on Macromolecular Chemistry, Section II [in Russian] (Moscow, 1960), p. 369.
11. N. N. Semenov, Chemistry and Technology of Polymers, No. 7-8 [in Russian] (1960), p. 196.
12. É. I. Adirovich, DAN, 136, 117 (1961).
13. V. A. Kargin, V. A. Kabanov, and G. P. Andrianova, Vysokomolek. Soed. 1, 301 (1959).
14. V. A. Kargin, V. A. Kabanov, and N. Ya. Rapoport, Molodtsova, Vysokomolek. Soed. 3, 787 (1961).

IGNITION LIMITS IN TURBULENT GAS MIXTURES

V. P. Karpov and A. S. Sokolik

Institute of Chemical Physics, Academy of Sciences, USSR
(Presented by Academician V. N. Kondrat'ev June 20, 1961)
Translated from Doklady Akademii Nauk SSSR, Vol. 141, No. 2,
pp. 393-396, November, 1961
Original article submitted June 20, 1961

The ignition of a gas mixture from a spark is one of the forms of thermal explosion, and the critical conditions for its occurrence exists when the rate of heat liberation from the reaction into the volume heated by the spark is equal to the heat conduction from the external surface of the region where the burning occurs into the surrounding gas (See [1], Sec. 15). A technique for producing artificial turbulence of the gas in a closed volume [2] makes possible a quantitative investigation of the effect of turbulence on the ignition of gases from a spark. The data given in Fig. 1. show that if the energy of the spark from a capacitor is constant the absolute intensity of turbulence ($U' \Sigma$)

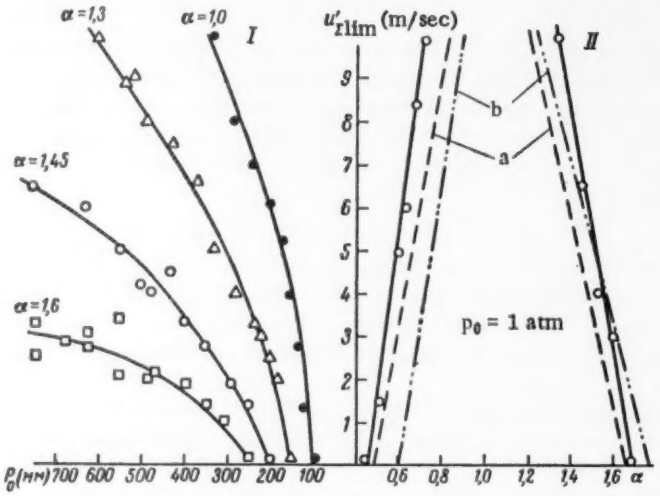

Fig. 1. Ignition limits of a propane-air mixture. I) As a function of pressure at various mixture compositions; II) as a function of concentration at P_0 = 1 atm with constant spark energy. a) With the spark energy reduced 20 times; b) ignition limits of the methane-air mixture.

produced in the bomb is increased and either the limits of concentration come closer together, or the lower pressure limit is raised. The limits of concentration also come closer together as the energy of the spark is reduced, the more so, the higher the intensity of turbulence. (see Fig. 1, II). Qualitatively, these results are in agreement with observations on a turbulent stream of gas – air mixture, i.e., the limiting ignition current is raised as the velocity of the stream is increased [3]. However, the value of the observations is not exhausted by demonstrating what, on the face of it, appears to be a trivial fact, namely, that increasing the turbulent heat conduction from the original focus of the reaction makes ignition from the spark difficult. Actually, with a turbulent heat exchange mechanism, the heat conductivity of the gas should have no effect on the heat conduction, and consequently, it should have no effect on the ignition limit. It is precisely for this reason that the turbulent combustion rate, which is determined directly by turbulent diffusion, is independent of the thermal conductivity of the gas mixture, and, by the same fact, is independent of the laminar combusion rate at constant partial pressures of the reacting components and constant

combustion temperature. This fact, which is one of the decisive indications that a turbulent combustion mechanism is inconsistant with the so-called "surface-laminar model," is clearly demonstrated by experiments on stoichimetric mixtures of propane and hydrogen with oxygen diluted with helium or argon, and all having the same combustion temperature (Fig. 2). The turbulent combustion rates are the same over wide ranges of change in the intensity of turbulence, with a difference in laminar combustion rates of approximately two-fold. But, as is also clear from Fig. 2, the ignition limit when diluted with helium occurs at a considerably lower intensity of turbulence than when diluted with argon. (In a propane mixture diluted with argon, the maximum intensity of turbulence at our disposal is in general not sufficient to reach the ignition limit.) The data obtained show that even with a twenty fold increase in spark energy, the ignition limit in mixtures diluted with helium remains considerably lower than with argon. It is, therefore, necessary to recognize that turbulent mixing of the gas makes spark ignition difficult, but that this occurs in the presence of a conductive mechanism of heat transfer from the original focus of the reaction. This may be explained by the fact that the heat transfer in the fresh gas is determined by the thermal resistance of the boundary layer surrounding the focus. With weak turbulence, the turbulence causes curvature of the surface of the original focus of the reaction, as may be seen from the series of pictures in Fig. 3b taken by Schlieren moving pictures. Only after a period of 1.5 milliseconds from the moment of spark discharge, beginning with picture No. 8, is there any visible breaking up of the focus to show that any actual turbulent transfer mechanism is entering into play. Conductive heat transfer through the boundary layer curved surface raises the heat conduction from the surface of the laminar plane, but it also slows up formation of the flame in the turbulent gas (See the series of pictures a, b) and narrows the ignition limits.

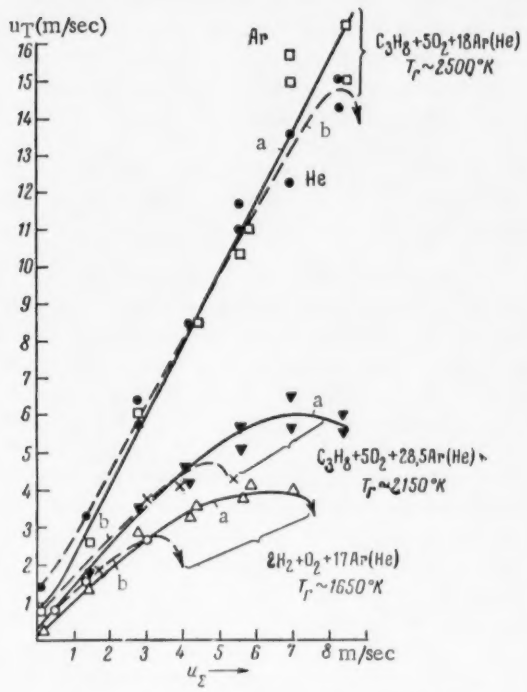

Fig. 2. Ignition limits of stoichiometric mixtures of propane and hydrogen with oxygen, diluted (a) with argon and (b) with helium.

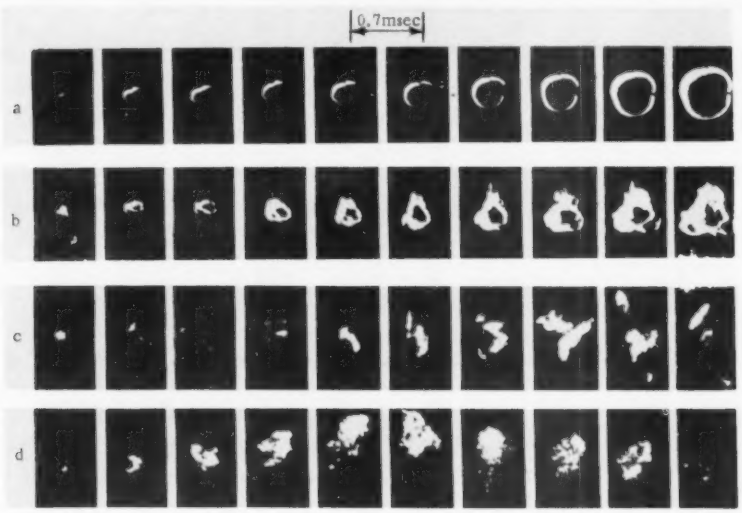

Fig. 3. Series of movie frames of hydrogen-air flames with $\alpha = 0.2$. a) Laminar flame; b) initial stage of propagation of a turbulent flame at $U'_\Sigma = 2.8$ meters/sec; c) breakup of the original focus at $U'_\Sigma = 7$ meters/sec; d) limit of propagation.

With strong turbulence, dissipation of the original focus occurs after it is torn loose from the electrodes as may be seen from Fig. 3c. The higher the intensity of turbulence, the earlier in the course of formation the focus is torn loose, then the greater the ratio of surface to volume of the focus of the reaction. The heat conduction from unit surface is, as before, determined by the thermal conductivity of the gas. Some particularly interesting things are to be found in the limits of turbulent ignition of hydrogen-air mixtures. As may be seen from Fig. 4, the ignition limit with excess hydrogen occurs at lower intensities of turbulence than with an excess of air, in spite of the higher combustion temperature of the rich mixtures. Thus, at $\alpha = 0.17$ (combustion temperature 1300°K), the limit is $U'_\Sigma = 2$ meters/sec, and at $\alpha = 5.6$ (combustion temperature 860°K), the limit is $U'_\Sigma > 5$ meters/sec.

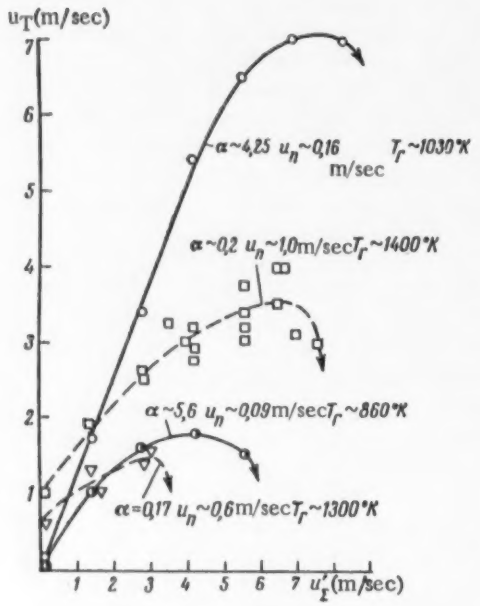

Fig. 4

In addition to the increased thermal conductivity, the lowering of the limit in rich hydrogen-air mixtures is markedly affected by the fact, that the reaction rate increases with the O_2/H_2 ratio. Thus, from experimental data [4] and from calculations [5], the maximum width of the chain ignition region corresponds with the composition $H_2 + 4O_2$, i.e., $\alpha = 8$ (see [5], page 76). An increase in the reaction rate in mixtures of hydrogen with excess air appears even in comparison with the turbulent combustion rates far from the ignition limits. Thus, U_T is considerably higher for a mixture with $\alpha = 4.25$ in a combustion temperature of 1030°K, than for $\alpha = 0.2$ and a combustion temperature of 1400°K. This again confirms the lack of correspondence between the rates of turbulent and laminar combustion: the latter are considerably higher in the rich mixtures with a higher molecular transfer coefficient. It follows from the data given in Fig. 1b, that for the same intensity of turbulence the poorer combustion limit for mixtures of methane is wider, than for propane mixtures, in spite of the fact that the thermal conductivity of the methane mixtures is higher. This difference must also be attributed to the greater reaction rate in the poorer methane mixtures in comparison with the higher alkanes, as were shown in our paper [6]. As may be seen from Figs. 2 and 4, the increase in the rate of turbulent combustion with intensity of turbulence is slowed up as the ignition limit is approached, and departs from the linear law $u_T \sim u'_\Sigma(t_0/\tau_i)$ [1]. However, a study of the movie frames, for example, Fig. 3c, shows that this deviation can not be ascribed simply through slowing up the turbulent propagation of the flame. Actually, it has to do with a profound change in the very nature of propagation of the flame, in particular with the fact, that at large intensities of turbulence the flame is propagated in separate tongues, and does not fill the whole volume, corresponding to the radius to which they extend out. If we calculate the circle of area equivalent to the total projection of the tongues of flame, we naturally find a reduction in the apparent flame velocity $U_f = dr/dt$. The ratio of the actual volume V_a, occupied by the individual tongues of flame, to the volume V_m of a sphere with a radius equal to the maximum distance to which the tongues go out, is a measure of the incompleteness of the filling of the volume by the free turbulent flame, and is a constant quantity $V_a/V_m \approx 0.35$, for the flames which we studied from air mixtures with methane, propane, and hydrogen right at the ignition limits. This value is a quantative measure of the probability of dissipation of a turbulent flame during propagation.

As may be seen from the series of pictures in Fig. 3d, at a sufficiently high intensity of turbulence, there is complete dissipation of the turbulent flame after it has occupied a considerable volume. Here we are dealing with the genuine limit of propagation of a turbulent flame before reaching the spark ignition limit. The fact, that increasing the turbulence, along with accelerating the combustion, leads, beginning at some value of U'_Σ, initially to an increase in the probability of dissipation, and then to complete dissipation of the developed turbulent combustion focus, this fact, we repeat, follows immediately from the ideas suggested by the new model, namely from the fact, that pulsating the ignition becomes impossible if the mixing time becomes less than the induction period for the ignition: $t_0 = l_1/U' < \tau_i$. This reduction of $t_0 = l_1/U'$ below the critical level corresponds with an increase in U', and, along with the pulsational velocity, it has a statistical character. With increasing mean square values of the intensity of turbulence, U'_Σ, the probability of achieving the above in equality becomes greater.

LITERATURE CITED

1. A. S. Sokolik, Self-Ignition, Flame and Detonation in Gases [in Russian] (Academy of Sciences Press, USSR, 1960).
2. A. S. Sokolik and V. I. Karpov, DAN, 129, 1, 168 (1959).
3. Kimura Itsuro and Kumagai Seiichiro, J. Phys. Soc. Japan, 5, 599 (1956).
4. N. M. Chirkov, Acta Physicochimica URSS, 6, 915 (1937).
5. A. B. Nalbandyan and V. V. Voevodskii, Mechanism of Oxidation and Combustion of Hydrogen [in Russian] (Academy of Sciences Press, USSR, 1949).
6. V. P. Karpov and A. S. Sokolik, DAN, 138, 4 (1961).

All abbreviations of periodicals in the above bibliography are letter-by-letter transliterations of the abbreviations as given in the original Russian journal. *Some or all of this periodical literature may well be available in English translation.* A complete list of the cover-to-cover English translations appears at the back of this issue.

DIFFUSION OF IODINE IN COMPRESSED CARBON DIOXIDE NEAR ITS CRITICAL POINT

I. R. Krichevskii, N. E. Khazanova, and L. R. Linshits

Government Scientific Research and Planning Institute of Nitrogen Industry and Products of Organic Synthesis
(Presented by Academician S. I. Vol'fkovich, June 20, 1961)
Translated from Doklady Akademii Nauk SSSR, Vol. 141, No. 2, pp. 397-399, November, 1961
Original article submitted May 26, 1961

Studies of molecular diffusion in double liquid systems have shown that at the critical separation point the diffusion rate is equal to zero [1-5]. From the thermo-dynamic standpoint, the critical point of any other type of equilibrium is in no way different from the critical point of a liquid – liquid equilibrium. Consequently, the diffusion rate at the critical point of double gas systems should also be zero.

Studies of molecular diffusion in gases under pressure present great experimental difficulties. Studies near the critical point are particularly difficult, and, therefore, up to the present time, nobody has made any. Making use of the fact that iodine gives colored solutions in gases, the authors have developed a technique of measuring the diffusion coefficient of iodine in compressed carbon dioxide. The experimental study is based on a method used by Furth to measure the diffusion coefficients in colored liquid solutions [6], which consists of following the rate of development of the colored layer, the intensity of the color being compared with the intensity of a standard colored solution.

The experimental technique was as follows. On the bottom of a high pressure ampule (Fig. 1, 1) with an inside diameter of about 3 mm, was placed iodine pressed into a tablet (2). The free space above the tablet was filled with thin glass rods (3) to keep convection currents from being formed (the free cross-section between the rods was not more than 0.1 mm^2). The ampule was closed with a stopper made of fluoroplast-4, and the opening was closed by the metal valve tip (4). The flanges on the stopper served as packing between the valve nipple and the end of the ampule. Tightening was done by the nut on top which drew the flanges of the ampule up against the valve nipple. The ampule thus assembled was evacuated and fastened into the holder (5). To keep down the vapor pressure of iodine, the end of the ampule was kept in a sack of dry ice before the holder was put into the thermostat. On the same holder as the test ampule was a control ampule (6) containing a solution of iodine in carbon dioxide. The color should be the same in all parts of the control ampule. After the holder was placed in the thermostat at a fixed temperature, carbon dioxide was admitted to the test ampule through a heated capillary tube. The pressure was measured with a visible reading manometer.

Near the critical point of carbon dioxide, a practically constant pressure is observed over a wide range of densities. In this case, the gas was added not in terms of pressure, but in terms of density. For this purpose, the balloon, from which the carbon dioxide was being added, was kept in a thermostat at a fixed temperature. Since the volume of the balloon was a thousand times greater than the volume of the ampule, it was possible to assume with a sufficient degree of approximation, that the density of the carbon dioxide in the ampule, connected to the balloon in the thermostat, was equal to the density of the carbon dioxide in the balloon. The density in the balloon was known from the volume (the balloon was calibrated) and the weight of carbon dioxide in it. A final check on the density of carbon dioxide in the ampule was made after the experiment.

After the carbon dioxide was admitted to the test ampule, the iodine began to diffuse into the compressed carbon dioxide. The moment the carbon dioxide is admitted directly to the surface of the tablet, this solution of the color front occurred. Therefore, moving the slit (7) immovably fastened with respect to the control ampule, a part of the test ampule was found at some distance above the surface of the iodine tablet, where there was the same intensity of color as in the control ampule. The displacement of this point along the ampule was measured on the

Diffusion Rate of Iodine in Compressed Carbon Dioxide

Run No.	Temperature, °C	Pressure, atm	Density, g/cm³	Length of run hours	Diffusion coefficient, $D_{I_2} \cdot 10^5 cm^2 \cdot sec^{-1}$
1	31.5	10.7	0.015	4.5	6.0
2	31.5	18.0	0.056	21.0	1.9
3	31.5	38.7	0.108	22.0	1.4
4	31.5	61.0	0.160	19.5	1.2
5	31.5	40.7	0.180	26.0	1.4
6	31.5	73.0	0.385	72.0	0.02
7	31.5	73.6	0.429	47.0	0.0
8	40.0	86.8	0.493	7.5	3.0
9	31.5	74.5	0.496	68.5	0.9
10	31.5	72.8	0.610	40.0	3.0
11	31.5	74.4	0.620	46.0	3.0
12	31.5	81.5	0.720	19.7	4.5

scale (8). The rate of this displacement corresponded with the diffusion rate. At the end of the experiment the actual carbon dioxide density in the ampule was found, by measuring the quantity of carbon dioxide in the free volume of the ampule. The quantity of carbon dioxide was determined from the difference in weight of the ampule with and without carbon dioxide. To determine the free volume, the glass rods were taken out of the ampule and weighed (the specific gravity of the glass of the rods is known), and the empty ampule was calibrated with mercury, taking account of the volumes of the stopper and the iodine tablet.

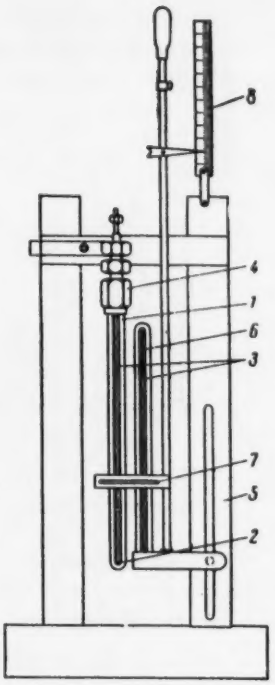

Fig. 1. Apparatus for measuring the diffusion rate of iodine in compressed carbon dioxide.

To check the method, the diffusion rate of iodine in liquid carbon dioxide was measured. The value of the diffusion coefficient at 20° was found to be equal to $1.5 \cdot 10^{-5}$ cm² · sec⁻¹, which agrees with the usual values of the diffusion coefficient in liquids. The visual observation error was ± 1.5 mm. Purified and dried carbon dioxide, containing up to 0.1% of inert gases, was used in the experiments.

The diffusion coefficient was calculated from the approximate equation [7]

$$D = \frac{l^2}{2t}, \qquad (1)$$

where D is the diffusion coefficient, l is the displacement, and t is the time. Since the square of the displacement is directly propertional to the time, in a plot of l^2 against t, the experimental points from each experiment should lie on a straight line, the slope of which gives the value of the diffusion coefficient. By way of illustration, Fig. 2 shows a straight line of this sort, constructed from the experimental points of run No. 9 (table). With the error of measurement mentioned above the minimum values of the diffusion coefficient which could be determined were of the order of $1 \cdot 10^{-7}$ cm² · sec⁻¹.

Equation (1) holds strictly for infinitely dilute solutions. Therefore, the values of the diffusion coefficients calculated from the experimental data are approximate. For the critical region, however, where the deviations from the ideal are considerable, Eq. (1) does not hold at all. Near the critical point, the authors did not make any visual observations on the displacement of the color, in spite of the long duration of the observation (table). Consequently, without recourse to calculation, the authors convinced themselves in a completely direct way that the diffusion stops near the critical point of the system.

The diffusion of iodine in compressed carbon dioxide was investigated at 31.5° and various carbon dioxide densities both above and below the critical density (table, Fig. 3).

There is no data in the literature on the critical parameters of the system iodine – carbon dioxide. However, it is to be assumed that because of the small solubility of iodine in carbon dioxide [8], the critical parameters of this system will be close to the critical parameters of pure carbon dioxide (temperature 31.06°, pressure 72.9 atm, density 0.467 g/cm^3).

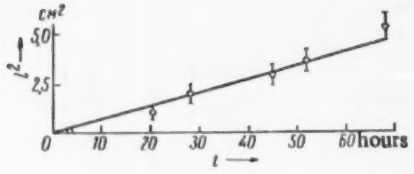

Fig. 2. Measurement of diffusion coefficient of iodine in carbon dioxide.

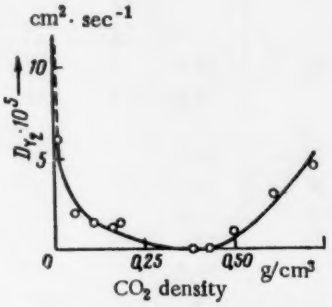

Fig. 3. Iodine diffusion in compressed carbon dioxide.

The experimental data obtained show that near the critical point, within the limits of error of our measurements, the diffusion of iodine practically stops. We observed the same thing at 32° and 73 atm [9]. As we get away from the critical point, the iodine diffusion proceeds at rates normal for compressed gases.

Measuring the diffusion rate at 40° and a density near critical (Run No. 8) showed that under these conditions the effect of the critical point was small. The diffusion coefficient has almost the usual value for compressed gases.

Molecular diffusion is a result of the Brownian motion of individual particles. As was shown in [10], at the the critical point, a Browian particle should be "squelched" on the spot, i.e., the effect of stopping the Brownian motion should be observable practically, and, consequently, the effect of stopping the molecular diffusion should be observable, too.

The data obtained by the authors on the diffusion of iodine in compressed carbon dioxide provides experimental confirmation of these views.

LITERATURE CITED

1. I. R. Krichevskii, N. E. Khazanova, and L. R. Linshits, DAN, 99, 113 (1954).
2. I. R. Krichevskii and Yu. V. Tsekhanskaya, ZhFKh, 30, 2315 (1956).
3. I. R. Krichevskii, N. E. Khazanova, and Yu. V. Tsekhanskaya, ZhFKh, 34, 1250 (1960).
4. H. L. Loretzen and B. B. Hansen, Acta Chem. Scand. 11, 893 (1957).
5. H. L. Lorentzen, Acta Chem. Scand. 12, 139 (1958).
6. R. Fürth, J. Sci. Instr. 22, 61 (1945).
7. A. Einstein and M. Smoluchowski, Collected Papers (1936).
8. E. L. Quinn, J. Am. Chem. Soc. 50, 672 (1928).
9. I. R. Krichevskii, N. E. Khazanova, and L. R. Linshits, Inzh.-Fiz. Zhurn. 3, 117 (1960).
10. I. R. Krichevskii and L. A. Rott, DAN, 136, 1368 (1961).

All abbreviations of periodicals in the above bibliography are letter-by-letter transliterations of the abbreviations as given in the original Russian journal. *Some or all of this periodical literature may well be available in English translation.* A complete list of the cover-to-cover English translations appears at the back of this issue.

THE TEMPERATURE DEPENDENCE OF THE COORDINATION NUMBERS OF PARTICLES IN LIQUID SOLUTIONS

V. I. Kuz'mich, V. K. Prokhorenko, O. Ya. Samoilov, and I. Z. Fisher

V. I. Lenin Belorussian Government University
N. S. Kurnakov Institute of General and Inorganic Chemistry, Academy of Sciences, USSR
(Presented by Academician I. I. Chernyaev, June 21, 1961)
Translated from Doklady Akademii Nauk SSSR, Vol. 141, No. 2, pp. 400-401, November, 1961
Original article submitted June 8, 1961

One of the fundamental characteristics of the structure of a liquid is the mean coordination number of the particles. More than once a close connection has been noted between the coordination number and the thermal (above all translational) motion of the particles of the liquid [1-3]. This connection shows up clearly in a high level of fluctuations of the coordination numbers [4, 5]. The temperature dependence of the coordination numbers is a matter of great interest. This dependence takes on special importance in the case of liquid solutions, since the various temperature changes of coordination number for different sorts of particles lead to substantial rearrangement of the structure of the solution as the temperature is changed: there is regrouping of the particles, as a result of which there is a change in the concentration in the solution of solvent particles which are not in the immediate vicinity of particles of the dissolved substance ("free" solvent).

Let us take a binary solution, consisting of particles of the sort a (solvent) and the sort b (dissolved substance). The change in the concentration of free solvent in the solution with change in temperature is related to the quantity

$$\delta_b = \left(\frac{\partial Z_{ba}}{\partial T}\right)_p - \left(\frac{\partial Z_{aa}}{\partial T}\right)_p, \tag{1}$$

where Z_{ba} is the mean number of particles of a surrounding a particle b in solution, and Z_{aa} is the same thing for the solvent particles.

The rearrangement of structure just mentioned is very important, in particular, in aqueous solutions of electrolytes. It is for just this reason that a number of the properties of such solutions are extremely dependent on the difference between the temperature variations of the coordination numbers of the ions in water solutions (the mean number of water molecules constituting the immediate surroundings of a given ion in solution) and the temperature variation of the coordination number of the molecules in the water. In [6] a thermochemical method was used to find the temperature variation of the coordination numbers of a number of monoatomic ions in dilute aqueous solutions. It was shown that the dependence of the corresponding quantities δ_i on the crystal-chemical radius of the ion r_i as a whole is given by a curve with a maximum at $r_i > r_{H_2O}$, where r_{H_2O} is the "radius" of a water molecule taken approximately equal to 1.38 A.

It is a matter of interest to find the value of δ_b for some liquid solution models. Let the solution consists of an assembly of a large number of spheres of diameter D_a forming the "liquid," to which is added a small number of spheres of diameter Db. The coordination number Z_{ba} is equal to

$$Z_{ba} = 2\lambda \int_0^{\rho_{\min}^{ba}} g_{ba}(\rho)\, \rho^2 d\rho, \tag{2}$$

where $\lambda = 2\pi D_a^3/v$ is the dimensionless density of the system, $g_{ba}(\rho)$ is the radial distribution function of the pair of particles b and a, and ρ^{ba}_{min} is the dimensionless distance from the origin of coordinates to the first minimum of the expression under the integral sign. Z_{aa} is expressed in a similar way. The function $g_{ba}(\rho)$ and $g_{aa}(\rho)$

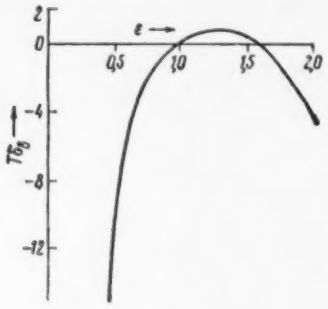

Fig. 1

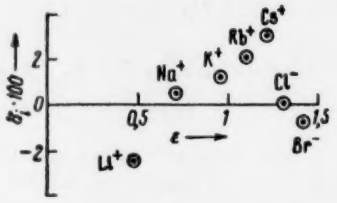

Fig. 2

have been found in the form of segments of series in powers of λ, by solving the Bogolyubov [7] integral equations for these functions for a system of spheres. Thus, $g_{ba}(\rho) = 0$ at $\rho < (1 + \varepsilon)/2$, and

$$g_{ba}(\rho) = 1 + \lambda g_{ba}^{(1)}(\rho) + \lambda^2 g_{ba}^{(2)}(\rho) + \ldots \tag{3}$$

at $\rho > (1 + \varepsilon)/2$. The functions $g^{(1)}_{ba}$ and $g^{(2)}_{ba}$ depend on the concentration of the solution n and the ratio of the particle diameters $\varepsilon = D_b/D_a$. The function $g_{aa}(\rho)$ is found from (3) at $\varepsilon = 1$. The series (3) were stopped in our work at the terms shown written, but it may be shown, that even at not small values of λ this does not lead to any substantial errors (although the whole calculation is then only qualitatively true). From (3) $(\partial Z_{ba}/\partial\lambda)$ and $(\partial Z_{aa}/\partial\lambda)$ may be found directly, and for a system of solid spheres, these values are independent of temperature. The derivatives $(\partial Z_{ba}/\partial T)_p$ and $(\partial Z_{aa}/\partial T)_p$ which interest us may be found from the relation

$$\left(\frac{\partial Z_{ba}}{\partial T}\right)_p = \frac{\partial Z_{ba}}{\partial \lambda}\left(\frac{\partial \lambda}{\partial T}\right)_p \tag{4}$$

using the equation of state of the system of spheres [7]

$$\frac{2\pi D_a^3}{kT} p = \lambda\left\{1 + \frac{1}{3}\lambda g_{aa}(1, \lambda)\right\}, \tag{5}$$

setting $n \to 0$ for a dilute solution.

We have made similar calculations for $\lambda = 5$, corresponding approximately with the density of a real aqueous solution, for 7 values of ε: 0.5, 0.75, 1.00, 1.25, 1.5, 1.75, and 2.00. The results of the calculations are given in Fig. 1 for a value of $T\delta_b$ from (1) as a function of ε. For comparison Fig. 2 gives the values of δ_i for monoatomic ions found in [6]. The obvious correspondence between the calculated results for a system of spheres and the experimental results of water solutions of electrolytes is important in connection with clearing up the nature of the function $\delta_i(r_i)$ for these solutions, in particular, the question of the extent to which the function $\delta_i(r_i)$ is determined by the specific interaction of the ions in molecules of water, and the extent to which it is determined by the ratio of the dimensions of the particles of the solution [6].

LITERATURE CITED

1. O. Ya. Samoilov, ZhFKh, 20, 1411 (1946).
2. O. Ya. Samoilov, Structure of Aqueous Solutions of Electrolytes and Hydration of Ions [in Russian] (Academy of Sciences Press, USSR, 1957).
3. I. Z. Fisher, Izv. AN SSSR, Metallurgiya i Toplivo, 6, 76 (1960).
4. V. K. Prokhorenko and I. Z. Fisher, ZhFKh, 31, 2145 (1957).
5. V. K. Prokhorenko and I. Z. Fisher, ZhFKh, 33, 1852 (1959).
6. M. N. Buslaeva and O. Ya. Samoilov, Zhurn. Strukturn. Khim. 2, 5, 551 (1961).
7. N. N. Bogolyubov, Problems of Dynamic Theory in Statistical Physics [in Russian] (Moscow, 1946).

POLARIZATION OF GAS ELECTRODES IN CONTACT WITH SOLID ELECTROLYTES

A. D. Neuimin, S. V. Karpachev, and S. F. Pal'guev

Institute of Electrochemistry of the Branch of the Academy of Sciences, USSR
(Presented by Academician A. N. Frumkin, June 24, 1961)
Translated from Doklady Akademii Nauk SSSR, Vol. 141, No. 2,
pp. 402-405, November, 1961
Original article submitted April 19, 1961

The question of the polarization of electrodes in the case of solid electrolytes is, at the present time, apparently, still completely uninvestigated. However, the study of this group of phenomena as applied to solid electrolytes is beyond any doubt a matter of interest.

As the electrolyte we chose a solid solution containing 85 mole % zirconium oxide and 15 mole % calcium oxide. From the data in the literature [1-4], the electrolyte mentioned is an ionic conductor at the temperatures at which our experiments were performed. Its electrical conductivity is caused, fundamentally, by the motion of oxygen ions, owing to the presence of a large number of empty oxygen nodes, arising during formation of the solid solution and the conductivity is substantially higher than in a number of other solid electrolytes. The free oxygen nodes arise in connection with the fact that when the solid solution is formed, the lattice of the cubic (stabilized) zirconium oxide is retained, and the calcium ions occupy part of the nodes intended for the zirconium ions [5-7].

The solid electrolyte was prepared by a method which has already been described in the literature [4]. In view of the nature of the electrolyte selected, it was decided to study the behavior of an oxygen electrode. To this end we investigated the following electrochemical circuit:

$$\text{Pt, } O_2 \;\Big|\; \begin{array}{l}\text{Solid electrolyte}\\ \text{85 mole \% } ZrO_2 + \text{15 mole \% CaO}\end{array} \;\Big|\; O_2\text{, Pt.} \qquad \text{(I)}$$

Setting up a cell of this sort is no different in principle from setting up the one described in detail in one of our papers [4]. We shall only note here, that the electrodes were thin porous layers prepared by bringing the necessary amount of platinum powder onto the electrolyte in a solution of rubber in benzene with subsequent backing.

The experiments with cell (I) were set up in the following way. Both platinum electrodes were in an atmosphere of air. A direct current was passed through the cell from an external source. One of the oxygen electrodes served as anode, the other as cathode. At each value of current, a potentiometer was used to measure the potential difference between the cell electrodes. The cell was kept in an electric furnace, the temperature of which was maintained with an accuracy of $\pm 2^\circ$ by a thermostat. The temperature was measured with a Pt – PtRh thermocouple. Before the measurements were started and after they were finished, the ohmic resistance of the electrolyte was measured with an alternating current bridge (frequency 3,000 cycles).

The measurements were made at temperatures of 900, 1000, 1100°C. The resistances of the electrolyte at these temperatures were respectively: 23.90, 7.93, and 3.80 ohms.

The relation between the current and the voltage at the cell electrodes taken from the measurements with direct current is shown graphically for the three temperatures in Fig. 1. It is clear from the figure that the voltage and the current are linearly related. The resistance of the electrolyte, found from the slope of the straight lines in Fig. 1, has the values 25.2, 8.3, and 3.86 ohms at 900, 1000, and 1100°C respectively. Comparing these figures with the values of electrolyte resistance measured directly, we can say that, at the temperatures indicated in the range of currents which we investigated, the overvoltage on the oxygen electrodes is insignificant. However, the possibility of a small over-voltage is not completely excluded, especially at 900°C. However, it must be kept in mind that we measured the total effect at both oxygen electrodes. For one oxygen electrode the effect would probably be less. Thus, it must be concluded that the over-voltage, if it exists at all on an oxygen electrode, is rather

small, and thus, at the temperatures mentioned it can be neglected in a number of cases. It is obvious that the oxygen pressure cannot be very small. Actually, the results of the experiments, which we made in a way similar to those described above, but with the air replaced by argon containing a small amount of oxygen ($P_{O_2} = 5 \cdot 10^{-4}$ atm), lead to the conclusion that there is considerable polarization of the electrodes, obviously due, basically, to concentration effects.

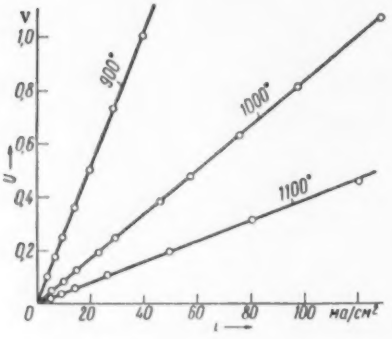

Fig. 1

In view of the small value of over-voltage on the oxygen electrode, it became possible to study the over-voltage on another electrode which replaced one of the oxygen electrodes in the cell (I). In order not to complicate the phenomenon being studied by having some solid substance liberated at one of the electrodes, we decided to investigate another gas electrode, choosing for this purpose a CO-electrode, and the following cell was considered

$$\text{Pt, CO+ CO}_2 \;\Big|\; \begin{matrix}\text{Solid electrolyte} \\ \text{85 mole \% + 15 mole \%}\end{matrix} \;\Big|\; \text{O}_2\text{, Pt.} \qquad \text{(II)}$$

The cell (II) was constructed in the same way as cell (I). Since, it contrast with cell (I), it gave an appreciable electromotive force, and the measurements could be made without an external source of the electromotive force. The cell was connected to a resistance box in series with an instrument for measuring the current. The current was varied by changing the resistance in the box. In this way a study was made of the anode polarization of the CO electrode.

The anode over-voltage on the CO electrode was determined from the following elementary equation

$$\eta = E_0 - Ir - IR, \qquad (1)$$

where η is the absolute value of the anode over-voltage at the CO electrode, E_0 is the absolute equilibrium value of the electromotive force of the cell (II), I is the current and r is the resistance of the electrolyte which was measured many times in the course of the experiment, always when changing from one current strength to another. IR is the potential drop in the external circuit measured directly with a potentiometer.

The oxygen electrode was bathed with a stream of pure oxygen, the CO electrode with a stream of the composition: 66 vol % CO + 34 vol % CO_2. The stream of this gas mixture was kept strong enough so that increasing it any more had no effect on the results of the measurements. The EMF of such a cell was sufficiently stable, that at temperatures above 900° it was practically equal to the thermodynamic value. This gives extra confirmation of the fact that the electrolyte selected is an ionic conductor, and shows that the electrodes being used at the above temperatures are reversible gas electrodes.

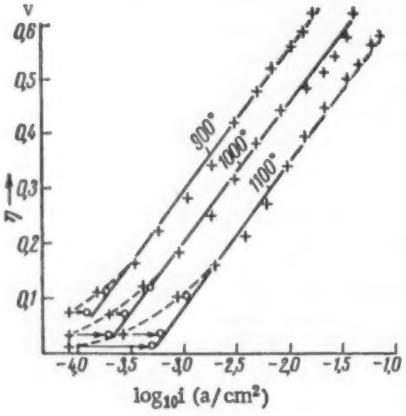

Fig. 2

In order to isolate the effect being measured in a more pure form, the surface of the CO electrode was taken twenty times less than the surface of the oxygen electrode.

The resistance of the solid electrolyte, measured on an alternating current bridge, drops somewhat as the current is increased. It is possible that this is caused by improvement in the contact between the electrodes and the solid electrolyte as the current strength increases. However, we did not make any special study of this phenomenon, since the ohmic potential drop in the electrolyte plays no particularly great role: at maximum current, it amounts to not more than 30% of the value of the over-voltage, and for mean values of current it is only about 6% of the over-voltage. The range from the smallest to mean currents includes more than half of all the measurements. Thus, even fairly inaccurate measurement of the ohmic resistance of the electrolyte introduces no substantial error into the over-voltage value.

	900°	1000°	1100°
b	0.258	0.250	0.260
α	0.45	0.51	0.52
a	1.068	0.953	0.866

Figure 2 gives a graphic representation at three temperatures of the over-voltage as a function of the logarithm of the current density at the CO electrode. As may be seen from the graph, at all three temperatures the relation between η and $\log_{10} i$ is expressed by straight lines, i.e.,

$$\eta = a + b \lg i. \tag{2}$$

Two electrons take part in the anode reaction at the CO electrode, so that it may be assumed that $b = \frac{2.3RT}{2F\alpha}$.

Table gives the values of b, α, and a for the three temperatures.

Talking about the temperature dependence of the quantities b, α and a does not seem to us to have much purpose, since the accuracy of our measurements is not great enough to establish a reliable relation from the relatively small temperature range over which we worked.

In considering Fig. 2, attention must be called to the fact that at small currents the experimental points depart very considerably from a straight line. It can be assumed, for example, that at small over-voltages the reverse current is not suppressed and has to be taken into account. In view of the fact that the value of α is only slightly different from 0.5 (see table) for the forward current, on the basis of Eq. (2) we can write:

$$\vec{i} = Ke^{\frac{\eta F}{RT}}. \tag{3}$$

The constant K may be expressed from (2) in terms of the constants a and b. We shall express the reverse current $\overleftarrow{i}$ by an equation, symmetric with (3):

$$\overleftarrow{i} = Ke^{-\frac{\eta F}{RT}}. \tag{4}$$

In the region of comparatively small over-voltages

$$\vec{i} = i + \overleftarrow{i}. \tag{5}$$

Here i is the measured current and $\vec{i}$ and $\overleftarrow{i}$ respectively the forward and reverse currents.

In the region of large over-voltages $\vec{i} \approx i$.

Using Eq. (4) for the points which deviate from the straight line in Fig. 2 the values of $\overleftarrow{i}$ were calculated, and then from (5) the values of $\vec{i}$. After this, the points in question were replotted on Fig. 2 with their abscissas changed from $\log_{10} i$ to $\log_{10} \vec{i}$. The change in these points is shown by arrows, and the new positions of the points are shown by circles. After being moved, the points fit well onto the straight lines. What we have said above enables us to conclude that the reverse reaction as small over-voltages is described by Eq. (4).

We note in conclusion that the CO electrode has a large over-voltage, the presence of which indicates retardation of the electrode reaction, in spite of the comparatively high temperatures at which the experiments were performed. To establish the mechanism of the phenomenon another series of investigations must be made.

LITERATURE CITED

1. K. Kuikkola and C. Wagner, J. Electrochem. Soc. 104, 379 (1959).
2. W. D. Kingery, J. Pappis, M. E. Doty, and D. C. Hill, J. Am. Ceram. Soc. 42, 393 (1959).
3. Z. S. Volchenkova and S. F. Pal'guev, Transactions of the Institute of Electrochemistry of the Ural'sk Branch of the Academy of Sciences, USSR [in Russian] (1960), No. 1, 119.
4. S. F. Pal'guev and A. D. Neuimin, Transactions of the Institute of Electrochemistry of the Ural'sk Branch of the Academy of Sciences, USSR [in Russian] (1960), No. 1, 111.
5. F. Hund, Zs. Phys. Chem. 199, 142 (1952).
6. A. I. Avgustinik and N. S. Antselovich, ZhFKh, 27, 973 (1953).
7. P. Duwerz, F. Odell, and F. H. Brown, J. Am. Ceram. Soc. 35, 107 (1952).

STRENGTHENING OF NICKEL SOLID SOLUTIONS

L. I. Pryakhina and L. A. Ryabtsev

A. A. Baikov Institute of Metallurgy, Academy of Sciences, USSR
(Presented by Academician I. I. Chernyaev, April 10, 1961)
Translated from Doklady Akademii Nauk SSSR, Vol. 141, No. 2,
pp. 406-408, November, 1961
Original article submitted April 8, 1961

Metals, which, in the solid state, are capable of dissolving atoms of other elements, undergo considerable strengthening in the process. This strengthening is caused by distortion of the crystal lattice of the solvent metal, as a result of which its mechanical strength is increased along with its specific electrical resistance, and other properties are changed as well. It was established a long time ago, and then repeatedly confirmed experimentally that there is a correlation between increased heat resistance of nickel solid solutions and an increase in the number of limitedly soluble elements making up the alloys [1, 2]. It was also shown that the greatest heat resistance is shown by alloys the composition of which is close to the maximum solubility limit [3-7]. It should be noted that these correlations were established in alloys belonging to various systems, in which the supersaturation of the solid solutions was brought about by introducing various types of elements. Therefore it was a matter of interest to study the laws governing the change in heat resistance of binary and more complicated nickel solid solutions by alloying them with some one element, for example aluminum, which forms limited solid solutions and metallic compounds with nickel.

As elements to be used to form a solid solution with nickel we selected the following: Cr, Ti, W, Mo, Nb, and Co. These elements form limited solid solutions with nickel, with the exception of cobalt, which forms a continuous series of solid solutions with nickel.

For the investigation we decided upon the following consistent set of nickel systems, each with a variable concentration of aluminum: Ni – Al, Ni – Cr – Al, Ni – Cr – Ti – Al, Ni – Cr – Ti – W – Al, Ni – Cr – Ti – W – Mo–Al, Ni – Cr – Ti – W – Mo – Nb – Al, Ni – Cr – Ti – W – Mo – Nb – Co – Al.

From the data on the limiting solubility of the above mentioned elements in nickel [8, 9], and the studies made previously [3-7], the compositions of the nickel solid solutions selected for our study were arranged in such a way that, except for aluminum, all the elements used would form unsaturated solid solutions. With this in mind, the alloys contained: Cr 10, Ti 2, W 6, Mo 3, Nb 2, and Co 5% by weight. Supersaturation of the solid solutions was brought about by one and only one element, namely aluminum, the concentration of which was varied from 0 to 12% by weight. At small aluminum concentrations the alloys were solid solutions. Increasing the aluminum concentration in the alloys caused supersaturation of the solid solutions accompanied by separation of the excess γ'-phase, which was the same for all the alloys studied, and the basis of which is the compound Ni_3Al, with a face-centered cubic lattice, differing somewhat from the lattice of nickel and its solid solutions.

The following data was taken on the samples alloyed in accordance with the above set of seven nickel systems: melting point of alloy, phase composition, physical chemical properties, including the crystal lattice parameters of the solid solutions, and tests were made on the heat resistance by the centrifugal method. This method made it possible to carry out a comparatively rapid study and establish a correlation between heat resistance and composition and structure of the alloys. All the alloys were tested under the same conditions: in the same furnace at 900°, and with the same constant stress of 12 kg/mm^2.

In figure based on our experiments [10], the upper part shows alloying diagrams, the phase composition of the alloys, and the solubility curves of aluminum in the alloys studied as a function of temperature. The middle part gives the crystal lattice parameters of nickel solid solutions at 1200°, and, finally, the bottom part gives composition – heat resistance diagrams for each of the alloy systems studied. The investigation has shown that as the aluminum concentration in each of the alloy systems is increased, strengthening of the solid solution occurs. This

is testified to by the curves and the composition – heat resistance diagrams, as well as the x-ray structure data, which showed that as the aluminum concentration in the alloys is increased an increase in the period of the crystal lattice of the nickel solid solutions occurs, and, consequently, there is an increase in the degree of deformation, which in turn causes strengthening of the solid solutions.

In every system studied, the greatest heat resistance is shown by the alloys in which increasing the aluminum concentration causes supersaturation of the solid solution and separation of excess γ'-phase in the finely dispersed state.

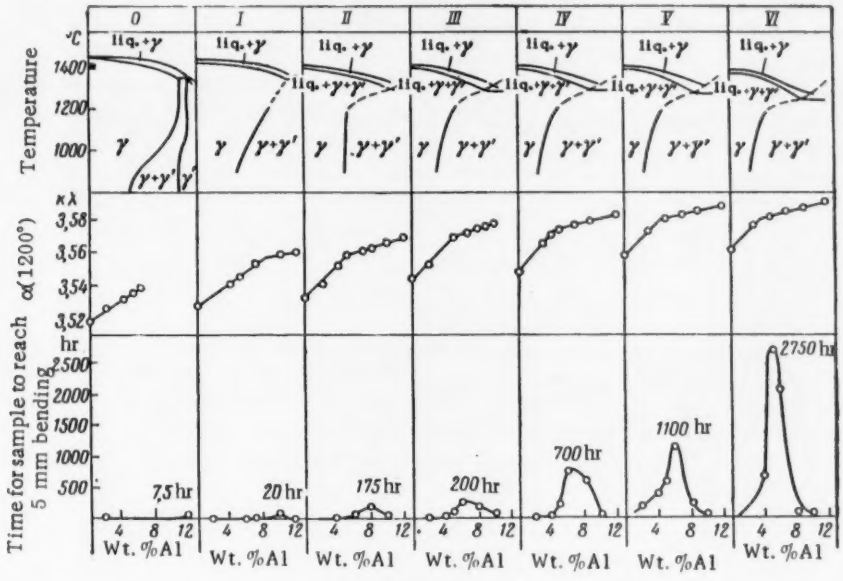

Fig. 1.

Comparing the heat resistance of alloys of different systems containing the same amount of aluminum shows that introducing an additional element into the nickel solid solution produces strengthening and increases the heat resistance of the alloy. Thus, for example, at 900° and a stress of 12 kg/mm^2, the alloy with 4% by weight of aluminum in the system Ni – Al was deformed to the limiting value in several minutes, an alloy with 4% by weight of aluminum in the system Ni – Cr – Ti – W – Al showed 5 mm bending after approximately 20 hours testing, while alloys with the same aluminum concentration in the systems Ni – Cr – Ti – W – Mo – Nb – Al and Ni – Cr – Ti – W – Mo – Nb – Co – Al showed 5 mm bending after 450 and 750 hours testing respectively.

X-ray structure studies have also shown that as the number of components in a nickel solid solution is increased, step-wise increase in the crystal lattice period occurs. The relative change in lattice period Δa from adding 1 atom % of an element to the solid solution increases in the order: Co, Cr, Ti, Mo, W, Nb. Consequently, the law which is followed is: as the element is further removed from nickel both in period and in group, the strenthening effect of the element on the nickel solid solution becomes greater.

This agrees with the data found in [11].

Comparison of the results for all the systems (see figure) shows that the absolute values of the heat resistance maxima of the alloys, found by the centrifugal method, increase in a step-wise fashion on going from a two component system to an eight component system as the number of elements entering into the composition of the solid solutions is increased. The highest heat resistance is shown by the alloys with the maximum amount of alloying in the eight component system.

Thus, the investigation again confirms the previously established correlation: increased heat resistance with increase in the number of organically dissolved elements entering into the solid solution.

The more complicated the chemical composition of the materials forming the base of the alloys of the solid solution, the greater the strength of the chemical bond between the diverse atoms and the nickel solid solution. Under conditions of limiting saturation and finely dispersed decomposition of the solid solutions, additional strengthening occurs.

LITERATURE CITED

1. I. I. Kornilov and L. I. Pryakhina, DAN, 112, 1, 70 (1957).
2. I. I. Kornilov, Izv. AN SSSR, OTN, 1, 119 (1956).
3. I. I. Kornilov, L. I. Pryakhina, and T. F. Chuiko, Izv. Sekt. Fiz.-Khim. Anal. 19, 437 (1949).
4. I. I. Kornilov and L. I. Pryakhina, Izv. AN SSSR, OTN, 7, 103 (1956).
5. I. I. Kornilov and L. I. Pryakhina, Collection of Papers on the Study of Heat Resistant Alloys [in Russian] (Academy of Sciences, USSR Press, 1956), p. 138.
6. I. I. Kornilov, L. I. Pryakhina, and O. V. Ozhimkova, Izv. AN SSSR, OKhN, 8, 885 (1956).
7. L. I. Pryakhina and L. A. Ryabtsev, Izv. AN SSSR, OTN, 12, 38 (1957).
8. I. I. Kornilov, Izv. AN SSSR, OKhN, 5, 475 (1950).
9. I. I. Kornilov, Izv. AN SSSR, OKhN, 6, 582 (1950).
10. I. I. Kornilov, L. I. Pryakhina, and L. A. Ryabtsev, Izv. AN SSSR, OTN, Metallurgiya i Toplivo, 2, 110 (1960).
11. Tyan' De-chen, Candidates Dissertation, A. A. Baikov Institute of Metallurgy, Academy of Sciences, USSR [in Russian] (1960).

All abbreviations of periodicals in the above bibliography are letter-by-letter transliterations of the abbreviations as given in the original Russian journal. *Some or all of this periodical literature may well be available in English translation.* A complete list of the cover-to-cover English translations appears at the back of this issue.

ELECTRON PARAMAGNETIC RESONANCE STUDY OF THE REACTION OF MOLECULAR OXYGEN WITH A STABLE FREE RADICAL IN SOLUTION

A. A. Revina and N. A. Bakh

Institute of Electrochemistry, Academy of Sciences, USSR
(Presented by Academician A. N. Frumkin, June 15, 1961)
Translated from Doklady Akademii Nauk SSSR, Vol. 141, No. 2,
pp. 409-412, November, 1961
Original article submitted May 13, 1961

In spite of the wide acceptance of the current radical-peroxide theory of the oxidation of organic compounds [1], there is still not much in the way of direct experimental data to give any idea of the initial products arising from combination with molecular oxygen. Recently, the EPR method has been used to observe and study the relatively stable peroxide radicals formed in the solid phase during the reaction of oxygen with the radicals arising from the action of ionizing radiation on teflon [2] and polyethylene [3], as well as during the reaction with the stable radical triparanitrothenylmethyl [4]. In contrast with solid polymers, in the majority of frozen low molecular compounds the stability of the radicals formed on irradiation is small at temperatures above 77°K, and the interaction with oxygen has been little studied.

In this respect, great interest is presented by the reactions taking place in the liquid phase during radiolysis, however, in view of the very small life time of the radicals arising in this case, any direct study of the transformations involved is a matter of great difficulty. Therefore, we felt that it was a good idea to make a preliminary EPR study of the reaction of oxygen with a stable radical dissolved in organic liquid. As the object of study we choose α,α'-diphenyl-β-picrylhydrazyl (DPPH), the EPR spectrum of which is quite well known. We know that at concentrations below 10^{-3} mole/liter a five-lined spectrum appears in DPPH solutions, corresponding with the interaction between an unpaired electron and the two nuclei of the central nitrogen atoms [5]. Recently, splitting of the lines of the five-lined DPPH spectrum has been observed experimentally, caused by the protons of the phenyl rings in the ortho and para position [6], as was predicted by theory [7].

This hyperfine structure appears, however, only after exceedingly careful removal of traces of oxygen, and with high resolving power of the apparatus. In our study, we have made use of a type ÉPR-2 IKhF [8] spectrometer. In benzene solutions of DPPH * the five-lined spectra were found, without any additional hyperfine structure. The number of paramagnetic centers in the sample was determined from the integrated area of the resonance absorption curve, calibrated by means of a carefully evacuated benzene solution of DPPH of known concentration. A 0.08 cc portion of solution was taken for each experiment. The reaction with oxygen was studied from the change in the EPR spectra.

Figure 1 shows the spectra obtained with fixed sensitivity of the apparatus in the initial solution evacuated to $8 \cdot 10^{-4}$ moles/liter (a), in the same sample after letting in air at atmospheric pressure (b), and oxygen (c), and, finally, after repeated evacuation just after letting in O_2 (d). As may be seen, the asymmetric spectrum characteristic of peroxide radicals does not appear. Contact with oxygen causes widening of the lines right up to complete disappearance of the hyperfine structure, and reduction of intensity, however, on removing the oxygen directly after it was let in, the original completely resolved spectrum is restored. Thus, the oxygen causes not only widening of the lines, but a reversible reduction in the total number of paramagnetic centers as well, as may be seen from the data given below, calculated from the spectra given in Fig. 1.

* A preparation recrystallized from benzene, prepared by the method of Arbuzov and Valitova [9] was kindly placed at our disposal by the inventors of the synthesis.

Atmosphere:	Vacuum	O_2, 150 mm Hg	O_2, 760 mm Hg	Vacuum
Number of paramagnetic centers	$4 \cdot 10^{16}$	$3.4 \cdot 10^{16}$	$3.0 \cdot 10^{16}$	$3.8 \cdot 10^{16}$
Width of spectrum	50 oersted	60 oersted	72 oersted	50 oersted

The sensitivity of measurement at the spectrum width in question was $3\text{-}4 \cdot 10^{14}$ paramagnetic centers in the sample.

To find the effect of length of time of interaction with O_2, the following experiments were set up: after preliminary evacuation and sealing off of 1-2 control samples, O_2 at atmospheric pressure was added simultaneously to 10-15 identical 0.08 cc portions of DPPH solution containing $4 \cdot 10^{16}$ paramagnetic centers each. The ampules were then sealed off at a ratio of gas to liquid volume of ~8, and stored at ordinary temperature.

Fig. 1. EPR spectra of benzene solutions of DPPH ($8 \cdot 10^{-4}$ moles/liter) signal from vacuum sample (a), after letting in air (b), oxygen (c) at atmospheric pressure, and after repeated evacuation of oxygen (d).

After definite periods of time the EPR spectra were taken, first in the presence of oxygen, and then directly after it had been removed by evacuation. Figure 2 gives the free radical content in oxygen and vacuum samples as a function of the time of contact between DPPH and oxygen. Both the number of radicals in the presence of oxygen and the number regenerated on evacuation drop off gradually. Simultaneously there is reduction in the intensity of the coloration characteristic of DPPH. After 90 24 hour periods, radicals are no longer observable in the presence of O_2, but they still show up again after the oxygen has been removed. In solutions which contain no O_2 in the first place, the number of radicals is practically unchanged in the same length of time.

The disappearance rate of DPPH depends on the total quantity of O_2 in the closed system, as illustrated by Fig. 3 in which the curves correspond with various O_2 ratios in the gaseous and liquid phase, from $V_{gas}/V_{liq} \sim 8$ to $V_{gas}/V_{liq} \sim 100$.

To changes just described in the DPPH resonance spectra in the presence of O_2 may be interpreted as a superposition of two different effects: 1) a purely physical interaction, caused by the paramagnetic properties of the O_2 molecule, which produces line broadening but has no effect on the number of unpaired electrons in the system, and 2) an interaction which may be regarded as chemical, leading to disappearance of the DPPH radicals from the formation of a non-radical compound of peroxide type, decomposing reversibly when the oxygen is removed, and converted to the final products of oxidation of DPPH when oxygen is present. As the peroxide disappears, being in equilibrium with the dissolved O_2 and the DPPH radicals, the latter should be consumed too, which is observed experimentally.

Comparison of the curves of Fig. 3 shows that the rate of consumption of the radicals, which is initially independent of the quantity of O_2 in the system, remains constant up to complete disappearance of the radicals only with a large excess of O_2. The less oxygen there is in the system, the earlier sharp retardation of the process sets in. This enables us to conclude that the formation of the primary norm-radical peroxide compound is a fast reaction, limited by the access of O_2 from the gaseous phase. The subsequent transformations are of a complicated sort, and to elucidate them requires more detailed study. Consideration should be given to the fact that the observed consumption of O_2 is substantially greater than the consumption of DPPH. This may be explained by the solvent being involved in the oxidation reaction, as shown by the presence of phenol among the reaction products in an amount exceeding the number of phenyl groups in DPPH, as well as by the effect of the nature of the solvent on the oxidation rate. Under these same conditions in n-heptane, the DPPH radicals disappear after several hours in the presence of O_2.

A similar sort of interaction with oxygen may be used to explain the observed reversible signal broadening and reduction in intensity in the presence of O_2 with crystalline DPPH [10], as opposed to the interpretation of the authors who assume that no actual reduction in the number of free radicals occurs.

The formation of a reversible molecular peroxide from the reaction of free radicals with oxygen in solution has, up to the present time, as far as we know, not been described in the literature, and represents a very early stage

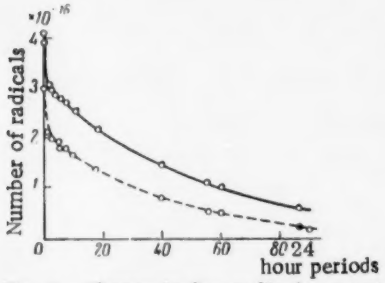

Fig. 2. Change in free radical content in vacuum (solid curve) and oxygen (dotted curve) samples with time of contact between DPPH and O_2.

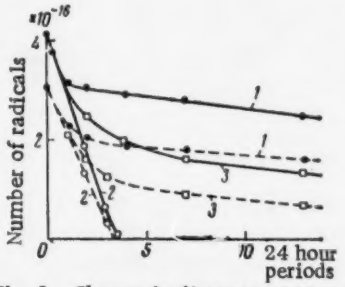

Fig. 3. Change in disappearance rate of DPPH as a function of the total amount of O_2 in the sample. Volume ratios of gaseous to liquid phase are ~ 8 (1), ~ 100 (2), ~ 50 (3). Solid curve for vacuum samples, dotted curve for oxygen samples.

of the oxidation reaction, which it was possible to observe by means of EPR. It may be assumed that a stage of this sort is a rather common thing in oxidation reactions. The mechanism of formation of the peroxide requires further consideration, as well as the problem of the similarities and differences between the formation of reversible peroxides in the liquid phase and on solid surfaces [11].

We consider it our pleasant duty to express sincere gratitude to Professor L. A. Blyumenfel'd for his valuable suggestions in discussing the results.

LITERATURE CITED

1. N. N. Semenov, Some Problems of Chemical Kinetics and Reactivity [in Russian] (Academy of Sciences Press, USSR, 1958).
2. Yu. D. Tsvetkov, Ya. S. Lebedev, and V. V. Voevodskii, Vysokomolek Soed. 1, 1518 (1959); A. N. Rexroad and W. Gordy, J. Chem. Phys. 30, 399 (1959); T. Matsugashita and K. Shinohara, J. Chem. Phys. 32, 954 (1960).
3. B. R. Loy, J. Polymer Sci. 44, 341 (1960).
4. F. M. Schimmel and F. W. Heineken, Physica, 23, 781 (1957).
5. C. A. Hutchinson and Y. R. C. Pastor, J. Chem. Phys. 20, 534 (1952); C. Kikuchi, Phys. Rev. 93, 394 (1954).
6. J. Deduchi, J. Chem. Phys. 32, 1584 (1960).
7. T. H. Brown, D. H. Anderson, and H. S. Gutowsky, J. Chem. Phys. 33, 720 (1960); H. S. Gutowsky, H. Kusumoto, T. H. Brown, and D. H. Anderson, J. Chem. Phys. 30, 960 (1959).
8. A. T. Semenov and N. N. Bubnov, Pribory i Tekhn. Eksperim. 1, 92 (1959).
9. A. E. Arbuzov and F. G. Valitova, ZhOKh, 27, 2354 (1957).
10. J. E. Bennett and E. J. H. Morgan, Nature, 182, 199 (1958).
11. A. N. Frumkin, Adsorption and Oxidation Processes, IV Bakhov Lecture [in Russian] (Academy of Sciences Press, USSR, 1951).

All abbreviations of periodicals in the above bibliography are letter-by-letter transliterations of the abbreviations as given in the original Russian journal. *Some or all of this periodical literature may well be available in English translation.* A complete list of the cover-to-cover English translations appears at the back of this issue.

DECOMPOSITION KINETICS OF ALKALI METAL AMALGAMS IN BUFFER SOLUTIONS

Academician A. N. Frumkin, V. N. Korshunov,

and Z. A. Iofa

M. V. Lomonosov Moscow State University
Translated from Doklady Akademii Nauk SSSR, Vol. 141, No. 2,
pp. 413-416, November, 1961
Original article submitted July 21, 1961

It has been shown previously [1] that the reaction rate of the decomposition of alkali metal amalgams by electrolyte solutions with a high pH value (> 10) in the absence of catalytically active impurities is independent of the composition, the concentration, and the pH of the solution, and is determined solely by the concentration of the amalgam, obeying the kinetic equation

$$i = kC_{am} \quad (1)$$

where i is the decomposition rate of the amalgam in amp/cm^2, C_{am} is the concentration of the amalgam in g.eq/liter and k is a constant. These facts have lead to the conclusion that in a strongly alkaline medium the decomposition of amalgams proceeds by direct interaction of the atoms of the metal in the amalgam with water molecules, without any particular cathode or anode processes, which occur only if impurities are present to lower the hydrogen overvoltage. On the other hand, according to data in the literature [2], the decomposition of dilute amalgams in buffer solutions with pH ~ 7-9 obeys the Bronsted-Kane equation

$$i = kC^{0.5}_{am} \quad (2)$$

which may easily be derived from electrochemical concepts [3, 4]. It seemed important to find out whether there is a real difference in mechanism between the decomposition of amalgams at higher and lower pH values, or whether the decomposition of the amalgam according to an electrochemical mechanism, as described in the references cited, occurs simply because catalytically active impurities are present. To elucidate this problem we made a study of the decomposition kinetics of potassium amalgams in 0.33 N phosphate buffer solutions in the pH range 7-10, using a technique or purifying the solutions and amalgams and measuring the decomposition kinetics which is practically identical with that described in [1]. The buffer solutions were prepared by mixing the necessary quantities of 0.33 N solutions of KOH and KH_2PO_4. The polystyrol apparatus in which the measurements were made was similar to that used in [1], but had smaller dimensions: the volume of solution was 100 ml, the area of the amalgam mirror was 4.5 cm^2, and the temperature was 20 ± 1°C.

The data which we obtained on the decomposition rate, or potassium amalgams of different concentrations (from 0.02 to 1.4 N) in 0.33 N phosphate buffer solutions (pH 7-10) is given in Fig. 1 in the coordinates: amalgam potential against normal claomel electrode-logarithm of the decomposition current density (curves 1-4). In the more acid buffer solutions we also made direct polarization measurements on the liberation of hydrogen at the mercury (curves 5-7).

As may be seen from Fig. 1 (curves 2-4), there is a linear relationship between the amalgam potentials and the logarithm of the decomposition rate with a slope b, close to 0.115 v. A similar relationship is also observed in the acid buffer solutions with cathode polarization of the mercury (curves 5-7), a potassium amalgam beginning to be formed at high current densities. In this case the polarization curve was taken by a method described in [5]. The probable cause of the kink in curve 1 will be spoken of below.

The data of Fig. 1 was used to construct Figs. 2 and 3. Figure 2 gives the electrode potential as a function of the pH of the solution for $i = 10^{-4}$ amp/cm^2. For comparison, the same figure shows similar data obtained previously by V. S. Bagotskii and I. E. Yablokova [6] from polarization measurements in acid buffer solutions, prepared by adding HCl to 0.3 N K_3PO_4 solution. As may be seen, their data is very close to ours.

Consideration of Fig. 2 shows that there is a continuous linear relationship between the electrode potential at i = const and the pH of the solution, right up to pH ~ 10 with a slope close to the theoretical value 0.111 v. This means that both in acid medium on mercury and in moderately alkaline medium on amalgams, the discharge of

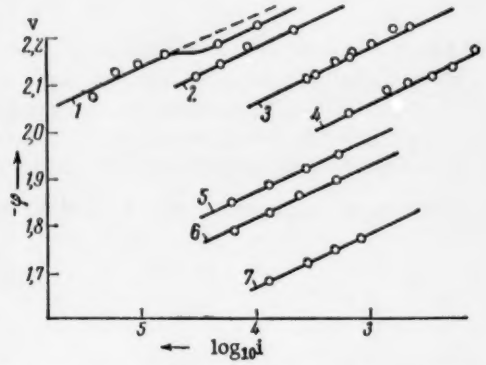

Fig. 1. φ–$\log_{10} i$ curves of potassium – mercury amalgams taken in 0.33 N phosphate buffer solutions. 1) pH 9.8; 2) pH 9.0; 3) pH 7.9; 4) pH 7.0; 5) pH 6.7; 6) pH 6.1; 7) pH 4.6.

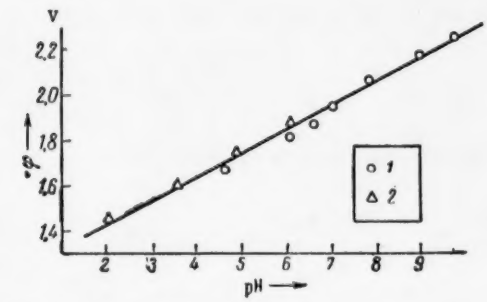

Fig. 2. Electrode potential as a function of pH at $i = 10^{-4}$ amp/cm^2. 1) Our data; 2) data of Bagotskii and Yablokova.

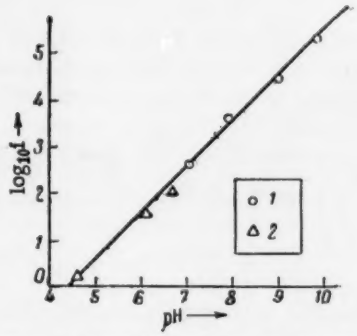

Fig. 3. Logarithm of current density of hydrogen liberation as a function of pH of buffer solution at φ = 2.100 v. 1) Points, taken on potassium amalgams; 2) on mercury.

H_3O^+ ions proceeds according to the electrochemical mechanism and the discharge rate is determined by the hydrogen overvoltage on the mercury under the prevailing conditions. The fact that the straight line φ – pH (i = const) as well as the straight lines $\varphi - \log_{10} i$ (curves 5-7) (Fig. 1) maintain constant slope up to high current densities also shows that the alkali metal dissolved in mercury has no substantial effect on the value of the hydrogen overvoltage. Analyzing the curve of Fig. 2 leads to the conclusion that up to pH ~ 10 neither the buffer anions nor the water molecules take part directly in the electrode reaction. Discharge of the latter, apparently, occurs only at the more negative potentials, attainable, for example, during cathode polarization of mercury in solutions of tetraalkylammonium salts [7].

Figure 3 illustrates the variation of the logarithm of the hydrogen liberation current density during mercury polarization and during decomposition of potassium amalgams in buffer solutions with variable pH of the solution and φ = const. As may be seen from the figure, there is direct proportionality between the hydrogen liberation rate (including decomposition of the amalgam) and the concentration of H_3O^+ ions. As far as from the theory of delayed discharge, an increase in the total concentration of the electrolyte at pH = const should increase the hydrogen overvoltage and reduce the discharge rate of the H_3O^+ ions, since the negative value of ψ_1-potential is reduced. This conclusion* is confirmed by the experiments, the results of which are given in table.

Thus, the decomposition kinetics of alkali metal amalgams in buffer solutions with pH < 10 depends, in accordance with the data in the literature, not only on the concentration of the amalgam, but on the composition

* In more concentrated buffer solutions, however, as the concentration of the buffer is increased, lowering of the hydrogen overvoltage is observed, the more so, the higher the concentration. This effect requires further investigation.

Composition of solution	pH	C_{am}(N)	$-\varphi$	$-\text{Log}\ i$
0.1 N (KOH + KH_2PO_4)	7.6	0.048	2.130	3.31
0.1 N (KOH P KH_2PO_4) + 1.25 N KCl	7.6	0.044	2.062	4.10

concentration, and pH of the solution, and obeys laws derived from the assumption of an electrochemical mechanism for the reaction. On the other hand, as was shown in [1] in a strongly alkaline medium there is a chemical reaction between the metal of the amalgam and the molecules of water. The difference in mechanisms causes the difference between the kinetic Eqs. (1) and (2). In order to give an over-all picture of the decomposition of alkali metal amalgams in aqueous solutions, we may assume that at any pH value two independent and simultaneous reactions occur:

a) An electrochemical reaction consisting of the conjugated stages – ionization of the metal of the amalgam:

$$MeHg \rightleftarrows Me^+ + e^- + Hg \tag{3a}$$

and the irreversible stage of the discharge of H_3O + ions:

$$H_3O^+ + e^- \rightarrow {}^1/_2H_2 + H_2O; \tag{3b}$$

b) A chemical stage, proceeding in one act according to the scheme:

$$MeHg + H_2O \rightarrow Me^+ + {}^1/_2H_2 + OH^- + Hg. \tag{4}$$

The kinetic equation for the reaction (3b), obtained by combining the electrochemical kinetic equation for the discharge reaction of the H_3O + ions:

$$i = k\,[H_3O^+]\,e^{-\alpha\varphi F/RT} \tag{5}$$

with the thermodynamic equation, relating the potential of the amalgam with its concentration,

$$\varphi = \varphi_0 - \frac{RT}{F}\ln\frac{a_{Me}}{a_{Me^+}} = \varphi_0' - B\log_{10}C_{am} \tag{6}$$

has the form:

$$i_e = k_1\,[H_3O^+]\,C_{am}^{B/0,116} = k_1\,[H_3O^+]\,C_{am}^n \quad (n \geqslant 0{,}5) \tag{7}$$

(the coefficient B, which takes account of the deviation of the amalgams from the properties of ideal solutions, is equal to 0.058 v at 20° for dilute amalgams, and rises rapidly for amalgams which are nearly saturated). Equation (7) goes over into the Bronsted-Kane equation (2) for dilute amalgams at constant solution pH. The kinetics of reaction (4) is determined by the equation:

$$i_x = k_2'C_{am}[H_2O] = k_2C_{am}. \tag{1a}$$

According to the assumption made above, the decomposition current density of an amalgam in any given case is the sum of the densities of the currents from the electrochemical and chemical components of the reaction, and is determined by the equation:

$$i_{dec} = i_e + i_{ch} = k_1\,[H_3O^+]\,C_{am}^n + k_2C_{am}. \tag{8}$$

In buffer solutions with not very high pH, the value of $k_1[H_3O^+]$ in Eq. (7) is large enough so that the electrochemical component of the current (7) is considerably higher than the current from the chemical reaction (1a), the rate constant k_2, of which is small [1]. The kinetics of the amalgam decomposition reaction under these conditions is determined by the rate of the reaction (3b), and obeys Eq. (7) of which Eq. (2) is a special case.

In solutions with high pH (> 10), the value of $k_1 [H_3O^+]$ becomes so small, that the current density from the chemical reaction (1a) becomes higher than the current from the electrochemical component (7). In this case the kinetics of the amalgam decomposition reaction is determined by the rate of reaction (4), and obeys Eq. (1).

In the range of solution pH about Fig. where the values of i_e and i_{ch} are comparable with one another a mixed type of kinetic law occurs. This latter fact is confirmed by consideration of the form of the curve 1 (Fig. 1), which is for a solution with pH 9.8. Calculation shows that for the potentials of the lower part of curve 1 discharge of H_3O^+ ions according to the electrochemical mechanism predominates, but after reaching considerable amalgam concentrations, the value of the current, calculated from (1a), increases, and, adding onto the current from the electrochemical component, distorts the linear relationship. Using the value of the constant k_2 which we found in [1] for a potassium amalgam, we made a correction to the decomposition current according to scheme (4). As a result of the correction, instead of the upper part of curve 1, we obtained the dotted straight line which is a projection of the original linear part of the curve.

The treatment here given of the process of hydrogen liberation from phosphate buffers is, however, incomplete, since we have not considered the question of sources for completing the discharged H_3O^+ ions. In the solutions which we have studied, the diffusion of H_3O^+ ions from the volume of the solution is of practically no importance because of the small concentration of these ions, and the proton donors in the volume of the solution must be water molecules or phosphoric acid anions. Calculation shows that the dissociation of water can provide a current density not exceeding $3 \cdot 10^{-6}$ amp/cm^2 at pH 8, and $3 \cdot 10^{-7}$ at pH 10 [8, 9]. Thus, the principle source of protons in the case under consideration must be buffer anions. The kinetic limitations, which the finite dissociation rate of the anion places on the hydrogen liberation reaction, were considered in [10]. Comparison of the conclusions of this paper with our results will be the object of subsequent investigation.

LITERATURE CITED

1. V. N. Korshunov and Z. A. Iofa, DAN, 141, 1 (1961).
2. J. Brönsted and N. Kane, J. Am. Chem. Soc. 53, 3624 (1931); F. Fletcher and M. Kilpatrick, J. Phys. Chem. 42, 113 (1938); W. Dunning and M. Kilpatrick, J. Phys. Chem. 42, 215 (1938); S. I. Sklyarenko and B. A. Sakharov, ZhFKh, 21, 97 (1947); G. Trümpler and K. Gut, Helv. Chim. Acta. 33, 1922 (1950); 34, 2044 (1951).
3. A. N. Frumkin, Zs. Phys. Chem. A160, 116 (1932).
4. L. Hammet and A. Lorch, J. Am. Chem. Soc. 54, 2128 (1932).
5. J. O' M. Bockris and R. Watson, J. Chim. Phys. 49, 70 (1952).
6. V. S. Bagotskii and I. E. Yablokova, ZhFKh, 23, 413 (1949).
7. Z. A. Iofa, A. N. Frumkin, and E. A. Maznichenko, ZhFKh, 31, 2042 (1957).
8. P. Delahay, J. Am. Chem. Soc. 74, 3497 (1952).
9. A. N. Frumkin, Advances of Electrochemistry, 1 (1961).
10. H. Nürnberg, G. Riesenbeck, and M. V. Stackelberg, Zs. Elektrochem. 64, 130 (1960); Collection, 26, 126 (1961).

All abbreviations of periodicals in the above bibliography are letter-by-letter transliterations of the abbreviations as given in the original Russian journal. *Some or all of this periodical literature may well be available in English translation.* A complete list of the cover-to-cover English translations appears at the back of this issue.

THE EFFECT OF OXYGEN ATOMS ON BURNING AT LOW PRESSURES

V. Ya. Basevich and S. M. Kogarko

Institute of Chemical Physics, Academy of Sciences, USSR
(Presented by Academician V. N. Kondrat'ev, May 12, 1961)
Translated from Doklady Akademii Nauk SSSR, Vol. 141, No. 3,
pp. 659-661, November, 1961
Original article submitted May 12, 1961

In observing the acceleration of burning processes at atmospheric pressure by the action of atoms and radicals [1-5] and in examining rarified atomic flames [6] the existence of which has been known for a long period of time [6], it is possible to discern common phenomena in the mechanism. In the first case if the admixture of atoms and radicals accelerate the oxidation process, then in the second case, under conditions of low temperatures, the reactions of the atoms and radicals with the fuel are the main process. An analogous phenomenon also occurs with spontaneous ignition [7-9].

In an earlier work [10] it was found in the case of acetylene and oxygen that there is a region where the atomic flames obtained at comparatively high pressures of several millimeters of mercury co-exist with the usual flames when burning may already occur independently. Commencing from the theory that the mechanism of atomic and usual flames are the same and also by considering the part played in the flames by the primary concentrations of the active reaction centers, in the present work we investigated the question of the action of atomic oxygen on the flame propagation velocity at low pressures and we also investigated the possibility of lowering the inflammable limit by varying the pressure before reaching the region where atomic flames exist.

Method. The oxygen atoms were obtained from a glow discharge by the well known method, only in this case in order to extend the region of the discharge ignition in the direction of higher pressures, the apparatus was designed so that it was possible to operate the apparatus with small distances between the electrodes (Fig. 1). Oxygen from a cylinder, after passing through an orifice plate and discharge tube through an expanding nozzle, with diameter 4 mm, enters into a reservoir, with diameter 60 · 110 mm. The combustible gas (commerical propane-butane) after passing through an orifice plate flows into the receiver through an annular orifice, width 1 mm, concentric with the nozzle. Central and lateral electrodes are placed in the reservoir to ignite the mixture with a spark of constant energy of about 0.45 joules. A frame enclosing a 15 μ wire gauze can be placed inside the nozzle thus serving for the recombination of oxygen atoms formed in the discharge. The frame is fastened to the central electrode. It is possible to replace the lateral electrode by a thermocouple, diameter 0.2 mm which either measures the heat of recombination or (with the insertion of the gauze) the temperature of the gas escaping from the nozzle. The reservoir was evacuated by a fore vacuum pump, the pressure being measured by a standard vacuum gauge. The visible flame propagation velocity was recorded photographically through an aperture. In some control experiments the contour of the flame front was photographed. The flame speeds were compared in the investigation because the degree of extension due to the flow from the receiver and the escape of heat at the wall could not be determined. In determining how the inflammability limit varies with pressure the flash was recorded in the whole volume of the receiver.

The experiments were carried out: 1) with cut-off of the glow discharge; 2) with the glow discharge but with the grating required for recombination set up in the nozzle; 3) with the glow discharge but without the gauze. In the second case there was either partial or complete recombination which depended on the discharge current and pressure. This may be established by the presence or absence of the afterflow of NO_2^* obtained as a consequence of the presence of some nitrogen in the oxygen. The existence of partial or complete recombination may also be found from the thermocouple readings: the temperature of the junction at maximum discharge currents in the tube ($i_2 \leq$ $\leq$ 900 mA) was $\leq 60°C$. In the last case, in the absence of the gauze, the temperature of the junction increased to 420° which permitted us to estimate the maximum concentration of oxygen over the nozzle section by an order of magnitude of 10%.

Obviously, the temperature of the gas coming from the glow discharge tube is close to room temperature (cf. also Harteck and Kopsch [6]) and in every case of the discharge in the presence of the gauze it was not less than that given by the discharge without a gauze because only a fraction of a second is required to heat the 15 μ wire gauze.

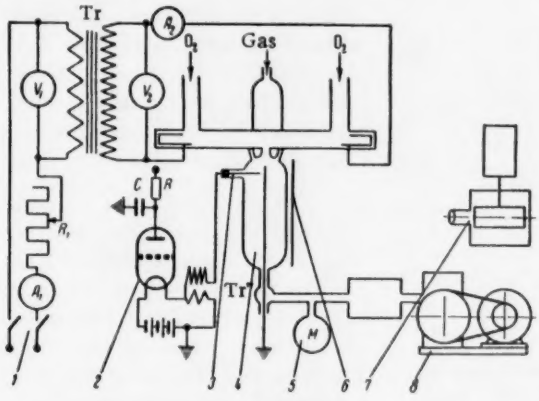

Fig. 1. Sketch of apparatus. 1) Electrical method for glow discharge; 2) generator for spark discharge; 3) discharge tube; 4) reservoir; 5) vacuum gauge; 6) aperture; 7) photo-recorder; 8) fore vacuum pump.

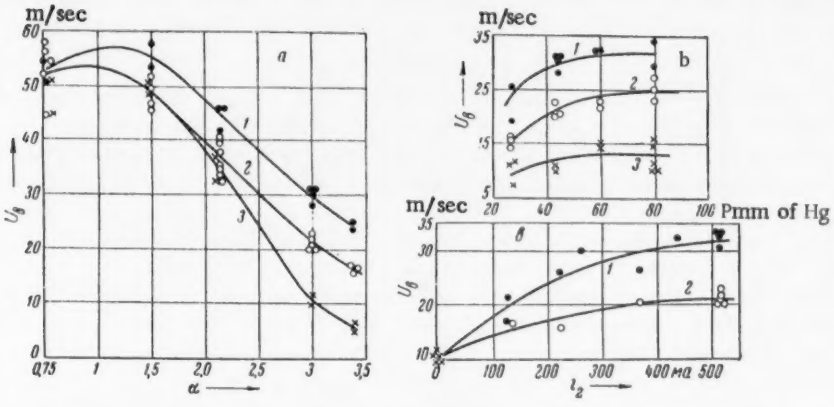

Fig. 2. Visible flame propagation speeds with a spark ignition: 1) Discharge; 2) discharge with the gauze in the nozzle; 3) without discharge. a) Variation of flame speed with composition, P = 43 mm of Hg; b) variation of flame speed with pressure, $\alpha = 3$; c) variation of flame speed with current, P = 43 mm of Hg; $\alpha = 3$.

Results and discussion. In the first series of experiments the distance between the electrodes of the glow discharge was 170 mm. The visible flame propagation speeds resulting from the spark were compared. In this series of tests the average flow velocity from the nozzle did not exceed 1 m/sec. The values of the flame speeds U_V at a pressure of P = 43 mm of Hg for different coefficients of excess oxygen are given in Fig. 2a. It is clear that in the presence of oxygen atoms the flame speed in regions of lean compositions rises very considerably. The discharge current field in the tube is selected so that by switching on, spontaneous ignition of the mixture in the reservoir does not occur. Consequently, the value of the flame speed differed depending on the composition of the mixture: greater with lean compositions and lower with rich mixtures right up to the value $\alpha = 0.75$. The seemingly small effect of the oxygen atoms on the value of U_V in regions of rich mixtures is also explained by the small permissible dis-

charge current field. Figure 2b gives the values of the speeds at different pressures with the coefficient of excess oxygen $\alpha = 3$, with the same discharge current. An increase of the discharge current leading to an increase in the concentration of oxygen atoms increases the visible flame speed (Fig. 2c). The measurements showed that an increase in the velocity of the gas from the discharge tube into the reservoir very noticeably increases the flame speed above the values referred to in the previous discussion. In the case of a discharge with and without the gauze, a similar change in the flow velocity does not cause a variation in the flame speed. The experiments showed a considerable increase in the flame luminescence in the presence of atomic oxygen.

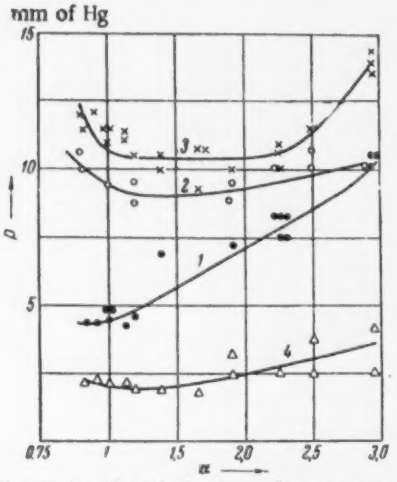

Fig. 3. Burning limits depending on pressure. Spark ignition: 1) Discharge; 2) discharge with the gauze in the nozzle; 3) without discharge; 4) spontaneous ignition.

In the second series of tests the possibility of reducing the inflammability limit with pressure which is obtained under the experimental conditions described (Fig. 3) was investigated. In this series of tests the oxygen supply was increased and the amount of combustible gas almost doubled and the distance between the electrodes increased to 1000 mm. As can be seen, the inflammability limit obtained with spark ignition is about 10 mm of Hg; with the glow discharge switched on first ($i_2 \leq 400$ mA), but in the presence of the grating the inflammability limit is about 9 mm of Hg. By increasing the discharge current in the tube to 900 mA it is possible to cause spontaneous ignition in the reservoir at a pressure of 2 mm of Hg which then corresponds to the region where atomic flames exist. Obviously, by increasing the rate of evacuation and the distance between the electrodes, the inflammability limit may be reduced to pressures at which work is usually carried out with atomic flames, i.e., 0.1-4 mm of Hg [6, 10].

LITERATURE CITED

1. S. W. Churchill, A. Weir, K. L. Gealer, and K. I. Kelley, Ind. and Eng. Chem. 49, 1419 (1957).
2. S. M. Kogarko, M. I. Devishev, and V. Ya. Basevich, Zhur. Fiz. Khim. 33, 2345 (1959).
3. S. M. Kogarko, M. I. Devishev, and V. Ya. Basevich, Dokl. Akad. Nauk. 127, 137 (1959).
4. S. M. Kogarko, M. I. Devishev, and V. Ya. Basevich, Izv. Akad. Nauk. SSSR, OTN, Energetics and Automatics, 3, 138 (1960).
5. S. M. Kogarko, V. V. Mikheev, and V. Ya. Basevich, Zhur. Fiz. Khim. 35, 10 (1961).
6. P. Harteck and U. Kopsch, Zs. Phys. Chem. B12, 327 (1931).
7. V. N. Semenov, F. I. Dubovitskii, and A. B. Nalbandyan, Trans. Farad. Soc. 29, 606 (1933).
8. A. Nalbandyan, Acta. Physicochem. USSR, 1, 305 (1934).
9. A. B. Nalbandyan, Phys. Zs. Soviet union, 4, 747 (1933).
10. A. G. Gaydon and H. G. Wolfhard, Proc. Roy. Soc. A213, 366 (1952).

All abbreviations of periodicals in the above bibliography are letter-by-letter transliterations of the abbreviations as given in the original Russian journal. *Some or all of this periodical literature may well be available in English translation.* A complete list of the cover-to-cover English translations appears at the back of this issue.

THE EFFECT OF THERMAL INTERACTION ON SYSTEMS CONSISTING OF POLYMERS AND DISPERSE METALS

S. D. Levina, K. P. Lobanova, and A. V. Vannikov

Institute of Electrochemistry, Academy of Sciences, USSR
(Presented by Academician A. N. Frumkin, July 11, 1961)
Translated from Doklady Akademii Nauk SSSR, Vol. 141, No. 3,
pp. 662-664, November, 1961
Original article submitted July 8, 1961

As we have shown [1], several systems consisting of organic polymers and highly disperse metals possess certain electrophysical properties characteristic for semiconductors. When compared with the many organic semiconductors described in the literature [2-8] these systems in the first place are characterized by small values of the electric resistance. So, at room temperature the resistance of metal-polymer systems amounts to a few ohms, sometimes even to tenths of an ohm. The values of the activation energy of conductivity, as were found from the relation between electric conductivity and temperature, varied between 0.08 and 0.2 ev.

By modifying the preparation method of some of these compositions we succeeded in obtaining systems having either p-type or n-type semiconductivity. Here the type of the conductivity was usually determined from the thermo-e.m.f. In those cases where the Hall effect was measured the same type of conductivity was found as was derived from thermo-e.m.f. Further on we will provisorily speak about p- and n-conductivity based on measurements of the thermo-e.m.f. It is interesting to note that nearly all organic polymers with semiconducting properties described in the literature have p-type semiconductivity. Because of the above mentioned differences between the properties of polymer-metal systems and those of organic semiconductors the notions, as were developed in the literature [6, 7], on the mechanism of the conductivity in the latter substances cannot be used without essential changes for the systems described by us.

The compositions we have studied most thoroughly contained iron powder with a high degree of dispersity. The polymers were added to the systems by vibro-milling iron powder in the liquid monomer, according to the method proposed by V. A. Kargin and N. A. Plate [9, 1]. In this way we prepared compositions of iron with polyisoprene, polymethylmethacrylate, polystyrene and polyacrylonitrile. All these compositions have n-conductivity.

An iron-polyisoprene system was also prepared by precipitating the finished polymer from its solution in benzene [1]. Here it was shown that, if the polyisoprene is added to the system from a solution, p-conductivity is found. But if, as has been shown above, the system is prepared by polymerization of isoprene in a vibro-mill, one finds n-conductivity. In order to clarify which is the structure of the conducting polymeric layer it seemed convenient to study compositions containing a polymer in which the passing of a current would be hampered. For this purpose we chose the system iron-polyisobutylene. The latter has a specific resistance of about 10^{14} ohm·cm and is saturated organic compound in which structural features facilitating the transfer of electrons are absent. Starting from the mentioned properties of polyisobutylene it is natural to suppose that at a considerable content of the latter the system will behave as an isolator.

Polyisobutylene was added to the system from a 1% solution in toluene. We studied samples with various amounts of polymer: 10, 20 and 30%. At 10% polyisobutylene content the specific resistance of the system was about $1 \cdot 10^{-2}$ ohm·cm; at 20% the specific resistance rises to $1 \cdot 10^{-1}$ ohm · cm . Both in this and in the former case the resistance practically does not change with temperature. As is found from thermo-e.m.f., in both cases the current carriers are those of p-semiconductors. Evidently, in these systems polyisobutylene does not interact with the surface of the metal particles and upon pressing the sample the separate metal particles come in direct contact with each other. This also explains the fact that, although the specific resistance of the samples markedly rises by the addition of polyisobutylene, nonetheless the temperature dependency of the electric conductivity remains the same as that of metals.

A radical change in the electric properties of the system takes place by the addition of 30% polyisobutylene. Under these conditions the resistance of the system rises sharply and becomes greater than $1 \cdot 10^4$ ohm. Polyisobutylene enwraps the metal particles and the contact between them is broken. However, if this composition is exposed to heating in vacuum at 180-200°, it acquires several new properties. The specific resistance at room temperature drops to 2-4 ohm · cm.

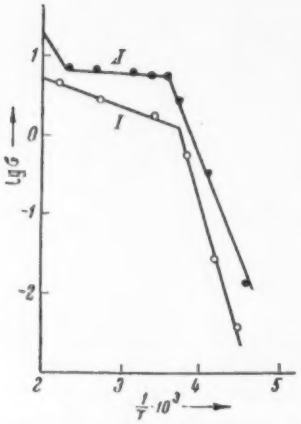

Fig. 1. The logarithm of the electric conductivity plotted versus inverse temperature. I) System iron-polyisobutylene; II) system iron-polyethylene.

As is evident from Fig. 1, the electric conductivity of such a system decreases, when the temperature is raised, and this is characteristic for semiconductivity. The plot of the logarithm of electric conductivity (log σ) versus inverse temperature (1/T) reminds that for extrinsic semiconductors. The plot consists of two linear sections with different values of the activation energy (ΔE). In the temperature range between 180° and 0° the value of ΔE is 0.07 ev; from 0° to −50° it is equal to 0.66 ev. These curves are reversible; at increasing temperature they coincide with the straight lines, especially in the region of low temperatures. In these systems the sign of the charge carriers corresponds to that in n-semiconductors.

In Fig. 2 a plot of the electric conductivity of pure polyisobutylene in the range from 30 to 160° is given. As may be seen, the conductivity increases by four orders of magnitude and comes back to its previous value, when the temperature is lowered again. This gives evidence that the thermal treatment of polyisobutylene in the said temperature range does not cause any radical change in the polymer structure. So, the above described changes in the electrophysical properties of the iron-polyisobutylene system result from a specific action of the iron powder on the state of the polymeric layers. The changes in these layers brought about by heating in the presence of iron are preserved even at room temperature. As yet it is not clear by which mechanism the said conducting structures originate. The above described experiments with the iron-polyisobutylene system indicate that the origin of the semiconducting properties is connected with a thermal interaction on the system. This conclusion may also be extended to the systems of iron with other polymers which we mentioned at the beginning of the paper and which too possess semiconducting properties. Since these systems were obtained by vibro-milling, during the preparation there occurred a strong local heating caused by the milling of the metal or, in any case, by stripping its surface layers. It should be noticed that in our measurements, which were carried out in vacuum, reproducible curves of the resistance as a function of temperature could only be obtained if the samples had been treated at 200-250°. So, in those cases too where the polymer is added to the system by precipitating it from a solution, in fact, a thermal treatment took place.

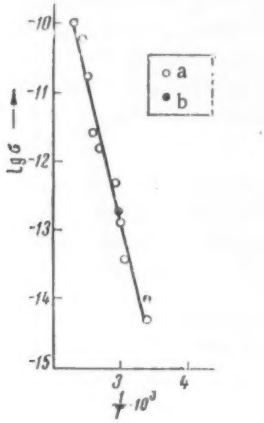

Fig. 2. The logarithm of the electric conductivity of polyisobutylene plotted versus inverse temperature. a) Measured at increasing temperature; b) measured in the reverse direction.

The system iron-polyethylene, obtained by precipitating polyethylene at about 140° from a solution in o-xylene, was studied too. The samples were exposed to a protracted heating in vacuum at 250°. Although the samples obtained are characterized by a relatively low resistance (about 14 ohm · cm at room temperature), they do not possess semiconducting properties. These properties make their appearance only after the samples have been ground and pressed for a second time and, moreover, heated again for a long time in vacuum. The curve of log σ versus 1/T (II) has about the same shape as that of the iron-polyisobutylene system (Fig. 1). The comparatively easy rearrangement of polyisobutylene when heated, obviously, may be explained by the fact that its chain contains tertiary carbon atoms, at which the chain is more easily broken so that new structures are formed.

At present we are carrying out investigations into the properties of the structures originating in our systems when they are treated thermally. Systems with other transition metals: nickel and cobalt and also with several metals belonging to other groups are studied too.

We gratefully acknowledge A. N. Frumkin for his interest in the investigation.

LITERATURE CITED

1. S. D. Levin, K. P. Lobanova, and N. A. Plate, DAN, 132, 1140 (1960).
2. A. T. Vartan'yan and I. A. Karpovich, ZhFKh, 32, 178 (1958); T. A. Vartan'yan, ZhFKh, 22, 769 (1948).
3. D. D. Eley, Nature, 162, 819 (1948); Res. in Appl. Ind. 12, 293 (1959).
4. A. V. Topchiev, M. A. Geiderikh, et. al., DAN, 128, 312 (1959).
5. A. Epstein and B. S. Wildi, J. Chem. Phys. 32, 324 (1960).
6. A. N. Terenin, Zhurn. Khim. Obshch. im. Mendeleeva, 5, 498 (1960).
7. V. A. Kargin, A. V. Topchiev, et. al., Zhurn. Khim. Obshch. im. Mendeleeva, 5, 507 (1960).
8. Semiconductors, Ed. N. B. Hannay, Am. Chem. Soc. Monogr. New York (1959).
9. V. A. Kargin and N. A. Plate, Vysokomolek. Soed. 1, 330 (1959).

All abbreviations of periodicals in the above bibliography are letter-by-letter transliterations of the abbreviations as given in the original Russian journal. *Some or all of this periodical literature may well be available in English translation.* A complete list of the cover-to-cover English translations appears at the back of this issue.

THE INFRARED SPECTRA OF CERTAIN R – O – Li COMPOUNDS

A. P. Simonov, D. N. Shigorin, T. V. Talalaeva,

and Corresponding Member of Academy of Sciences,

USSR, K. A. Kocheshkov

L. Ya. Karpov Physico-Chemical Institute
Translated from Doklady Akademii Nauk SSSR, Vol. 141, No. 3,
pp. 665-667, November, 1961
Original article submitted July 13, 1961

In an earlier communication [1] we had shown that R – O – Li compounds are strongly associated through the formation of intermolecular O – Li . . . O bonds. Infrared bands in the 400-600 cm^{-1} region were assigned to the vibrations of the O – Li group in the investigated lithium alcoholates; derivatives of normal aliphatic alcohols and tert-C_4H_9OLi were examined [1].

In the work here discussed the IR spectra of three lithium alcoholates with branched aliphatic radicals – iso-C_3H_7OLi, iso-C_4H_9OLi, and $(C_2H_5)_2CHOLi$, and of two isotopically substituted derivatives – CH_3OLi^6 and CD_3OLi were examined. The first three compounds are crystalline solids readily soluble in ordinary organic solvents and can be sublimed without decomposition in vacuo ($5 \cdot 10^{-2}$ mm Hg) at temperatures between 100 and 150° (the tert-C_4H_9OLi has similar properties [1]). These lithium alcoholates are also very strongly associated in solution. V. A. Dubovitskii and O. V. Nogina have determined molecular weights of these compounds cryoscopically. In cyclohexane and benzene 1 mole % solutions of all these compounds yield an association factor 5 while 0.5% solutions yield a factor of 3. This seems to indicate that all these compounds are associated in a similar manner. The pentamers are probably tetrahedral in structure while the trimers are composed of three-membered rings.

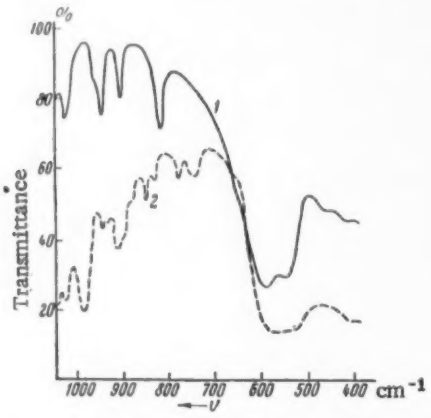

Fig. 1. The spectra of sublimed crystalline samples of: 1) iso-C_4H_9OLi; 2) $(C_2H_5)_2CHOLi$.

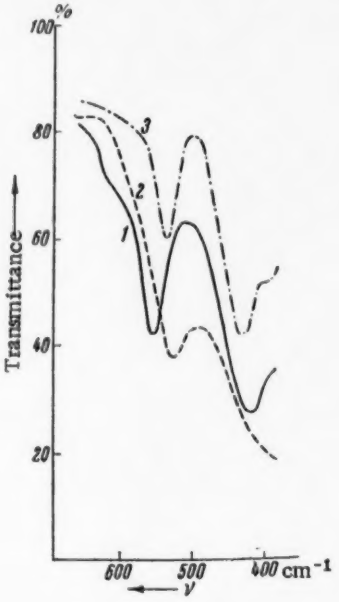

Fig. 2. The spectra of isotopically substituted lithium methylates (in nujol mull): 1) CH_3OLi^6; 2) CD_3OLi; 3) CH_3OLi.

TABLE 1

iso-C_3H_7OLi			iso-C_4H_9OLi			$(C_2H_5)_2CHOLi$			Assignment
crystal sublimate	crystal in nujol	0.3 N solution in cyclohex., 100 μ	crystal sublimate	crystal in nujol	1.05 N solution in hexane, 100 μ	crystal sublimate	crystal in nujol	0.24 N solution in cyclohex., 100 μ	
1455 (s)	~1455 (s)		1455 (m)	1453 (m)	1450 (m)	1468 (s)	~1450 (s)		} C – H deformation
1367 (s)	~1370 (s)	1365 (m)	1387 (m)	1387 (m)	1385 (m)	1370 (s)	~1370 (s)	1365 (m)	
1350 (v.s)	1350 (s)	1353 (m)	1357 (m)	1355 (m)	1360 (m)				
1327 (m)	1330 (w. sh)	1330 (m)	1330 (v.w)	1330 (w)		1303 (w) 1182 (m)	1300 (w)		
1150 (v.s)	1155 (s)	1155 (s)	1133 (w)	1133 (s)	1130 (s)	1145 (s)	1140 (v.s)	1137 (s)	} C – O stretch
1123 (v.s)	1123 (m)	1120 (m)	1090 (v.w)	1087 (v.s)	1090 (v.s)	1115 (m.)	1113 (s)	1110 (m)	
1060 (w)	1055 (w)					1067 (m. sh)	1067 (m.sh)	1066 (w)	
						1050 (m)	1047 (m)	1048 (w)	
						1027 (m)	1025 (s)	1025 (m)	
975 (v.s)	975 (s)	975 (s)	1020 (m)	1017 (m)	1020 (m)	987 (s)	985 (s)	985 (m)	>C – O – Li deformation
			955 (w)	953 (m)	955 (w)				
			943 (m)	940 (m)	940 (m)	945 (w)	948 (m)	947 (w)	C – C stretch
						915 (m)	915 (m)	915 (w)	
			903 (m)	900 (m)	903 (m)	906 (w. sh)	905 (m)		
						853 (m)	853 (w)		
820 (s)	820 (m)	820 (m)	820 (m)	820 (m)	820 (m)				
						783 (m)	785(v.w)		
						~750(m)	747 (w)		
~575 (s.b.)	575 (s. b)	~585(m.b)	~595(v.w.b.)	~580(v.s.b.)	~600(s.b.)	~570(m)	~600(s.b.) ~560(s.b.)	~590(m.b.)	} Vibrations of associated O – Li groups.
~525 (s.b.)	~520(s.b)	~540(m.b)	~545(s.b)		~550(s.b.)	~530(s.b.)	~490(m.b)	~500(m.b)	
~470 (s.b.)	~470(v.s.)	~490 (m)	~460(s.b)	~465(s.b)	~470(s.b.)	~420(s.b.)	~425(m.b)		C – C – C deformation

• v.s.) Very strong; s) strong; m) medium; w) weak; v.w) very weak; sh) shoulder; b) broad. Since bands in the 500-600 cm^{-1} region are broad and poorly resolved the table gives only their centers.

TABLE 2

CH_3OLi	CH_3OLi^6	CD_3OLi	Frequency assignment
2923 (m)	2942 (m)		C – H stretch
2842 (s)	2858 (s)		
2792 (s)	2803 (s)		
		2260 (m)	C – D stretch
		2170 (s)	
		2122 (s)	
		2092 (s)	
2080 (w)	2062 (m)		$2\nu_{C-O}$
1435 (s)	~1455 (m)		C – H deformation
1368 (s)	~1370 (w)		
1160 (m)	1168 (m)		$-OCH_3$
		1145 (s)	C – D deformation
		1040 (w)	$-OCD_3$ (?)
1060 (v.s.)	1065 (v.s.)	1005 (s)	C – O stretch
		907 (m)	C – D deformation
537 (s)	560 (s)	530 (s)	Associated O – Li vibrations
428 (s)	~ 430 (v.s.)		CH_3 deformation (rocking)

The IR spectra were recorded on a Hilger model H-800 double-beam spectrometer over the range of wavelenths from 5 to 25 μ. The spectra of sublimed samples were obtained by (using a special cell in which a thin solid film was sublimed directly on top of a potassium bromide plate and remained in vacuo during the measurements. All the operations involving these compounds were performed under dry argon. In Table 1 we have compiled the frequencies of all the bands except the very weak ones.

The Table shows that the spectra of sublimates, or of the crystals ground with nujol, differ very little from the ones recorded in solution (the same holds for tert-C_4H_9OLi). In the 400-600 cm^{-1} region the spectra of the investigated alcoholates, and of the alcoholates examined before [1], exhibit intense broad bands (Fig. 1) which apparently should be assigned to the vibrations of associated O – Li groups. In order to verify our assignment we recorded the spectra of two isotopically substituted derivatives of lithium methylate, CH_3OLi^6 and CD_3OLi (Table 2). Table 2 shows that the 537 cm^{-1} band of CH_3OLi (which was assigned to the vibration of associated O – Li groups [1] shifts by about 25 cm^{-1} towards higher frequencies when Li^7 is replaced by Li^6, while the replacement of H atoms in the methyl group by D has very little effect on this band (Fig. 2). These data confirm to a certain extent the previously made assignments.

Thus the investigated lithium alcoholates are strongly associated through intermolecular O – Li . . . O bonds; complex vibrations of the associated O – Li groups seem to fall in the 400-600 cm^{-1} region and may possibly also show up in the far infrared region.

LITERATURE CITED

1. A. P. Simonov, D. N. Shigorin, T. V. Talalaeva, and K. A. Kocheshkov, DAN, 136, 634 (1961).

All abbreviations of periodicals in the above bibliography are letter-by-letter transliterations of the abbreviations as given in the original Russian journal. *Some or all of this periodical literature may well be available in English translation.* A complete list of the cover-to-cover English translations appears at the back of this issue.

ISOTOPIC EXCHANGE BETWEEN O_2^{18} AND MOLTEN $Na_2WO_4^{16}$

V. I. Spitsyn, V. G. Finikov, and G. N. Zykova

Institute of Physical Chemistry, Academy of Sciences, USSR
Translated from Doklady Akademii Nauk SSSR, Vol. 141, No. 3,
pp. 668-669, November, 1961
Original article submitted August 8, 1961

By using the procedure described in [1] we studied isotopic exchange between gaseous oxygen containing 1.360 at. % O^{18} and molten Na_2WO_4 of normal isotopic composition at 720, 745 and 764°C (the temperature was kept constant with an accuracy of ± 0.5°). The melt surface, which had the shape of a rectangle with sizes 4 · 0.5 cm, was practically identical in all experiments. To find out how the kinetic characteristics depend on the thickness of the molten layer we carried out three series of experiments with 1.0, 4.4 and 7.4 g sodium tungstate, respectively, and this corresponds to a layer thickness of approximately 1, 5, and 8 mm. The isotopic analysis of oxygen in the gas phase by means of a MS-4 mass spectrometer was done by V. L. Litvakov and the authors gratefully acknolwedge him. Knowing the weight of sodium tungstate and the flow rate of gas in the system we calculated the degree of exchange, the reaction rate constant and the activation energy from the change of the O^{18} content in the gas with time.

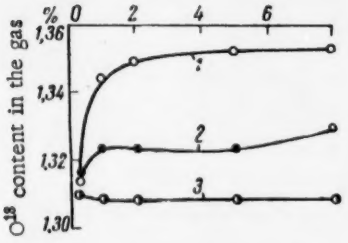

Fig. 1. The change of the O^{18} content in the gas phase with time of isotopic exchange in the system $Na_2WO_4^{16} - O_2^{18}$ at 720°. Weights of Na_2WO_4: 1) 1.0 g; 2) 4.4 g; 3) 7.4 g.

In Fig. 1, it is shown how the O^{18} content in the gas phase changes with time at the temperature 720°. It is remarkable that the reaction rate is constant over many hours. About 10^{15} O ions per 1 cm^2 are found in the surface of the melt. The number of collisions with the surface of the melt amounts to $2 \cdot 10^{23}$ $sec^{-1} \cdot cm^{-2}$. An estimate from the experimental results indicates that at 720° every second $5 \cdot 10^{14}$, $15 \cdot 10^{14}$ and $1.5 \cdot 10^{14}$ – or on the average $7 \cdot 10^{14}$ – O^{18} atoms are transferred to the liquid phase for the weights 1.0, 4.4 and 7.4 g, respectively, that is, just as many as or somewhat fewer than the number of oxygen ions in the surface layer. The theory of absolute reaction rates gives the relation

where V is the reaction rate (molecules $cm^{-2} \cdot sec^{-1}$), N_q the number of collisions onto the surface (molecules $cm^{-2} \cdot sec^{-1}$). By substituting the afore mentioned values into this relation we find an activation energy of 38.4 kcal/mole. For the temperatures 745 and 764° the results are similar.

Table 1 contains data on the degrees of exchange attained in eight hours at the temperatures used.

Application of the formula $Kt = \ln \frac{100}{100 - \alpha}$, where K is the reaction rate constant, t time, α the degree of exchange in percents, allowed us to calculate the rate constants given in Table 2. Figure 2 where the results for the temperature 720° are plotted illustrates how strictly the linear relation is satisfied by the experimental data. The apparent activation energies calculated by the method of least squares are found to be 30.6, 22.7 and 13.2 kcal/mole and they are a linear function of the weight of the sample (Fig. 3). Extrapolation to an infinitely thin (or rather to a monomolecular) layer gives an activation energy of 33.5 kcal/mole.

The following interpretation of the obtained results seems to be a possible one. In this case isotopic exchange is accomplished by exchange between gaseous oxygen, probably entirely in the form of atoms, and oxygen anions of sodium tungstate, which are present in the surface of the melt, because atoms are displaced in collisions. This exchange proceeds at a very low rate, the number of effective collisions with the surface is very small, because only 10^{-13} % of the molecules is in the state of thermal dissociation (10^4 pairs of atoms per cm^3 in our case). The linear decrease of the activation energy at raised layer thickness (increased weight) of the molten sodium tungstate and the fact that for small weights it tends to the limit value 33.5 kcal/mole differing only 12% from the theoretically

TABLE 1. Degrees of Exchange (in percent) Attained in Eight Hours in the System $Na_2WO_4^{16}$–O_2^{18}

Weight of tungstate, g	Temperature °C		
	720	745	764
1.0	45.6	57.9	65.4
4.4	22.4	28.6	33.9
7.4	10.6	13.4	13.8

TABLE 2. Rate Constants for Isotopic Exchange of Oxygen in the System $Na_2WO_4^{16}$–O_2^{18} (hr^{-1})

Weight of tungstate, g	Temperature °C		
	720	745	764
1.0	0.0631	0.1040	0.1229
4.4	0.0317	0.0421	0.0525
7.4	0.0140	0.0179	0.0186

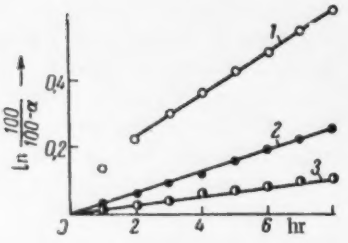

Fig. 2. Plot of $\ln \frac{100}{100-\alpha}$ versus time for isotopic exchange of oxygen in the system $Na_2WO_4^{16}$–O_2^{18} at 720°. Weights of Na_2WO_4: 1) 1.0 g; 2) 4.4 g; 3) 7.4 g.

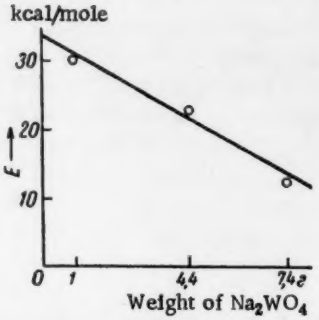

Fig. 3. The activation energies of isotopic exchange in the system $Na_2WO_4^{16}$–O_2^{18} plotted versus the weight of Na_2WO_4 used.

calculated one give reason to consider the obtained value to be a quantitative indication for the strength of the oxygen bond in the tungstate anion of the sodium salt. The lower accuracy of the values used in the theoretical calculation allow one to take the value 33.5 kcal/mole as more close to the actual one.

LITERATURE CITED

1. V. I. Spitsyn and V. G. Finikov, DAN, 108, 491 (1956).

All abbreviations of periodicals in the above bibliography are letter-by-letter transliterations of the abbreviations as given in the original Russian journal. *Some or all of this periodical literature may well be available in English translation.* A complete list of the cover-to-cover English translations appears at the back of this issue.

ADSORPTION OF AROMATIC AND HYDROAROMATIC COMPOUNDS AT A MERCURY-SOLUTION INTERFACE

A. N. Frumkin, R. I. Kaganovich, and É. S. Bit-Popova

M. V. Lomonosov Moscow State University
Translated from Doklady Akademii Nauk SSSR, Vol. 141, No. 3,
pp. 670-673, November, 1961
Original article submitted July 21, 1961

By comparing the adsorption of polar aromatic compounds at a solution-air and a mercury-solution interface it was shown that at the latter interface, when compared with the former, one observes that the adsorbability on a positively charged surface is enhanced and finds higher negative values of the adsorption potential [1]. It was suggested that these effects result from a flat arrangement of the molecules in the adsorbed layer, which facilitates the interaction between the negative atoms of the polar groups and the metal. An investigation into the electrocapillary behavior of nonpolar aromatic compounds carried out later in our laboratory by Gerovich [2] showed that such substances as benzene, naphthalene etc. are adsorbed preferentially on a positively charged mercury surface and displace the point of zero charge in the direction of negative potentials.

A comparison of the electrocapillary curves for aromatic compounds with the corresponding curves for hydroaromatic compounds (benzene-cyclohexane, naphthalene-decalin) led to the conclusion that the shift of the point of zero charge and the change in the adsorption at positive charges of the surface are caused not only by the flat orientation of the molecules of the aromatic compounds but also by the presence of π-electrons, which interact with the mercury surface, especially, when it has a positive charge.

In agreement with previously exposed ideas, the presence of a polar group in the aromatic ring (phenol) intensified the effects observed in the adsorption of nonsubstituted hydrocarbons.

It was of interest to study the adsorption of other polar benzene derivatives.

For aqueous solutions of the substances studied the electrocapillary curves, which express the interface surface tension σ as a function of the electrode potential φ (refered to a normal calomel electrode), were taken by means of Gouy's electrometer. The substances used in the study were purified by a double distillation or by recrystallization. V. Gerovich synthesized hexahydrobenzoic acid by means of Zelinskii's method.

The electrocapillary curves of aniline (2) and cyclohexylamine (3) compared with that of 1 N Na_2SO_4 + 0.01 N NaOH (1) are shown in Fig. 1. From Fig. 1 it is evident that aniline is adsorbed on a positively charged mercury surface, whereas in the case of cyclohexylamine and increase of the positive charge results in the disappearance of adsorption. On the other hand, on the original noncharged or negatively charged mercury surface the adsorbability of cyclohexylamine exceeds that of aniline.

The electrocapillary curve of 1.1 N H_2SO_4 (1) and those of H_2SO_4 containing aniline- (2) or cyclohexylamine sulfate (3) in the concentration 0.1 M are represented in Fig. 2. As is evident from Fig. 2, on a positively charged mercury surface the adsorption of the cyclohexylamine anion ceases completely, the electrocapillary curve of this salt runs parallelly to that of the solvent H_2SO_4. In the case of aniline sulfate, as has already been shown previously in [3], the cations are still adsorbed, even when the surface gets a positive charge and this indicates that the forces of the π-electron interaction of the aromatic ring prevail over the electrostatic repulsion forces.

We have also studied the electrocapillary behavior of aniline and cyclohexyl amine in a medium with HCl and HBr [4]. It turns out that adsorption of the aniline ion on a positively charged mercury surface is enhanced in the sequence $SO_4^{2-} < Cl^- < Br^-$. When Br^- ions are present, some adsorption of the cyclohexyl ammonium ion too is observed. These data make us suggest that the adsorption of cations is raised owing to the interaction between the flatly orientated cations in the adsorbed layer and the specifically adsorbed anions.

Primary solution	Substance studied	Concentration, mole/liter	$\Delta\sigma_1$	$\Delta\sigma_2$
1 N Na_2SO_4	Aniline	0.1	47.0	10.0
1 N Na_2SO_4	" "	0.0045	10.0	–
1.1 N H_2SO_4	" "	0.1	6.0	0.4
1.1 N HBr	" "	0.1	11.3	0.7
1 N Na_2SO_4	Cyclohexyl amine	0.1	43.7	23.6
1 N Na_2SO_4	" "	0.01	23.6	–
1.1 N Na_2SO_4	" "	0.1	7.5	1.0
1.1 N HBr	" "	0.1	13.0	1.3
0.1 N H_2SO_4	Benzoic acid	0.01	19.2	2.5
0.1 N H_2SO_4	" "	0.0005	2.5	–
0.01 N KOH	" "	0.05	20.5	0.4
0.1 N H_2SO_4	Hexahydrobenzoic acid	0.01	20.5	6.0
0.1 N H_2SO_4	" "	0.0027	6.0	–
0.01 N KOH	" "	0.05	2.5	–

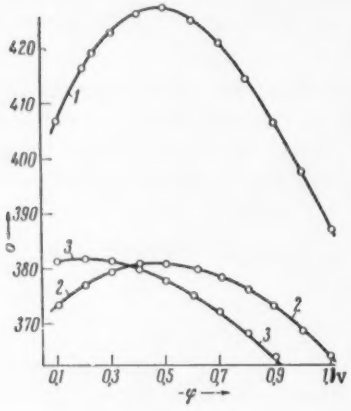

Fig. 1. Electrocapillary curves of the solutions: 1) 1 N Na_2SO_4 + 0.01 N NaOH; 2) 1 N Na_2SO_4 + 0.1 M $C_6H_5NH_2$; 3) 1 N Na_2SO_4 + 0.1 M $C_6H_{11}NH_2$, σ in d/cm.

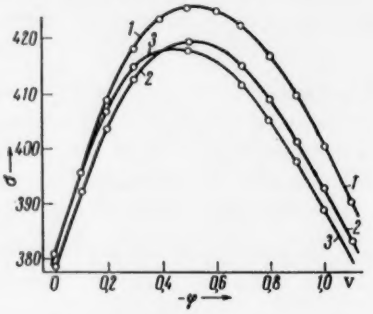

Fig. 2. Electrocapillary curves of the solutions: 1) 1.1 N H_2SO_4; 2) 1 N H_2SO_4 + + 0.1 M $C_6H_5NH_2 \cdot \frac{1}{2} H_2SO_4$; 3) 1 N H_2SO_4 + + 0.1 M $C_6H_{11}NH_2 \cdot \frac{1}{2} H_2SO_4$.

In order to compare the surface activity of the substances studied on the water-air with that on the water-mercury interface we did some measurements of the surface tension by means of the method of maximum bubble pressure and their results are assembled in Table 1. $\Delta\sigma_1$ designates the lowering found in the interfacial surface tension when one passes from the maximum in the electrocapillary curve of the primary solution to the maximum in the presence of a substance which is adsorbed, $\Delta\sigma_2$ represents the corresponding lowering in the surface tension of the primary solution.

From table it follows that the surface activity of the compounds studied increases substantially upon going from the free solution surface to the interface with mercury. Upon assuming that equal lowerings of the interfacial tension in both interfaces correspond to equal adsorption magnitudes, that is, upon supposing that the equations of state for both interfaces are identical, then from the data of table by means of the equation $|\Delta g_0| = RT \ln(C_1/C_2)$ one may calculate $|\Delta g_0|$, that is, the increase in the absolute standard free energy for the transition from the solution-air to the solution-mercury interface (C_1 and C_2 are the concentrations of the dissolved substance which give an equal lowering of σ in the boundary with air and in that with mercury respectively. In the case of aniline (at $\Delta\sigma_1 = \Delta\sigma_2 = 10.0$) $|\Delta g_0| = 1.80$ kcal),in the case of cyclohexyl amine (at $\Delta\sigma_1 = \Delta\sigma_2 = 23.6$) $|\Delta g_0| = 1.34$ kcal), It is noteworthy that in the case of cyclohexyl amine the gain in adsorption energy upon passing to the interface

with mercury is markedly higher than that found, for instance, for aliphatic alcohols with a long chain [1]. Possibly, this effect is connected with the flat arrangement of the adsorbed cyclohexyl amine molecules. The said gain in energy increases by $\Delta|\Delta g_0| = 0.46$ kcal upon passing from cyclohexyl amine to aniline; this points out that the interaction with the π-electrons of the ring, albeit to a much less extent than on a positively charged surface, is manifested on a noncharged mercury surface too. On the free solution surface the surface activity of cyclohexyl amine because

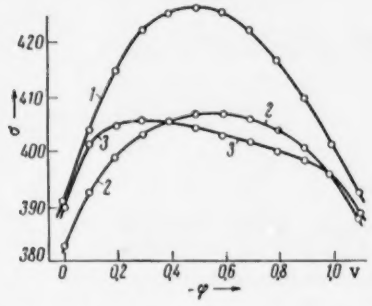

Fig. 3. Electrocapillary curves of the solutions: 1) 0.1 N H_2SO_4; 2) 0.1 N H_2SO_4 + + 0.01 M C_6H_5COOH; 3) 0.1 N H_2SO_4 + + 0.01 M $C_6H_{11}COOH$.

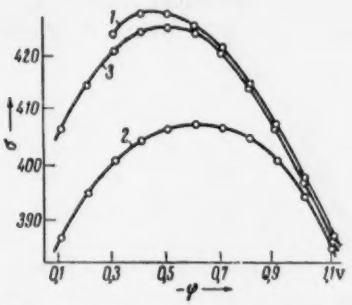

Fig. 4. Electrocapillary curves of the solutions: 1) 0.01 N KOH; 2) 0.05 N KOH + 0.05 N C_6H_5COOK; 3) 0.05 N KOH + 0.05 N $C_6H_{11}COOK$.

of its high molecular volume is markedly higher than that of aniline; owing to the π-electron interaction this difference disappears upon passing to the interface with mercury. The surface activity of the cations of aniline and cyclohexyl amine is much less than that of the corresponding neutral molecules, but between the adsorbability of both cations the same ratio is preserved as is found for the molecules. Whereas the cyclohexyl ammonium cation is adsorbed by about 2-2.5 times more strongly than the aniline ion on the interface with air, this difference is smoothed out upon passing to the interface with mercury. In this case $\Delta|\Delta g_0| \approx 0.4$ kcal. As is evident from Fig. 2, although the cation as a whole is repelled, the π-electron interaction increases, when the mercury surface has a positive charge.

The effect which the interaction between the π-electrons and the mercury surface has in the adsorption of aniline- and other analogous cations in a 0.1 N HCl solution was also pointed out by Blomgren and Bockris [5], who have quantitatively studied this adsorption at various potentials. However, these authors did not take into account that, as is evident from the example of cyclohexyl ammonium, appreciable adsorption effects are found even in the absence of such an interaction. In the case of a free water surface the latter effects result, because the organic cation is forced out from the bulk of the solution.

The electrocapillary curves for 0.01 M solutions of benzoic (2) and hexahydrobenzoic acid (3) compared with that of 0.1 N H_2SO_4 (1) are represented in Fig. 3. Evidently, the curve for hexahydrobenzoic acid, when one passes to positive surface charges, runs almost parallel to that of the primary solution and this indicates that adsorption ends under these conditions, whereas the adsorption of benzoic acid retains an appreciable magnitude under those same conditions.

The results obtained, when we investigated the electrocapillary behavior of the potassium salts of benzoic (Fig. 4, 2) and hexahydrobenzoic acid (Fig. 4, 3), indicate to which extent the surface activity of the anion increases as a result of the π-electron effect.

A comparison of the surface activities of benzoic and hexahydrobenzoic acid on the solution-air interface with those on the solution-mercury interface leads to conclusions similar to those found for aniline and cyclohexyl amine. The value of $|\Delta g_0|$ for benzoic acid (at $\Delta\sigma_1 = \Delta\sigma_2 = 2.5$) is equal to 1.74 kcal and for hexahydrobenzoic acid (at $\Delta\sigma_1 = \Delta\sigma_2 = 6.0$) it is only 0.76. So, the extra gain in energy resulting from the interaction with the π-electrons of the ring attains nearly 1 kcal in this case. It is noteworthy that the surface activity of benzoic acid on the interface with mercury decreases only by a factor five upon passing from the neutral molecule to the anion, whereas for hexahydrobenzoic acid the corresponding factor is about 40.

LITERATURE CITED

1. A. N. Frumkin, A. A. Donde, and R. M. Kul'varskaya, Zs. Physikal. Chem. 123, 326 (1926); A. N. Frumkin, Ergebn. Exakt. Naturwiss, 7, 235 (1928); Coll. Symp. Annual. 7, 89 (1930).
2. M. A. Gerovich, ZhFKh, 28, 19 (1954); DAN, 96, 3 (1954); DAN, 105, 6, 1278 (1955).
3. M. A. Gerovich and N. S. Polyanovskaya, Nauchn. Dokl. Vysshei Shkoly. Khim. i Khim. Tekhnol. 4, 651 (1958).
4. A. N. Frumkin, Electrochim. Acta (in the press).
5. E. Blomgren and J. O'M. Bockris, J. Phys. Chem. 63, 1475 (1959).

All abbreviations of periodicals in the above bibliography are letter-by-letter transliterations of the abbreviations as given in the original Russian journal. *Some or all of this periodical literature may well be available in English translation.* A complete list of the cover-to-cover English translations appears at the back of this issue.

INTRAMOLECULAR ENERGY MIGRATION IN THE RADIOLYSIS OF ALKYLBENZENES

Kh. S. Bagdasar'yan, N. S. Izrailevich, and V. A. Krongauz

Karpov Institute of Physical Chemistry
(Presented by Academician S. S. Medvedev July 6, 1961)
Translated from Doklady Akademii Nauk SSSR, Vol. 141, No. 4,
pp. 887-890, December, 1961
Original article submitted May 22, 1961

Intramolecular energy migration in unconjugated molecules has often been invoked to explain effects produced in polymers and biological objects by light and ionizing radiation. All the same, there has been very little done on simple compounds, especially under conditions such that the effect should be detectable. A point to remember here, of course, is that intramolecular migration may be masked or suppressed by intermolecular transfer even in one-component systems. Polymers are unsuitable objects here, because the effects of radiation on them seldom allow an unambiguous interpretation.

The arylalkanes and mixtures of aromatic and aliphatic hydrocarbons are much more radioresistant than the aliphatic ones, so energy transfer can be detected by means of any deviation from additivity. Burton et al [1] have shown in this way that the yield of gases from a radiolyzed alkylbenzene is much less than that to be expected from a mixture of benzene with the corresponding alkane. However, it is not known whether the aromatic ring protects the alkyl radical by intramolecular or intermolecular transfer (the latter effect occurs in cyclohexane mixed with benzene [2]).

Alexander et al [3] have found that naphthyldodecane is much more resistant to radiation-induced cross-linking than is decyldodecane; moreover, the naphthyl group is most effective if it is attached at the middle of the chain in the dodecane. This is clear evidence for intramolecular migration. Even better evidence would be provided by measurements of the chain-rupture probability as affected by the naphthyl group. Voevodskii et al [4] have made ESR studies of the frozen-in radicals produced from 1,1-substituted dodecanes at – 196°; the substituents were phenyl and cyclohexyl rings. They found that the energy migrated readily from the aliphatic groups to the phenyl rings, with the result that the yield of radicals was reduced greatly. The mechanism of the transfer is not altogether clear; the phenylcyclohexyl derivative gave a yield smaller than that given by an equimolecular mixture of the diphenyl and dicyclohexyl derivatives, but this might be caused by large-scale inhomogeneity in the dodecane mixtures rather than by a preference for intramolecular transfer as against intermolecular transfer.

The most direct evidence is provided by the yields of primary radicals from alkylbenzenes relative to those from mixtures of benzene with the corresponding alkanes. Schuler et al [5] have used x-rays for this purpose; some of their results are given in table, which also gives values we have calculated on the basis of additivity for toluene and ethylbenzene. The formula used was

$$G_a = \varepsilon_A G_A + \varepsilon_{Ph} G_{Ph}, \quad (1)$$

in which ε_A and ε_{Ph} are the electron contributions from the chain and ring respectively, while G_A and G_{Ph} are the radical yields for the alkanes and benzene. Table shows that the calculated G is close to the actual one for toluene and for ethylbenzene, which clearly does not agree with the other results quoted.

We have used γ-rays in similar measurements on toluene, ethylbenzene, cumene, n-butylbenzene, and n-octylbenzene, as well as on an equimolecular mixture of benzene with n-octane. We also measured the radical yields for benzene, n-hexane, and n-octane. The radical acceptor was iodine. The benzene, toluene, ethylbenzene, and cumene were purified by repeated shaking with concentrated sulfuric acid; they were dried over sodium metal, and then were distilled (in a column of 25-30 theoretical plates) to give fractions boiling within limits of 0.1°. The

Compound	Schuler's results		Our results	
	G	G_a	G	G_a
Benzene	0.6	(0.6)	0.6	(0.6)
Toluene	2.4	2.0	0.8	1.0
Ethylbenzene	2.8	2.6	0.85	2.3
Cumene	–	–	0.7	2.8
Butylbenzene	–	–	0.9	3.1
Octylbenzene	–	–	0.9	3.9
Octane + +benzene (1:1)	–	–	2.1	3.9
Hexane	7.4	(7.5)	5.8	(6.0)
Octane	7.6	(7.5)	6.4	(6.0)

Note. The G are mean values.

butylbenzene and octylbenzene were made by Wurtz synthesis from bromobenzene and the corresponding alkyl bromides. The butylbenzene was fractionated in the column; the octylbenzene was distilled under reflux several times.

The iodine was used in a concentration of $5 \cdot 10^{-4}$ to $5 \cdot 10^{-3}$ M; the concentration had no effect on the yield within these limits and was measured spectrophotometrically at the absorption peaks for the solutions (490-520 mμ). The compounds were irradiated in the absence of air; the dissolved air was removed by freezing and thawing the compounds repeatedly under vacuum.*

The radiation source was Co^{60}; ferrous sulfate dosimetry was used. The dose rate was $1.8 \cdot 10^{18}$ electron-volts per liter per sec.

Table gives the radical yields.

The results for the alkanes are somewhat lower than those of Weber et al [5] but agree with Schuler's [6]. Our G for toluene and ethylbenzene are much lower than Schuler's. The G for toluene were checked for the effects of impurities by using various specimens of toluene and several methods of purification. In every case the value was close to that given in the table. The yield as measured with DPPH was 1.1, which agrees with Schapiro's value [7]. Further, the alkylbenzenes all gave G of 0.8-0.9, which indicates that this is the correct value; the high ones given by Weber et al [5] are wrong.

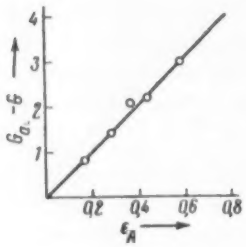

Table shows that the actual G are always much less than the ones derived by addition; the phenyl group protects the aliphatic chain, as has been demonstrated in other ways. In particular, octylbenzene gives a radical yield much lower than that for an equimolecular mixture of octane and benzene, which shows that here the intramolecular transfer is much more important than intermolecular transfer. The relative probabilities of the two processes may be estimated by reference to these two equations for the steady state for excited aliphatic chains A^* and excited phenyl rings Ph^* :

$$a_A J \varepsilon_A = k_{\dot{A}} [A^*] + k_A [A^*] + k_{APh} [A^*] [Ph] + k_M [A^*]; \quad (2)$$

$$a_{Ph} J \varepsilon_{Ph} = k_{\dot{P}h} [Ph^*] + k_{Ph} [Ph] - k_{APh} [A^*] [Ph] - k_M [A^*], \quad (3)$$

in which J is the dose rate, the ε are as before, ε_A and ε_{Ph} are the rate constants for the formation of radicals from the corresponding excited molecules or groups, k_A and k_{Ph} are deactivation constants, k_{APh} is the rate constant for the intermolecular transfer of energy from the aliphatic chain to the phenyl ring, k_M is the same for intramolecular transfer, [Ph] is the concentration of these rings, and the a are the yields of A^* and Ph^* per unit absorbed energy.

Then G is given by (2) and (3) as

$$G_a - G = \varepsilon_A \frac{\theta}{1+\theta} \left(G_A - \frac{a_A}{a_{Ph}} G_{Ph} \right),$$

* The iodine color weakened considerably when air-free solutions in octane or octylbenzene were frozen and then allowed to thaw. The original color was restored completely when the solution was exposed to a bright light or to the γ-rays. The iodine presumably forms rather unstable molecular compounds with these hydrocarbons.

in which

$$\theta = \frac{k_M + k_{APh}[Ph]}{k_A + k_A} . \quad (5)$$

Figure shows $(G_a - G)$ as a function of ε_A; the straight line passes through the origin, so $\theta / (1 + \theta)$ is nearly constant.

We must know a_A/a_{Ph} in order to deduce θ from (4). The lowest excited level for the aliphatic chain lies below the same for the ring, so a_A/a_{Ph} cannot be larger than 1; the θ corresponding values for an equimolecular mixture of benzene and octane give θ' as 1.2 and 1.08 ($\theta' = \frac{k_{APh}[Ph]}{k_A + k_A}$, because $k_M = 0$ for the mixture).* Now $(\theta - \theta')$ equals $k_M/(k_A + k_A)$ and so its values are 11.3 and 6.0. Finally we find for $\frac{\theta - \theta'}{\theta'} = \frac{k_M}{k_{APh}[Ph]}$ values of 9.5 and 5.5 (for octylbenzene). This means that intramolecular migration is very much more probable than intermolecular transfer from the aliphatic chain to the ring.

Avivi et al [8] have found that the efficiency of transfer from polystyrene to 2,5-diphenyloxazole and anthracene is unaffected if the phosphor is bound chemically to the polystyrene chain. This does not conflict with our result for intramolecular migration from the aliphatic chain. Energy absorbed by the aliphatic chain in polystyrene migrates to the adjacent phenyl rings (not to molecules of the phosphor), for these rings lie at the ends of the molecule. The luminescence results from intermolecular transfer from these rings to the phosphor.

LITERATURE CITED

1. M. Burton, S. Goren, and R. Hentz, J. Chim. Phys. 48, 190 (1951).
2. P. Manion and M. Burton, J. Phys. Chem. 56, 560 (1952).
3. P. Alexander and A. Charlesby, Nature, 173, 578 (1954).
4. Yu. N. Molin, I. I. Chkheidze, A. A. Petrov, N. Ya. Buben, and V. V. Voevodskii, DAN, 131, 125 (1960).
5. E. Weber, P. Forsyth, and R. Schuler, Radiation Res. 3, 68 (1955).
6. R. Schuler, J. Phys. Chem. 63, 925 (1959).
7. A. Schapiro, J. Phys. Chem. 63, 801 (1959).
8. P. Avivi and A. Weinreb, J. Chem. Phys. 27, 716 (1957).

All abbreviations of periodicals in the above bibliography are letter-by-letter transliterations of the abbreviations as given in the original Russian journal. *Some or all of this periodical literature may well be available in English translation.* A complete list of the cover-to-cover English translations appears at the back of this issue.

---

* We note that since [Ph] = 4 moles/liter, then from the found value of Θ' it follows that $\frac{k_{APh}}{k_A + k_A} = 0{,}25$.

EFFECTS OF EXTERNAL IRRADIATION OF SORPTION PARAMETERS OF $BaSO_4$

V. V. Gromov and Academician V. I. Spitsyn

Institute of Physical Chemistry, Academy of Sciences, USSR
Translated from Doklady Akademii Nauk SSSR, Vol. 141, No. 4,
pp. 891-893, December, 1961
Original article submitted July 13, 1961

We have found [1, 2] that the behavior of precipitated radioactive barium sulfate with respect to dyes is dependent on the dye and on the type and energy of the radiation. For example, prolonged exposure to the S^{35} in $BaSO_4$ reduces the capacity of the sorbent [2]. We have now examined this effect in more detail by means of external radiation; the uptake of dye was measured as a function of dose rate and of integral absorbed dose for barium sulfate exposed to high-energy electrons. In certain cases we also used $BaSO_4$ that had been exposed to a proton beam.

Electrons of energy 800 kev were produced in an accelerator fed from a capacitor-type voltage-multiplying rectifier (1.2 Mev). The beam current at the specimen was monitored by means of the current received by the beryllium exit window after suitable calibration.

The proton beam (energy 1.5 Mev) was taken from a 2.5 Mev electrostatic generator.* The irradiations were done at a pressure of 10^{-5} to 10^{-6} mm Hg. The target was water-cooled, but the specimen reached a temperature of 100-150° during the irradiation. The specimens showed no induced activity.

The barium sulfate (chemically pure) was heated to 300-350° for 2 hr under vacuum (10^{-3} mm Hg) in a stainless-steel cylinder. Then the cylinder was filled with nitrogen to a pressure of 5 atm. The resulting material was used in the irradiations. It was exposed to the electron beam in an aluminum holder which was water-cooled in nitrogen. The preliminary treatment with nitrogen and the irradiation in nitrogen together prevented the $BaSO_4$ from occluding ozone, which is formed from atmospheric oxygen and which can effect the results. In this case the water cooling enabled us to restrict the temperature to 30-60°. The temperature was monitored throughout the irradiation by means of a copper-constantan thermocouple. In no case was the weight of the specimen altered by the irradiation.

Some 30-40 min after the irradiation, a weighed amount of the $BaSO_4$ was transferred to a flask containing a solution of acid orange or methylene blue; the mixture was stirred for 1 hr, and then the uptake of dye was measured. A specimen of unirradiated $BaSO_4$ was treated in the same way at the same time. The proportions used were 0.4 g of $BaSO_4$ to 25 ml (acid orange) and 3 g of $BaSO_4$ to 25 ml (methylene blue).

The dye concentrations were measured with an SF-2M spectrophotometer; the solutions were centrifuged first. The divergence between three or four parallel measurements of the absorption was 3-4% for acid orange and 5-8% for methylene blue. The initial concentrations were 50, 100, 200, 300, and 450 mg/liter at pH 5-6 (acid orange) and 25, 50, 100, and 150 mg/liter at pH 5-5.5 (methylene blue).

Figures 1 and 2 show the uptake by the $BaSO_4$ as a function of integral absorbed dose.

Curves 2-4 of Fig. 1 and 2-5 of Fig. 2 relate the specimens given various integral doses at a dose rate of $1.3 \cdot 10^{20}$ ev/g-sec. Curve 5 of Fig. 1 and curve of Fig. 2 show the effects of reducing the dose rate to $1.3 \cdot 10^{19}$ ev/g-sec. Figures 1 and 2 and Table 1 showed that the uptake falls as the electron dose increases for both dyes; Fig. 3 shows the same.

The use of protons instead of electrons reduces the capacity of $BaSO_4$ for acid orange very greatly (Table 1).

* The $BaSO_4$ was irradiated with the proton beam in I. Ya. Barit's laboratory at the Physics Institute, Academy of Sciences of the USSR.

TABLE 1. Effects of Dose Rate on the Uptake by $BaSO_4$

Radiation	Absorbed dose, ev/g	Dose rate, ev/g-sec	Maximal dye uptake, g/m²	Dye
Electrons	$1.3 \cdot 10^{23}$	$1.3 \cdot 10^{20}$	22.5	Methylene blue
	$1.3 \cdot 10^{23}$	$1.3 \cdot 10^{19}$	17.5	" "
	$1.3 \cdot 10^{23}$	$1.3 \cdot 10^{20}$	300.0	Acid orange
	$1.3 \cdot 10^{23}$	$1.3 \cdot 10^{19}$	235.0	" "
Protons	$0.4 \cdot 10^{21}$	$0.5 \cdot 10^{19}$	250.0	" "

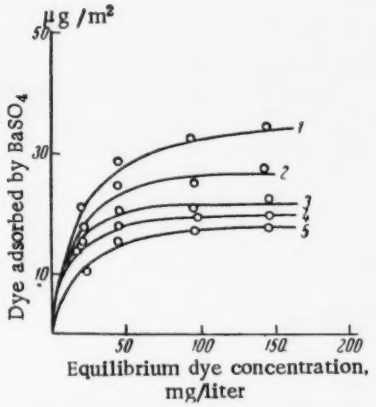

Fig. 1. Sorption of methylene blue by $BaSO_4$; electron-beam doses in ev/g: 1) 0; 2) $1.3 \cdot 10^{22}$; 3) $1.3 \cdot 10^{23}$; 4) $1.3 \cdot 10^{24}$; 5) $1.3 \cdot 10^{23}$. a) Dye adsorbed by $BaSO_4$; b) equilibrium dye concentration, mg/liter.

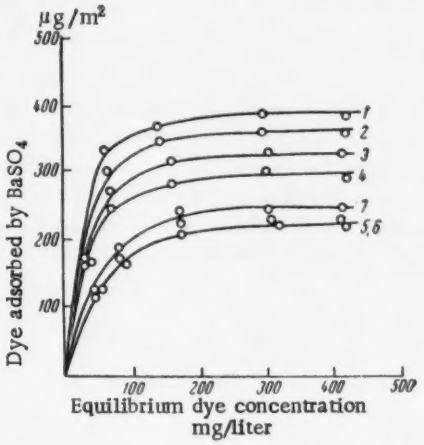

Fig. 2. Sorption of acid orange by $BaSO_4$; electron-beam doses in ev/g: 1) 0; 2) $1.3 \cdot 10^{21}$; 3) $1.3 \cdot 10^{22}$; 4) $1.3 \cdot 10^{23}$; 5) $1.3 \cdot 10^{24}$; 6) $1.3 \cdot 10^{23}$; 7) proton-beam dose of $0.4 \cdot 10^{21}$. a) Dye adsorbed by $BaSO_4$; b) equilibrium dye concentration, mg/liter.

Table 1 shows that the lower electron dose rate is more effective in depressing the uptake by the $BaSO_4$. This means that the β-rays emitted by sulfur-35 in $BaSO_4$ do reduce the capacity, although these β-rays have a maximum energy of only 162 kev.

TABLE 2

Specimen	Specific surface, m^2/g
Control	7.7
Electron dose of $1.3 \cdot 10^{22}$ ev/g	7.8
Electron dose of $1.3 \cdot 10^{24}$ ev/g	7.7
Proton dose of $0.4 \cdot 10^{21}$ ev/g	7.7

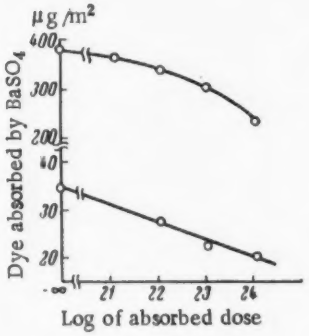

Fig. 3. Uptake of dye by $BaSO_4$ as a function of electron dose: 1) Acid orange; 2) methylene blue. a) Dye adsorbed by $BaSO_4$; b) log of absorbed dose.

It might be supposed that the high dose rates produced by the beams have the effect of reducing the surface area of the $BaSO_4$, which would explain the reduced uptake. But results given below show that the specific surface of the $BaSO_4$ is not affected,* so some other factor must be responsible.

The radiation dose may reduce the number of active centers; it may, as it were, polish the surface of the $BaSO_4$. This is only one possible cause for the reduced capacity, though. Another is that the damage to the sorbent affects the electron-density distribution [3-5]. In particular, the beams altered the color from white to light gray or brown. This color was lost within a week or so no matter whether the specimen was kept in air or nitrogen, but the $BaSO_4$ did not recover its former uptake. The color was also lost when the specimens were heated to 200-250° for 1 hr; the capacity increased somewhat, but still remained below the initial value. The weights of its specimens were not altered by the heating.

We are indebted to P. Ya. Glazunov and I. Ya. Barit for assistance in this work.

LITERATURE CITED

1. Vikt. I. Spitsyn and V. V. Gromov, DAN, 123, 722 (1958); Radiokhimiya, 1, 181 (1959).
2. Vikt. I. Spitsyn and V. V. Gromov, Summaries of Papers at the Second All-Union Conference on Radiation Chemistry, October 10-14 [in Russian] (1960), p. 90.
3. G. J. Diches and G. H. Vineyard, Radiation Effects in Solids, New York – London (1957).
4. B. Sfech, Zs. Naturforsh. 7a, 175 (1952).
5. Effects of Ionizing Radiations on Inorganic and Organic Systems [in Russian] (Izd. Akad. Nauk SSSR, 1958).

---

* The specific surface of the $BaSO_4$ was measured in Deryagin's apparatus. It had previously been shown (by adsorption of nitrogen) that the $BaSO_4$ did not contain blind pores (possible error 10%).

RATE OF DISSOCIATION OF THE OXYGEN MOLECULE AT HIGH TEMPERATURES

S. A. Losev

Lomonosov State University, Moscow
(Presented by Academician V. N. Kondrat'ev June 28, 1961)
Translated from Doklady Akademii Nauk SSSR, Vol. 141, No. 4,
pp. 894-896, December, 1961
Original article submitted June 22, 1961

The interactions between molecules that lend to dissociation are of interest in relation to the states of gases at the high temperatures developed in shock waves. Measurements have been made of the rates of decomposition for O_2, Br_2, I_2, and the like, alone or mixed with other gases [1].

I have made measurements on O_2 at temperatures up to 7000°K; the methods were the same as those used previously at lower temperatures [2], in which the initial stages of the process are examined in order to minimize the fall in temperature associated with the dissociation. The essential features of the shock-tube system have been described already [3].

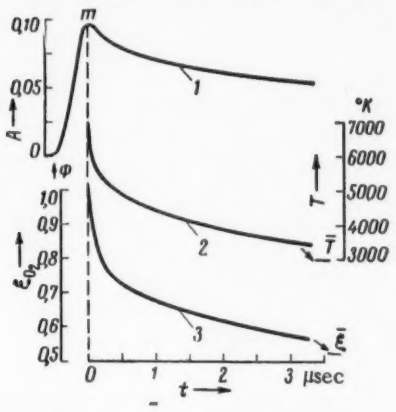

Fig. 1. 1) Absorptivity A; 2) temperature T; and 3) ξ_{O_2} the concentration of molecular oxygen (molarity of O_2) behind a shock wave (speed 4.1 km/sec) in oxygen. Here T and ξ represent the equilibrium values; Φ is the shock-wave front. Pressure 0.11 atm, laboratory time.

The absorptivity (at 2275 A) was measured with high time resolution (0.025 μsec) for the region behind a shock wave (Fig. 1, curve 1). Only vibrationally excited molecules of O_2 ($v^* \approx 4.5$) absorb in this spectral region, so any absorption must be associated with excitation, and loss of absorption implies dissociation. The relation of the absorptivity A to the concentration n_{O_2} of oxygen molecules and to the temperature T was derived by measuring A for the equilibrium region (far behind the front) and at the point of maximum absorption. The first measurements of A were for $T < 3000$-$4000°$; extrapolation to larger T on the basis of a Boltzman distribution for the initial levels gave results identical (within the errors of experiment) with the A as measured at point m (Fig. 1) for T up to 7000°K, if we assume that vibrational relaxation has ceased by this point and dissociation is not yet appreciable.* These assumptions are not strictly correct (particularly for high temperatures), for vibrational relaxation overlaps with dissociation near m. However, the relation of A to T shows that the effect is unimportant for T of 5000-7000°. Further, A is proportional to n_{O_2} if it is 0.2-0.3 (if the vibrations are in equilibrium):

$$A = n_{O_2}\varphi(T), \tag{1}$$

in which $\varphi(T)$ is the relation to temperature. The relation between n_{O_2} and T implied by the law of conservation of energy is

$$n_{O_2} = p\,\frac{\frac{D}{2kT} + \frac{5}{2} - \frac{mV^2}{4kT}\left[1 - \left(\frac{\rho_0}{\rho}\right)^2\right]}{\frac{D}{2} + \frac{5}{2}kT + \frac{mV^2}{4}\left[1 - \left(\frac{\rho_0}{\rho}\right)^2\right] - h(T)} \tag{2}$$

* Here T and the other parameters are calculated in accordance with the laws of conservation of mass, energy, and momentum as applied to the equation of state in accordance with the measured wave speed (known to 1-2%) and with the conditions in front of the wave.

(in which D is the dissociation energy, k is Boltzman's constant, m and h(T) are the mass and enthalpy of the oxygen molecule, V is the wave velocity, p and ρ are the gas pressure and density behind the front, and ρ_0 is the density before the front), so we can eliminate n_{O_2} from (1). The second term inside the square bracket is less than 0.015, so any change in it can be neglected; a mean ρ/ρ_0 may be used. Further, p varies little behind the wave, so it too can be assigned a mean value. Then (1) and (2) give us a relation between T, V, and A, which enables us to deduce T (curve 2 of Fig. 1) and also $\xi_{O_2} = n_{O_2}(kT/p)$ (Fig. 1, curve 3).

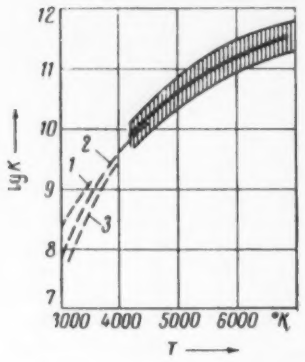

Fig. 2. Plot of log K (dimensions cm^3/mole · sec) for the dissociation of oxygen. Broken lines: 1) [2]; 2) [8]; 3) [5].

If we neglect recombination (which is possible for states far from equilibrium), we get for the region behind the shock wave that

$$\frac{d\xi_{O_2}}{dt} = -(1 + \xi_{O_2})\frac{p}{kT}\left[K\ (O_2, O_2)\,\xi_{O_2}^2 + K\ (O_2, O)\,\xi_{O_2}(1 - \xi_{O_2})\right], \tag{3}$$

in which $K(O_2, O_2)$ and $K(O_2, O)$ are the rate constants for dissociation consequent upon $O_2 - O_2$ and $O_2 - O$ collisions respectively. Values have been given for $K(O_2, O)$ [4, 5], so (3) gives us $K(O_2, O_2)$ for 4000-7000°K. This region is shown hatched in Fig. 2, the central line being the mean value. The scatter is large on account of several errors of experiment (width of oscilloscope beam, photomultiplier noise, etc.).

We may put K as an Arrhenius plot $K = PZ\exp\{-(D/kT)\}$, in which Z is the number of collisions in unit volume per sec per molecule. It is usually assumed that P may be represented reasonably well as $(D/kT)^n$; it is found [6, 7] that n is about 1.5 for collisions between atoms and diatomic molecules. This is closely so for O_2-Ar collisions [4]; Matthews [8] finds that n = 3 for $O_2 - O_2$ collisions at 2400-4600°K. My results imply an n of about 4. One possible cause of this marked variation in P with T is [4] that vibrational equilibrium does not occur completely at high temperatures. Incomplete relaxation at the start of dissociation limits the possibility of determining the rate constant as a function of temperature, because K will depend on the elapsed time after the passage of the wave as well as on the temperature at the higher speeds (temperatures). The range from 2400 to 7000°K is covered by the relation

$$K\ (O_2, O_2) = 2\cdot 10^{-2}\left(\frac{D}{kT}\right)^3 Z\ \exp\left\{-\left(\frac{D}{kT}\right)\right\}, \tag{4}$$

but caution is needed in extrapolating this relation to higher T.

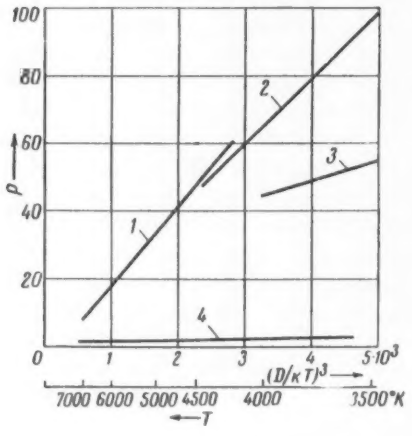

Fig. 3. Mean values of P as a function of $(D/kT)^3$ for $O_2 - O_2$ collisions (curves 1-3) and O_2-Ar collisions (curve 4). 1) Present results; 2) from [8]; 3) from [5]; 4) from [4].

Comparison of the P for $O_2 - O_2$ and O_2 – Ar collisions enables us to distinguish effects dependent on the structure of the particles. Figure 3 shows $P(O_2, O_2)$ and $P(O_2, Ar)$ as a functions of $(D/kT)^3$; the ratio α of the two decreases rapidly (from 30-40 at 3500°K to 5-10 at 7000°K). Nikitin [9] states that allowance for the transfer of rotational energy in $O_2 - O_2$ collisions gives an α of about 20, which is not dependent on temperature. The actual behavior of P indicates that our picture of the process needs revision.

I am indebted to N. A. Generalov for assistance in this work.

LITERATURE CITED

1. S. A. Losev and A. I. Osipov, Usp. Fiz. Nauk. 73, 3, 392 (1961).
2. S. A. Losev, DAN, 120, 6, 1291 (1958).
3. N. A. Generalov and S. A. Losev, Prikl. Mekh. i. Tekh. Fiz. 2, 64 (1961).
4. M. Camac and A. Vaughan, J. Chem. Phys. 34, 2, 460 (1961).

5. S. R. Bayron, J. Chem. Phys. 30, 6, 1380 (1959).
6. E. E. Nikitin, DAN, 119, 3, 526 (1958).
7. E. V. Stupochenko and A. I. Osipov, ZhFKh, 33, 7, 1526 (1959).
8. D. Matthews, Phys. Fluids, 2, 2, 170 (1959).
9. E. E. Nikitin, DAN, 132, 2, 395 (1960).

All abbreviations of periodicals in the above bibliography are letter-by-letter transliterations of the abbreviations as given in the original Russian journal. *Some or all of this periodical literature may well be available in English translation.* A complete list of the cover-to-cover English translations appears at the back of this issue.

ELECTROCHEMICAL HYDROGENATION OF ALLYL ALCOHOL

M. E. Manzhelei and A. F. Sholin

Kishinev State University
(Presented by Academician A. A. Balandin, July 3, 1961)
Translated from Doklady Akademii Nauk SSSR, Vol. 141, No. 4,
pp. 897-899, December, 1961
Original article submitted June 29, 1961

The present study was made for the purpose of elucidating the mechanism of cathode reduction of allyl alcohol on electrodes made of platinized platinum. This question was studied as early as 1906 by S. Fokin, who first pointed out the possibility of reducing allyl alcohol by means of an electric current. The product of the reaction, in his opinion, was propyl alcohol [1].

Several techniques have been adopted to solve the problem posed. Polarization curves have been taken i.e., measurements have been made of the value of the potentials set up when the strength of the polarizing current is varied from 0.001 to 10 ma. These measurements have been accompanied by a measurement of the volume, and a detailed analysis of the gas liberated. The gas to be analyzed was collected in an ampule (Fig. 1) (chromatographic method).

Fig. 1

A study was made of the reaction of allyl alcohol with the degassed electrode surface, i.e., of the adsorption (potentiometric method). The reaction in the layer of adsorbed hydrogen was also studied [2, 3]. The electrode material was a sheet of platinized platinum ($S_{apparent}$ = 2 cm^2, S_{actual} = 3000 cm^2) with a clean surface, and different amounts of mercury and arsenic added. The technique of applying these to the electrode surface is described in [4]. Preliminary measurements were made of the charging curves of the electrodes used [5] to find out how the hydrogen adsorptivity and the binding energy changes with electrode surface as affected by the above additives. The principal electrolyte was a 0.1 N solution of H_2SO_4. All measurements were made with respect to the potential of a reversible hydrogen electrode in this solution.

The electroreduction of allyl alcohol over the whole range of current densities from $3 \cdot 10^{-10}$ to $3 \cdot 10^{-6}$ a/cm^2 occurs at potentials corresponding, according to the charging curve, with adsorbed hydrogen present on the electrode surface. Here a characteristic phenomenon is observed, namely, the liberation of gaseous products, beginning at a potential 150 mv more positive than the reversible value of the hydrogen electrode potential. The composition of these products, as determined by gas chromatography, is given in table in mole percent, and the amounts of mercury and arsenic are given in percentages of the total number of surface platinum atoms. (In experiments Nos. 5 and 6, the electrode was platinized platinum wire.)

From the data of table and a comparison of the volume of gas liberated with the current passed, it is clear that the reduction of allyl alcohol in an acid medium on a cathode made of platinized platinum occurs mainly with the formation of C_3H_8, C_3H_6, and small quantities of CH_4, C_2H_4, C_2H_6, and H_2.

If the electrode potential is shifted to the negative side, the amount of propylene is reduced on account of an increase in the amount of propane (Experiments Nos. 1-3). At potentials in the further overvoltage range, the reduction stops (Experiment No. 4). In alkaline medium, the course of the reaction is markedly different; the liberation of gaseous products occurs only at potentials corresponding with the hydrogen overvoltage region. The reaction products are preponderantly hydrogen, the liberation of which initially (Experiment No. 5) consumes a part of the applied current, and then (Experiment No. 6) consumes the whole current. Thus, the conclusion may be reached that in an alkaline medium the reduction of allyl alcohol occurs through the formation of propyl alcohol.

Adsorption measurements in both acid and alkaline media have shown that $H_2C = CH - CH_2OH$ as well as CH_3OH, C_2H_5OH, and C_3H_7OH are adsorbed on the electrode giving a sharp change in potential toward the negative

Experiment No.	φ, mv	C_3H_8	C_3H_6	C_2H_4 + C_2H_6	CH_4	H_2
Electrolyte H_2SO_4						
1	80-50	29.8	66.3	1.3	1.2	1.4
2	40-20	32.5	62.4	1.8	1.3	2.0
3	−60	10.0	69.3	2.7	2.5	15.5
4	−260	2.7	10.8	−	−	86.5
Electrolyte NaOH						
5	−70	4.1	1.4	−	−	94.5
6	−270	0.8	−	−	−	99.2
Electrolyte H_2SO_4, on 20% Hg Electrode						
7	−60	0.4	10.2	−	−	89.4
Electrolyte H_2SO_4, on 10% As Electrode						
8	−150	−	−	−	−	100

side (Fig. 2, 1). It may be assumed that the $H_2C = CH - CH_2OH$ molecules are oriented horizontally on adsorption. Apparently, vertical orientation is also possible, as supported by the fact that large quantities of propylene are formed.

The reactions between allyl alcohol and the hydrogen adsorbed on the platinum are also markedly different in acid and in alkaline media. In acid medium, parallel with the change in potential toward the positive side, there is liberation of gas bubbles from the electrode, the chromatogram of which has one peak, corresponding with propane.

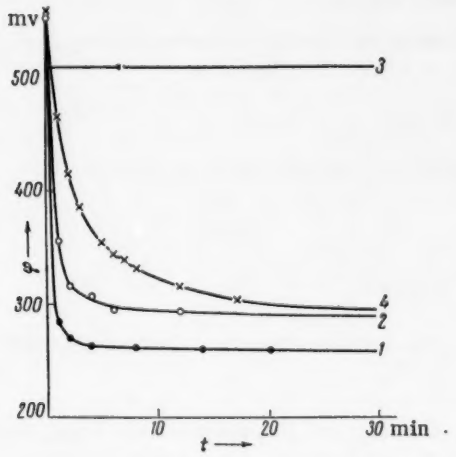

Fig. 2

If there are small quantities of mercury on the electrode, the hydrogenization by previously adsorbed hydrogen, and the electrohydration go in the same direction as on a clean platinum surface, but at a slower rate. Both reactions stop if the quantities of mercury are such that, according to the charging curves, the platinum loses its ability to adsorb hydrogen. The potential shift is reduced on adsorbing allyl alcohol, and at large fillings it becomes equal to zero (Fig. 2, 2, 3). Thus, on a mercury electrode, allyl alcohol is not reduced in agreement with polarographic data [6]. Arsenic, which causes a strengthening of the bond of the hydrogen adsorbed on the platinum, and to a considerable degree lowers the adsorption rate of allyl alcohol (Fig. 2, 4), causes a sharp reduction in the rate of both hydrogenization processes, and to large extent of the hydrocarbon formation reaction. At as little as ~ 4% coating with arsenic, the polarization curves at current densities of $1 \cdot 10^{-8}$ a/cm^2 go over into the overvoltage region, and repeat the hydrogen overvoltage curves.

The data given speak for a wide ranging similarity between hydration in the adsorbed hydrogen layer and electrohydration. Both these reactions are catalytic in nature, and are brought about by interaction between the adsorbed allyl alcohol molecules and the adsorbed hydrogen.

The data on the composition of the products resulting from the hydrogenization of allyl alcohol on a platinum catalyst electrode make possible a proposal as to the scheme of the reaction. The theoretical basis must be grounded on the calculations made by A. A. Balandin using the energetics aspect of the multiplet theory of catalysis. A. A. Balandin [7] has shown that, for a nickel catalyst, there is a sequence of possible reactions with alcohols, the indices of which may be written in the order of increasing energy barriers:

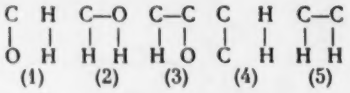

With unsaturated alcohols, precedence should be given to the index, corresponding with a reaction which saturates a multiple bond. A series of reactions of this sort is also completely possible on a platinum catalyst, since it has been shown [8] that the energies of the bond between the atoms in the indices and the catalyst surface change very little on going from metal to metal in the group Ni, Pt, Pd. With the adsorbed hydrogen present on the electrode surface, the most probable reactions are those with indices (1) and (4). It is well known that platinum is not a catalyst for the reaction with index (3).

In addition, in view of the fact that a large amount of propylene is found in the products of the reaction, the above reactions are possible without preliminary hydration of the double bond. In this case, hydrogenolysis of the C – O bond should be facilitated because a double bond is present in the allyl alcohol molecule in the $\alpha - \beta$ -position, which leads to lability of the OH group. Additional experiments have shown that CH_3OH, C_2H_5OH, and C_3H_7OH are not reduced. This confirms what has been said above. In addition, the polarized, adsorbed hydrogen atoms, H^+_{ads}, should cause polarization of the alcohol molecule at the place where the C – OH bond is located, and the hydrogen ions, located in the electric double layer of the electrolyte, should cause shifts in equilibrium toward the side of water formation. This last assumption is based on data from an experiment in alkaline medium, where the H^+ ions in the electric double layer were replaced by Na^+ ions, and formation of hydrocarbons does not occur.

Everything that has been said leads to the reaction scheme:

$$H_2C = CH - CH_2OH + H^+_{ads} = H_2C = CH - CH_2^+ + H_2O;$$
$$H_2C = CH - CH_2^+ + H^-_{ads} = H_2C = CH - CH_3.$$

The existence on the surface of metallic adsorbents of two oppositely charged hydrogen ions is something that has been proposed by many investigators in the field of adsorption and catalysis [9].

In addition to the main reaction, saturation of the double bond occurs as a parallel or consequent stage, as well as partial hydrogenolysis of the C – C bond to form hydrocarbons of lower molecular weight.

LITERATURE CITED

1. S. Fokin, ZhRFKhO, 38, 419 (1906).
2. A. I. Shlygin, Transactions of the Conference on Electrochemistry [in Russian] (Academy of Sciences, USSR, Press, 1953), p. 322.
3. M. E. Manzhelei, Uch. Zap. Kish Gos. Univ. 27, 179 (1957).
4. M. E. Manzhelei and L. V. Voitenko, ZhFKh, 34, 27 (1960).
5. A. I. Shlygin and A. N. Frumkin, Akta Physicochim. USSR, 3, 701 (1935).
6. M. Stackelberg and W. Stacke, Zs. Elektrochem. 53, 118 (1949).
7. A. A. Balandin, in Collection: Questions of Chemical Kinetics, Catalysis, and Reactivity [in Russian] (Academy of Sciences, USSR, Press, 1955), p. 474.
8. S. A. Kiperman and A. A. Balandin, ZhFKh, 33, 2045 (1959).
9. S. Z. Roginskii, Kinetika i Kataliz. 1, 15 (1960); R. Suhrmann, G. Wedler, and D. Schiephane, Zs. Phys. Chem. 12, 128 (1957); L. E. Moore and P. Selwood, J. Am. Chem. Soc. 78, 647 (1956); T. Toya, J. Res. Inst. Catal. 6, 388 (1956).

COMBINATIONAL LIGHT SCATTERING SPECTRA OF $AgClO_4$ AND ITS COMPLEX WITH BENZENE

Sh. Sh. Raskin

Scientific Research Physics Institute, Leningrad State University
(Presented by Academician A. N. Terenin, July 13, 1961)
Translated from Doklady Akademii Nauk SSSR, Vol. 141, No. 4,
pp. 900-903, December, 1961
Original article submitted June 17, 1961

$AgClO_4$, like $SbCl_3$ and some other complex-forming substances, forms compounds with benzene and its derivatives. It is a matter of importance that in recent years the crystal structure of the $AgClO_4 \cdot C_6H_6$ complex has been studied repeatedly by x-ray methods [1, 2], and in [2] it was possible to determine the deformation of the carbon skeleton of the benzene ring, as well as to give a value for the energy of the donor-acceptor bond in this complex. Up to the present time a number of investigations have been carried out on the spectra of $AgClO_4$ complexes. For example, in [3], a study was made of the infrared spectra not only of $AgClO_4 \cdot C_6H_6$, but of the compound $2SbCl_3 \cdot C_6H_6$ in the solid phase, which we studied previously. The results obtained confirm the data of our studies on the combination scattering spectra of the complexes which $SbCl_3$ forms with benzene and its derivatives [4]. Since the nature of the change in the spectra, in the opinion of the author of [3], is not identical in these two complexes, the conclusion is reached that there is a different type of bond in them.

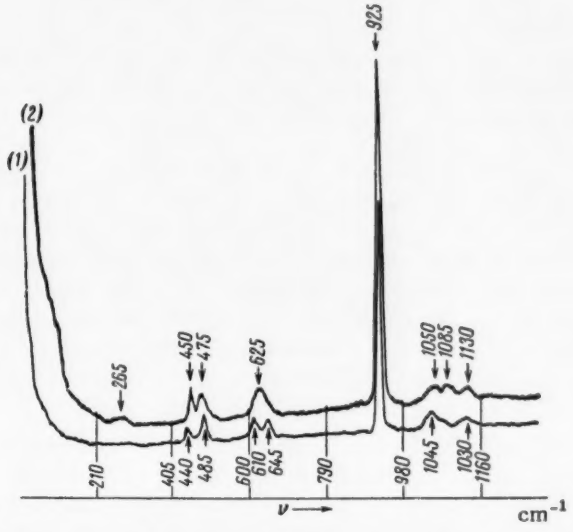

Fig. 1. Traces of combinational scattering spectra of (1) Anhydrous, and (2) hydrated $AgClO_4$ on the DFS-12 spectrometer.

In the present paper, a study has been made of the combinational scattering spectra of the polycrystalline complex $AgClO_4 \cdot C_6H_6$ on a DFS-12 apparatus with a double grating monochromator and photoelectric recording of the spectrum (dispersion 5.2 A/mm, relative aperture 1 : 53). The spectrum was excited from the line 4358 A, obtained from a low pressure mercury spiral arc with cooled electrodes, built in the laboratory. The short wave length part of the arc spectrum was filtered out with a saturated solution of $NaNO_2$.

At the same time, studies were also made on the spectra of anhydrous $AgClO_4$ and its monohydrate. The frequencies of the spectra obtained are given in table, and the traces of the spectra on the DFS-12 are reproduced in Figs. 1 and 2. The spectra of anhydrous and hydrated $AgClO_4$ are markedly different from one another as may be seen from table. It should be noted above all that the frequencies 1045 and 1130 cm^{-1} go over on hydration into a triplet band with the maxima 1050, 1085 and 1130 cm^{-1}. Further, the two frequencies 610 and 645 cm^{-1} of anhydrous $AgClO_4$ go over into the band 625 cm^{-1} (possibly with structure). We note further, that on hydration the frequencies 440-485 cm^{-1} of anhydrous $AgClO_4$ come together and form a band with the wide maxima 540 and 475 cm^{-1}.

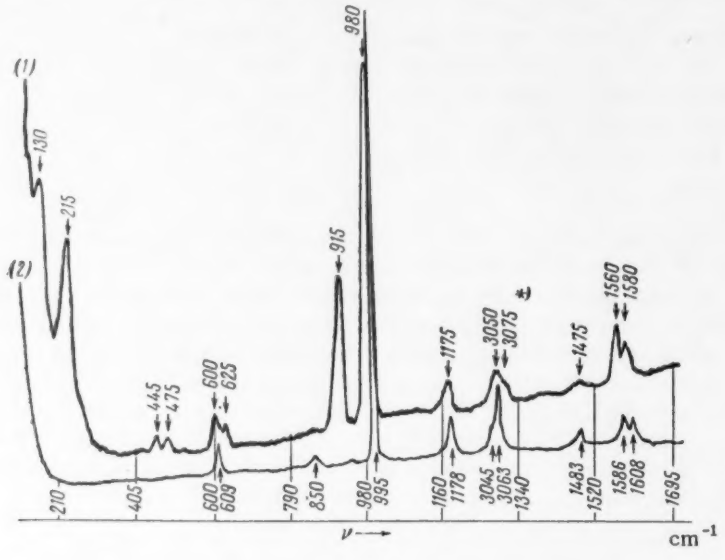

Fig. 2. Traces of combinational scattering spectra of (1) the polycrystalline complex $AgClO_4 \cdot C_6H_6$, and (2) of liquid benzene on the DFS-12 spectrometer.

On examination, the spectrum of the $AgClO_4 \cdot C_6H_6$ complex in the $AgClO_4$ frequency region, as may be seen from table, suggests the spectrum of hydrated rather than anhydrous $AgClO_4$. It should be noted that the two new intense frequencies 130 and 215 cm^{-1} appear, and that the frequency of the intense (Cl – O) line at 925 cm^{-1} is reduced by 10 cm^{-1}. As to the frequencies in the region of vibration of the second component of the complex, we can point to a lowering of the frequency 995 cm^{-1} in C_6H_6 by 15 cm^{-1} when the complex is formed, and a similar reduction in the frequencies of the doublet 1586-1608 cm^{-1} by about 25 cm^{-1}. The C – H frequencies (from λ 4047), marked in Fig. 2 with an asterisk, were also observed. In the spectrum of the complex they are represented by a diffuse band, possibly with the two maxima 3050 and 3075 cm^{-1}, having not very different intensities, while in the spectrum of pure C_6H_6 there are two lines with different intensities in the frequencies 3045 and 3063 cm^{-1}.

There is some point in comparing our results with the data on the combinational scattering spectra of monocrystals of the intermolecular compounds of $SbCl_3$ with benzene and its derivatives [4]. As has been shown, when these complexes are formed, the following changes occur in the spectra: first, in the valence vibration region of $SbCl_3$, the spectra of the complex show a larger number of lines than can be ascribed to the $SbCl_3$ molecule (even in the case of the two $SbCl_3 \cdot C_6H_6$ complex, where the spectra of the components of the complex do not overlap). As to the origin of these lines, the proposal has been made that they should probably be ascribed to new bonds, formed in the complex. Second, new lines are observed in the region of the organic component of the complex, which, as we have proposed, are due to violation of the selection rules. Third, there is splitting and displacement of a number of lines in the spectra. Thus, for example, the above-mentioned frequency 995 cm^{-1} in the spectrum of the intermolecular compound $2SbCl_3 \cdot C_6H_6$ is lowered 4 cm^{-1}, and the 1586-1608 cm^{-1} doublet is lowered 6-7cm^{-1}.

In spite of the relatively small magnitude of these shifts, and in view of the fact that it is observed systematically in a number of other complexes, we proposed earlier [4], that the lowering in frequency of these lines with ben-

Combinational Scattering Spectra of $AgClO_4$, and the Complex $AgClO_4 \cdot C_6H_6$

$AgClO_4$		$AgClO_4 \cdot C_6H_6$	C_6H_6
anhydrous	hydrate		
		130(7)	
		215(6)	
	265(<1/2)		
440(1/2)		445(1/2)	
	450(>1)		
	475(<1)	475(1/2)	
485(1)			
		600 (1)	609(<1)
610(<1)			
	625(1)	625(<1)	
645(<1)			850(1/2)
		915(4 1/2)	
925(10)	925(10)		
		980(10)	
			995 (10)
1045(1)	1050(1/2) *		
	1085(1/2)		
1130(1/2)	1130(1/2)		
		1175 (1)	1178 (1)
		1475 (1/2)	1483(1/2)
		1560 (1 1/2)	
		1580 (1)	1586 (1/2)
			1608 (1/2)
		3050 (1)	3045 (1/2) *
		3075 (<1)	3063 (1 1/2)

* Band with maxima.

zene and its derivatives is characteristic of the formation of π-complexes. As we have seen, in analyzing our data on the combinational scattering spectra of $AgClO_4 \cdot C_6H_6$, we also observed the same characteristic changes, but to a greater extent.* The question naturally arises, is it possible, since the above-mentioned line shifts in the spectra of the compounds $AgClO_4 \cdot C_6H_6$ and $2SbCl_3 \cdot C_6H_6$ are known and the value of the energy of the $Ag - C_6H_6$ bond is known from [1], – is it possible to make some sort of statement as to the bond energy in the catalytic complex $2SbCl_3 \cdot C_6H_6$? It seems to us that it is impossible to do this simply on the basis of the results which we have. First, there is no x-ray data on the structure of the crystal or the complex; second, there are indirect indications, which suggest the idea that the interaction in this intermolecular compound is no longer so small. Some qualitative indications of this sort are to be found in Menshutkin's paper [5], as well as in our experiments. In addition, the question is not yet cleared up for compounds of this type, whether or not there is a correspondence between the interaction of the components in the complex and the observed spectroscopic changes.

In conclusion, we wish to point out the following. In recent years, some new studies have appeared on the spectra of $SbCl_3$ and its complexes [6, 7]. In particular, [7] repeated our studies on the combination scattering spectra of $SbCl_3$ with benzene and its derivatives [4], and all our experimental results were confirmed.

As the authors of [7] state, in the spectrum of pure liquid $SbCl_3$, in the neighborhood of the intense band at 357-380 cm^{-1} are to be found weak additional maxima, which explain the appearance of the new lines in the spectrum of the two $SbCl_3 \cdot C_6H_6$ complex. However, repeated studies on the shape of the 357-380 cm^{-1} band both by photographic and by photoelectric methods (on the DFS-12), have failed to confirm the existence of these weak maxima.

The authors expresses his gratitude to E. V. Pershina for her assistance in the work.

LITERATURE CITED

1. R. E. Rundle and J. H. Goring, J. Am. Chem. Soc. 72, 5337 (1950).
2. H. G. Smith and R. E. Rundle, J. Am. Chem. Soc. 80, 5075 (1958).
3. L. W. Daasch, Spectrochim. Acta. 9, 726 (1959).
4. Sh. Sh. Raskin, DAN, 100, 3, 485 (1955); Optika i Spektroskopiya, 1, 4, 516 (1956); DAN, 123, 4, 645 (1958).
5. B. N. Menshutkin, The Effect of Substituents on Some Reactions of Benzene and Its Substituted Derivatives [in Russian] (SPb, 1912).
6. A. Tramer, Bull. Acad. Polon. Sci. Ser. Math. Astron. Phys. 6, 10, 659 (1958); P. W. Davis and R. A. Octjen, J. Molec. Spectrosc. 2, 253 (1958); L. W. Daasch, J. Chem. Phys. 28, 1005 (1958); Watari Fumio and Kimaki Susumi, Bull. Chem. Res. Inst. Non-Aqueous Solut. Tohoku Univ. 9, 1 (1959); K. Wilmshurst, J. Molec. Spectrosc. 5, 343 (1960).
7. P. Simova and R. Angelieva, Bulletin of the Bulgarian Academy of Sciences, Physics Series [in Bulgarian] (1959), Vol. 7, No. 333.

* It, therefore, seems to us that the conclusion reached in [3] to the effect that the compounds $2SbCl_3 \cdot C_6H_6$ and $AgClO_4 \cdot C_6H_6$ are of a different nature since the changes in their spectra are different, is a little ahead of itself. The question cannot be definitely solved without x-ray data on the structure of the crystal and the compound.

OXIDATION-REDUCTION POTENTIAL OF THE SYSTEM U^{3+}/U^{4+} IN A NaCl – KCl MELT

M. V. Simirnov and O. V. Skiba

(Presented by Academician V. I. Spitsyn, June 2, 1961)
Translated from Doklady Akademii Nauk SSSR, Vol. 141, No. 4,
pp. 904-907, December, 1961
Original article submitted May 30, 1961

The oxidation-reduction potential of the system U^{3+}/U^{4+} gives not only the equilibrium between metallic uranium and its tri-quadrivalent ions in the melt, but also the residual current from the electrolysis of uranium tetrachloride in fused alkaline metal chlorides, caused by the change in charge from U^{4+} to U^{3+}. In the literature there are two papers [1, 2] in which the oxidation-reduction potential of uranium was measured in a fused eutectic LiCl – KCl mixture at a temperature of 600°C. Unfortuantely, the measurements were made not with the same, but with different, although metallic comparison electrodes: silver in [1], and platinum in [2]. This fact makes it difficult to compare the published results of the investigations, and very much complicates the thermodynamic interpretation. But even allowing for the possibility of errors in reducing the potentials to any one comparison electrode, there is still considerable divergence between them. Thus, it follows from the paper by Trzebiatowski and Kisza [1] that, referred to a platinum comparison electrode at 450° in a LiCl – KCl melt [3], $E^0_{U^{3+}/U^{4+}} = -0.813$ v, while according to the direct measurements of Hill, Perano, and Osteryoung [2] under these same conditions $E^0_{U^{3+}/U^{4+}} = -1.25$ v. It may be seen that the difference amounts to 0.44 v.

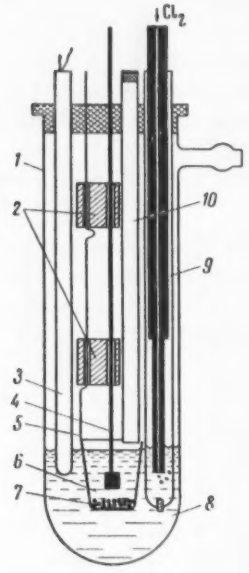

Fig. 1. Cell. 1) Quartz tube; 2) porcelain spacers; 3) thermocouple; 4) Pt and Mo electrode; 5) alundum crucible with Mo suspension; 6) electrolyte under test; 7) metallic uranium; 8) NaCl – KCl melt; 9) chlorine comparison electrode; 10) quartz tube for adding uranium.

We have measured the oxidation-reduction U^{3+}/U^{4+} potential at the higher temperatures 690-810° in a fused 1 : 1 NaCl – KCl mixture. As the comparison electrode we chose a chlorine electrode, which is at equilibrium relative to the electrolyte under study. The method used was the one which we had tested previously on the system Ti^{2+}/Ti^{3+} [4] involving potentiometric titration UCl_4 in a NaCl – KCl melt with metallic uranium. This enabled us to avoid the errors associated with the difficulties in making an accurate measurement in the melt of the ratios of the concentrations of quadri- and trivalent uranium caused by the greater reactivity of the latter.

The cell in which the measurements were made is shown schematically in Fig. 1. The chlorine comparison electrode was in a separate quartz tube having an opening filled by an asbestos disphragm. The indicator electrode, which took on the potential of the system U^{3+}/U^{4+}, was a platinum or molybdenum wire, which was rotated to stir the electrolyte and was prepared by fusing an equi-molar mixture of chemically pure sodium and potassium chlorides in vacuum. The uranium tetrachloride was prepared by chlorinating uranium dioxide with carbon tetrachloride vapor, followed by purification consisting of 2-3 fold volatilization in vacuum. In the various experiments, the electrolyte contained from 0.6 to 9.6% U by weight. The gas volume above the salt mixture was filled with pure argon after evacuation. The cell was placed in a previously heated furnace, and held until the desired temperature was reached, which was kept constant to ± 1°. Then the metallic uranium was charged into the melt, and with constant stirring of the electrolyte the potential of the indicator electrode was measured once every minute. The results of the measurements, plotted relative to time, give distorted potentiometric titration curves. In course of time, these curves become more and more

Experiment No.	Temp °C	Uranium concentration in original melt: U, % by wt.	Uranium concentration in original melt: $[U^{4+}]$	Indicator electrode material	E.M.F.	Experiment No.	Temp °C	Uranium concentration in original melt: U, % by wt.	Uranium concentration in original melt: $[U^{4+}]$	Indicator electrode material	E.M.F.
1	698	1,77	$5,0 \cdot 10^{-3}$	Mo	1,432	9	715	5,55	$1,7 \cdot 10^{-2}$	Mo	1,422
2	701	4,75	$1,4 \cdot 10^{-2}$	Mo	1,423	10	720	2,24	$6,5 \cdot 10^{-3}$	Mo	1,414
3	701	9,6	$2,8 \cdot 10^{-2}$	Mo	1,423	11	740	2,10	$6,0 \cdot 10^{-3}$	Pt	1,404
4	708	7,92	$2,3 \cdot 10^{-2}$	Mo	1,416	12	786	4,21	$1,2 \cdot 10^{-2}$	Pt	1,377
5	714	1,52	$4,3 \cdot 10^{-3}$	Mo	1,418	13	790	0,6	$1,7 \cdot 10^{-3}$	Pt	1,376
6	714	7,95	$2,3 \cdot 10^{-2}$	Pt	1,416	14	802	1,86	$5,3 \cdot 10^{-3}$	Mo	1,376
7	705	1,98	$5,7 \cdot 10^{-3}$	Mo	1,428	15	805	2,86	$8,1 \cdot 10^{-3}$	Pt	1,372
8	715	2,14	$6,1 \cdot 10^{-3}$	Mo	1,416						

stretched out, since as the concentration of quadrivalent uranium in the melt decreases, the rate of the heterogeneous reduction reaction $3U^{4+}_{melt} + U_T = 4U^{3+}_{melt}$ falls off. Nevertheless, all the curves obtained show wiggles, which correspond with reaching a state of equality between the U^{4+} and U^{3+} concentrations in the electrolyte. This appears with special clarity in the differential curves, the most typical of which are given in Fig. 2.

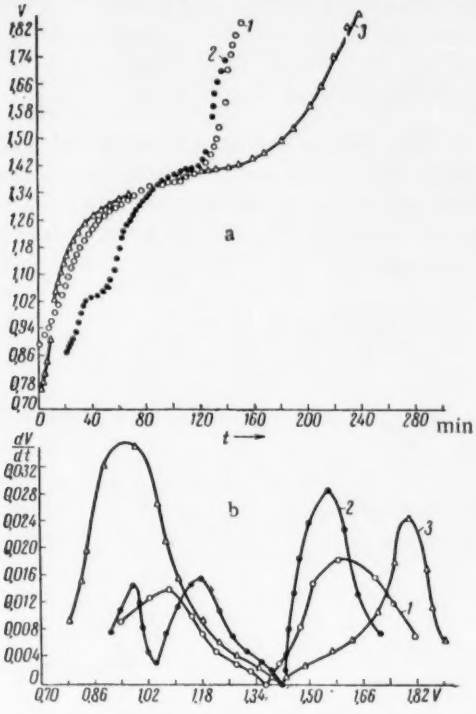

Fig. 2. Potentiometric titration curves with metallic uranium. 1) Experiment No. 13; 2) experiment No. 7; 3) experiment No. 6.

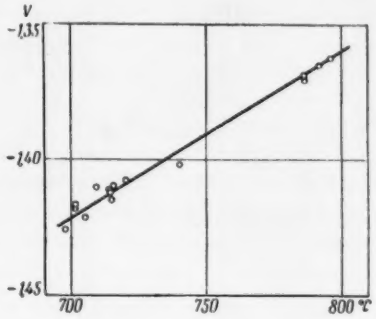

Fig. 3. Temperature dependence of the oxidation-reduction potential of the system U^{3+}/U^{4+}

With a molybdenum indicator electrode, the curves show an additional wiggle, lying at the more positive potentials of about −1 v. With a platinum electrode under the same conditions there is no such wiggle. Obviously, it came from solution of molybdenum according to the reaction:

$$Mo_T + 3U^{4+}_{melt} = Mo^{3+}_{melt} + 3U^{3+}_{melt}.$$

Table shows, for various temperatures and concentrations of quadrivalent uranium in the original melt, the e.m.f.'s of the cell, which correspond with the wiggles in the potentiometric titration curves. Corrected for the thermal e.m.f. between the cell electrodes, (C − Mo or C − Pt), they give us the desired values of the oxidation-reduction potential $E^0_{U3+/U4+}$, relative to a chlorine comparison electrode. The corresponding points, given in the curve of Fig. 3 as a function of the temperature, give a good fit to the straight line described by the empirical equation

$$E^0_{U^{3+}/U^{4+}} = -1,906 + 4,83 \cdot 10^{-4} T \pm \pm 0,003 \text{ v}.$$

In spite of the fact that the ion fraction concentration of uranium in the original solutions changes almost 17 times (from $1.7 \cdot 10^{-3}$ to $2.8 \cdot 10^{-2}$), the magnitude of $E^0_{U^{3+}/U^{4+}}$ remains constant within the limits of possible experimental error. This shows that the salt mixtures $UCl_3 - UCl_4 - NaCl - KCl$ of the compositions investigated behave as ideal solutions.

The U^{3+}/U^{4+} oxidation-reduction potential in a NaCl – KCl melt is considerably more positive than the Th^{2+}/Th^{4+} potential. At 1000°K, the difference in the potentials reaches a value $E^0_{U^{3+}/U^{4+}} - E^0_{Th^{2+}/Th^{4+}} = 0.517$ v. From the previously [5] found value of $E^0_{Th^{2+}/Th^{4+}} = -1{,}945 - 0{,}95 \cdot 10^{-4}T$ v in a NaCl – KCl melt relative to a chlorine comparison electrode, expressions may be found for the equilibrium constant of the reaction $2U^{4+}_{melt} + Th^{2+}_{melt} \rightleftharpoons 2U^{3+}_{melt} + Th^{4+}_{melt}$

$$\lg K = \lg \frac{[Th^{4+}][U^{3+}]^2}{[Th^{2+}][U^{4+}]^2} = 5{,}82661 + \frac{391}{T}.$$

Hence it follows that, for example, at 1000°K, reduction in a 99% U melt $U\left(\frac{[U^{3+}]}{[U^{4+}]} = 99\right)$ is accompanied by reduction of only 0.6% of the Th $\left(\frac{[Th^{2+}]}{[Th^{4+}]} = 0{,}0061\right)$.

From measurements on the equilibrium potentials of uranium in a NaCl – KCl melt [6], it was found that $E^0_{U/U^{4+}} = -3.010 + 6.65 \cdot 10^{-4}$ T v relative to a chlorine comparison electrode. This makes it possible, using the equation $E^0_{U^{3+}/U^{4+}} = 4E^0_{U/U^{4+}} - 3E^0_{U/U^{3+}}$ to calculate the value of the standard electrode potential, U/U^{4+}

$$E^0_{U/U^{4+}} = -2{,}734 + 6{,}14 \cdot 10^{-4}T \text{ v}$$

Since the value of $E^0_{U/U^{4+}}$ is given relative to a reversible chlorine electrode, it may be taken directly for calculation of the thermodynamic quantities, which express the state of the uranium tetrachloride in the NaCl – KCl melt. If it is born in mind that UCl_4 solutions in the melt behave ideally at concentrations which correspond essentially with mixtures of the congruently melting compound K_2UCl_6 [7] with NaCl and excess KCl, the decomposition voltage of UCl_4 at an ion fraction concentration of uranium $[U^{4+}] = 0.2$ is given by

$$\varepsilon_{melt} = -E^0_{U/U^{4+}} - 0{,}496 \cdot 10^{-4}T \lg 0{,}2,$$
$$\varepsilon_{melt} = 2{,}734 - 5{,}79 \cdot 10^{-4}T \text{ v}.$$

This quantity is a direct measure of the change in isobaric potential in the formation of uranium tetrachloride from its elements in a melt of the composition in question:

$$U_T + 2Cl_{2g} = UCl_4 \text{ melt},$$
$$\Delta Z = -4F\varepsilon_{melt} = -252\,206 + 53{,}41\,T \text{ cal/mole}.$$

Hence, the heat and entropy of the reaction are equal to:

$$\Delta H_{UCl_4\,melt} = -252\,206 \text{ cal/mole}$$
$$\Delta S_{UCl\,melt} = -53{,}41 \text{ cal/°C-mole}$$

From the thermodynamic data in the literature [7], it is possible to calculate the change in the isobaric potential for the formation of pure liquid uranium tetrachloride from its elements:

$$\Delta Z_2 = -253\,561 + 49{,}34T \text{ cal/mole}.$$

Thus, it is clear that mixing liquid uranium tetrachloride with fused NaCl – KCl is accompanied by a considerable change in the isobaric potential, equal to:

$$\Delta Z_{mixed} = \Delta Z_1 - \Delta Z_2 = -18\,645 + 4{,}07T \text{ cal/mole}.$$

This gives a hint of the formation in a fused UCl_4 – NaCl – KCl mixture of stable complex anions

$$U^{4+}_{melt} + 6Cl^{-}_{melt} \rightarrow UCl_6^{2-}{}_{melt}.$$

This reaction proceeds with a liberation of heat $\Delta H = -18.6$ kcal/g-ion, and a small reduction in the entropy of the system, $\Delta S = -4.07$ entropy units because of some ordering in the mutual orientation of the ions in the melt.

Knowing the quantities $E^0_{U/U^{3+}}$ and $E^0_{U/U^{4+}}$, we can obtain the expressions for the variation and isobaric potential, and the equilibrium constant of the reaction $3U^{4+}_{melt} + U_T \rightleftharpoons 4U^{3+}_{melt}$

$$\Delta Z = -276\,744\,(E^0_{U/U^{4+}} - E^0_{U/U^{3+}}) = -76381 + 14{,}11T \text{ cal},$$

$$\lg K = \lg \frac{[U^{3+}]^4}{[U^{4+}]^3} = \frac{120000}{1{,}984T}(E^0_{U/U^{4+}} - E^0_{U/U^{3+}}) = -3{,}0845 + \frac{16690}{T}.$$

In contrast with thorium dichloride [5], uranium trichloride in a NaCl – KCl melt is stable over the whole range of attainable temperatures (a lack of proper proportional relationship to UCl_4 and U should begin at temperatures above 5000°).

LITERATURE CITED

1. W. Trzebiatowski and A. Kisza, Bull. Acad. Polon. Sci. Ser. Chem. Geol. Et Geogr. 7, 781 (1959).
2. D. L. Hill, J. Perano, and R. A. Osteryoung, J. Electrochem. Soc. 107, 698 (1960).
3. H. A. Laitinen and C. H. Liu, J. Am. Chem. Soc. 80, 1015 (1958).
4. M. V. Smirnov, L. A. Tsiovkina, and N. A. Loginov, DAN, 136, 1388 (1961).
5. M. V. Smirnov and L. D. Yushina, Izv. AN SSSR, OKhN, 2, 251 (1959).
6. O. V. Skiba and M. V. Smirnov, Electrochemistry of Fused Salts and Solid Electrolytes [in Russian] (Transactions of the Institute of Electrochemistry, Ural Branch, Academy of Sciences, USSR, 1956), No. 2.
7. J. Katz and E. Rabinowitz, Chemistry of Uranium [Russian translation] (IL, 1954), Vol. 1.

THE SLOWING DOWN LIMIT IN THE THERMAL CRACKING OF ALKANES AS AFFECTED BY THE NATURE OF THE INHIBITOR

A. D. Stepukhovich

N. G. Chernyshevskii Saratov Government University
(Presented by Academician V. N. Kondrat'ev, March 28, 1961)
Translated from Doklady Akademii Nauk SSSR, Vol. 141, No. 4,
pp. 908-910, December, 1961
Original article submitted March 21, 1961

In 1934, we first observed the slowing down effect of propylene additives on the thermal cracking rate of butane. Subsequently, in studying the slowing down effect of propylene additives on the thermal decomposition rate of ethane [2], one of the most interesting phenomena in the field of thermal cracking was discovered, namely, the existence of the slowing down limit of an inhibitor. The essence of this phenomenon consists in the fact that if the inhibitor concentration is increased, the alkane cracking rate falls to some value and does not change with further increase in the inhibitor concentration. It has been shown in our later papers that the phenomenon of the slowing down limit is characteristic of the effect of different inhibitors on the decomposition of various alkanes [3-10]. Staveley and Hinshelwood [11, 12] came to the same conclusion in their studies on the effect of NO on the thermal decomposition of alkanes.

The residual rate of completely inhibited alkane cracking was interpreted by us as the rate of a residual chain reaction [4] or, at least, as the rate of primary decomposition into radicals [3, 13]. In connection with these investigations, the question arose as to how the various inhibitors effect the thermal cracking rate of a given alkane. A priori, it could only be assumed that, if thermal cracking of an alkane is a homogeneous reaction, and the residual rate at the slowing down limit is of the same order of magnitude as the homogeneous radical production rate, then different inhibitors should slow down the radical-chain decomposition of a given hydrocarbon to one and the same limit. Naturally, difference in nature of the inhibitors would show up only in that different quantities of inhibitor would be required to reach the well defined production rate.

The very first calculations [3, 14] showed that the residual rate at the slowing down limit is many times greater than the homogeneous radical production rate, and, consequently, it could not be interpreted as the primary rate of dissociation of the hydrocarbon into radicals. This encouraged us to start considering thermal cracking as a process involving heterogeneous production of radicals [14, 15]. In the formation of chains on walls, because of the ease of formation of radicals on a surface from simple chemisorption (or even from activated adsorption), the production rate was increased many times, and approached the observed residual rate. In addition, as shown by experiment, the chain length was also reduced, approaching that observable from the composition of the products [4, 14-16].

With heterogeneous production of radicals and a homogeneous action of the inhibitors, one can imagine that different inhibitors, rupturing the chains in the volume, were the cracking rate of a given alkane to the same value. In making an experimental study of the effect of different inhibitors on the cracking rate of the same alkane, for example of propylene or isobutylene on the thermal decomposition rate of propane (butane or isobutane), we found that the olefine inhibitors mentioned reduced the decomposition rate of the hydrocarbon in question down to practically the same limiting value [7-9]. However, we explained this fact in terms of the similarity in structure of the inhibitors, whose mode of action consists in carrying off H atoms from the methyl groups in the olefins by means of active radicals, and forming low activity allyl radicals [5, 16]. The fact is that the residual rate at the slowing down limit is still several times greater than the heterogeneous radical formation rate, and may be interpreted as the rate of a residual chain reaction for some chain length [4, 16]. In this case, naturally, the slowing down limit should be different for different inhibitors, i.e., it should depend on the nature of the inhibitor.

At almost the same time, Hinshelwood and his coworkers [17, 18] found that even more widely different inhibitors (such, for example, as NO and propylene) reduce the pentane decomposition rate to the same limiting value.

Thus, both from our studies, and from the work of Hinshelwood and his coworkers, it was possible to come to the conclusion that the slowing down limit is independent of the nature of the inhibitor for any given hydrocarbon. However, this contradicts the idea of the residual rate as being the rate of a chain reaction. Actually, Hinshelwood, basing his arguments on the fact that the rate at the slowing down limit is independent of the nature of the inhibitor, interpreted the residual decomposition rate of a hydrocarbon as the rate of a molecular reaction, on which, naturally, inhibitors have no effect. In the opinion of these authors, thermal cracking is a combination of a molecular and a chain reaction.

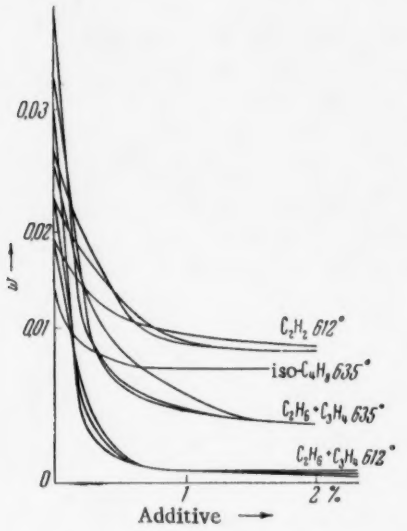

Ethane cracking rate as a function of inhibitor concentration.

Based on the idea that the slowing down rate is independent of the nature of the inhibitor, Voevodskii and his coworkers [19, 20] proposed an hypothesis, in which the inhibitor prevents the formation of radicals on the walls, but has no effect on the development of chains in the volume, i.e., it acts in an exclusively heterogeneous way. The fact that the slowing down limit is the same for different inhibitors finds just as simple an explanation on Voevodskii's hypothesis, as in Hinshelwood's work, and is, that to block an active center on a surface requires just one inhibitor particle of any given kind. Here, the residual rate can be interpreted only as a rate of formation, and the developing chains in the volume are very long (of the order of several hundred links).

Without rejecting the advantages of this hypothesis in explaining the observed fact, one must, however, recognize that the point of view relative to the absolute nature of the fact itself is subject to doubt. This doubt is based on the facts presented in our work, which testify to the fundamentally homogeneous nature of the action of olefin inhibitors, although NO as a radical can affect heterogeneous chain formation. The doubt is further based on the ideas, derived from this work, relative to the hetero-homogeneous chain character of the residual rate.

In view of the wide development of studies that have been made on the effect of different alkane cracking products on the course of the reaction, we were able to subject our doubts to test. In particular, we tried to show which products slow up ethane cracking, since adding ethylene does not show any inhibiting effect, and propylene was not observed either in the initial or in the later stages of ethane cracking [16]. In experiments on ethane cracking made by the authors, E. K. Mogileva and N. S. Sukhova, it was shown that small additions of allene and acetylene act like effective inhibitors [16], and here they reduce the cracking rate to a different limiting value.

Data on the variation of the initial cracking rate of ethane (after 10, 30 and 60 seconds) with the amount of added isobutylene, allene, and acetylene at different temperatures (612 and 635°) and different initial pressures (10 mm for added iso-C_4H_8, 20 mm for added C_3H_4 and C_2H_2, and t = 60 sec) are given in figure. The curves demonstrate clearly that at 612° the added allene and acetylene slow up the reaction rate to different limiting values. At 635°, with added allene and isobutylene a difference was also observed in the cracking rate at the limit of inhibitor action which lies beyond the limits of possible error in the rate determination. These results prove directly that the slowing down limit does depend on the nature of the inhibitor, and, together with this, they prove the radical-chain character of the residual reaction at the limit, which occurs in the volume. It should be noted that if the chain formation reaction on the walls is prevented by the inhibitor, as occurs from the effect of adding NO, no absolute significance is to be attached to the fact that their residual rate is independent of the nature of the inhibitor either, at least in the sense of there being any difference in the adsorptional properties of the inhibitors or of their reactivities with respect to centers on the surface. In the light of all this, the fact that the limits are the same for some olefins and NO in the case of propane or pentane cannot have any absolute significance.

LITERATURE CITED

1. A. I. Dintses, A. D. Stepukhovich, and D. V. Frost, Byull. Gos. Khim. Nauchno-Issl. Inst. Vysokikh Davlenii, 6, 4 (1934).
2. A. I. Dintses, D. A. Kvyatkovskii, A. D. Stepukhovich, and A. V. Frost, ZhOKh, 7, 1754 (1937).
3. A. D. Stepukhovich, Candidates Dissertation [in Russian] (Saratov, 1938).

4. A. D. Stepukhovich, ZhFKh, 24, 513 (1950); ZhFKh, 31, 511 (1957).
5. A. D. Stepukhovich, DAN, 89, 889 (1953); 92, 213 (1953).
6. A. D. Stepukhovich and A. G. Finkel', ZhFKh, 26, 1413 (1952).
7. A. D. Stepukhovich and É. S. Shver, DAN, 89, 1067 (1953); ZhFKh, 27, 1013 (1953).
8. A. D. Stepukhovich and A. M. Chaikin, ZhFKh, 27, 1737 (1953).
9. A. D. Stepukhovich and G. P. Vorob'eva, ZhFKh, 28, 1361 (1954).
10. A. D. Stepukhovich and L. V. Derevenskikh, ZhFKh, 28, 1413 (1952); 28, 1720 (1954); 29, 2129 (1955).
11. L. Staveley, Proc. Roy. Soc. A. 162, 557 (1937).
12. I. E. Hobbs and C. Hinshelwood, Proc. Roy. Soc. A. 167, 447 (1938).
13. A. I. Dintses, Usp. Khim. 7, 404 (1938).
14. A. D. Stepukhovich, ZhFKh, 28, 1882 (1954).
15. I. F. Bakhareva, Candidates Dissertation [in Russian] (Saratov, 1954).
16. A. D. Stepukhovich, Doctors Dissertation [in Russian] (Moscow, 1958).
17. F. I. Stubbs and C. Hinshelwood, Proc. Roy. Soc. A. 200, 4158 (1950); A. 201, 18 (1950).
18. K. U. Ingold, F. I. Stubbs, B. C. Spall, and C. Hinshelwood, Proc. Roy. Soc. A. 214, 20 (1952).
19. V. V. Voevodskii, DAN, 90, 5 (1953).
20. V. V. Voevodskii and V. A. Poltorak, DAN, 91, 3 (1953).

All abbreviations of periodicals in the above bibliography are letter-by-letter transliterations of the abbreviations as given in the original Russian journal. *Some or all of this periodical literature may well be available in English translation.* A complete list of the cover-to-cover English translations appears at the back of this issue.

THE E.P.R. SPECTRUM OF IRRADIATED FROZEN BENZENE

V. A. Tolkachev, Yu. N. Molin, I. I. Chkheidze,

N. Ya. Buben, and Corresponding Member, Academy

of Sciences, USSR, V. V. Voevodskii

Institute of Chemical Physics, Academy of Sciences, USSR
Institute of Chemical Kinetics and Combustion, Siberian Division,
Academy of Sciences, USSR
Translated from Doklady Akademii Nauk SSSR, Vol. 141, No. 4,
pp. 911-912, December, 1961
Original article submitted August 21, 1961

One of our previously published papers [1] gives the e.p.r. spectrum of benzene irradiated at 100°K. The spectrum shows a well resolved triplet, each component of which is split into a quadruplet. The central component of the triplet has a considerably greater integral intensity than is given by the 1 : 2 : 1 binomial intensity distribution law. This spectrum may be explained by the superposition of a 1 : 2 : 1 triplet and a single line, the position of which coincides with the central component of the triplet. On the basis of this and chemical data on the radiolysis of liquid C_6H_6 [2, 3] the conclusion was reached that in the radiolysis of solid C_6H_6 the two radicals $C_6H_5^{\cdot}$ and $C_6H_7^{\cdot}$ are formed.

Here it was assumed that the spectrum with the hyperfine structure (h.f.s.) corresponds with the radical

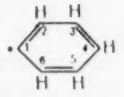

The triplet with a total splitting of about 90 oersted is caused by the interaction of the unpaired electron with the two β-hydrogens (2 and 6), and the additional splitting of each component of the triplet into four lines is caused by interaction with hydrogen atoms 3, 4, and 5.

The single unresolved line was ascribed to the $C_6H_7^{\cdot}$ radical [1].

Recently, a more detailed theoretical analysis has given rise to the idea that this explanation of the observed spectrum cannot be considered conclusive, and that a h.f.s. of $3 \cdot 4 = 12$ components in the e.p.r. spectra may also be caused by the radical

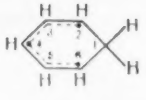

if it is assumed that the unpaired electron is localized mainly in the 2, 4, and 6 positions, and that the two hydrogens of the $>CH_2$ group give a triplet with a total spreading ~ 90 oersteds and the hydrogen atoms in the 2, 4, and 6 positions give approximately the same spreading of about 10 oersteds each.*

By slowly heating the sample to 220°K, and keeping it at this temperature for 20-30 min (see figure), we were able to improve the resolution of the spectrum considerably. Here the relative intensity of the central part of the

* The large splitting at the hydrogens of the $>CH_2$ group may be due to several causes: first, the splitting at the β-hydrogens is usually greater than at the α-hydrogens, second, the interaction with the hydrogens of the $>CH_2$ group comes not from one position, but from two (2 and 6), and finally, distortions of the geometric structure of the radical are possible.

spectrum is greatly reduced. Apparently, the radical giving the single line has undergone a considerable amount of recombination. The most important result is the additional splitting of each quadruplet line into a triplet with a total splitting of ~7 oersteds. (In the central part of the spectrum this splitting shows up less clearly, because of the partial superposition of the single line.) This result completely excludes the possibility of ascribing the h.f.s. spectrum to the $C_6H_5^{\cdot}$ radical, since the spectrum of this radical cannot contain more than 18 components. The idea that the h.f.s. spectrum is caused by the $C_6H_7^{\cdot}$ radical is supported by the following considerations.

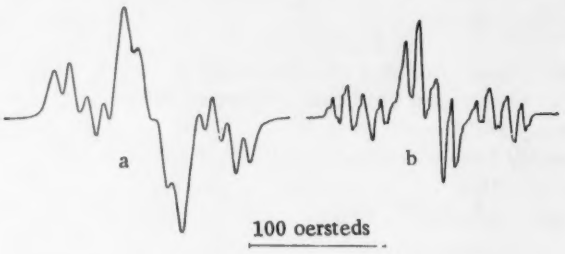

Spectrum of irradiated benzene; a) 146°K, b) 220°K.

It is known from studies on aromatic ion-radicals [4] that the total splitting of an unpaired p-electron at hydrogens lying in the plane of the aromatic ring cannot exceed 22-23 oersteds (excluding an alternating sign for the spin density). The total splitting at all the hydrogens of the ring found in our experiments (determined from the total splitting in one component of the fundamental triplet) is equal to 38 oersteds. This means that there is alternation of sign of the spin density in the ring, the total splitting at hydrogens corresponding with negative spin density being equal to $(38 - 22)/2 = 8$ oersteds.

It is clear from the C_6H_7 radical scheme that the negative spin density can be localized only in positions 3 and 5. Hence, it follows that if the explanation of the spectrum which we have proposed is correct, the additional splitting at each of these hydrogens must be close to $8/2 = 4$ oersteds. Experiment gives 3.5 oersteds. The proposal to ascribe the h.f.s. spectrum to the $C_6H_7^{\cdot}$ radical is in agreement with the data obtained in [5], which gives the e.p.r. spectra of the radicals formed by the action of hydrogen atoms on polystyrene. In the discussion at this same symposium, Cochrane and Adrian reported that they had also found a spectrum with hyperfine structure in the photolysis of HI with C_6H_6 present in the solid matrix.

The authors express their thanks to G. K. Voronova for her help in working up the results.

LITERATURE CITED

1. I. I. Chkheidze, Yu. N. Molin, et al. DAN, 130, 1291 (1960).
2. J. P. Manion and M. Burton, J. Phys. Chem. 56, 560 (1952).
3. W. N. Patrick and M. Burton, J. Am. Chem. Soc. 76, 2626 (1954).
4. D. J. E. Ingram, Free Radicals as Studied by Electron Spin Resonance, London (1958).
5. R. B. Ingalls and L. A. Wall, Transactions of the Fifth Symposium on Frozen Radicals [in Russian] (Uppsala, Sweden, July, 1961).

All abbreviations of periodicals in the above bibliography are letter-by-letter transliterations of the abbreviations as given in the original Russian journal. *Some or all of this periodical literature may well be available in English translation.* A complete list of the cover-to-cover English translations appears at the back of this issue.

A STUDY OF THE STRUCTURE OF PASSIVE OXIDE FILMS ON THE SURFACE OF TITANIUM

N. D. Tomashov, R. M. Al'tovskii, and M. Ya. Kushnerev

Physical Chemistry Institute, Academy of Sciences, USSR
(Presented by Academician V. I. Spitsyn, July 5, 1961)
Translated from Doklady Akademii Nauk SSSR, Vol. 141, No. 4,
pp. 913-916, December, 1961
Original article submitted July 4, 1961

There are several reports in the literature on the composition and structure of the oxide films formed on the surface of titanium under conditions of high-temperature oxidation in air, oxidation in boiling solutions of oxidizing agents, and anodic oxidation at high positive potentials [1-3]. The data of various authors together with the results of the present work are given in Table 1. There are no data in the literature on the structure of passive films formed on the surface of titanium during spontaneous passivation in solutions at room temperature or during anodic passivation in solutions at comparatively low positive potentials.

In a number of our earlier works [4, 5] it was shown that titanium can renew spontaneously its protective oxide film after the latter has been removed mechanically under dilute (up to 5%) solutions of sulfuric and hydrochloric acids. Later it was also established that titanium undergoes spontaneous passivation after its surface has been cleaned in solutions of sodium chloride, caustic soda, or nitric acid. In sulfuric and hydrochloric acids with a concentration of 10% and above, titanium can be passivated only by anodic polarization [5-7]. The passive state is attained when the potential of the titanium becomes more positive than the potential of complete passivation in the given acid

TABLE 1. The Structure of Oxide Films Formed on Titanium under Different Oxidation Conditions

Conditions and duration of oxidation	Temp. °C	Composition of oxide film	Literature source
Oxidation in air for 10 days	18-20	TiO with a small quantity of Ti_3O_5	[8]
Corrosion in 92% H_2SO_4 for 100 hr	18-20	Ti_3O_5	[15]
Spontaneous passivation in solutions: 5% HCl, 5% H_2SO_4, 6% HNO_3, 1 N NaCl, 1 N NaOH for 10 days	18-20	$Ti_2O_3 \cdot 3\text{-}4TiO_2$	Authors' data
Anodic oxidation in 40% H_2SO_4. At potentials of − 0.05 and + 1.0 v for 5 hr	18-20	$Ti_2O_3 \cdot 3\text{-}4\,TiO_2$	The same
Oxidation in air	875-1050	Laminated scale of TiO, Ti_2O_3, and TiO_2 rutile	[1]
Oxidation in 10% CrO_3 for 10 hr	Boiling	TiO_2, anatase and rutile	[2]
Oxidation in aqua regia for 0.5 hr	" "	TiO_2, anatase	[2]
Oxidation in 50% HNO_3 for 2 hr	" "	The same	[2]
Anodic oxidation in 0.1 N H_2SO_4. At a potential of +8.0 v for 5 hr	18-20	" "	[3]
Oxidation in 65% HNO_3 for 5 hr	Boiling	TiO_2, anatase with a small quantity of rutile	Authors' data
Anodic oxidation in 40% H_2SO_4. At a potential of +8.0 v for 15 min	18-20	The same	The same

TABLE 2. Interplanar Spacings d and Qualitative Characterization of the Intensities of the Diffraction Lines I for the Electron-Diffraction Patterns of Oxide Films Obtained on Titanium in H_2SO_4 and HNO_3

No.	Spontaneous passivation in 5% H_2SO_4, transmission method				Anodic oxidation in 40% H_2SO_4, reflection method						Oxidation in boiling 65% HNO_3 for 5 hr			
	kept in solution for 1 day		kept in solution for 10 days		treatment for 5 hr				treatment for 15 min at a potential of +8.0v		transmission method		reflection method	
					−0.05 v		+ 1.0 v							
	d	I*	d	I*	d	I*	d	I*	d	I	d	I	d	I
1	2	3.49	3	3.50					7	3.52	7	3.51	6	3.52
2	2	3.4-2.8							2	3.24	2	3.21		
	Diffuse								Blurred		Blurred			
3	6	2.46	5	2.46	5	2.42	4	2.43	3	2.44	4	2.44	1	2.46
4									4	2.34	5	2.35	3	2.34
5	5	2.10	4	2.09	3	2.03	2	2.03	3	2.13	2	2.04		
6	2	1.90	2	1.89					5	1.88	6	1.89	4	1.88
7	2	1.69	3	1.67					7	1.66	7	1.67	5	1.68
									Broad		Broad			
8	6	1.43	6	1.43	4	1.47	3	1.49	4	1.46	5	1.47	4	1.46
9			2	1.34					4	1.32	4	1.33	2	1.32
									Broad		Broad			
10			2	1.24	3	1.29	2	1.29	4	1.25	4	1.24	3	1.25
11					2	1.22								
12	2	1.17	2	1.18										
13									3	1.16	3	1.15	2	1.14
14			2	1.03					1	1.03	2	1.03	1	10.3
			Blurred											
15											1	0.95		
16			2	0.90							1	0.91		
			Blurred											
17											1	0.88		
18											1	0.83		

* The line intensities were estimated qualitatively on a ten-division scale: extremely strong 10, very strong 9, strong 8, moderately strong 7, moderate 6, moderately weak 5, weak 4, very weak 3, extremely weak 2, just perceptible 1.

solution. For example, in 40% H_2SO_4 solution at room temperature, the potential of complete passivation of titanium is equal to about ± 0.1 v,* so that the anodic passivation of titanium under these conditions becomes possible if the potential has any positive value [7]. In the examination of the passive properties of titanium, considerable interest is attached to the determination of the composition and structure of the passivating films formed during spontaneous passivation in different solutions and also during anodic passivation.

In our previous study we determined the composition and structure of the oxide film formed on titanium and some of its alloys (VT5, VTZ, and VTZ-1) during oxidation in air at room temperature. It was shown that the oxide film consists of the titanium oxide TiO [8]. For the study of the structure of the film, the latter was removed from the surface of the metal in an anhydrous 5% solution of bromine in methyl alcohol and examined by the "transmission" method of electron-diffraction analysis [8].

* All the potentials in the present article are quoted relative to the normal hydrogen electrode.

In the present work the separation of the oxide film for study of its structure by the transmission method was carried out in the same way. In some cases electron-diffraction diagrams were obtained by the reflection method. The patterns were recorded on an EM-4 electron-diffraction apparatus with a constant of 39.8 for operation by the transmission method and 38.9 for operation by the reflection method. The voltage in all cases was 40 kv.

We studied the composition and structure of oxide films formed on titanium: 1) during spontaneous passivation in solutions of 5% HCl, 5% H_2SO_4, 6% HNO_3, 1 N NaCl and 1 N NaOH at room temperature; 2) during anodic oxidation in 40% H_2SO_4 at potentials of −0.05, + 1.0 and +8.0 v; and 3) during oxidation in boiling 65% HNO_3 solution.

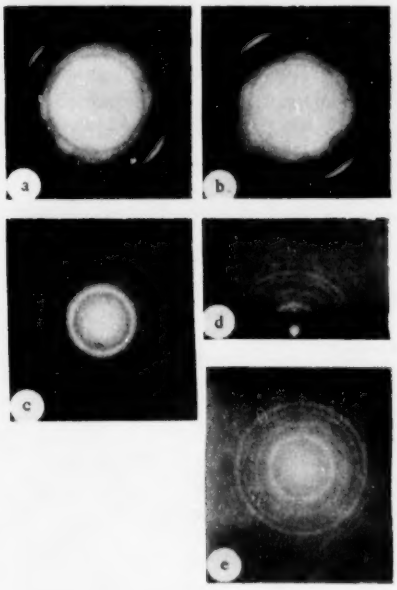

Electron-diffraction patterns for oxide films obtained on the surface of titanium under different oxidation conditions. a) 5% H_2SO_4 for 1 day; b) 5% H_2SO_4 for 10 days; c) 65% boiling HNO_3 for 5 hr; d) 65% boiling HNO_3 for 5 hr (reflection method); e) 40% H_2SO_4, anodic oxidation at a potential of 8 v for 15 min.

Table 2 gives the results of the electron-diffraction studies. The results of the analysis of the oxide films formed during spontaneous passivation are given only for 5% H_2SO_4, since similar electron-diffraction patterns were obtained for all the solutions studied. The diffraction lines in almost all cases showed textural maxima (figure). This indicates orientation of the crystals in the oxide film, apparently produced by orientation in the surface layers of the metal, resulting from the polishing of the surface.

Comparison of the experimental interplanar spacings and line intensities with the tabulated data for the various oxides and other compounds of titanium showed that the diffraction patterns obtained for the oxide films formed during the spontaneous passivation of titanium in all the solutions listed above (case 1) and also during the anodic passivation in 40% H_2SO_4 at potentials of −0.05 and +1.0 v show best agreement with the pattern obtained from the titanium oxide with composition $Ti_2O_3 \cdot 3\text{-}4TiO_2$. The slight scatter observed in the line intensities for the oxide films obtained in different solutions is apparently due to distortion of the crystal lattice of this intermediate oxide as a result of deviation from the stoichiometric composition, and also to the texturing effect. The oxide of composition $Ti_2O_3 \cdot 4TiO_2$ is intermediate between the oxides Ti_2O_3 and TiO_2. This oxide was first detected in [9], where the results of its x-ray diffraction study are also given. Later the results of this work were confirmed in [10] and also in [11, 12]. In the latter works cited, the two oxides Ti_5O_9 and Ti_6O_{11} correspond to the oxide of composition $Ti_2O_3 \cdot 3\text{-}4TiO_2$.

It is interesting to note that the oxide films formed on the surface of titanium in 40% H_2SO_4 in a passive state maintained by external anodic polarization at a potential (+1.0 v) much more positive than the potential of complete passivation of titanium in 40% H_2SO_4, which is equal to 0.0 v, and also at a potential slightly more negative (−0.05 v), consist of the same oxide film. Thus the conversion of titanium to the passive state at the potential of complete passivation can be interpreted as involving conversion from a state of incomplete covering of the surface by the oxide film (at potentials more negative than the potential of complete passivation) to a state of complete covering of the surface by the oxide film (at potentials more positive than the potential of complete passivation); the composition and structure of the oxide layer remain the same.

It should also be pointed out that during the anodic passivation of titanium (at potentials not higher than +1 to +2 v) and during spontaneous passivation in solutions, oxide films of the same composition are formed. This result emphasizes the correctness of the conclusion previously reached in the literature regarding the absence of any fundamental difference between the chemical and anodic passivation of metals [13, 14].

Analysis of the electron-diffraction patterns for the oxide films obtained during the oxidation of titanium in 40% H_2SO_4 at more positive potentials, for example +8.0 v, and also during oxidation in boiling 65% HNO_3, shows that in these cases the film consists of the higher titanium oxide TiO_2 with the anatase structure, together with a small quantity of rutile. These results which we have obtained agree with those of [2, 3]. In Table 2 the lines Nos. 1, 4, 6-10, and 13-18 refer to the anatase structure and the lines Nos. 2, 3 and 5 to the rutile structure. The slightly

higher intensity of line No. 7 compared with the other lines in the anatase structure, together with the broadening of this line, are probably due to the superposition of the reflections from this oxide and from rutile in the pattern of which this line has the highest intensity. Table 2 also shows that electron-diffraction studies by the transmission and reflection methods give the same structure for the oxide film formed during the oxidation of titanium in boiling 65% HNO_3. This indicates that the structure of the film is preserved during the removal of the oxide films from the titanium surface in a solution of bromine in methyl alcohol.

Analysis of the data in Table 1, which gives the results of the study of the structure of the oxide films, obtained in the present work, together with the data available in the literature, leads to the conclusion that the oxide corresponding to the highest degree of oxidation of titanium – TiO_2 – appears on the titanium surface under the most severe oxidation conditions. These conditions are: oxidation in air at high temperature, oxidation in solution at the boil, and anodic oxidation at high positive potentials. Under less severe oxidation conditions: spontaneous passivation in solutions at room temperature or anodic oxidation in solution at comparatively low positive potentials, an oxide of lower degree of oxidation than TiO_2, namely the oxide of composition $Ti_2O_3 \cdot 3\text{-}4TiO_2$, is formed on the titanium surface. Under even milder oxidation conditions, the formation of lower oxides of titanium is possible. For example, during the spontaneous dissolution of titanium in H_2SO_4, we have detected on its surface the oxide Ti_3O_5 [15], and during oxidation in air at room temperatures, as already pointed out above, the oxide TiO is formed [8].

LITERATURE CITED

1. P. H. Morton and W. M. Baldwin, Trans. Am. Soc. Metals, 44, 1004 (1953).
2. S. Ogawa and D. Watanabe, Sci. Rep. Res. Inst. Tohoku Univ. 2, 184 (1955).
3. O. Rüdiger, W. R. Fischer, and W. Knorr, Zs. Metallukunde, 47, 11, 8 (1956).
4. N. D. Tomashov, R. M. Al'tovskii, and A. G. Arakelov, DAN, 121, 5, 885 (1958).
5. N. D. Tomashov, G. P. Chernova, R. M. Al'tovskii, and G. K. Blinchevskii, Zav. Lab. 3, 299 (1958).
6. N. D. Tomashov, R. M. Al'tovskii, and A. G. Arakelov, Izd. Fil. VINITI, Theme 13, M-59-239/26 (1959).
7. N. D. Tomashov, G. P. Tschernova, and R. M. Altovsky, Zs. Phys. Chem. 214, 312 (1960).
8. N. D. Tomashov, R. M. Al'tovskii, and M. Ya. Kushnerev, Zav. Lab. 3 (1960).
9. N. E. Filonenko, V. I. Kudryavtsev, and I. V. Lavrov, DAN, 86, 3, 561 (1952).
10. N. V. Ageev, V. A. Reznichenko, T. P. Ukolova, and M. S. Model', Collection, Titanium and Its Alloys [in Russian] (1949), No. 2, 64, (1949).
11. S. Anderson, B. Collin, U. Knylonstierka, and A. Magnelli, Acta. Chem. Scand. 11, 11 (1957).
12. S. Asbrink and A. Magnelli, Acta. Chem. Scand. 11, 9, 1606 (1957).
13. N. D. Tomashov, The Theory of Metal Corrosion [in Russian] (Moscow, 1952).
14. Ya. M. Kolotyrkin, Collection, Problems in Physical Chemistry [in Russian] (Moscow, 1958), No. 1, p. 81.
15. N. D. Tomashov, R. M. Altov'skii, A. V. Prosvirin, and R. D. Shamgunova, Collection, The Corrosion and Protection of Constructional Materials [in Russian] (Moscow, 1961), p. 151.

MEASUREMENT OF THE POTENTIAL DROP AT A PLATINUM ANODE WHEN THE POLARIZING CURRENT IS BROKEN

Academician A. N. Frumkin and V. V. Sobol'

M. V. Lomonosov Moscow State University

Translated from Doklady Akademii Nauk SSSR, Vol. 141, No. 4,
pp. 917-920, December, 1961
Original article submitted July 4, 1961

During the measurement of anodic polarization curves on platinum in perchloric [1] and sulfuric [2, 3] acids, a sudden increase in the potential is observed in a definite range of current density, characteristic of the acid concentration being studied and the method used to prepare the electrodes. In [1] it was suggested that the potential jump during the anodic polarization of platinum is related to the formation, within the potential range 2.2-3.0 v, of a new form of the surface oxide, accompanied by a decrease in the energy of adsorption of the O atoms or OH radicals formed by the discharge of water molecules. This leads to an increase in the overvoltage, it is assumed that the latter is determined by the retardation of the electrochemical formation of adsorbed oxygen. An analogous explanation was put forward by Ruetschi and Delahay [4] to explain the shape of the polarization curves observed by Hickling and Hill [5] for the liberation of oxygen from alkaline solutions at Pd and Au. Study of the dependence of the position and magnitude of the potential jump on the nature and concentration of the acid anion leads to the conclusion that the formation of the chemisorbed layer involves the participation not only of oxygen and water but also of the acid anions, and experiments with ClO_4^- anions labeled with O^{18} have shown that at potentials above the upper boundary of the jump, exchange between the adsorbed oxygen and oxygen present in the ClO_4^- anion becomes possible [6].

Anodically polarized platinum can also be studied by measuring the curves for the potential drop when the current is broken [5, 7]. In our work we have used the drop curves to calculate the capacity of the electrode from the formula $C = (i_0 t/\Delta\varphi)$, where $\Delta\varphi$ is the initial section of the potential drop during time t and i_0 is the polarization current density before the current is broken [8]. This formula is applicable with the condition that the self-discharge current in the initial period of the potential drop is equal to the polarization current. In the calculation of the capacity we neglected the ohmic potential drop calculated from Kabanov's formula [9]. Parallel calculations of the capacity were carried out by making use of the points lying on the drop curve, as a result of which the ohmic drop was eliminated. In this case i_0 in the formula was replaced by i'_0, which was determined from the polarization curve with allowance for the potential drop before the readings were started. The position of the section of the curve was chosen in such a way that, on the one hand, it was as close as possible to the potential at which the circuit was broken, and on the other hand, the current i'_0 lay in the region of the polarization curve not distorted by the ohmic potential drop. The results of the two determinations agreed within the limits of experimental error.

The potential drop was measured by means of an electronic oscillograph with delayed scanning. The potential-drop curve consisted of a series of points determining the time scale (time marks) with intervals of $5.4 \cdot 10^{-6}$, $1.29 \cdot 10^{-5}$, $2.55 \cdot 10^{-5}$, and $2.02 \cdot 10^{-4}$ seconds. In the experiment, the current was switched off by an electronic assembly for 10^{-1}-10^{-3} seconds and the potential-drop curve obtained on the oscillograph screen was recorded by means of a photographic attachment, after which the polarization was applied again automatically. When a stable potential had again become established, the potential-drop curve corresponding to the next point on the polarization curve was recorded. The current was maintained for 2 minutes before the circuit was broken. The potential drop when the current was broken for a longer period of up to 10 seconds was studied on an MPO-2 loop oscillograph with electronic amplifier. We also carried out visual measurements by means of a cathodic voltmeter and stopwatch.

The experiments were carried out in a cell with separated electrodes and the potential was measured relative to a hydrogen electrode in the same solution. Two electrodes of platinum wire with areas of 0.01 and 0.15 cm^2 were used as anodes. Particular attention was paid to the preparation of the electrodes. Before each experiment the electrodes were washed in dilute nitric acid and then in concentrated sulfuric acid, after which they were sub-

jected to anodic polarization for 30 minutes in 1 N H_2SO_4 by a current of $6 \cdot 10^{-4}$ amp/cm^2. Deviation from the procedure for preparing the electrodes had a marked effect on the polarization curves and on the results of the capacity measurements. The experiments were carried out in 0.6, 1.35, 4.3, and 10 N solutions of perchloric acid. The relationship between the electrode capacity and log i, together with the polarization curves, are shown in Fig. 1. At potentials corresponding to the lower branch of the polarization curve, at concentrations of 0.6 and 1.35 N $HClO_4$ (curves 1 and 2), the observed value of the capacity is approximately 100 μf/cm^2; the capacity increases as the current density at which the potential jump takes place is approached. In some experiments the potential jump took place at higher current densities than usual, for example at $8 \cdot 10^{-1}$ amp/cm^2 instead of the normal value of $6 \cdot 10^{-1}$ amp/cm^2. In this case the capacity increases to approximately 200-250 μf/cm^2. The reasons for these deviations in the behavior of the electrode are not yet clear. The observed high values of the capacity, exceeding considerably the capacity of the double layer, indicate an increase in the covering of the surface with increase in polarization by an electrochemically active substance, i.e., a substance capable of ionizing. It may be assumed that in this range of potentials, on part of the surface at least, the slowest stage is not the transfer of electrons from water molecules to the electrode but the decomposition of surface compounds with the formation of oxygen.

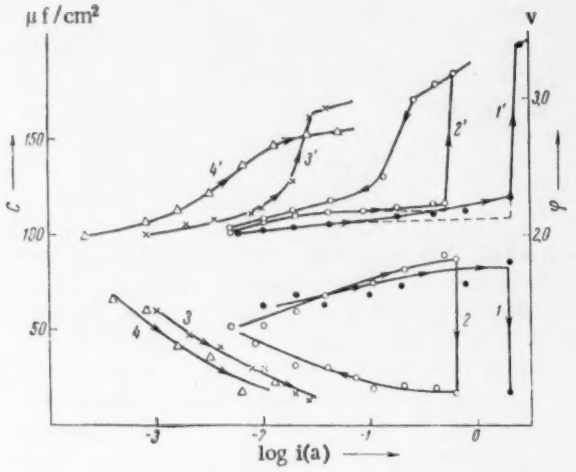

Fig. 1. Relationship between the capacity and current density in $HClO_4$ solutions: 1) 0.6 N; 2) 1.35 N; 3) 4.3 N; 4) 10 N. 1',2',3',4' – polarization curves for the same solutions. The arrows indicate the direction in which the curves were recorded. The dotted line shows the polarization curves corrected for the ohmic potential drop.

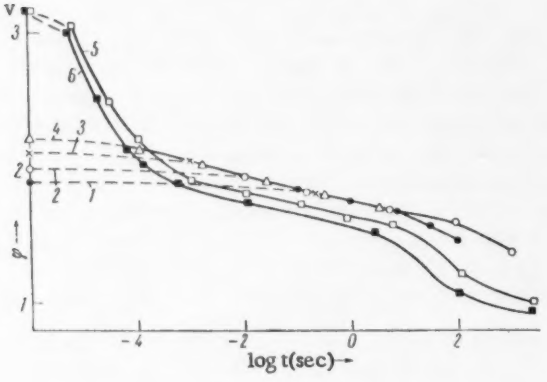

Fig. 2. Curves showing the relationship between the potential drop and the time from the moment when the current is broken in 1.35 N $HClO_4$. 1) $i = 10^{-4}$ amp/cm^2; 2) 10^{-3} amp/cm^2; 3) 10^{-2} amp/cm^2; 4) 10^{-1} amp/cm^2; 5) $6 \cdot 10^{-1}$ amp/cm^2; 6) potential drop after polarization by a current of $6 \cdot 10^{-1}$ amp/cm^2 for 1 hr.

Determination of the capacity at potentials lying on the upper boundary of the potential jump, or at potentials exceeding this limit, lead to different results. In this case the value of C amounts to 20 ± ± 2 μf/cm^2, which is characteristic of the capacity of the double layer. Due to the insufficient frequency of the time marks and the high value of the potential drop $\Delta\varphi$, which reaches 1 v in 10^{-4} seconds, the calculation of the capacity for the upper branch of the polarization curve is inaccurate. Moreover, the high value of the drop in this potential range makes doubtful the assumption that the self-discharge current is equal to the value of i_0, although the error cannot be too great, since according to measurements carried out by the polarographic method [10], the change in the magnitude of the current within this potential range lies within narrow limits. The most simple explanation of the observed phenomena is to be found in the suggestion that as the surface layer becomes covered with oxygen, there is a gradual shutting-off of the centers available on the surface with a high energy of adsorption of the O atoms and OH radicals which are formed as a result of the discharge of water molecules. As a result of this, the rate of the discharge reaction decreases sharply and in order to maintain a constant current density, an increase in the electrode potential to a value corresponding to the resulting overvoltage of the discharge of water molecules becomes necessary. Thus in this case it is suggested that the nature of the jump is related to a change in the nature of the slowest stage in the over-all process.

The measurements of the capacity from the potential drop, carried out in more concentrated solutions (curves 3 and 4) give in general a similar picture of the relationship between capacity and log i, i.e., a decrease in the capacity to a value of approximately 20 $\mu f/cm^2$ with the rise in potential to the upper branch of the polarization curve. In this case however the change in the capacity is much more marked; the capacity on the lower section of the polarization curve does not exceed 70 $\mu f/cm^2$ and gradually decreases with increase in the slope of the polarization curve. Hysteresis is observed when the polarization curves are recorded from the high current densities corresponding to the upper branch of the polarization curve to lower values. In this case the capacity increases only to values not exceeding 50 $\mu f/cm^2$. This result indicates that the change in the electrode surface after the jump is irreversible.

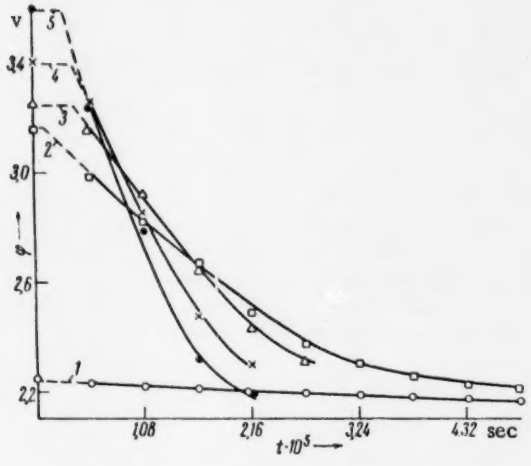

Fig. 3. Curves showing the potential drop after the current is broken: 1) $i = 5.2 \cdot 10^{-1}$ amp/cm²; 2) $6.4 \cdot 10^{-1}$ amp/cm²; 3) 1.3 amp/cm²; 4) 2.6 amp/cm²; 5) 5.2 amp/cm².

Figure 2 gives complete curves for the potential drop in 1.35 N $HClO_4$ after the current is broken, plotted against the logarithm of the time. Figure 2 shows that the curves for the drop, starting from potentials corresponding to the lower branch of the polarization curve for initial current densities of 10^{-4}-10^{-1} amp/cm² (curves 1-4) come out on a straight line. The slope of this line is 0.1 v, which coincides approximately with the slope of the polarization curve in the same current density range. This result indicates that in the potential range 1.6-2.2 v the evolution of oxygen takes place by an unchanged mechanism, so that the nature of the surface is preserved.

For a drop from a potential of 3.2 v (curve 5), the start of the drop curve shows a region of rapid decrease in potential, followed by a section with a slope equal to the slope of the lower branch of the polarization curve, and at the end of the drop an increase in the slope is observed. The cause of this last phenomenon is not clear and requires further study. It should be noted that the drop starting from potentials corresponding to the upper branch of the polarization curve takes place to lower potentials than the drop from potentials of the lower branch, i.e., intersection of the potential-drop curves is observed. This phenomenon is shown particularly clearly at high anodic potentials (the upper section of the polarization curve, see Fig. 3). One possible reason for this intersection is that after the surface is covered with oxides there is an increase in the stability of the surface compound with the application of high polarization, i.e., there is an interaction between the surface groups, which might be described as two-dimensional crystallization and which leads to a decrease in the electrochemical activity of the polarized electrode.

In [11] an increase in the stability of the oxide film with time was observed at lower anodic potentials than those considered here. We have also observed a relationship between the behavior of a platinum electrode and the time for which the current is passed at higher potentials. When a current of $4 \cdot 10^{-1}$ amp/cm² is passed for a prolonged period at an initial potential of 2.2 v, there is a gradual increase in potential, which after 1 hr rises to 0.1-0.2 v, while the capacity decreases from 80-90 $\mu f/cm^2$ to 25-30 $\mu f/cm^2$ in the same period. Thus the covering of the adsorption centers with oxygen increases with time, and as a result, the transition to the upper branch of the polarization curve takes place at lower current densities. Prolonged polarization of an electrode by a current of $6 \cdot 10^{-1}$ amp/cm² in 1.35 N $HClO_4$ at a potential of 3.2 v on the upper branch of the polarization curve also influences the rate of the drop. Figure 2 (curves 5 and 6) shows that the potential drop after polarization for one hour is more rapid than that after polarization for 2 minutes. The rate of the drop in the time range from 10^{-5} to 10^{-4} seconds after the circuit is broken increases from $1.4 \cdot 10^4$ v/sec to $2.1 \cdot 10^4$ v/sec. These results can also be related to an increase in the stability of the surface oxides with time.

LITERATURE CITED

1. R. I. Kaganovich, M. A. Gerovich, and E. Kh. Enikeev, DAN, 108, 107 (1956).
2. I. A. Izgaryshev and E. A. Efimov, ZhFKh, 27, 130, 310 (1953); V. A. Kheifets and I. A. Rivlin, ZhPKh, 28, 1294 (1955).

3. V. I. Veselovskii, Proceedings of the 4th Conference on Electrochemistry [in Russian] (1959), p. 241.
4. P. Rüetschi and P. Delahay, J. Chem. Phys. 23, 556 (1955).
5. A. Hickling and S. Hill, Discuss. Farad. Soc. 236, 254 (1947).
6. M. A. Gerovich, R. I. Kaganovich, V. M. Vergelesov, and L. N. Gorokhov, DAN, 114, 1049 (1957).
7. W. R. Busing and W. Kauzmann, J. Chem. Phys. 20, 1129 (1952).
8. N. A. Fedotov, ZhFKh, 25, 3 (1951).
9. B. N. Kabanov, ZhFKh, 8, 486 (1936).
10. R. I. Kaganovich and M. A. Gerovich, ZhFKh, 32, 958 (1958).
11. Ts. I. Zalkind and B. V. Ershler, ZhFKh, 25, 565 (1951); V. I. Nesterova and A. N. Frumkin, ZhFKh, 26, 1178 (1952); A. D. Obrucheva, ZhFKh, 26, 1448 (1952).

All abbreviations of periodicals in the above bibliography are letter-by-letter transliterations of the abbreviations as given in the original Russian journal. *Some or all of this periodical literature may well be available in English translation.* A complete list of the cover-to-cover English translations appears at the back of this issue.

STABILIZATION OF FREE RADICALS IN IONIC CRYSTAL MATRICES

Yu. M. Boyarchuk and N. Ya. Buben

Institute of Chemical Physics, Academy of Sciences, USSR
(Presented by Academician V. N. Kondart'ev, July 13, 1961)
Translated from Doklady Akademii Nauk SSSR, Vol. 141, No. 5,
pp. 1120-1123, December, 1961
Original article submitted June 27, 1961

For studying free radicals the method of stabilizing them in various matrices is widely used [1]. Then the stability of the radicals – the temperature at which they are found to recombine at a measurable rate – to a considerable extent is determined by properties of the matrix. Radicals formed by radiolysis or photolysis of frozen organic substances recombine rapidly, when in amorphous substances they are heated to the vitrification temperature or near to the melting point in crystalline ones [2]. In certain cases, recombination even takes place at a lower temperature, namely, in the region where some molecular motions in the matrix are set free. Therefore, it may be expected that the use of more stable matrices will enable one to prevent recombination of organic radicals up to higher temperatures. An attempt to use an ionic crystal lattice for this purpose was done in the paper [3]: a mechanical mixture of KCl and small admixtures of some solid organic substances was exposed to photolysis. In the opinion of the said authors, the thus found small effect resulted from radical stabilization of the surface of the microcrystals.

It is of interest to find out whether stabilization of organic radicals in an ionic lattice used as matrix is possible under such conditions that the original organic molecules and the matrix substance are present in comparable amounts and form a chemically homogeneous system. For this purpose, for instance, crystalline solvates – molecular compounds of inorganic salts and organic solvents – which are crystals of known composition [4], may be used. When irradiating such compounds by gamma-rays or fast electrons, one may expect that the stability of the formed radicals will be enhanced considerably. Although this method of introducing organic compound into an ionic crystal lattice is not generally applicable, yet it may be used in many cases, since the number of compounds of this type is quite high. In the present study we investigated the radicals formed by irradiating the compounds of normal alcohols (methyl, ethyl and n-propyl) with magnesium chloride or calcium chloride having the composition $MgCl_2 \cdot 6ROH$ and $CaCl_2 \cdot 4ROH$ [5]. The said compounds were obtained by the method described in the paper [6]. The samples were irradiated at $-170°$ by fast electrons with 1.6 Mev energy at doses up to about 40 Mrad. The radicals formed were recorded by electron paramagnetic resonance (EPR). The concentration of paramagnetic centers in the irradiated samples amounted to $\sim 10^{20}$ paramagnetic centers per gram. The EPR spectra observed upon irradiating alcohols in the $CaCl_2$ and $MgCl_2$ matrices coincide with those of the corresponding alcohols irradiated at the temperature of liquid nitrogen [7]. This allows one to conclude that in both cases mainly the same radicals are formed. For three of the studied compounds the EPR spectra are shown in Fig. 1 (a, c, d). It is interesting that the lines which usually are observed, when ionic crystals are irradiated, and which result from the formation of trapping centers are absent in our spectra. This may be explained by a loosening of the crystal lattice in the formation of a compound with alcohol, as a result of which the depth of the electron traps is decreased.

To get information on the stability of alcohol radicals in frozen alcohol when compared with that in an ionic crystal matrix we studied the change in radical concentration at raised temperature. For this purpose the irradiated sample together with the standard was kept in a dry nitrogen current of a given temperature. When the sample had come to the temperature of the current, the EPR spectrum of the radicals was recorded, then the temperature of the current was raised and so on. During about 15 min the temperature of the sample was kept constant and meanwhile no noticeable decrease whatever of the radical concentration took place. Such measurements do not allow one to get quantitative informations on the kinetics of radical recombination, but they indicate at once in which temperature range the radicals start to disappear rapidly. Curves of the change in free radical concentration at raised temperature for frozen methyl alcohol and the compound $MgCl_2 \cdot 6CH_3OH$ are shown in Fig. 2.

As can be seen by comparing these curves, in an ionic crystal lattice one may easily observe alcohol radicals at temperatures considerably exceeding the melting point of methyl alcohol. Up to −30° the radical recombination in the matrix proceeds slowly; in 15 min their concentration does not change noticeably. At higher temperatures the radical concentration is found to fall rapidly with time, but, obviously, this mainly results, because the compound $MgCl_2 \cdot 6CH_3OH$ itself decomposes when the sample is kept in the current of nitrogen. Radicals formed by irradiating ethyl and n-propyl alcohols were observed in the matrices $CaCl_2$ and $MgCl_2$ up to the temperature −30° too.

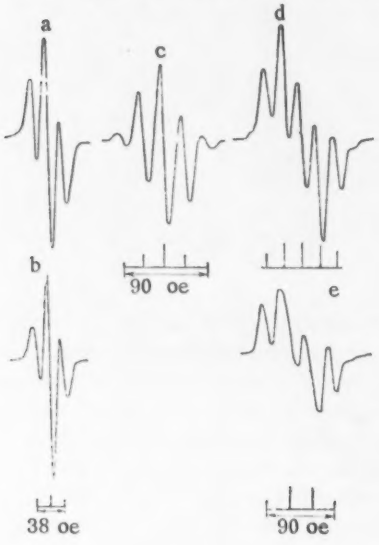

Fig. 1. EPR spectra of alcohols irradiated in the matrix $MgCl_2$: a) methyl alcohol at −150°; b) methyl alcohol at −40°; c) ethyl alcohol at − 80°; d) n-propyl alcohol at −150°; e) n-propyl alcohol at −90°.

The possibility of observing in a broader range of temperatures the free radicals formed in the radiolysis of normal alcohols allowed us to get new informations on the nature and the properties of these radicals.

1. The EPR spectrum of the CH_2OH radical observed in irradiated $MgCl_2 \cdot 6CH_3OH$ at −150° is shown in Fig. 1a. The amplitude ratio in the hyperfine structure of the first derivative spectrum at this temperature is approximately equal to 1 : 1.7 : 1. At raised temperature a relative increase in the amplitude of the center component is found. This is illustrated in Fig. 1b where the spectrum of this same radical at −40° is give. In Fig. 3 it is shown how the ratio of the height of the center component (H_1) to that of the outer components (H_2) depends on temperature. The changes in the EPR spectrum are reversible, that is, at lowered temperature H_1/H_2 decreases in the same way. An analysis of the $\dot{C}H_2OH$ radical spectrum leads to the conclusion that the change of H_1/H_2 with temperature results from a decreased width of the central component in the hyperfine structure at raised temperature; at the same time the width of the outer components hardly changes.

As was shown in the papers [8, 9], effects of this type are common ones for $R\dot{C}H_2$ radicals and originate, because at raised temperature the rotation of the $\dot{C}H_2$ group around the R − C = bond is set free. When the rotation is quite rapid, in the center component of the triplet the broadening resulting from anisotropic hyperfine interaction is completely removed, whereas that for the side components stays.

So, stabilization of $\dot{C}H_2OH$ radicals in an ionic crystal matrix enabled us to observe the onset of the internal rotation of the $\dot{C}H_2$ group in these radicals.

2. In several papers [10, 11] it has been noted that in radiolysis of normal alcohols the expulsion of a hydrogen atom preferentially take place in the α-position under formation of $RCH_2\dot{C}HOH$ radicals. The EPR spectrum found upon irradiating frozen ethyl alcohol consists of a quintuplet with a binominal intensity distribution, which finds a good explanation in the formation of a $CH_3 - \dot{C}HOH$ radical, since in the latter the hydrogen atoms in the α- and β-position are equivalent. Some difficulties arose in the interpretation of the EPR spectra of n-propyl alcohol and other higher normal alcohols irradiated at a low temperature. The point is that in the spectra of all these alcohols one observes five main lines with the intensity distribution 1 : 2 : : 2 : 2 : 1. To ascribe such a spectrum to a $RCH_2\dot{C}HOH$ radical it must be assumed that the unpaired electron interacts with three hydrogen atoms, but the constant for the interaction with one of the β-hydrogen is two times greater than the constants for the interaction with the two other hydrogen atoms.* However, there existed no direct proofs that this interpretation of

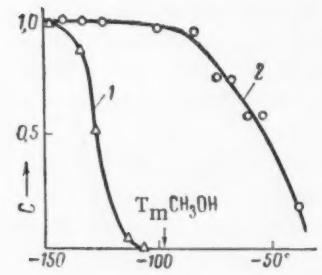

Fig. 2. Change in CH_2OH radical concentration (rel. unit) with temperature: 1) In frozen methyl alcohol; 2) in $MgCl_2 \cdot 6CH_3OH$.

* This interpretation of the EPR spectra found for irradiated higher normal alcohols was proposed by V. K. Ermolaev and Yu. N. Molin.

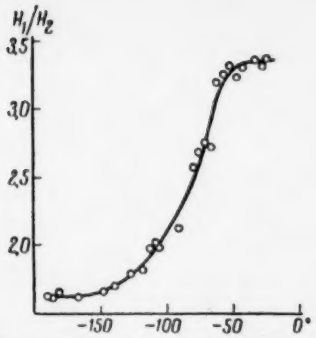

Fig. 3. The ratio of the height of the central component to that of the outer ones in the h.f.s. of the first derivative spectrum for the $\dot{C}H_2OH$ radical plotted versus temperature.

the spectra was right. In the present study it was discovered that the quintuplet of the EPR spectra of n-propyl and n-amyl alcohol irradiated in a matrix changes reversibly into a quartet with an intensity ratio close to 1 : 3 : 3 : 1, when the temperature is raised to about − 100° and − 90° shown in Fig. 1d, e. In the spectrum of irradiated ethyl alcohol no changes in multiplicity were found at raised temperature.

The discovered change with temperature in the spectral multiplicity for irradiated normal alcohols* indicates that rotation of the CH_2 group in the $RCH_2\dot{C}HOH$ radical is set free and, because of this, both β-hydrogens become equivalent and one observes the spectrum characteristic for an interaction of the unpaired electron with three equivalent hydrogen atoms. These observations confirm the rightness of the proposed interpretation for the EPR spectra of the radicals formed in the radiolysis of higher normal alcohols.

In the future the proposed stabilization method will be extended to other classes of organic radicals, it is also intended to find out which is the highest attainable concentration of free radicals in ionic crystal matrices.

In conclusion the authors thank I. N. Blazhevich for his assistance in some of the experiments and Yu. N. Molin for discussing the results.

LITERATURE CITED

1. The Formation and Trapping of Free Radicals, Ed. by A. M. Bass and H. P. Broida, New York (1960).
2. V. K. Ermolaev and others, Abstracts of Proceedings of the Second All-Union Conference on Radiation Chemistry [in Russian] (Moscow, 1960), p. 46.
3. Stabilization of Free Radicals at Low Temperatures, Ed. by A. M. Bass and H. P. Broida, NBS Monograph, 12 (1960), p. 95.
4. B. N. Menshutkin, Etherates and Other Molecular Compounds of $MgBr_2$ and MgI_2 [in Russian] (1907), p. 48.
5. I. W. Mellor, A Comprehensive Treatise on Inorg. and Theor. Chemistry, 3 (1928), p. 712; 4 (1923), p. 305.
6. A. S. Osokin, ZhOKh, 8, 583 (1938).
7. R. S. Alger, T. H. Anderson, and L. A. Webb, J. Chem. Phys. 30, 695 (1959).
8. G. M. Zhidomirov and Yu. N. Molin, Zh. Strukturn. Khimii, 3 (1962) (in the press).
9. E. L. Cochran, F. J. Adrian, and V. A. Bowers, J. Chem. Phys. 34, 1161 (1961).
10. H. Zeldes and R. Livingston, J. Chem. Phys. 30, 40 (1959).
11. R. S. Alger, T. H. Anderson, and L. A. Webb, Bull. Am. Phys. Soc. 5, 156 (1960).
12. M. Fujimoto and D. Y. E. Ingram, Trans. Farad. Soc. 54, 1304 (1958).

* A changed multiplicity in the EPR spectrum at −160° was observed previously for isopropyl alcohol [12].

THE CONDENSATION (STICKING) COEFFICIENT OF GAS MOLECULES WHEN CHEMISORBED ON A METAL SURFACE

V. M. Gavrilyuk

Institute of Physics, Academy of Sciences, USSR
(Presented by Academician A. N. Frumkin, June 26, 1961)
Translated from Doklady Akademii Nauk SSSR, Vol. 141, No. 5,
pp. 1124-1226, December, 1961
Original article submitted May 23, 1961

Numerous studies are devoted to the experimental and theoretical investigation of the problem to be discussed. However, just after Becker's paper [1] several studies [2-4] were carried out and experimental data were obtained both on the magnitude of the condensation (sticking) coefficient $\varkappa$ and its dependence on the concentration $\underline{n}$ of adsorbed atoms or molecules. By these studies it was established that $\varkappa$ for the gases studied (H_2, O_2, CO, N_2) is almost constant in a certain range of $\underline{n}$ and always smaller than one ($\varkappa \approx 0.5$-0.1). When $\underline{n}$ is further raised, the coefficient $\varkappa$ begins to fall sharply and attains values of about 10^{-3}-10^{-4}.

There are known several attempts [2, 5] to explain the dependence of $\varkappa$ on $\underline{n}$, but they were not successful. All authors started from the assumption that the measured decrease of $\varkappa$ at rising $\underline{n}$ actually takes place.

This paper is based on the assumption that the sticking coefficient $\varkappa$ does not depend on the concentration $\underline{n}$ of adsorbed molecules. The experimentally observed decrease of $\varkappa$ at rising $\underline{n}$ originates from the evaporation of part of the adsorbed molecules resulting, because by the interaction between the adsorbed molecules the heat of chemisorption falls sharply at increasing $\underline{n}$; in a preceding paper [6] we have developed a theory for the said interaction.

We will distinguish the sticking coefficient $\varkappa = dn/dN$ and the mean sticking coefficient $K = \underline{n}/N$ where $\underline{n}$ is the number of molecules adsorbed from the total number N of molecules hitting the metal surface in a given interval of time so that

$$K = \overline{\varkappa} = \frac{1}{n}\int_0^n \varkappa\, dn. \tag{1}$$

To form an electronic bound with the surface, obviously, a certain time, longer than the duration of a molecular collision with the surface, is required. Therfore, we assume that chemisorption is always preceded by physical adsorption and the latter is characterized by its own sticking coefficient $\varkappa_{ph}$. Correspondingly, chemisorption is characterized by its sticking coefficient $\varkappa_{ch}$. In the experiment one usually measured the apparent sticking coefficient of chemisorption

$$\tilde{\varkappa}_{ch} = \frac{d(n - n_v)}{dN} = \frac{dn_{ch}}{dN}$$

or the mean apparent sticking coefficient of chemisorption $\tilde{K}_{ch} = n_{ch}/N$ where $n_{ch} = n_{ch} - n_v$ Here n_{ch} is the number of molecules chemisorbed and staying per unit surface area, n_v the number of molecules evaporated from a unit surface area in the same time.

Let a flow dN/dt hit the surface, then the change in concentration of physically adsorbed molecules dn_{ph}/dt will be

$$\frac{dn_\Phi}{dt} = \varkappa_\Phi \frac{dN}{dt} - n_\Phi a e^{-q_\Phi/kT} - n_\Phi b e^{-\varepsilon/kT}. \tag{2}$$

Here the second and the third term at the right hand side, according to the theory of absolute reaction rates [7], are equal to the number of physically adsorbed molecules which evaporate and that of the molecules passing from the physically adsorbed to the chemisorbed state; q_{ph} is the heat of physical adsorption; ε the activation energy for the transition from the physically adsorbed to the chemisorbed state; $\underline{k}$ Boltzmann's constant; $\underline{h}$ Planck's constant; $\underline{a}$ and $\underline{b}$ are the ratios of the partition function for the activated complex to that of an adsorbed molecule for the transition from the physically adsorbed state to the gas phase and to the chemisorbed state, respectively. Upon solving this equation we find the value of n_{ph} for the case $T \neq 0$

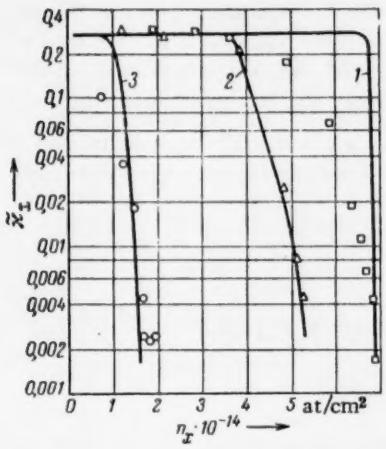

$$n_{\Phi} = \frac{\varkappa_{\Phi}\, dN/dt}{ae^{-q_{\Phi}/kT} + be^{-\varepsilon/kT}}. \tag{3}$$

The change in concentration of chemisorbed molecules dn_{ch}/dt will be

$$\frac{dn_{ch}}{dt} = n_{\Phi} b e^{-\varepsilon/kT} - n_{ch} a_{ch} e^{-q_{ch}/kT}. \tag{4}$$

Here q_{ch} is the heat of chemisorption and a_{ch} is a ratio like $\underline{a}$ but now for desorption from the chemisorbed state; the second term at the right hand side is equal to the number of chemisorbed molecules evaporated.

By substituting (3) into (4) we find the sticking coefficient of chemisorption $\varkappa_{ch}$ (evaporation is not taken into account)

$$\varkappa_{ch} = \frac{d(n_{ch} + n_v)}{dN} = \frac{\varkappa_{\Phi}}{\frac{a}{b} e^{-(q_{\Phi}-\varepsilon)/kT} + 1}, \tag{5}$$

and also the apparent sticking coefficient $\tilde{\varkappa}_{ch}$ (evaporation is taken into account)

$$\tilde{\varkappa}_{ch} = \frac{dn_{ch}}{dN} = \frac{\varkappa_{\Phi}}{\frac{a}{b} e^{-(q_{\Phi}-\varepsilon)/kT} + 1} - \frac{n_{ch} a_{ch} e^{-q_{ch}/kT}}{dN/dt}. \tag{6}$$

The second term in the right hand side of (6) originates from the decrease of $\tilde{\varkappa}_{ch}$ at rising n_{ch} caused by evaporation.

The apparent mean sticking coefficient is equal to

$$\tilde{K}_{ch} = \frac{1}{n_{ch}} \int_0^{n_{ch}} \tilde{\varkappa}_{ch}\, dn_{ch} = \frac{\varkappa_{\Phi}}{\frac{a}{b} e^{-(q_{\Phi}-\varepsilon)/kT} + 1} - \frac{a_{ch}}{n_{ch}\, dN/dt} \int_0^{n_{ch}} n_{ch} e^{-q_{ch}/kT}. \tag{7}$$

From (5) it follows that always $\varkappa_{ch} \leq \varkappa_{ph}$. Usually, in physical adsorption of gases q_{ph} is small. Therefore, Lennard-Jones' [8] theory of the sticking coefficient, according to which $\varkappa_{ph} < 1$ and practically independent of temperature, is applicable here. For instance, in the case of hydrogen adsorption on metals in [8] there were found values lying in the range 0.16-0.3 and this is in good agreement with the experiment [3]. Hence it becomes also understandable why in the adsorption of oxygen on W the coefficient $\varkappa_{ch}$ is independent of temperature in the broad temperature range detected in the experiments by N. D. Morgulis and A. G. Naumovets [9] and also in adsorption of H_2 on W (see [3]) in that same range, where evaporation as yet does not manifest itself. In these cases $\varepsilon \approx 0$ and $q_{ph} \approx$ $\approx$ 0.1-0.2 ev. It should be noted that Lennard-Jones' theory [8] does not take into account that $\varkappa_{ph}$ may depend on the concentration of adsorbed molecules, because the conditions of phonon exchange may be altered as surface coverage increases. The relations (6) and (7) describe how $\tilde{\varkappa}_{ch}$ and $\tilde{K}_{ch}$ depend on n_{ch}. Here it should be underlined that q_{ch} is a function of n_{ch}, that is, as a result of the interactions between the adsorbed atoms or molecules, q_{ch} falls sharply at raised n_{ch} [6]. Therefore, the magnitude of the second term in (6) and (7) will depend strongly on the value of q_{ch}/kT and, consequently, on n_{ch} and T.

Curves of $\tilde{\varkappa}_{ch}(n_{ch})$ calculated by means of (6) for hydrogen at sorption on W for the three substrate temperatures: 1) 310°K, 2) 610°K, 3) 740°K are shown in figure. The relation $q_{ch}(n_{ch})$ was taken from the work of O. Beeck. All these curves were calculated for three different values of dN/dt. We used the simplification that a_{ch} is equal to kT/h (where h is Planck's constant). In this same figure we have plotted the experimental data of Eisinger. It may be said that the agreement between the calculated and experimental relations $\tilde{\varkappa}_{ch}(n_{ch})$ is satisfactorily. It should be noted that at raised dN/dt or lowered temperature the n_{ch} value at which $\tilde{\varkappa}_{ch}$ begins to fall will be higher. At temperatures close to the absolute zero point, $\tilde{\varkappa}_{ch}$ will be constant for all n_{ch}.

However, the here exposed ideas are in agreement, at least qualitatively, with Eisinger's experimental data [3] on the way $\tilde{\varkappa}_{ch}$ depends on n_{ch} in the adsorption of N_2, O_2 and CO on W. For a quantitative comparison one should have data on the relation $q_{ch}(n_{ch})$, which are lacking at present.

LITERATURE CITED

1. J. A. Becker and C. Hartman, J. Phys. Chem. 57, 157 (1953).
2. G. Eilich, J. Phys. Chem. 60, 1388 (1956).
3. J. Eisinger, J. Chem. Phys. 27, 1206 (1957); 28, 165 (1958); 29, 1154 (1958); 30, 412 (1959).
4. R. E. Schlier, J. Appl. Phys. 29, 1162 (1958).
5. P. Kisliuk, Phys. Chem. Solids. 3, 95 (1957).
6. V. M. Gavrilyuk, Ukr. Fiz. Zhurn. 4, 734 (1959).
7. S. Glasstone, K. Laidler, and H. Eyring, Theory of Absolute Reaction Rates [Russian translation] (IL, 1948).
8. J. E. Lennard-Jones and A. F. Devonshire, Proc. Roy. Soc. A156, 6 (1936).
9. N. D. Morgulis and A. G. Naumovets, Izv. AN SSSR, Ser. Fiz. 24, 6 (1960).
10. O. Beeck, Catalysis [Russian translation] (IL, 1955).

All abbreviations of periodicals in the above bibliography are letter-by-letter transliterations of the abbreviations as given in the original Russian journal. *Some or all of this periodical literature may well be available in English translation.* A complete list of the cover-to-cover English translations appears at the back of this issue.

AUTO-DIFFUSION OF ALKALI IONS IN SILICATE MELTS

V. I. Malkin and B. M. Mogutnov

I. P. Bardin Central Scientific Research Institute of Heavy Metallurgy
(Presented by Academician G. V. Kurdyumov, July 14, 1961)
Translated from Doklady Akademii Nauk SSSR, Vol. 141, No. 5,
pp. 1127-1130, December, 1961
Original article submitted July 14, 1961

The results of transference number measurements in acid silicate melts [1-3] show that in three-component melts containing two cations a mutual effect of the cations on their relative mobility is observed. A cause of this mutual effect may be that the strength of the bond between one cation and the silicic acid anion depends on the strength of the bond between this anion and the other cation, due to mutual polarization of oxygen by both cations.

Another factor which is responsible for this mutual effect is the change in degree of looseness of the structure when cations of different sizes are joined in pairs. It has been pointed out [1] that the relative role of the two factors in melts of this sort depends on the difference in coordination numbers of the pair of cations. As the difference increases, a more important role is assumed by the factor related to the degree of looseness of the structure (the "geometric" factor), since it leads to a reduction in the relative mobility of the larger cation. If the difference becomes smaller the role of the bond strength factor becomes more important, since it increases the relative mobility of the larger cation.

There is some interest in pursuing the question of how various paired cation combinations influence not only the relative, but the absolute mobility as well. To this end, the present paper gives results of measurements on the auto-diffusion coefficients of potassium and sodium cations in the following silicate melts:

$Na_2O \cdot 2SiO_2$, $Na_2O \cdot Li_2O \cdot 4SiO_2$, $Na_2O \cdot K_2O \cdot 4SiO_2$, $K_2O \cdot 2SiO_2$,
$K_2O \cdot Li_2O \cdot 4SiO_2$, $Na_2O \cdot MgO \cdot 4SiO_2$, $Na_2O \cdot CaO \cdot 4SiO_2$,
$Na_2O \cdot SrO \cdot 4SiO_2$, $Na_2O \cdot BaO \cdot 4SiO_2$, $K_2O \cdot MgO \cdot 4SiO_2$,
$K_2O \cdot CaO \cdot 4SiO_2$, $K_2O \cdot SrO \cdot 4SiO_2$, $K_2O \cdot BaO \cdot 4SiO_2$.

We have given a detailed description of the measurement technique in [4]. The radioactive isotopes Na^{24} and K^{42} were used.

The measurements were made in the temperature range 850-1210°C with melts containing only alkali metal cations, and 1100-1300° with the melts containing cations of alkali and alkaline earth metals. The experiments have shown that the temperature dependence of the auto-diffusion coefficients of the cations is well described by the equation $D = D_0 e^{-\frac{E}{RT}}$, where E is the activation energy as may be seen from figure where the straight lines $\log_{10} D_{Na} = f(1/T)$ are given as an example. In no case did the error of measurement exceed 10%, except that with the $K_2O \cdot CaO \cdot 4SiO_2$ melt the error was larger ($\approx 20\%$), in view of which a considerably larger number of measurements was made in this melt.

The results of the measurements are given in table, which shows D_0 and E, as well as the values of the auto-diffusion coefficients at t = 1200°, for which the transference numbers were found.

In [4] it was shown that the mechanisms of diffusion and electrical conductivity are equivalent in a $Na_2O \cdot 2SiO_2$ melt. If this is also true for three-component melts, the ratio of the auto-diffusion coefficients in the melts should be equal to the ratio of the transference numbers. The transference numbers calculated from the auto-diffusion coefficients for the sodium ion at 1200° in the $Na_2O \cdot K_2O \cdot 4SiO_2$ and $Na_2O \cdot CaO \cdot 4SiO_2$ melts (in the latter melt the auto-diffusion coefficient of the Ca^{++} ion was measured at 1200°) are equal respectively to 0.53 and 0.75, while the values measured directly are 0.52 and 0.70, i.e., even in three-component melts, the mechanisms are the same. With this in mind, the mobility of one of the cations may be used with the data on the transference numbers to find the mobility of the other cation.

Chemical composition	Diffusing cation	Radius of second cation, A	$D_{1200°}$, cm^2/sec	D_0 cm^2/sec	E, cal/mole	ΔF^* cal/mole	ΔH^* cal/mole	ΔS^* cal/mole
$Na_2O \cdot 2SiO_2$	Na^+	—	$3{,}2 \cdot 10^{-5}$	$1{,}8 \cdot 10^{-3}$	11900	23700	9000	—10
$Na_2O \cdot Li_2O \cdot 4SiO_2$	Na^+	0,60	$2{,}9 \cdot 10^{-5}$	$2{,}8 \cdot 10^{-3}$	13400	24000	10500	—9,2
$Na_2O \cdot K_2O \cdot 4SiO_2$	Na^+	1,33	$2{,}6 \cdot 10^{-5}$	$6{,}3 \cdot 10^{-3}$	16100	24200	13200	—7,5
$Na_2O \cdot BaO \cdot 4SiO_2$	Na^+	1,35	$1{,}6 \cdot 10^{-5}$	2,3	34800	25700	31900	4,2
$Na_2O \cdot SrO \cdot 4SiO_2$	Na^+	1,13	$1{,}5 \cdot 10^{-5}$	$1{,}1 \cdot 10^{-1}$	26200	25900	23300	—1,8
$Na_2O \cdot CaO \cdot 4SiO_2$	Na^+	0,99	$1{,}3 \cdot 10^{-5}$	$1{,}2 \cdot 10^{-2}$	19900	26300	17000	—6,3
$Na_2O \cdot MgO \cdot 4SiO_2$	Na^+	0,65	$1{,}4 \cdot 10^{-5}$	$1{,}6 \cdot 10^{-2}$	20500	26000	17600	—5,7
$K_2O \cdot 2SiO_2$	K^+	—	$2{,}7 \cdot 10^{-5}$	$8{,}7 \cdot 10^{-4}$	10200	25400	7700	—12
$K_2O \cdot Li_2O \cdot 4SiO_2$	K^+	0,60	$1{,}7 \cdot 10^{-5}$	$8{,}7 \cdot 10^{-3}$	18200	26300	15300	—7,5
$K_2O \cdot Na_2O \cdot 4SiO_2$	K^+	0,95	$2{,}3 \cdot 10^{-5}$	$5 \cdot 10^{-3}$	15800	25600	12900	—8,6
$K_2O \cdot BaO \cdot 4SiO_2$	K^+	1,35	$8{,}9 \cdot 10^{-6}$	56	45900	28300	43000	10
$K_2O \cdot SrO \cdot 4SiO_2$	K^+	1,13	$6{,}8 \cdot 10^{-6}$	$4{,}8 \cdot 10^{-1}$	32700	29000	29800	0,51
$K_2O \cdot CaO \cdot 4SiO_2$	K^+	0,99	$6{,}6 \cdot 10^{-6}$	$1{,}7 \cdot 10^{-1}$	29800	29300	26900	—1,6
$K_2O \cdot MgO \cdot 4SiO_2$	K^+	0,65	$5{,}2 \cdot 10^{-6}$	$9{,}3 \cdot 10^{-3}$	21900	29800	19000	—7,3

It follows from the results given in table that the auto-diffusion coefficient in melts, containing alkali metal cations alone, is greater than in melts containing cations of both alkali and alkaline earth metals. The activation energy in the first group is less than in the second. This last condition is a result of the fact that the bivalent cations of the alkaline earth metals form bridges between the silicate anion complexes, and in this way densify the structure of the melt. In the first group of melts, going from binary to tertiary melts causes the auto-diffusion coefficient to drop and the activation energy to rise.

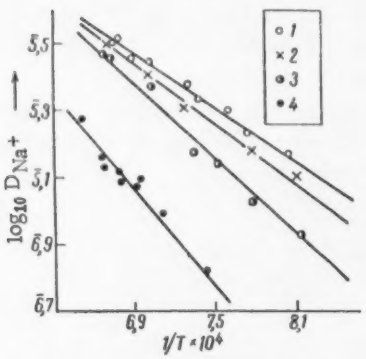

$\log_{10} D_{Na^+}$ as a function of 1/T. 1) $Na_2O \cdot 2SiO_2$ melt; 2) $Na_2O \cdot Li_2O \cdot 4SiO_2$ melt; 3) $Na_2O \cdot K_2O \cdot 4SiO_2$ melt; 4) $Na_2O \cdot CaO \cdot 4SiO_2$ melt.

Going from the $Na_2O \cdot 2SiO_2$ melt to the $Na_2O \cdot Li_2O \cdot 4SiO_2$ melt, in spite of weakening of the Na — O bond, lowers the mobility of the sodium ion, because of the effect of the "geometric factor."

Replacing the lithium oxide in the tertiary melt with potassium oxide causes an even greater reduction in mobility of the sodium ion, since in this case both the "geometric" and the bond strength factor are acting in a direction to reduce the mobility.

In the series of melts $K_2O \cdot 2SiO_2$, $K_2O \cdot Na_2O \cdot 4SiO_2$, and $K_2O \cdot Li_2O \cdot 4SiO_2$, densification of structure predominates, and therefore the auto-diffusion coefficient of the potassium ion drops.

In the second group of melts, containing alkaline earth metal ions as in the series of melts $K_2O \cdot BaO \cdot 4SiO_2$, $K_2O \cdot SrO \cdot 4SiO_2$, $K_2O \cdot CaO \cdot 4SiO_2$, and $K_2O \cdot MgO \cdot 4SiO_2$, the auto-diffusion coefficient of the potassium cation is reduced, while the transference number of the potassium ion is increased. In this series, densification of structure occurs, and the strength of the bond between the potassium ion and the anions is reduced, while the strength of the bond between the alkaline earth cations and the anions is increased. The densification of structure reduces the mobility of both the potassium ion and the ions of alkaline earth metals, but the mobility of the latter is reduced to a larger extent, because the bond which they form with the anions is strengthened. For this reason, the transference number of the potassium ion increases in this series in spite of the fact that the auto-diffusion coefficient is reduced.

In second group melts containing sodium, the auto-diffusion coefficient of the sodium ion changes very little. At the same time, the data on the transference numbers testify to the fact that the relative mobility of the sodium ion in this group of melts drops on going from the $Na_2O \cdot MgO \cdot 4SiO_2$ melt to the $Na_2O \cdot CaO \cdot 4SiO_2$ melt on account of an increase in bond strength caused by the greater strength of the magnesium cation as compared with the potassium cation. On going from the $Na_2O \cdot CaO \cdot 4SiO_2$ melt to the $Na_2O \cdot SrO \cdot 4SiO_2$ melt and further to $Na_2O \cdot BaO \cdot 4SiO_2$, the transference number of the sodium ion increases because of the densification of structure, which hinders the motion of the alkaline earth metal ions, the more so, the bigger they are.

Comparing the data of table with the results for the transference numbers brings us to the conclusion that the increase in relative mobility of the sodium ion in the series $Na_2O \cdot CaO \cdot 4SiO_2$, $Na_2O \cdot SrO \cdot 4SiO_2$, and $Na_2O \cdot BaO \cdot 4SiO_2$, what is responsible is the reduction in mobility of the alkaline earth metal atoms resulting from the effect of the "geometric" factor. It is interesting to consider the results obtained in the light of the theory of absolute reaction rates.

According to the theory [5]

$$D = \lambda^2 \frac{kT}{h} e^{\frac{\Delta S^*}{R}} e^{-\frac{\Delta H}{RT}} = \lambda^2 \frac{kT}{h} e^{-\frac{\Delta F^*}{RT}}, \quad (1)$$

while λ is the distance between two equilibrium positions of the diffusing particle, k is the Boltzman's constant, h is Planck's constant, T is the absolute temperature, R is the gas constant, ΔH^* is the heat of activation of the diffusion process, ΔS^* is the entropy of the process, and ΔF^* is the free energy of activation.

The structural models discussed in [6] were used to calculate λ. For the melts containing sodium oxide, λ = = 5.75 A, and with potassium oxide, 6.67 A.

Table gives values of ΔF^*, ΔH^* and ΔS^* calculated from Eq. (1) at 1200° for sodium and potassium ions. The values of $\Delta F^*_{1200^\circ}$ vary from melt to melt according to the change in D_{1200°.

The value of ΔS^* is the difference between the entropies of the transitional (S_{trans}) and the ground states (S_{ground}) of the diffusing particle. The entropy in each of the states mentioned will be increased if the bond strength is reduced, and the looseness of the structure is increased. It may be assumed that the effect of these factors on going from melt to melt will in large measure effect the ground state, since there is a less degree of freedom in the transitional state, and this state should be less different for the various melts.

As a result of this, bearing in mind that $\Delta S^* = S_{trans} - S_{ground}$, an increase in bond strength reduces S_{ground} and increases S^*, while loosening the structure increases S_{ground} and reduces ΔS^*.

Let us consider the change in the values of ΔH^* and ΔS^* in the first group of melts. In the series $K_2O \cdot 2SiO_2$, $K_2O \cdot Na_2O \cdot 4SiO_2$, and $K_2O \cdot Li_2O \cdot 4SiO_2$, the effect of the "geometric" factor is to increase ΔH^*. In this same series, the value of ΔS^* increases (by becoming less negative) as a result of the effect of the same "geometric" factor (densification of the structure with reduction in S_{ground}).

On going from the $Na_2O \cdot 2SiO_2$ melt to the $Na_2O \cdot Li_2O \cdot 4SiO_2$ melt, in spite of the reduction in bond strength resulting from densification of the structure, what occurs is an increase in both ΔH^* and ΔS^* (reduction of S_{ground}). If Li_2O is replaced by K_2O, what occurs is further densification of the structure and in addition strengthening of the bond, as a result of which a further increase in ΔH^* and ΔS^* is observed.

In the second group of melts (the melts, containing alkaline earth metal ions), the values of ΔH^* and ΔS^* noticeably exceed those for melts of the first group. This fact is an expression of the denser structure of these melts caused by the presence of bivalent cations which play the role of bridges between the anions. In the series of melts $Na_2O \cdot BaO \cdot 4SiO_2$, $Na_2O \cdot SrO \cdot 4SiO_2$, and $Na_2O \cdot CaO \cdot 4SiO_2$, what occurs is loosening of the structure and reduction in bond strength, which causes a reduction in ΔH^* and ΔS^*. However, on going from the $Na_2O \cdot CaO \cdot 4SiO_2$ melt to the $Na_2O \cdot MgO \cdot 4SiO_2$ melt, the role of the "geometric" factor increases along with the further reduction in bond strength. The effect of the "geometric" factor is predominating, and, therefore, ΔH^* and ΔS^* increase somewhat. In the series of melts $K_2O \cdot BaO \cdot 4SiO_2$, $K_2O \cdot SrO \cdot 4SiO_2$, $K_2O \cdot CaO \cdot 4SiO_2$, and $K_2O \cdot MgO \cdot 4SiO_2$, the strength of the bonds between the potassium ion and the anions is reduced, and the role of the "geometric" factor increases. In this group the bond strength plays a large role, thus reducing ΔH^* and ΔS^*.

It is interesting to note that for all the melts studied the increase in ΔH^* is accompanied by a simultaneous increase in ΔS^*. According to the compensation rule [7], and increase in activation energy is accompanied by an increase in D_0. From the point of view of the concepts presented it is understandable that this general rule would be obeyed when applied to the diffusion of cations in the melts studied. The "geometric" and bond strength factors affect ΔH^* and ΔS^* in such a way that E and D_0 change in the same direction.

LITERATURE CITED

1. V. I. Malkin, ZhFKh, 35, 2, 336 (1961).
2. I. O'M. Bockris, J. A. Kitchener, and A. E. Davies, Trans. Farad. Soc. 48, 536 (1952).

3. V. I. Malkin and L. V. Shvartsman, Problems in Metallurgy and the Physics of Metals, Sixth Collection of Papers [in Russian] (Moscow, 1959).
4. V. I. Malkin and B. M. Mogutnov, Izv. AN SSSR, OTN, Metallurgiya i Toplivo, 2, 37 (1960).
5. S. Glasstone, K. Laidler, and H. Eyring, The Theory of Rate Process, New York (1941).
6. E. M. Levin and S. Block, J. Am. Ceram. Soc. 40(3), 95 (1957).
7. P. Rüetschi, Zs. Phys. Chem. 14 (516), 277 (1958).

All abbreviations of periodicals in the above bibliography are letter-by-letter transliterations of the abbreviations as given in the original Russian journal. *Some or all of this periodical literature may well be available in English translation.* A complete list of the cover-to-cover English translations appears at the back of this issue.

THE LEADING STAGE OF COMBUSTION

A. D. Margolin

Institute of Chemical Physics, Academy of Sciences, USSR
(Presented by Academician V. N. Kondrat'ev June 23, 1961)
Translated from Doklady Akademii Nauk SSSR, Vol. 141, No. 5,
pp. 1131-1134, December, 1961
Original article submitted June 21, 1961

According to present day concepts, the combustion of gunpowders and explosive substances proceeds in several spatial stages [1-6]. In the general case, the combustion rate of the system depends on the interaction of all the stages of combustion. But in a number of cases, some one stage of combustion determines the rate of flame propagation in the whole system, while the remaining stages "add onto" the leading stage. Discovering what the leading stage is one of the fundamental problems of the theory of combustion. Because of the complexity of the combustion process, it is a good idea to consider a simplified scheme, which, nevertheless, takes account of the fundamental properties of the real process.

In the Belyaev-Zel'dovich model [1, 2], on the surface of a burning second-order explosive substance, evaporation or gasification occurs, and the vapors formed burn up to give the end products in the gaseous phase. The leading stage, which determines the combustion rate, is the combustion in the gaseous phase. The combustion of gunpowders is a more complicated process. As P. F. Pokhil [3] has shown, in the reacting layer on the surface of the condensed gunpowder phase, over-all exothermic reactions occur, which are accompanied by dispersion of a considerable part of the material. There is a "cold" flame located on the surface of the gunpowder in which a smoke-gas mixture is burning into intermediate products, which are burnt up in a second, luminous flame.

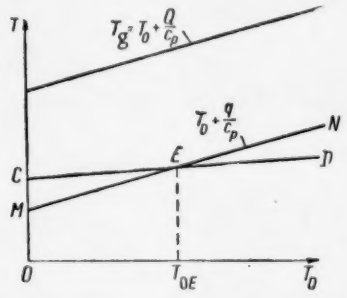

Scheme showing the surface temperature of the condensed phase of gunpowder, and the combustion temperature T_g as a function of the initial temperature of the powder, T_0.

Here it will be shown that for various values of the parameters, which affect the combustion process, the leading stage of combustion may be either the combustion of the smoke-gas mixture, or the combustion in the reacting layer of the condensed phase, although the stage of combustion in the reacting layer of the condensed phase can be the leading one only if the reaction going on there liberates heat.

First, we shall trace how changing the initial temperature affects the process of combustion. The line CED (figure) is the surface temperature of the condensed phase, when the leading stage is in the gaseous phase. The line MEN is the temperature to which the surface of the condensed phase is heated by heat liberation q in the reacting layer of the condensed phase,

$$T_{MEN} = T_0 + \frac{q}{c_p}. \qquad (1)$$

If the combustion goes according to a three-stage scheme, with a condensed stage, a smoke-gas stage, and a luminous flame, T_g will be the temperature reached when the smoke-gas mixture burns in the second stage of combustion.

The surface of the condensed phase of the powder is heated in the process of combustion by the heat liberated in the condensed phase, q, and the heat coming from the gaseous phase Δq $\left(T_p = T_0 + \frac{q}{c_p} + \frac{\Delta q}{c_p}\right)$. The ratio of combustion of the condensed phase is sharply increased by raising the surface temperature T_p. Over the range of initial temperatures $0 < T_0 < T_{0E}$, the leading stage of combustion is the combustion in the smoke-gas phase.

Regulation of the rate of combustion of the condensed phase is accomplished by the heat Δq. At $T_0 > T_{0E}$, we have $\Delta q = 0$ if heat is liberated in the gaseous phase. The surface temperature T_p increases, to a first approximation, along the curve CEN as T_0 is increased. At $T_0 > T_{0E}$, the leading stage is the combustion in the reacting layer of the condensed phase. The rate of combustion in the condensed phase ($T_0 > T_{0E}$) exceeds the rate of combustion of the smoke-gas mixture of a given composition, therefore, either the combustion front in the gas phase will be removed from the surface until it is extinguished, or the combustion process goes over into a burn-up process, the (mass) rate of which is determined only by the rate at which products are supplied from the burning in the preceding stage.

The initial temperature, T_{0E}, at which the leading role is transferred from one stage of combustion to another is determined in the following way:

$$T_{0E} = T_{pE} - \frac{q}{c_p}. \tag{2}$$

In the general case, at the point of intersection, we may have

$$\left(\frac{\partial T_{CED}}{\partial T_0}\right)_E \lesseqgtr \left(\frac{\partial T_{MEN}}{\partial T_0}\right)_E. \tag{3}$$

The leading role passes from the gaseous phase to the condensed phase on raising the initial temperature, if

$$\left(\frac{\partial T_{CED}}{\partial T_0}\right)_E < \left(\frac{\partial T_{MEN}}{\partial T_0}\right)_E.$$

This case was examined above (see figure). The leading role moves from the condensed stage to the gaseous stage at $T_0 > T_{0E}$, if

$$\left(\frac{\partial T_{CED}}{\partial T_0}\right)_E > \left(\frac{\partial T_{MEN}}{\partial T_0}\right)_E.$$

The way in which the curves CED and MEN interesect determines the relation between the temperature coefficients of the combustion rate $\beta = (\partial \ln u/\partial T_0)_p$ at $T_0 > T_{0E}$ (index +), and below the point of intersection (index −):

$$\left(\frac{\partial u_+}{\partial T_0}\right)_E \gtreqless \left(\frac{\partial u_-}{\partial T_0}\right)_E; \quad \beta_+ \gtreqless \beta_-;$$
$$\left(\frac{\partial \ln u_+}{\partial \ln T_0}\right)_E \gtreqless \left(\frac{\partial \ln u_-}{\partial \ln T_0}\right)_E \quad \text{at} \quad \left(\frac{\partial T_{CED}}{\partial T_0}\right)_E \lesseqgtr \left(\frac{\partial T_{MEN}}{\partial T_0}\right)_E. \tag{4}$$

If the over-all kinetics of the chemical reactions in the gaseous phase and in the reacting layer of the condensed phase is described by a Arrhenius law with activation energies E_g and E_p respectively, Eq. (3) is ($E/RT \gg 1$) approximately equivalent to the expression

$$\frac{E_g}{T_g^2} \lesseqgtr \frac{E_p}{T_p^2}\left(1 + \frac{\partial}{\partial T_0}\frac{q}{c_p}\right). \tag{5}$$

We shall now apply the concepts presented to some problems in the theory of combustion. Raising T_0 of the powder above some level causes a substantial increase in β [7-9]. Thus, O. I. Leipunskii and A. I. Korotkov have shown [9] that raising the initial temperature of nitroglycerin N powder ~above 40°C causes an increase in β of approximately seven fold at atmospheric pressure. On the basis of what has been said above it may be assumed that a β (T_0) relation of this sort is to be explained by a transfer of the leading role at $T_0 > T_{0E}$ from combustion in the smoke-gas phase to combustion in the reacting layer of the condensed powder phase. Let us try the value of T_{0E} in formula (2). P. F. Pokhil [3] has experimentally produced flameless combustion of powder in vacuum, which is propagated stably only on account of the heat liberation in the condensed phase, and he has shown that $q = 80$ cal/g, $c_p = 0.3$-0.4 cal/g · deg, with $T_p \approx 300°$. Calculation gives $T_{0E} \simeq 30$-$100°$, which agrees qualitatively with the data in [9]. Assuming the $T_0 > T_{0E}$ the leading stage of combustion is the combustion in the condensed phase, we were able to find the effective activation energy of the reactions going on in the reacting layer of the condensed

powder phase, which was equal to 25 kcal/mole, starting from the experimental relation between the combustion rate and T_0 [9], and Eq. (1). The value of T_{0E} was taken from [9], and T_{pE} was taken equal to 300° (q/c_p = const).

By experimentally determining the point T_{0E} where the break in the $\beta(T_0)$ curve occurs at constant pressure and T_{pE}, it is possible in principle to find q for any pressure

$$q = c_p (T_{pE} - T_{0E}). \tag{6}$$

Ya. B. Zel'dovich's theory [2] predicts that raising the initial temperature of a condensed explosive or a powder at constant pressure can increase the combustion rate by no more than e (2.7) times. It is known [9] that the actual combustion rate may be increased by raising the temperature of the powder by more than ten times. We are of the opinion that Zel'dovich's derivation can be used only below the temperature T_{0E}, when the leading stage of combustion is in the gaseous phase. Actually, below the point T_{0E}, where the break in the $\beta(T_0)$ curve occurs, the combustion rate changes more than e times [9]. The combustion rate of nitroglycol changes not more than e times with change in the initial temperature at constant pressure [7], which is in agreement with what has been presented above, since in nitroglycol the q value is small, and therefore the leading stage of combustion is located in the gaseous phase for any possible range of initial temperatures.

It is known that the combustion rate of powder at any temperature is dependent on the pressure. This relationship, when the leading stage is combustion in the reacting layer of the condensed phase, can probably be explained in the following way. The value of q, and, consequently, T_{MEN} may depend on the pressure, and in addition, the reacting layer of the condensed phase will contain gaseous products [3-5], which may also cause the combustion rate, which is determined by processes in the reacting layer of the condensed phase, to be dependent on the pressure

$$u \sim p^{\nu_1} e^{-E_p/2RT_p(p)}, \tag{7}$$

from which we have the following expression for ν_p = d ln u/d ln p, when the leading stage is the combustion in the condensed phase:

$$\nu_p = \frac{p}{u}\frac{\partial u}{\partial p} + \frac{p}{u}\frac{\partial u}{\partial T_p}\frac{dT_p}{dp} = \nu_1 + p\frac{E_p}{4RT^2}\frac{dT_p}{dp},$$

where

$$\frac{dT_p}{dp} = \frac{1}{c_p}\frac{dq}{dp}.$$

The effect of pressure on the transition of the leading role from one stage of combustion to another may be analyzed in the same way as the effect of temperature.

In particular, Eq. (4) continues to hold, if T_0 is everywhere replaced by P. The physical meanings of the lines CED and MEN remains the same as before ($T_{MEN} = T_0 + q/c_p$).

With increase in pressure, the leading stage of combustion is shifted from the gaseous phase to the condensed phase, if $(\nu_n/\nu)_E > 1$ $((\partial T_{MEN}/\partial p)_E > (\partial T_{CED}/\partial p)_E)$ and from the condensed phase to the gaseous phase, if $(\nu_n/\nu)_E < 1$ $((\partial T_{MEN}/\partial p)_E < (\partial T_{CED}/\partial p)_E)$.

P. F. Pokhil and V. M. Mal'tsev have shown experimentally that the specific amount of heat, liberated in the reacting layer of the condensed phase of nitroglycerin powder, increases with increase in pressure, i.e., there is actually a tendency for the leading role to be transferred to the reaction going on in the reacting layer of the condensed phase, i.e., the case $(\nu_p/\nu)_E > 1$ is realized, where ν relates to the gaseous phase.

The relation between the surface temperature T_p in the pressure, when the leading stage is located in the gaseous phase is described approximately ($E/RT \gg 1$) by the formula

$$\frac{dT_p}{dp} = \frac{\nu - \nu_1}{p}\frac{4RT_p^2}{E_p}. \tag{9}$$

The work presented is in complete agreement with the physical bases of the theory of combustion of gunpowder, formulated by P. F. Pokhil [3].

LITERATURE CITED

1. A. F. Belyaev, ZhFKh, 12, 93 (1938).
2. Ya. B. Zel'dovich, ZETP, 12, 498 (1942).
3. P. F. Pokhil, Collection: Physics of Explosion [in Russian] (1953), No. 2; 3 (1955); 5, (1956).
4. O. K. Rice and R. Ginell, J. Phys. Coll. Chem. 54, 885 (1950).
5. R. G. Parr and B. L. Crawford, J. Phys. Coll. Chem. 54, 929 (1950).
6. Dzh Korner, Internal Ballistics of Artillery [in Russian] (Moscow, 1953).
7. K. K. Andreev, Thermal Decomposition and Combustion of Explosives [in Russian] (Moscow and Leningrad, 1957).
8. K. K. Andreev and A. E. Varga, Addendum to the Russian translation of the Book by M. Patri, Combustion and Detonation of Explosives [in Russian] (1953), No. 2.
9. A. I. Korotkov and O. I. Leipunskii, Collection: Physics of Explosion [in Russian] (1953), No. 2 .

All abbreviations of periodicals in the above bibliography are letter-by-letter transliterations of the abbreviations as given in the original Russian journal. *Some or all of this periodical literature may well be available in English translation.* A complete list of the cover-to-cover English translations appears at the back of this issue.

THE DISTRIBUTION OF POTENTIAL AT A GERMANIUM – ELECTROLYTE SOLUTION BOUNDARY

Yu. V. Pleskov and V. A. Tyagai

Electrochemistry Institute, Academy of Sciences, USSR
(Presented by Academician A. N. Frumkin, July 21, 1961)
Translated from Doklady Akademii Nauk SSSR, Vol. 141, No. 5,
pp. 1135-1138, December, 1961
Original article submitted July 20, 1961

The electrical double layer at a semiconductor-solution boundary is in the simplest case formed by the diffuse charge in the semiconductor and the electrostatically adsorbed ions of the solution; the Galvani potential at the phase interphase is made up of the potential jumps in the Helmholtz layer and in the region of spatial charge in the semiconductor. According to [1, 2], in the case of a nondegenerate surface in the absence of surface states* and dipole layers the potential drop in the Helmholtz layer constitutes an insignificant part of the total potential jump at the semiconductor-solution boundary both at equilibrium and with polarization of the electrode. The distribution of the potential at the surface of a semiconducting electrode can be estimated from the relationship between the magnitude of the spatial charge and the electrode potential; for this purpose we used a method involving measurement of the rate of surface recombination and the photopotential, i.e., the instantaneous measurement of the electrode potential with impulse illumination).

The rate of surface recombination s, which depends on the external electric field, has a maximum value when the concentrations of holes and electrons on the surface of the semiconductor are equal (with the condition that the capture cross-sections for capture of an electron or a hole by the recombination center are equal [3]). In this case the surface potential φ_s, i.e., the difference between the Fermi level E_F and the center of the forbidden zone on the surface, divided by the charge on the electron q, is equal to zero, irrespective of the concentration of electrons in the bulk.

The magnitude of the photoeffect is large in the case where an inversion layer is formed on the surface, and small in the case where an accumulative layer is formed. The photoeffect disappears when the spatial charge in the semiconductor is equal to zero (in the absence of surface states [4]). The electrode potential corresponding to this state of the surface has been called the planar zone potential, since in this case there are no inflections in the energetic zones of the semiconductor at its surface. The surface photopotential is conveniently measured by determining the planar zone potential [5]. At the planar zone potential, the energy of the center of the forbidden zone on the surface has the same value E_i as in the bulk of the semiconductor, and

$$\varphi_s = \frac{E_F - E_i}{q}.$$

Thus by measuring simultaneously the rate of surface recombination and the photopotential as functions of the electrode potential φ, we can "tie" φ_s for each specimen to definite values of φ from two characteristic values. It can readily be seen that in the case of a semiconductor with inherent conductivity ($E_F = E_i$) the surface potentials, zero photoeffect, and maximum rate of surface recombination are practically identical and equal to approximately zero.

According to [1, 2], the magnitude of the Galvani potential at a semiconductor-solution boundary depends on the concentration of free electrons in the bulk of the semiconductor in the same way as the Fermi level E_F (i.e., it

* I.e., particles specifically adsorbed on the surface and present in equilibrium with the free charges in the semiconductor.

changes by 59 mv when the electron concentration changes by a factor of 10). Since the potential jump in the Helmholtz layer is independent of E_F it is the second component of the Galvani potential – the potential drop in the region of the spatial charge V_s – which reflects the change in E_F with change in the electron concentration in the semiconductor. At the planar zone potential $V_s = 0$. If it is assumed that the potential jump in the Helmholtz layer depends little on the polarization of the semiconducting electrode, i.e., that change in the electrode potential is accompanied chiefly by a change in V_s (which is apparently true in the case of a nondegenerate surface in the absence of surface states [1]), then the magnitude of the polarization necessary to make the zones planar is close to V_s. Consequently, with change in the electron concentration in the semiconductor, the planar zone potential changes in the same way as V_s, i.e., it practically follows the Fermi level E_F. If however the concentration of surface is high, then a considerable fraction of the applied voltage falls in the Helmholtz layer.

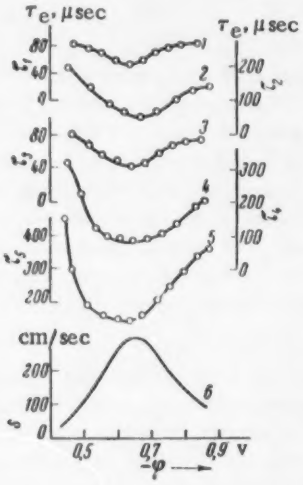

Fig. 1. The electrophysical properties of the specimens.

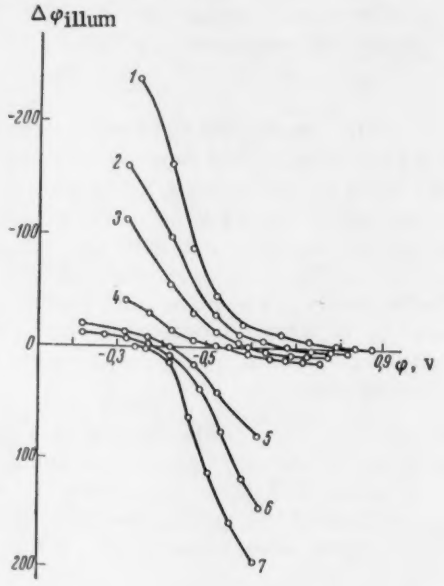

Fig. 2. The electrophysical properties of the specimens

Curve No.	Type of conductivity	Specific resistance, ohm · cm	Diffusion length of minority carriers, mm
1	p	3	0.7
2	n	3	0.7
3	p	20	1.0
4	n	20	1.5
5	n	40	2.5

Curve No.	Type of conductivity	Specific resistance, ohm·cm	Curve No.	Type of conductivity	Specific resistance, ohm·cm
1	n	0.004	5	p	10
2	n	3	6	p	3
3	n	20	7	p	0.5
4	n	40			

On the other hand, the surface potential $\varphi_s = \frac{E_F - E_i}{q} + V_s$ is practically independent of E_F* and is only a function of the electrode potential [1]. It may therefore be expected that the potential of the maximum rate of surface recombination, which is unambiguously determined by the surface potential, will be independent of E_F, i.e., independent of the specific resistance of the germanium.

* More accurately, its change with change in E_F is compensated by the change, of opposite sign, in V_s.

The rate of surface recombination s on a germanium-solution boundary was measured by recording the drop in the photoconductivity in specimens with dimensions 15 · 5 mm and thickness 0.2-0.5 mm. For the measurement of the conductivity, a low voltage (50 mv) was applied to the ends of the plate by means of 2 ohmic contacts. The specimen was illuminated by the impulse lamp of a PST-1 strobotachometer (frequency of flashing 20-40 sec^{-1}, duration of flash approximately 3 μsec). The signal, which is proportional to the photoconductivity, was amplified by means of a USh-2 wide-band amplifier and reproduced on the screen of an IO-4 impulse oscillograph; the constant for the photoconductivity drop, i.e., the effective life-time of the minority carriers τ_e, was determined by means of a system of time marks. The photopotential $\Delta\varphi_{illum}$ was measured by means of the same apparatus. In both cases the magnitude of the illumination chosen was so small that the polarization of the electrode on illumination changed by not more than 0.01 v.

Before the measurements, the contacts were insulated by means of purified paraffin wax and the electrode was treated in SR-4A etching agent and placed in 1 N NaOH solution. After nitrogen had been passed for a prolonged period through the solution, the curve showing the relationship between τ_e and the potential was recorded. For the determination of $\Delta\varphi_{illum}$ the surface of the germanium was subjected to anodic etching for a short period in the solution in which the measurements were carried out, as a result of which the rate of surface recombination decreased considerably. It should be noted that it is impossible to determine s and $\Delta\varphi_{illum}$ for absolutely identical treatment of the surface, since the exact measurement of $\Delta\varphi_{illum}$ is possible only in the absence of appreciable recombination.

Figure 1 shows the relationship between the effective life-time of the minority carriers τ_e and potential for 5 specimens of germanium with different bulk electrophysical properties (curves 1-5), together with the curve, calculated from the experimental data for specimen 4, for the relationship between the rate of surface recombination s and the electrode potential φ (curve 6). The relationship between the instantaneous photopotential and the electrode potential in 1 N NaOH solution is shown in Fig. 2. At a definite value of the potential for each specimen, the value of $\Delta\varphi_{illum}$ passes through zero and changes sign. The value of the potential φ_z, at which the photopotential is equal to zero, depends on the concentration of free electrons in the germanium, as can be seen from Fig. 3 (1 – in 1 N NaOH solution, 2 – in 1 N H_2SO_4 solution).

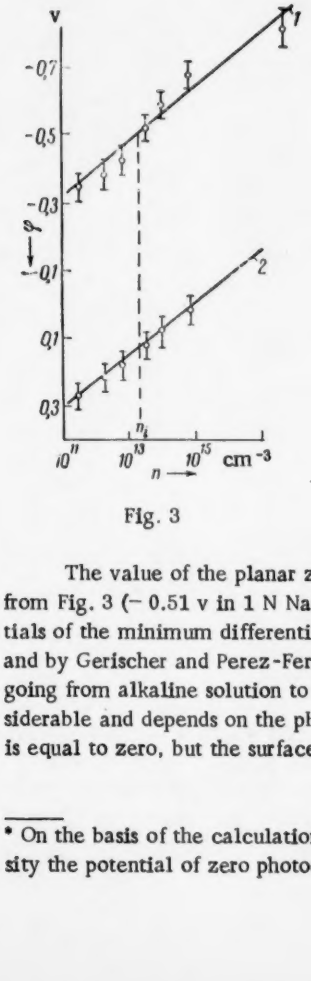

Fig. 3

The experimental data which we have obtained confirm the applicability of the above theories to the germanium-electrolyte interface. The potential of the maximum rate of surface recombination (i.e., of the minimum τ_e) is practically independent of the specific resistance of germanium (Fig. 1) and is equal to −0.63 v in 1 N NaOH solution, while the potential of zero photoeffect, i.e., the planar zone potential, changes regularly with change in the concentration of free electrons in the semiconductor (Fig. 3). This gives grounds for assuming that under the conditions of our experiments (slight anodic etching of the germanium directly before the measurements) the density of surface states is not very high.* Nevertheless a considerable fraction of the applied voltage (about 30%) falls in the Helmholtz layer, as indicated by the difference between the slope of the straight lines in Fig. 3 (0.080 v for one order of magnitude of the free electron concentration) and the theoretical slope (0.059 v).

The value of the planar zone potential for germanium with inherent conductance, determined by interpolation from Fig. 3 (− 0.51 v in 1 N NaOH solution and 0.13 v in 1 N H_2SO_4 solution), show good agreement with the potentials of the minimum differential capacity, measured by Bohnenkamp and Engell [6] (−0.5 and 0.3 v respectively) and by Gerischer and Perez-Fernandez [7] (−0.52 and 0.2 v). The displacement of the planar zone potential on going from alkaline solution to acid solution indicates that the equilibrium Helmholtz potential difference is considerable and depends on the pH of the solution. At the planar zone potential the spatial charge in the semiconductor is equal to zero, but the surface of the electrode appears to be negatively charged as a result of oxidation, the mag-

* On the basis of the calculations of Garrett and Brattain [4], it may be concluded that at a high surface state density the potential of zero photoeffect depends little on E_F.

nitude of the charge depending on the pH of the solution. The production of this charge brings about electrostatic adsorption of cations from the solution. Thus the structure of the double layer on the germanium-solution surface at the planar zone potential resembles the surface of mercury at the zero point with specific adsorption of iodide ions (the absence of charge in the metal does not exclude the formation of ionic double layers).*

LITERATURE CITED

1. J. F. Dewald, Semiconductors, Ed. N. B. Hannay, New York (1959), p. 727.
2. M. Green, Modern Aspects of Electrochemistry, Ed. J. O'M. Bockris, 2 (1959), p. 343.
3. A. Many, E. Harnik, and Y. Margoninski, Semiconductor Surface Physics, Ed. R. H. Kingston, New York (1957), p. 85.
4. C. G. B. Garrett and W. H. Brattain, Phys. Rev. 99, 376 (1955).
5. J. F. Dewald, The Surface Chemistry of Metals and Semiconductors, Ed. H. C. Gatos (1960), p. 205.
6. K. Bohnenkamp and H. J. Engell, Zs. Elektrochem. 61, 1184 (1957).
7. H. Gerischer, Advances in Electrochemistry, New York (1961).
8. E. A. Efimov and I. G. Erusalimchik, ZhFKh, 33, 441 (1959).

All abbreviations of periodicals in the above bibliography are letter-by-letter transliterations of the abbreviations as given in the original Russian journal. *Some or all of this periodical literature may well be available in English translation.* A complete list of the cover-to-cover English translations appears at the back of this issue.

---

* In [8] a minimum differential capacity was observed for a germanium electrode at −0.6 v (in 0.1 N HCl solution), and the authors related this to the zero point of germanium. Before the measurements, however, the electrodes were subjected to prolonged cathodic polarization, which apparently leads to degeneration of the free carriers on the surface. The problem of the zero charge potential of the ionic face of the double layer on germanium and of the zero point of a degenerate semiconductor is being made the object of further study.

THE ELECTROLYTIC REDUCTION OF ANIONS AT POLAROGRAPHIC MAXIMA OF THE 2ND TYPE

S. Sat'yanarayan and N. V. Nikolaeva-Fedorovich

M. V. Lomonosov Moscow State University
(Presented by Academician A. N. Frumkin, July 1, 1961)
Translated from Doklady Akademii Nauk SSSR, Vol. 141, No. 5,
pp. 1139-1142, December, 1961
Original article submitted June 21, 1961

In the study of the electrolytic reduction of anions at a dropping mercury electrode, a sudden retardation of the reaction is observed on going to potentials corresponding to negative charges on the surface; this retardation is related to the repulsion of the negatively charged particles from the negatively charged surface of the electrode. At more negative potentials the rate of the reaction again increases [1]. It appeared to us of interest to study the reduction of the $S_2O_8^{2-}$ ion under conditions involving a sudden increase in the reaction current as a result of the tangential movements of the mercury electrode surface at high rates of flow of the mercury, i.e., for a maximum of the 2nd type. It might be assumed that under the conditions of a maximum of the 2nd type, when the solution is vigorously agitated, the reduction current for $S_2O_8^{2-}$ would be determined by the kinetics of the electrochemical process and that the diffusion limitationswhich arise in the conditions under which the $I - \varphi$ curves are usually recorded would be eliminated.

The work was carried out with a capillary with constants: m = 6.18 mg/sec and τ = 1.35 sec in 0.1 M KCl solution with open circuit. All the potentials in this paper are given relative to the normal calomel electrode.

Figure 1 gives the $I - \varphi$ curve for the reduction of $4.4 \cdot 10^{-4}$ M $K_2S_2O_8$ in the presence of 0.001 M KCl. With positive charges on the surface, a clearly-defined current maximum is observed. Since the rate of flow of mercury was high, and the electrical conductivity of the solution low, the observed maximum is the result of the interaction of movements of the first and second type, i.e., it must be regarded as an inverted maximum of the 1st type [2].

On going from positive values of the charge on the electrode surface to negative values, there is a sharp drop in the current, which decreases by a factor of approximately 100 and starts to increase again only at negative potentials. In this case the retardation of the reaction was more sharp than in other works, since the rate of reaction before the drop in the current was much higher as a result of the additional agitation by the tangential movements of the surface of the mercury drop. When $6 \cdot 10^{-4}$ M tetraamylammonium (TAA) bromide was added to the solution under study, we obtain a normal polarization curve with a clearly-defined limiting-current plateau (Fig. 1, 2). This change in the shape of the $I - \varphi$ curve is related to the fact that the adsorption of TAA leads to a retardation of the movements of the surface of the mercury drop and the current maximum falls to the values of the normal limiting current [3]; simultaneously the TAA cation increases the rate of reduction of the anion, so that the minimum on the $I - \varphi$ curve disappears when TAA is added [4].

Analogous effects were obtained in the case of solutions in which the supporting electrolyte was 0.01 M KCl. The current drop in this case was slightly smaller, however, since the retardation of the reduction of the $S_2O_8^{2-}$ is partly eliminated by the K^+ cations (Fig. 2, 3). In the region of the maximum, the magnitude of the current for the reaction is several times greater than the value of the limiting current, and it might be assumed that the current at the maximum is determined by the kinetics of the electrochemical process and is not complicated by concentration-polarization phenomena. In order to verify this assumption, we recorded curves for the reduction of $S_2O_8^{2-}$ at different rates of flow of mercury (Fig. 2). If the current for $\varphi = -1.0$ is corrected for concentration polarization, the current at the minimum will be practically independent of the height of the mercury column H,* i.e., it will

* Figure 2 shows the dependence of the $I - \varphi$ curves not on H but on the time for the formation of one drop $\tau = \frac{K}{H}$.

be determined by the rate of the electrochemical reaction. In the region of the limiting current, I is proportional to $\sqrt{H}$, and consequently is determined by the rate of the diffusion process. Figure 2 shows that the current at the maximum depends on H and that the diffusion limitations cannot be eliminated completely, even with the vigorous agitation of the solution at high rates of flow of mercury.

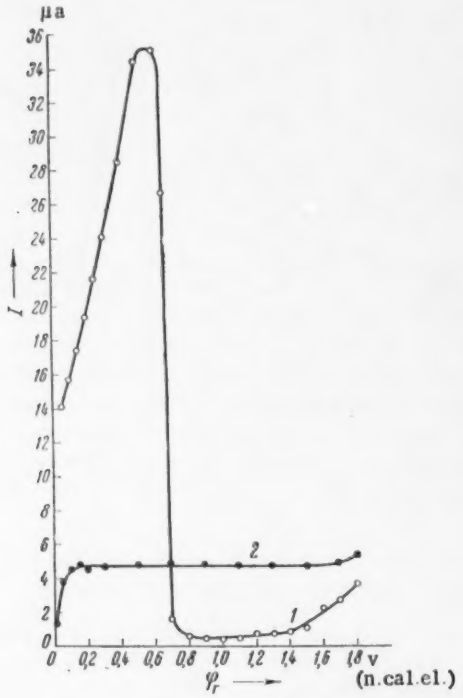

Fig. 1. Polarization curves for the reduction of $4.4 \cdot 10^{-4}$ M $K_2S_2O_8$ + 0.001 M KCl: 1) Without additive; 2) with the addition of $6 \cdot 10^{-4}$ M $[(C_5H_{11})_4N]Br$.

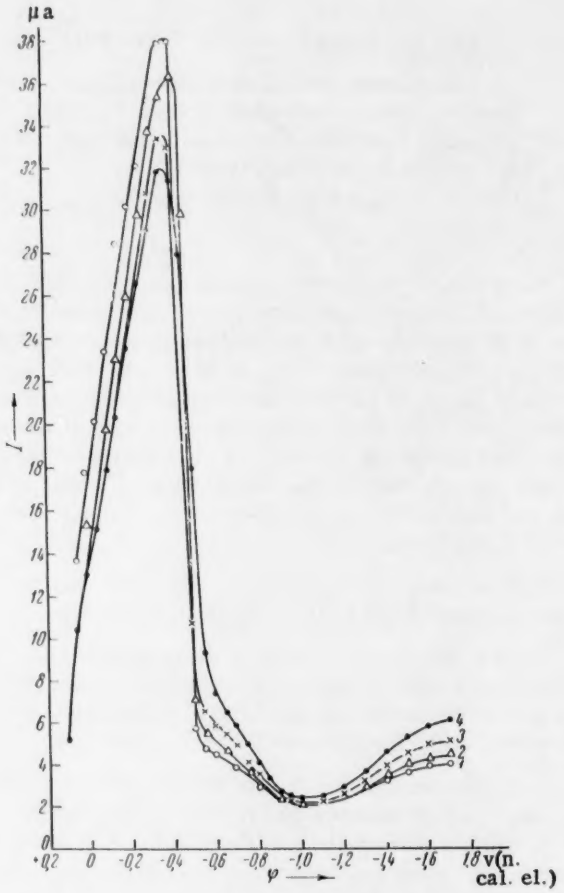

Fig. 2. Polarization curves for the reduction of $4.4 \cdot 10^{-4}$ M $K_2S_2O_8$ + 0.01 M KCl at different values of τ: 1) 2.75 sec; 2) 2.2 sec; 3) 1.7 sec; 4) 1.2 sec.

In fact, as Yu. M. Povarov has shown,* the rate of reaction is controlled by diffusion, even when a current density equal to $1.5 \cdot 10^{-3}$ amp/cm^2 is reached, on a rotating amalgamated copper electrode in a solution of the same composition as that which we studied. In our experiments the highest current at the maximum of the curve amounted to only $\sim 1 \cdot 10^{-5}$ amp/cm^2, i.e., the reaction in this case takes place according to diffusion kinetics.

It is known that increase in the concentration of the cations of the supporting electrolyte eliminates the retardation of the reduction of $S_2O_8^{2-}$ and in this case we observe no drop in the current. Figure 3, 1 gives the $I - \varphi$ curve for the reduction of $4.4 \cdot 10^{-4}$ M $K_2S_2O_8$ in the presence of 0.1 M KCl. The maximum of the 2nd type is most clearly developed in the region of the potential of zero charge. Increase in the charge on the mercury surface retards the movement, and the current drops almost to the value of the limiting diffusion current. The introduction of the TAA cation to the solution leads to a retardation of the movements of the mercury surface and the $I - \varphi$ curve does not show a maximum of the 2nd type. At the potential of desorption of the TAA cation, a slight increase in the current is observed, and this makes it possible to estimate the magnitude of the effect of agitation at this potential (Fig. 2, 2).

* Unfinished work.

In concentrated solutions of the supporting electrolyte, the charges have a much smaller retarding effect on the movement of the surface and a maximum of the 2nd type is observed throughout the whole range of potential on the $I - \varphi$ curve (Fig. 4, 1). The addition of the TAA cation leads to retardation of the movements and the current falls to the values of the limiting diffusion current, within a certain range of potentials (1.0-1.5). At $\varphi = -1.58$,

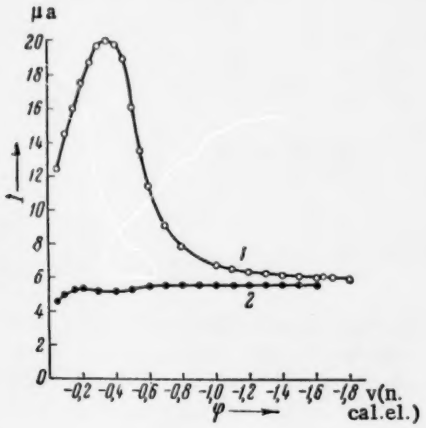

Fig. 3. Polarization curves for the reduction of $4.4 \cdot 10^{-4}$ M $K_2S_2O_8$ in the presence of: 1) 0.1 M KCl; 2) 0.1 M KCl + $6 \cdot 10^{-4}$M $[(C_5H_{11})_4N]Br$.

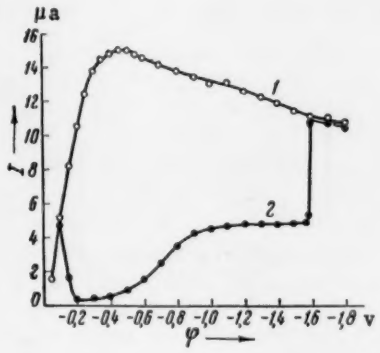

Fig. 4. Polarization curves for the reduction of $4.4 \cdot 10^{-4}$ M $K_2S_2O_8$ in the presence of: 1) 2.0 M KCl; 2) 2.0 M KCl + $6 \cdot 10^{-4}$M $[(C_5H_{11})_4N]Br$.

desorption of the TAA cation from the surface of the mercury electrode takes place, the movements of the surface develop again, and the current reaches the same values as in solutions to which no organic substance has been added [3]. At positive or small negative charges on the surface, the $I - \varphi$ curve for the reduction of $S_2O_8^{2-}$ in the presence of KCl and $6 \cdot 10^{-4}$ M TAABr shows a clearly-defined retardation of the reduction of $S_2O_8^{2-}$ (Fig. 4, 2). In this case the phenomenon of retardation is related to the attraction of the anions of the supporting electrolyte into the electrical double layer by the surface-active organic cations, as has been shown earlier [5].

Thus the effects observed earlier during the reduction of highly-charged anions can be observed even more distinctly when the surface of the mercury electrode undergoes intensive tangential movements.

LITERATURE CITED

1. T. A. Kryukova, DAN, 65, 517 (1949); A. N. Frumkin and G. M. Florianovich, DAN, 80, 907 (1951); ZhFKh, 29, 1827 (1955); A. N. Frumkin and N. V. Nikolaeva-Fedorovich, Vestn. Moskovsk. Univ. 4, 169 (1957); A. N. Frumkin, O. A. Petriii, and N. V. Nikolaeva-Fedorovich, DAN, 128, 1006 (1959); O. A. Petrii and N. V. Nikolaeva-Fedorovich, ZhFKh, 35, 8 (1961).
2. T. A. Kryukova, ZhFKh, 21, 365 (1947).
3. T. A. Kryukova, ZhFKh, 20, 1179 (1946).
4. N. V. Nikolaeva and B. B. Damaskin, Proceedings of the Conference on the Influence of Surface-Active Agents on the Electrodeposition of Metals [in Russian] (Vil'nyus, 1957), p. 33; N. V. Nikolaeva-Fedorovich, B. B. Damaskin, and O. A. Petrii, Coll. Czechoslov. Chem. Commun. 25, 2982 (1960).
5. A. Frumkin, Trans. Farad. Soc. 55, 156 (1959); N. V. Nikolaeva-Fedorovich and L. A. Fokina, DAN, 118, 987 (1958).

EFFECT OF VARIOUS KINDS OF RADIATION ON CATALYTIC DEHYDRATION OF n-DECYL ALCOHOL

Academician V. I. Spitsyn, Ion Maksim, G. N. Pirogova,

I. E. Mikhailenko, and P. N. Kodochigov

Institute of Physical Chemistry, Academy of Sciences, USSR
Institute of Atomic Physics, Academy of Sciences, Rumanian People's Republic
Translated from Doklady Akademii Nauk SSSR, Vol. 141, No. 5,
pp. 1143-1146, December, 1961
Original article submitted July 24, 1961

A great number of papers devoted to the effect of radiation on heterogeneous catalyst has been published. The effect of γ-rays, neutrons, beams of positive ions and other kinds of radiation has been investigated. In some cases the activity of the catalyst after irradiation was enhanced [1-5], in others it was lowered [6, 7] and sometimes it remained unchanged [8]. In studies of the last years the important role of radioactive atoms introduced directly into the catalysts has been established [9-11]. But in the literature there are almost no studies in which the effect of different kinds of radiation on a same catalytic reaction was compared. The aim of the present investigation was to study this problem by taking the dehydration of n-decyl alcohol over Al_2O_3 as an example. The alumina used had the following composition: 99.87% Al_2O_3; 0.11% Fe_2O_3; traces SiO_2.

The investigation was carried out along three routes:

1) The catalyst was exposed in an uranium pile to neutrons and γ-rays during various times an thereafter tested in the catalytic reaction. In this case by the action of slow neutrons with a flux density of $\sim 0.8 \cdot 10^{13}$ $cm^{-2} \cdot sec^{-1}$ some contaminations present in the aluminum oxide are activated and the radioactive isotopes: Na^{24}, Fe^{59} and Cu^{64} are formed (Fig. 1). Under these conditions aluminum and oxygen do not form long-living radioactive isotopes and neither does silicon present as a small contamination. The distribution of the induced activity was the following: 98% Na^{24}, 2% Fe^{59}, traces Cu^{64}. The catalytic activity was studied during three days after the catalyst had been withdrawn from the pile.

2) The radioactive isotope in the form of $\overset{\times}{C}eCl_3$ was introduced into the alumina and prallelly the reaction was tested on the nonradioactive catalyst to which stable $CeCl_3$ had been added. However, we did not succeed in preparing catalysts of one and the same chemical composition. The radioactive $CeCl_3$ contained the chlorides of Ca, Ba, Cr, Mn, Mg and Fe, and upon impregnating the alumina by the $\overset{\times}{C}eCl_3$ solution the amount of these contaminations attained 0.005% per gram Al_2O_3. The nonradiactive sample was prepared from $CeCl_3$ (pure) and contained 0.005 weight % of it.

3) During the reaction the catalyst and the alcohol vapor were irradiated by fast electrons. Their source was 1 Mev accelerating electronic tube. At the catalyst surface the energy of the electrons amounted to 760 kev. The dose, which was determined by means of ferrosulfate, was of the order of 10^{20} ev/g per 10 min.

The characteristics of the catalysts irradiated in the pile are given in table. The absolute radioactivity was measured in a gas-flow 4π-counter. The degree of n-decyl alcohol conversion was found from the bromine number. The reaction was tested in an apparatus of the horizontal type, the space velocity of n-decyl alcohol was 0.32 min^{-1}, the weight of catalyst amounted to 0.3 g. The experimental results are shown in Fig. 2, A.

The alumina irradiated by neutrons during one day showed a sharply lowered catalytic activity (decreased by a factor 1.5-2 in the temperature range 275-350°). Its induced radioactivity was small (0.09 m Cu/g). As far as is known from previous investigations [9], at such a low specific radioactivity of the catalysts no changes in their catalytic activity resulting from the induced radioactive radiation are observed. Evidently, the impingement of slow neutrons lowers the number of active centers on the catalyst surface in the same way as was found for the sorp-

Sample No.	Duration of irradiation in the pile	Absolute activity, mCu/g.	Yield of unsaturated hydrocarbons, %	Change in degree of conversion when compared with nonirradiated Al_2O_3
1	–	–	45	–
2	1	0.09	28	– 38
2'	1 (49 days after the irradiation)	0.0002	37	– 18
3	5	0.13	42	– 7
4	10	0.14	51	+ 13

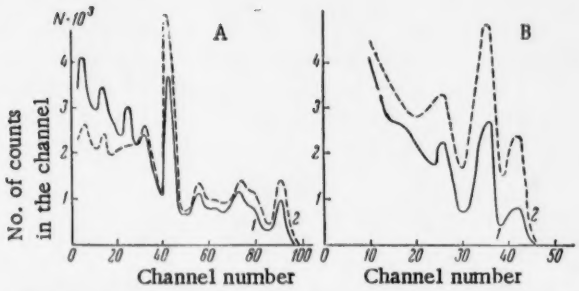

Fig. 1. Gamma spectrum of the catalyst three days (A) and 30 days (B) after the irradiation. 1) The Al_2O_3 catalyst; 2) Na^{24} (A) and Fe^{59} (B).

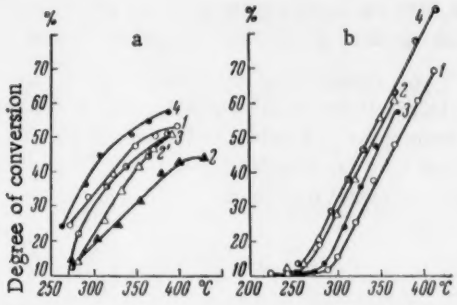

Fig. 2. Dehydration of n-decyl alcohol on Al_2O_3 in a horizontal (A) and in an upright (B) reactor. 1) Al_2O_3; 2) Al_2O_3 irradiated one day in the pile; 2') Al_2O_3 irradiated one day in the pile and then tested during 49 days; 3) Al_2O_3 irradiated five days in the pile; 4) Al_2O_3 irradiated ten days in the pile. B, 2) Al_2O_3 + $CeCl_3$ (0.005%), B,3) Al_2O_3 + Ce^{144}, specific activity 11.2 m Cu/g,B,4) Al_2O_3 at irradiation by electrons from the outside. Dose 10^{20} ev/g per 10 min.

tion capacity of barium sulfate, after it had been irradiated by electrons or positively charged ions [12]. Exposition to neutrons during five days too results in a lowered catalytic activity of the aluminum oxide, although the decrease here is not so great. Finally, an irradiation in the pile during ten days somewhat improves the catalytic properties of Al_2O_3 when compared with those of the nonirradiated sample. We assume that under these conditions the said changes in their properties cannot be caused by the induced radioactivity of the catalyst samples, being of the magnitude (0.13 and 0.14 m Cu/g) which we found. As will be noted below, by the introduction of a foreign radioisotope, even at a specific radioactivity higher by two orders of magnitude, the catalytic activity of aluminum oxide is only insignificantly raised.

It should be kept in mind that at a protracted irradiation by slow neutrons both constitutive elements of alumina are converted into short-living radioactive isotopes: Al^{28} ($T_{1/2}$ = 2.3 min) and O^{19} ($T_{1/2}$ = 29.5 sec) with a very high radiation energy. The crystal lattice defects originated by their decay will raise the catalytic activity of the original sample. A similar phenomenon (accumulated radiation effect) was observed in solid potassium sulfate as a result of protracted S^{35} decay in a study of sulfur isotope exchange in the system $K_2SO_{4s} - \overset{\times}{S}O_{3g}$ at high temperature [13]. So, two factors may have an opposite effect on the catalytic activity of a solid: The formation of crystal lattice defects and the appearance of electric charges by radioactive decay, on the one hand; the decreased number of active centers on the surface caused by the peculiar "polishing" action of irradiation [12], on the other hand. A protracted test (49 days) with an Al_2O_3 sample irradiated one day in the pile gave interesting results. At the comparatively low temperature (280°) of the test the catalytic activity of this sample did not change with time. It rises rapidly, when the temperature is raised, and at 390° it approaches the catalytic activity of the nonirradiated alumina. It may be taken that in this case the irradiation by neutrons was of too short duration and did not result in the formation of a

noticeable number of crystal lattice defects. The heating makes the catalyst surface becomes nearly normal, as was also found in an investigation of the sorption capacity of barium sulfate irradiated by electrons or protons [12].

In an upright reactor we studied dehydration of decyl alcohol on alumina to which Ce^{144} had been added or which during the reaction was irradiated from the outside by electrons. The space velocity of alcohol was 0.68 cm^{-1}. The weight of catalyst amounted to 0.15 g. Irradiation by electrons increases the conversion rate of decyl alcohol, especially at the temperatures 250-300° (Fig. 2B). So, at 280° the yield of unsaturated hydrocarbons is raised by ten times. At higher temperatures the radiation effects provoked by the fast electrons begin to be annealed and the yield of unsaturated hydrocarbons is raised to a less extent, at 390° by no more than 30%. Evidently, the bombardment by electrons, on the one hand, disturbs the crystal lattice of alumina, on the other hand, excites protons on the catalyst surface and alcohol molecules too and this favors the dehydration reaction.

The degree of n-decyl alcohol conversion on alumina impregnated by a solution of $Ce^{144}Cl_3$, in spite of the rather high specific radioactivity, is not noticeably higher than that of pure Al_2O_3. The addition of nonradioactive $CeCl_3$ to the catalyst gives a greater effect. Possibly, contaminations present in the solution of radioactive $CeCl_3$ have a poisoning effect on the catalyst studied.

So, simultaneous irradiation of the catalyst and n-decyl alcohol vapor by fast electrons gave the greatest effect in the reaction studied. Some increase in the catalytic activity of Al_2O_3 was found upon introducing a radioactive β-emitter into the oxide. Irradiation of alumina by neutrons and γ-rays gave the smallest effect or even negative results. A more detailed investigation into the mechanism of radiative catalysis by using n-decyl alcohol dehydration as a model is going on.

LITERATURE CITED

1. E. H. Taylor and H. W. Kohn, J. Am. Chem. Soc. 79, 252 (1957).
2. R. W. Clarke and E. J. Gibson, Nature, 180, 140 (1957).
3. H. W. Kohn and E. H. Taylor, J. Phys. Chem. 63, 500 (1959); 63, 966 (1959).
4. E. H. Gibson, R. W. Clarke, T. A. Dorling, and D. Pope, Proc. Sec. Intern. Confer. Peaceful Uses of Atomic Energy, U. N. 29, 312, Paper N P/63 (1958).
5. J. Turkevich, Proc. Sec. Intern. Confer. Peaceful Uses of Atomic Energy, U. N. 29, 375, Paper N P/934 (1958).
6. E. H. Taylor and J. A.Wethington, J. Am. Chem. Soc. 76, 971 (1954).
7. P. J. Lucchesi, D. L. Baeder, J. P. Londwell, and M. C. Schroeder, J. Chem. Phys. 31, 558 (1959).
8. E. H. Taylor, H. W. Kohn, and G. E. Moore, Large Radiat. Sources. Ind. 2, 119 (1960).
9. A. A. Balandin, V. I. Spitsyn, N. P. Dobrosel'skaya, and I. E. Mikhailenko, DAN, 121, 495 (1958); 137, 648 (1961).
10. A. A. Balandin, V. I. Spitsyn, N. P. Dobrosel'skaya, I. E. Mikhailenko, I. V. Vereshchinskii, and P. Ya. Glazunov, Izv. AN SSSR, OKhN, 565 (1961).
11. V. I. Spitsyn, I. E. Mikhailenko, and G. N. Pirogova, DAN, 140 (1961).
12. V. I. Spitsyn and V. V. Gromov, Abstracts of Proceedings of the Second All-Union Conference on Radiation Chemistry, October 10-14, 1960 [in Russian] (Acad. Sci. USSR Press, 1960), p. 90.
13. I. E. Mikhailenko and V. I. Spitsyn, DAN, 131, 129 (1960).

All abbreviations of periodicals in the above bibliography are letter-by-letter transliterations of the abbreviations as given in the original Russian journal. *Some or all of this periodical literature may well be available in English translation.* A complete list of the cover-to-cover English translations appears at the back of this issue.

AFTER-EFFECTS IN THE ACTION OF ELECTRON PULSES ON SULFURIC ACID SOLUTIONS OF FERROUS SULFATE SATURATED WITH AIR AND CONTAINING ETHYL ALCOHOL

L. E. Stolyarchik and A. K. Pikaev

Institute of Physical Chemistry, Academy of Sciences, USSR
Institute of Nuclear Research, Polish Academy of Sciences
(Presented by Academician V. I. Spitsyn, July 17, 1961)
Translated from Doklady Akademii Nauk SSSR, Vol. 141, No. 5, pp. 1147-1150, December, 1961
Original article submitted July 10, 1961

It is known that organic contaminations raise $G(Fe^{3+})$ in a dosimetric solution of ferrous sulfate [1-8]. Dewhurst [2, 3] has proved that addition of sodium chloride suppresses the effect of organic substances on the magnitude of the final yield $G(Fe^{3+})$ and has given some suggestions for the reason why the Fe^{3+} yield is greater, when alcohols are present. Until now it has not been studied in detail how the radiolytic oxidation of Fe^{2+} proceeds in the course of time, when the solution contains organic compounds. Only Vermeil [5] in the action of x-ray observed a small after-effect in the oxidation of Fe^{2+} in a solution saturated with air and containing hydrocarbons. Evidently, the kinetics of such an ensuing reaction may be studied more precisely, only if electron pulses are used. In this case the transfer of relatively high doses to the system in very short times is made possible.

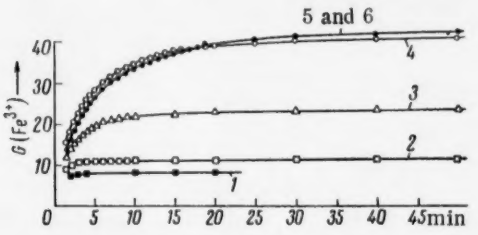

Fig. 1. $G(Fe^{3+})$ as a function of the time passed after transmitting a pulse to an air-saturated solution in 0.4 M sulfuric acid: 1) $2.5 \cdot 10^{-4}$ Fe^{2+}; 2) $2.5 \cdot 10^{-4}$ M Fe^{2+}, 10^{-4} M C_2H_5OH; 3) $2.5 \cdot 10^{-4}$ M Fe^{2+}, $4 \cdot 10^{-4}$ M C_2H_5OH; 4) $2.5 \cdot 10^{-4}$ M Fe^{2+}, 10^{-3} M C_2H_5OH; 5) $2.5 \cdot 10^{-4}$ M Fe^{2+}, 10^{-2} M C_2H_5OH; 6) $2.5 \cdot 10^{-4}$ M Fe^{2+}, 10^{-1} M C_2H_5OH.

In the present study a directly accelerating electron tube with special equipment enabling to generate single intensive electron pulses of $5 \cdot 10^{-6}$ sec duration was used as a source of ionizing radiation to investigate after-effects in irradiated 0.4 M sulfuric acid solutions of ferrous sulfate saturated with air and containing ethyl alcohol. The procedure of obtaining and measuring these pulses has been described in a previous communication [9] by one of the authors of the present paper. The energy of the electrons was equal to 0.8 Mev; the absorbed dose per pulse amounted to $1\text{-}2 \cdot 10^{-3}$ ev (in the entire volume of the solution) and this corresponded to a dose intensity of about $2.5 - 5 \cdot 10^{22}$ ev/ml sec.

The solutions were prepared from doubly distilled water; all reagents used were of a sufficient degree of purity. The irradiated samples containing Fe^{2+} were transferred to a cell (8 ml volume)provided with a glass diaphragm. By means of a special transition this cell was connected to the cell of the spectrophotometer and this enabled us to measure more rapidly and accurately. The determination of the Fe^{3+} concentration was done by the usual spectrophotometric method.

The results obtained are given in Figs. 1-4. In Fig. 1 $G(Fe^{3+})$ is plotted versus the time passed after transmitting a single electron pulse to the solution at a constant Fe^{2+} concentration ($2.5 \cdot 10^{-4}$ M) and various concentrations of ethyl alcohol. Fig. 2 gives an similar plot at various Fe^{2+} contents and a constant concentration of ethyl alcohol (10^{-2} M). The curve in Fig. 3 shows how the final yield of Fe^{3+} depends on the initial Fe^{2+} concentration in the solution and Fig. 4 gives the final yield of Fe^{3+} as a function of the initial concentration of ethyl alcohol in the solution.

The results obtained by studying solutions which during the irradiation did not contain Fe^{2+} ions are assembled in table. In this case the solutions were irradiated in a cell (6.5 ml volume) provided with a glass diaphragm. After

Dependence of $G(Fe^{3+})$ on Time for Solutions Obtained by Mixing an Irradiated Solution without Fe^{2+} with Solution of Ferrous Sulfate

Time min	a	b	c	d	e	Time min	a	b	c	d	e
1,0	2,4	—	5,6	5,1	4,9	10,0	—	12,9	—	—	14,6
1,5	2,7	5,2	7,1	6,3	6,8	11,0	—	13,3	—	—	—
2,0	2,9	6,4	8,2	7,2	8,1	12,0	—	13,6	—	—	—
2,5	3,0	7,1	9,3	8,0	8,9	13,0	—	13,9	16,9	—	—
3	3,0	7,7	10,3	8,9	9,7	14,0	—	—	—	14,0	—
3,5	3,1	8,4	11,0	9,8	10,5	15,0	—	—	—	—	15,6
4,0	—	9,0	11,6	10,5	11,3	18,0	—	14,8	17,1	—	—
4,5	3,1	9,6	—	—	12,0	19,0	—	—	—	14,5	—
5,0	—	10,0	12,8	11,4	12,4	20,0	—	—	—	—	15,9
5,5	3,1	10,5	—	—	—	23,0	—	15,3	—	—	—
6,0	—	10,9	13,8	11,9	13,2	28,0	—	—	17,1	—	—
7,0	—	11,5	14,8	12,4	13,7	30,0	—	15,7	—	14,7	16,1
8,0	—	12,1	15,5	13,0	14,0	40,0	—	15,8	—	14,9	16,3
9,0	—	12,6	—	13,3	14,3	∞	3,1	15,9	17,1	15,1	16,4

Note.	a	b	c	d	e
Composition of the irradiated solution	H_2O	H_2O	0.4 M H_2SO_4	0.4 M H_2SO_4	0.15 M C_2H_5OH
Composition of solution after mixing	$2.5 \cdot 10^{-4}$ M Fe^{2+} + + 0.4 M H_2SO_4	$2.5 \cdot 10^{-4}$ M Fe^{2+} + + 0.1 M C_2H_5OH	$2.5 \cdot 10^{-4}$ M Fe^{2+} + + 0.1 M C_2H_5OH	$2.5 \cdot 10^{-4}$ M Fe^{2+} + + 0.1 M C_2H_5OH	$2.5 \cdot 10^{-4}$ M Fe^{2+} + + 0.1 M C_2H_5OH
Time passed between transmitting the pulse and mixing the solution, min	2	2	2	1	20

that, 3.5 ml of a solution containing Fe^{2+} and other substances in the amount required for the comparison were added to the irradiated solution. After mixing we transferred a sample of the solution obtained to the cell of the spectrophotometer. The concentration of the final solution is given without correcting for the concentration changes caused by the precision in the determination of the absorbed dose (± 10%). The relative error for various points on one and the same curve is connected with the accuracy of rapid measurements in the photometer. In the first five minutes this relative error does not exceed ± 2% and later ± 1%.

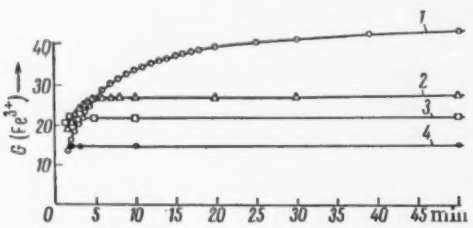

Fig. 2. $G(Fe^{3+})$ as a function of the time passed after transmitting the pulse for 0.4 M sulfuric acid solutions saturated with air: 1) $2.5 \cdot 10^{-4}$ M Fe^{2+}, 10^{-2} M C_2H_5OH; 2) $5 \cdot 10^{-4}$ M Fe^{2+}, 10^{-2} M C_2H_5OH; 3) 10^{-3} M Fe^{2+}, 10^{-2} M C_2H_5OH; 4) $2.5 \cdot 10^{-3}$ M Fe^{2+}, 10^{-2} M C_2H_5OH.

From Figs. 1 and 2 it is evident that in irradiated sulfuric acid solutions of ferrous sulfate saturated with air and containing ethyl alcohol a considerable Fe^{2+} oxidation is found to proceed long after the irradiation. Oxygen plays an important role in this reaction. Upon irradiating a solution of the following composition: $2.5 \cdot 10^{-4}$ M Fe^{2+}, 0.4 M H_2SO_4 and 10^{-1} M C_2H_5OH from which air had been removed by bubbling argon through the solution we got a value of $G(Fe^{3+})$ equal to about 5 ions/100 ev. No aftereffect whatever was detected.

By our study it has been established after irradiation is over, the oxidation of bivalent iron goes on during a time varying from a few minutes to one hour, dependent on the concentrations of Fe^{2+} and C_2H_5OH. The rise of

* The argon was purified by passing it over a sodium-potassium alloy.

$G(Fe^{3+})$ resulting from the after-effect is the greater the lower the concentration of Fe^{2+} ions. For small ethyl alcohol concentrations (up to 10^{-3} M) this rise is nearly proportional to the C_2H_5OH concentration. At high C_2H_5OH concentrations (above 10^{-2} M) further raising the said concentration does not result in an increased $G(Fe^{3+})$. In so-

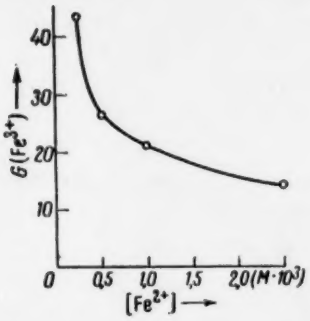

Fig. 3. The final Fe^{3+} yield (at $t = \infty$) as a function of the initial Fe^{2+} concentration in 0.4 M sulfuric acid solutions saturated with air and containing 10^{-2} M C_2H_5OH.

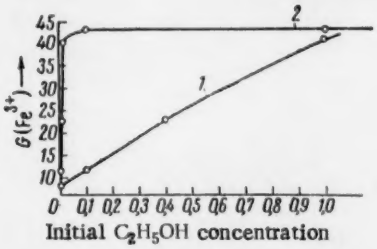

Fig. 4. The final Fe^{3+} yield (at $t = \infty$) as a function of the initial ethyl alcohol concentration in 0.4 M sulfuric acid solutions saturated with air and containing $2.5 \cdot 10^{-4}$ M Fe^{2+}. 1) Initial C_2H_5OH concentration in $M \cdot 10^3$; 2) initial C_2H_5OH concentration in $M \cdot 10^1$.

lutions containing more than 10^{-3} M C_2H_5OH and less than $5 \cdot 10^{-4}$ M Fe^{2+} the value of $G(Fe^{3+})$ is more than two times higher than that for solutions without alcohol. The oxidation of Fe^{2+} which takes place in the course of time, when C_2H_5OH is present, may be initiated by hydrogen peroxide.

Evidently, the radiolytic oxidation of Fe^{2+} in the presence of ethanol and oxygen and also the analogous process initiated by hydrogen peroxide are chain reactions. Obviously, this process is described by the mechanism suggested by Dewhurst [3]:

$$H_2O \text{---vvv}\rightarrow H, OH, H_2, H_2O_2; \qquad (0)$$

$$H + O_2 \xrightarrow{k_1} HO_2; \qquad (1)$$

$$Fe^{2+} + OH \xrightarrow{k_2} Fe^{3+} + OH^-; \qquad (2)$$

$$CH_3CH_2OH + OH \xrightarrow{k_3} CH_3\dot{C}HOH + H_2O; \qquad (3)$$

$$CH_3\dot{C}HOH + O_2 \xrightarrow{k_4} CH_3\underset{\displaystyle O_2^{\bullet}}{\underset{|}{C}}HOH; \qquad (4)$$

$$Fe^{2+} + \underset{\displaystyle O_2^{\bullet}}{\underset{|}{CH_3C}}HOH + H^+ \xrightarrow{k_5} Fe^{3+} + \overset{\displaystyle OOH}{\overset{|}{CH_3C}}HOH; \qquad (5)$$

$$Fe^{2+} + \underset{\displaystyle OOH}{\underset{|}{CH_3C}}HOH \xrightarrow{k_6} Fe^{3+} + \underset{\displaystyle O^{\bullet}}{\underset{|}{CH_3C}}HOH + OH^-; \qquad (6)$$

$$Fe^{2+} + \underset{\displaystyle O^{\bullet}}{\underset{|}{CH_3C}}HOH + H^+ \xrightarrow{k_7} Fe^{3+} + CH_3CHO + H_2O; \qquad (7)$$

$$CH_3CH_2OH + \underset{\displaystyle O^{\bullet}}{\underset{|}{CH_3C}}HOH \xrightarrow{k_8} CH_3CHO + CH_3CHOH + H_2O; \qquad (8)$$

$$Fe^{2+} + HO_2 + H^+ \xrightarrow{k_9} Fe^{3+} + H_2O_2; \qquad (9)$$

$$Fe^{2+} + H_2O_2 \xrightarrow{k_{10}} Fe^{3+} + OH + OH^-. \qquad (10)$$

The process initiated by hydrogen peroxide comprises the reactions (10), (2)-(8).

When the solution contains more than 10^{-3} M C_2H_5OH and less than $5 \cdot 10^{-3}$ Fe^{2+} the chain embraces the reactions (4)-(6) and (8), whereas its length is greater than one. The dependency of $G(Fe^{3+})$ on the concentrations of Fe^{2+} and C_2H_5OH is connected with the magnitude of the rate constant ratios k_2/k_3 and k_7/k_8. Obviously, because at high ethanol concentrations other reactions take place, $G(Fe^{3+})$ no longer depends on the said concentration. This may result, for instance, from the recombination of peroxide radicals [10]:

$$2CH_3\underset{\underset{O_2^{\cdot}}{|}}{C}HOH \rightarrow CH_3\underset{\underset{OOH}{|}}{C}HOH + CH_3CHO + O_2. \qquad (11)$$

The authors reckon it their pleasant duty to acknowledge Academician V. I. Spitsyn for his interest in the present investigation and also P. Ya. Glazunov and his team for assistance in the study.

LITERATURE CITED

1. G. Harker, Nature, 133, 373 (1934).
2. H. A. Dewhurst, J. Chem. Phys. 19, 1329 (1951).
3. H. A. Dewhurst, Trans. Farad. Soc. 48, 905 (1952).
4. E. J. Hart, J. Am. Chem. Soc. 74, 4174 (1952).
5. C. Vermeil, J. Chim. Phys. 52, 587 (1955).
6. C. Vermeil, Ann. Chim. 1, 641 (1956).
7. A. I. Chernova, V. D. Orekhov, and M. A. Proskurnin, Collection: Transactions of the First All-Union Conference on Radiation Chemistry [in Russian] (Acad. Sci. USSR Press, 1958), p. 55.
8. J. Teply and J. Bednar, Proc. 2nd United Nations Conf. Peaceful Uses Atomic Energy, 29, p. 71, Paper 2114, Geneva (1958).
9. P. A. Glazunov and A. K. Pikaev, DAN, 130, 5, 1051 (1960).
10. G. G. Jayson, G. Scholes, and J. Weiss, J. Chem. Soc. 1358 (1957).

THE RADIOLYSIS OF n-HEXANE AT LOW INTEGRAL DOSES ($3 \cdot 10^{18}$ - $1 \cdot 10^{20}$ ev/ml)

V. G. Berezkin, A. E. Mysak, and L. S. Polak

(Presented by Academician A. V. Topchiev, July 19, 1961)
Translated from Doklady Akademii Nauk SSSR, Vol. 141, No. 6,
pp. 1397-1399, December, 1961
Original article submitted July 19, 1961

The interest in the radiolysis of n-hexane at temperatures between 15 and 25° stems from the fact that it may elucidate certain general problems connected with the radiolysis of liquid n-alkanes. This explains why the radiolysis of n-hexane has been so thoroughly investigated [1-4]. Yet as far as we know the rates of production and the composition of radiolysis products have only been examined at doses greater than $0.5\text{-}1 \cdot 10^{21}$ ev/ml, in what is known as a non-linear region [5].

We have investigated in this work the amounts of hydrocarbons C_1-C_4 produced when n-hexane is radiolyzed at considerably smaller integral doses, $3\text{-}100 \cdot 10^{18}$ ev/ml; the dose intensity was maintained at $6.60 \cdot 10^{14}$ ev/ml · sec. A Co^{60} source served as emitter of γ-radiation. Degassed 0.2-0.3 ml samples of pure n-hexane were irradiated in small sealed glass tubes (0.4-0.5 in volume) at room temperature.

The commercial n-hexane was treated with fuming sulfuric acid, purified by passage through a column packed with ASK silica gel, and distilled at atmospheric pressure. The absence of aromatic hydrocarbons and dienes was verified by examining the ultraviolet absorption spectra of the material; the purity of n-hexane was also checked chromatographically and mass-spectroscopically.

Gaseous radiolysis products C_1-C_4 were analyzed by gas chromatography. A chromatographic column $75 \cdot 0.6$ cm was packed with a "ASK" silica gel which had previously been coated with KOH (2 wt. %). Samples of irradiated hexane were chromatographed at room temperature; the carrier gas (hydrogen) was circulated at the rate of 40 ml/min. To avoid loosing any of the gaseous radiolysis products when the sample is introduced into the column we used a specially designed gadget [6] for breaking the irradiated tubes.

Since the sensitivity of a catarometer is obviously inadequate to detect some of the products produced in the radiolysis of hexane at low integral doses, we used a highly sensitive flame-ionization detector [7] the design* of which is shown in Fig. 1. Weak ionization currents of the hydrogen flame were amplified by a "cactus" model microroentgenometer; the chromatograms were registered by means of model EPP-09 automatic recording potentiometer (with a 10 mv scale and 2.5 sec response time). By using the flame-ionization detector we could analyze impurities present in the starting mixture in amounts less than 10^{-5} wt %. The detector was sensitive to amounts of propane no less than $2 \cdot 10^{-10}$ mole (input resistance 10 g · ohm). The detector and the apparatus for introducing the samples were maintained at a constant temperature of 60°. The quantities of analyzed gaseous products were determined by absolute calibration. The calibration constant was determined with an accuracy of ± 5%.

In Table 1 we have compiled the average yields of gaseous products (in milliliters of gas per 1 ml of liquid hexane) generated at various integral radiation doses. To show how reproducible our data were we have also recorded the analytical results for individual tubes exposed to a dose of $29.4 \cdot 10^{18}$ ev/ml. The relative deviations from the average did not exceed ±10%.

Figure 2 shows a log-log plot of the total yield of certain gaseous products versus the integral radiation dose. By expressing the experimental data in logarithmic coordinates we can represent much more clearly the relationship

* The design was worked out in cooperation with S. K. Krasheninnikov, engineer SKB INKhS.

TABLE 1. The Yield of Gaseous Products from n-Hexane Radiolyzed by γ-Rays

Radiolysis products	Integral dose, ev/ml											
	$3.0 \cdot 10^{18}$		$11.5 \cdot 10^{18}$		$19.5 \cdot 10^{18}$						$100 \cdot 10^{18}$	
					analysis of individual tubes				average			
	a	b	a	b	a	b	a	b	a	b	a	b
Methane	0,66	10,8	2,21	10,6	4,47	4,06	4,53	4,80	4,65	10,8	16,7	11,6
Ethane	1,25	20,4	4,03	19,3	9,28	9,50	9,53	9,00	9,33	21,6	33,7	23,4
Ethylene	1,10	18,1	3,24	15,6	6,82	7,53	8,45	7,66	7,62	17,7	23,2	16,2
Propane	1,30	21,2	4,00	19,2	8,05	7,90	7,80	8,50	8,06	18,7	28,0	19,4
Propylene	0,35	5,7	1,71	8,2	3,50	3,06	3,70	3,40	3,41	7,9	9,9	6,9
Butane	1,05	17,2	4,30	20,6	7,62	7,45	6,75	7,45	7,32	17,0	26,9	18,7
Butene-1	0,40	6,6	1,35	6,5	2,98	2,56	2,34	2,76	2,66	6,3	5,5	3,8
	6,11	100,0	20,84	100,0	42,72	42,06	43,10	42,57	43,05	100,0	143,9	100,0

Note: a gives the yield of gas in ml · 10^3 per 1 ml of liquid C_6H_{14}; b is the same yield expressed in mole percent.

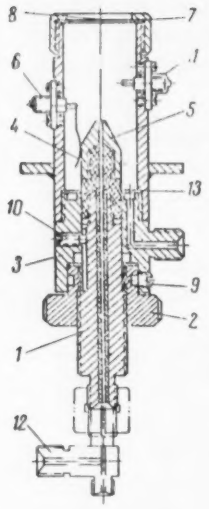

Fig. 1. Flame-ionization detector. 1) The core of the central duct; 2) a nut for regulating the distance between the nozzle and the electrode; 3) the base; 4) insulating teflon sleeve; 5) a stainless steel nozzle; 6) electric junction to the nozzle; 7) crucible; 8, 13) a wire mesh; 9, 10) set screws; 11) a junction to the recording electrode; 12) a T-joint.

between the yield and the dosage. As one can see in Fig. 2 $\log P = \log k + \log D$, i.e., $P = kD^2$, where $a_{C_1 - C_4} = 0.92$, $a_{C_2 - C_4}$ (alkanes) = 0.92; $a_{C_2 - C_4}$ (olefins) = = 0.88. Hence within the investigated range of small integral doses the yield of gaseous radiolysis products tends to deviate from a linear relationship.

We would like to point out that within the investigated range of integral doses unsaturated compounds apparently undergo hydrogenation by thermal hydrogen atoms (we have assumed that the reaction takes place in the entire vapor phase and not just along the radiation path).

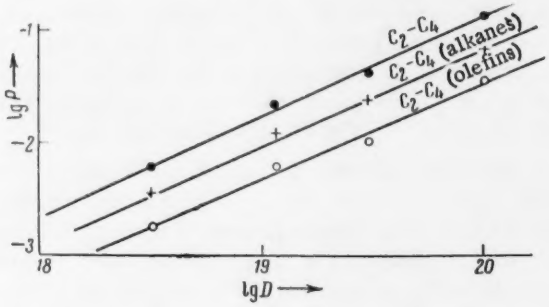

Fig. 2. The yield of gaseous products in the radiolysis of hexane as a function of the radiation dose. P is the yield of gaseous products in ml of gas per ml of liquid n-hexane; D is the radiation dose in ev/ml.

Certain workers [8] have ignored this reaction claiming that the stripping of hydrogen atoms from alkanes is the predominant reaction,

$$H^{\cdot} + C_6H_{14} \rightarrow H_2 + C_6H_{13}^{\cdot}. \qquad (1)$$

By examining the rate constants of the corresponding gas-phase reactions [9] one can see that even at low doses, when the total concentration of unsaturated products is still very low, the predominant reaction is the hydrogenation of olefins,

TABLE 2

Product	Moles/100 ev	Mole %
Methane	0.41	11.0
Ethane	0.82	22.0
Ethylene	0.62	16.6
Propane	0.68	18.2
Propylene	0.31	8.3
Butane	0.65	17.5
Butene-1	0.24	6.4
	3.73	100.0

$$H^{\cdot} + M(C=C) \rightarrow MH^{\cdot}. \qquad (2)$$

In fact

$$\frac{k_1 [C_6H_{14}] \cdot [H^{\cdot}]}{k_2 [M(C=C)]\ [H^{\cdot}]} \approx \frac{5 \cdot 10^9 \cdot 15}{3 \cdot 10^9 [M(C=C)]} \approx \frac{\sim 2{,}5 \cdot 10^{-5}}{[M(C=C)]}.$$

Thus when the concentration of olefins in solution becomes $2.5 \cdot 10^{-5}$ moles/liter the rates of the two reactions become approximately equal. Hence the sharp deviations from linearity observed in the case of gaseous olefins (propylene and butene-1) can apparently be attributed to hydrogenation reactions (Table 1). It should be pointed out that under our experimental conditions most of the ethylene is in the gas phase.

From the experimental data given in Table 1 we have calculated the radiochemical yields, G-values (moles/100 ev), for the gaseous radiolysis products; these are presented in Table 2.

The G-values obtained by us, except for methane, are essentially close to those obtained by Futrell [10] but differ from those reported by Dewhurst [3]. The low G-value previously reported for methane [10] may be the result of different catarometer sensitivity with respect to methane and other hydrocarbons; this possibility was not examined in [10]. We would like to mention that Kunz [11] reported a G = 0.4 for methane.

LITERATURE CITED

1. H. A. Dewhurst and E. H. Winslow, J. Chem. Phys. 26, 969 (1957).
2. W. H. T. Davison, Chem. and Ind. 662 (1957).
3. H. A. Dewhurst, J. Phys. Chem. 62, 15 (1958).
4. T. J. Hardwick, J. Phys. Chem. 64, 1623 (1960).
5. V. G. Berezkin, I. M. Kustanovich, et al., DAN, 131, 593 (1960).
6. V. G. Berezkin, Trans. Tashkent Conference on the Peaceful Uses of Atomic Energy [in Russian] (Tashkent, 1960), Vol. 2, p.425.
7. J. G. McWilliam and R. A. Dewar, Nature, 8, 760 (1958).
8. C. D. Wagner, J. Phys. Chem. 64, 231 (1960).
9. V. N. Kondrat'ev, The Kinetics of Gas-Phase Reactions [in Russian] (Izd. AN SSSR, 1958).
10. J. H. Futrell, J. Am. Chem. Soc. 81, 5921 (1959).
11. F. H. Kunz, Nature, 176, 1113 (1955).

THE EFFECT OF RADIATION ENERGY ON THE SUBLIMATION RATE OF SOLIDS

I. E. Zimakov and Academician Vikt. I. Spitsyn

Institute of Physical Chemistry, Academy of Sciences, USSR
Translated from Doklady Akademii Nauk SSSR, Vol. 141, No. 6,
pp. 1400-1402, December, 1961
Original article submitted July 22, 1961

In an earlier communication [1] we have shown that the sublimation rate of molybdenum trioxide depends on the level of emitted radiation. In the work reported here we have examined how the sublimation rate of MoO_3 is affected by the introduction of various radioactive isotopes emitting radiation of different energies. We used the following β-ray emitters: Y^{90} (E_m = 2.18 Mev), Mo^{99} (E_m = 1.23 Mev), and W^{185} (E_m = 0.43 Mev). Molybdenum trioxide samples containing Y^{90} were prepared as follows: powdered MoO_3 was soaked in a fixed volume of an yttrium nitrate solution, dried, heated to a constant weight, and passed through a sieve; only the fraction with particles ranging in size from 0.25 to 0.5 mm was collected. The specific radioactivities of resulting samples were expressed relative to the amount of MoO_3 since the net yttrium content was negligible. Control samples of MoO_3 containing non-radioactive yttrium were prepared under similar conditions.

Samples of MoO_3 containing W^{185} were prepared by adding a fixed amount of radioactive ammonium tungstate to an ammonium molybdate solution. After the solution was evaporated the solid residue was wetted with a few drops of HNO_3 to prevent any reduction of the hexavalent Mo and W and fired. Fractions with particles ranging from 0.25-0.5 mm in size were used.

The way in which various amounts of Mo^{99} are introduced into MoO_3 have been described before [1].

The apparatus used for the determination of the sublimation rate (Fig. 1) consisted of a vertical quartz tube (1) placed in an electric furnace (2). The upper part of the tube had a larger diameter and protruded above the furnace. A quartz jacket (3) with a ground joint at the top (4) was sealed inside the tube and a quartz coil spring (6) was suspended form a plug (5) fitting into the ground joint. A quartz crucible (7) was suspended from the spring on a quartz thread. A side-arm (8) was sealed to the upper end of tube (1) through which air or other gases could be introduced. The lower portion of the tube terminated in a vapor trap (9) cooled with liquid nitrogen. Stretching of the coil spring was observed by means of a cathetometer which was rigged up with an adjustable telescopic micrometer enabling us to follow the level of indicator (10). The described quartz ballance had a sensitivity of $7 \cdot 10^{-5}$ g per micrometer division.

The experiments were done in the following way. A weighed sample of the investigated material (~200 mg) was placed in the quartz crucible, suspended from the coil, and placed inside the tube. After the temperature was raised to 700 ± 1° a stream of dry air or nitrogen was passed through the system at the rate of 10 ml/min. Changes in the weight were recorded every hour. The data thus obtained were used for constructing a sublimation curve. In each case a number represents an average of several parallel experiments.

The experimentally determined sublimation rates of MoO_3 in the presence of Y^{90} are plotted in Fig. 2. The sublimation rates of samples containing non-radioactive yttrium or with an activity of only 1.0 or 2.0 mC/g remain practically unchanged. As the specific radioactivity is raised to 3 mC/g and higher the sublimation rate of MoO_3 changes appreciably. In each case the sublimation rate increases with time, since the removal of MoO_3 raises the specific activity of the residue.

In Fig. 3 we have plotted the sublimation rates of MoO_3 containing W^{185} One can readily see that here again the radiation affects the sublimation rate of MoO_3. The sublimation rates of samples with an activity of 5 mC/g and higher differ greatly from the rate in MoO_3 containing non-radioactive tungsten, and the difference increases with increasing activity.

When the sublimation rate of MoO^3 was investigated in the presence of Y^{90} and W^{185} no radioactive material was detected in the sublimate.

It is important to point out that the relationship between the specific radioactivity and the sublimation rate of MoO_3 detected in this work by using a quartz balance and passing a stream of gas over the crucible containing the sample (Fig. 4) does not differ from the results published before [1], which were obtained in an apparatus where the gas was passed through a MoO_3 layer.

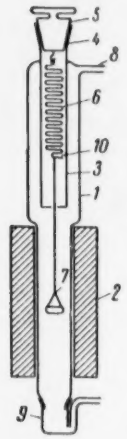

Fig. 1. The absorption used for studying the sublimation rate of MoO_3.

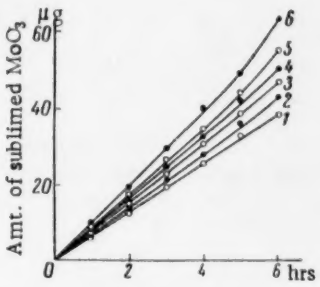

Fig. 2. The sublimation rate of MoO_3 samples labeled with the radioactive isotope Y^{90}. 1) MoO_3 containing non-radioactive Y_2O_3; 2) 4 mC/g; 3) 6 mC/g; 4) 8 mC/g; 5) 10 mC/g; 6) 20 mC/g.

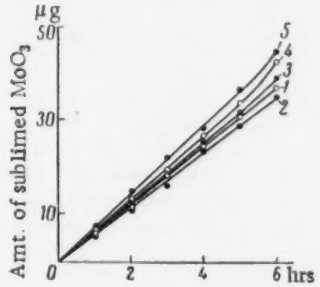

Fig.3. The sublimation rate of MoO_3 samples labeled with the radioactive isotope W^{185}. 1) MoO_3 containing non-radioactive WO_3; 2) 7 mC/g; 3) 10 mC/g; 4) 12 mC/g; 5) 15 mC/g.

In Fig. 4 we have shown how the sublimation rate of MoO_3 depends on the specific radioactivity of the samples and on the type of radioactive material introduced. One must conclude therefore that different radiation energies affect differently the sublimation rate. It is interesting to note that the initial branches of all three curves coincide. This would indicate that small amounts of radioactive isotopes introduced into MoO_3 have very little effect on the sublimation rate. In the presence of W^{185}, which has the lowest radiation energy among the isotopes used by us, a change in the sublimation rate of MoO_3 becomes noticeable when the specific radioactivity reaches 5 mC/g. After that the sublimation rate slightly declines until an activity of 7-8 mC/g is attained. Subsequent increase in the radioactivity gradually raise the sublimation rate of MoO_3. The mechanism responsible for this behavior is apparently similar to the one described before [1] for the case of MoO_3.

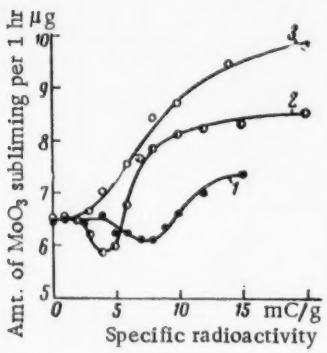

Fig. 4. The sublimation rate of MoO_3 as a function of the specific radioactivity of various β-emitters introduced into the sample: 1) MoO_3 containing W^{185}; 2) MoO_3 containing Mo^{99}; 3) MoO_3 containing Y^{90}.

The sublimation rate curve of MoO_3 containing various amounts of Mo^{99} differs considerably from the sublimation curve of samples containing W^{185}. The sublimation rate undergoes an appreciable change at lower radioactivities. The minimum is also much more pronounced. At high specific radioactivities the sublimation rates of MoO_3 are also increased by a greater amount. When Y^{90} is introduced into MoO_3, as soon as the specific radioactivity exceeds 3 mC/g the sublimation rate begins to rise without passing through a minimum as in the two cases where Mo^{99} or W^{185} was added.

The absence of minimum in this case is apparently connected with the fact that the high energy β-particles emitted by Y^{90} have a stronger effect on the surface charge and ionize more readily the evaporation MoO_3 molecules, which are repelled by the positively charged surface, than in cases where radioactive isotopes of lower energy are used.

Thus the sublimation rate of molybdenum trioxide depends on both the radioactivity of the sample and on the energy of the radiation emitted

by the radioactive isotope introduced into the sample. At any given radiation level the higher the energy the greater the change in the sublimation rate of MoO_3. It should be pointed out that the sublimation rate of MoO_3 can be altered not only by introducing a radioactive molybdenum isotope but also by introducing other radioactive elements into the solid phase.

LITERATURE CITED

1. Vikt. I. Spitsyn and I. E. Zimakov, DAN, 139, 3 (1961).*

All abbreviations of periodicals in the above bibliography are letter-by-letter transliterations of the abbreviations as given in the original Russian journal. *Some or all of this periodical literature may well be available in English translation.* A complete list of the cover-to-cover English translations appears at the back of this issue.

---

* The following corrections should be made in [1]: a) All the numbers in column 3 of Table 1 should be reduced by a factor of 10. b) all the numbers on the ordinates of Fig. 2, 3, and 4 should be reduced by a factor of 10.

THE THEORY OF ELECTRICAL DOUBLE LAYERS IN CONCENTRATED SOLUTIONS

Corresponding Member, Academy of Sciences, USSR,

V. G. Levich and V. S. Krylov

Institute of Electrochemistry, Academy of Sciences, USSR

Translated from Doklady Akademii Nauk SSSR, Vol. 141, No. 6,
pp. 1403-1405, December, 1961
Original article submitted September 12, 1961

In a number of earlier publications [1-3] dealing with the quantitative aspects of the discrete charge distribution in ionic layers adsorbed on various interfaces the bulk phase electrolyte concentrations were assumed to be either infinitely large, in which case the potential drop in the diffusion layer could be neglected, or infinitely small, so that the potential gradient in the diffusion layer could be represented by a linear Poisson-Boltzmann equation. However, since in practice one usually has to deal with intermediate concentrations (between 0.01 and 1 moles/liter) it was interesting to attempt a quantitative treatment of the diffusion layer, taking into account electrostatic correlations and short range interactions between ions at bulk phase concentrations exceeding those used in the Guy-Stern theory by several orders of magnitude. The treatment attempted in this paper was based on the statistical theory of correlation functions developed by a number of workers [4-8]. Kirkwood and co-workers [5, 6] derived the correlation functions for the ionic distribution in the bulk of the solution and in the diffusion layer by expanding these functions in power series and selecting the charge of an arbitrary ion as the expansion parameter; this last choice not only aroused certain doubts as to the validity of the method but also made it impossible to determined how widely applicable the method itself is.

We are going to show that if the diffusion layer consists of a medium with a rather large dielectric constant while the solid portion of the double layer is covered with a discrete layer of adsorbed like-charged ions Kirkwood's method will yield valid results if in the zeroth order approximation the parameter $\varepsilon_1 = cr_0^3$ (where c is the average electrolyte concentration, r_0 is the mean effective radius for short range interactions between ions of the electrolyte) and in the first order approximation $\varepsilon_2 = e^2c^{1/3}/D_3kT$ and $\varepsilon_3 = |e\bar{\psi}_3(\gamma)|/kT$ (where D_3 is the dielectric constant of the diffusion layer, $\bar{\psi}_3(\gamma)$ is the average potential in a plane where the ions of the diffusion layer approach most closely the interface). If we let θ represent the fraction of the surface covered with the adsorbed ions, then for mono – monovalent electrolytes and an uncharged interface the discussed approximation is valid when $c \lesssim 0.5$ moles/liter and $\theta \lesssim 0.1$. If the interface has a charge density q and the adsorbed ions have a charge z_0, then the condition that $|q + ez_0\theta/\sqrt{3}\gamma^2| \lesssim 5$ coulombs/cm^2, where γ is the half width of the solid portion of the double layer, must also be fulfilled.

Using this approximation to calculate the space charge density in the diffusion layer and assuming that the adsorbed ions remain attached in one position we can determine the potential distribution throughout the entire space.

Suppose the electrolyte solution lies in the region $x \geqslant -\beta$, the solid portion of the double layer has a width $\delta = \beta + \gamma$ and a dielectric constant D_2, and the centers of the adsorbed ions lie in the plane x = 0. The potential distribution in such a system would have the form

$$\psi_1(\mathbf{r})_{(x \leqslant -\beta)} = \begin{cases} \sum_{mn} \int_0^\infty A_1(\lambda)\, e^{\lambda x} J_0(\lambda R_{mn})\, \lambda\, d\lambda & \text{(dielectric-solution)}, \\ \psi_0 = \text{const} & \text{(metal-solution)}; \end{cases}$$

$$\psi_2(\mathbf{r}) = \begin{cases} \sum_{mn}\int_0^\infty \left\{A_2^{(1)}(\lambda)e^{\lambda x} + B_2^{(1)}(\lambda)\,e^{-\lambda x} + \right. \\ \left. + \frac{ez_0}{D_2\lambda}\,e^{-\lambda|x|}\right\} J_0(\lambda R_{mn})\,\lambda d\lambda & \text{(dielectric-solution)} \\ \sum_{mn}\int_0^\infty \left\{A_2^{(2)}(\lambda)e^{\lambda x} + B_2^{(2)}(\lambda)e^{-\lambda x} + \right. \\ \left. + \frac{ez_0}{D_2\lambda}\,e^{-\lambda|x|}\right\} J_0(\lambda R_{mn})\lambda d\lambda + \\ + M(x+\beta) + \psi_0 & \text{(metal solution);} \end{cases}$$

$$\psi_3(\mathbf{r}) = \begin{cases} \sum_{mn}\int_0^\infty A_3^{(1)}(\lambda)\{a(\lambda)\,e^{-\xi_1(\lambda)x} - \\ - b(\lambda)\,e^{-\xi_2(\lambda)x}\}\,J_0(\lambda R_{mn})\,\lambda d\lambda & \text{(dielectric-solution)} \\ \sum_{mn}\int_0^\infty A_3^{(2)}(\lambda)\{a(\lambda)\,e^{-\xi_1(\lambda)x} - \\ - b(\lambda)\,e^{-\xi_2(\lambda)x}\}\,J_0(\lambda R_{mn})\,\lambda d\lambda + \\ + C\{a(0)e^{-\xi_1(0)x} - b(0)e^{-\xi_2(0)x}\} & \text{(metal-solution)} \end{cases}$$

Here $J_0(\lambda R_{mn})$ is a first order Bessel function; $R^2_{mn} = (y - y_{mn})^2 + (z - z_{mn})^2$; the subscripts m and n fix the position of the centers of the adsorption ions in the plane x = 0; the functions $A_1(\lambda)$, $A_2(\lambda)$, $B_2(\lambda)$ and $A_3(\lambda)$ can be expressed in terms of simple but hard to evaluate parameters $a(\lambda)$, $b(\lambda)$, $\xi_1(\lambda)$ and $\xi_2(\lambda)$, where:

$$a(\lambda) = \left(\frac{\varkappa r_0}{y_1^{(0)}}\right)^2; \qquad b(\lambda) = \left(\frac{\varkappa r_0}{y_2^{(0)}}\right)^2 \exp\left\{(y_2 - y_1)\left(\frac{\gamma}{r_0} - 1\right)\right\};$$

$$r_0\xi_j(\lambda) = y_j \quad (j = 1, 2),$$

where $\varkappa$ is the inverse Debye radius; $y_j^{(0)}$ are the complex roots of the equation $y^2 - (\varkappa r_0)^2 \operatorname{ch} y = 0$ which fall in the right hand half of the plane and in which the real component is minimum for a given $\varkappa r_0$. For each $y_j^{(0)} = \alpha_j + i\beta_j$ we must set up a corresponding function $y_j = p_j + iq_j$ such that

$$p_j^2 = {}^1/_2\{\sqrt{(\alpha_j^2 - \beta_j^2 + \lambda^2 r_0^2)^2 + 4\alpha_j^2\beta_j^2} + (\alpha_j^2 - \beta_j^2 + \lambda r_0^2)\};$$

$$q_j^2 = {}^1/_2\{\sqrt{(\alpha_j^2 - \beta_j^2 + \lambda^2 r_0^2)^2 + 4\alpha_j^2\beta_j^2} - (\alpha_j^2 - \beta_j^2 + \lambda^2 r_0^2)\}.$$

The constants ψ_0, M, and C depend on $y_j^{(0)}$ and on other properties of the double layer. The functions expressing the corresponding relationships will not be given due to their complexity.

Our calculations, which are in full accord with previously published results [1-3], indicate that if one assumes an arbitrary charge distribution in the adsorbed layer the potential drop in the solid portion of the double layer would be

$$\delta\psi = \begin{cases} \frac{4\pi\sigma\gamma}{D^2} & \text{(dielectric-solution)} \\ \frac{4\pi\sigma\gamma}{D_2} + \frac{4\pi q(\beta+\gamma)}{D_2} & \text{(metal-solution)} \end{cases}$$

where σ is the average density of the adsorbed charges.

We also examined the behavior of the average potential

$$\bar{\psi}_3(x) = \lim_{S\to\infty}\frac{1}{S}\iint_{-\infty}^{\infty}\psi_3(\mathbf{r})\,dy\,dz$$

and showed that at moderate bulk electrolyte concentrations (~ 0.5 moles/liter) the potential declines much more rapidly in the direction of the solution than would be expected from the Guy-Stern theory. This is well illustrated in the figure;

$$Z^{(0)}(x^*) = \frac{\bar{\psi}_3^{(0)}(x)}{\bar{\psi}_3^{(0)}(\gamma)}, \quad Z(x^*) = \frac{\bar{\psi}_3(x)}{\bar{\psi}_3^{(0)}(\gamma)},$$

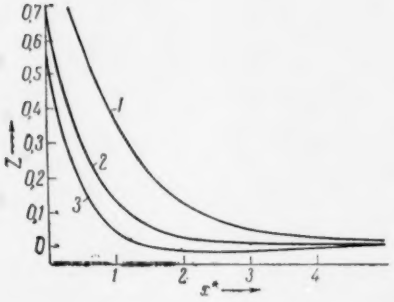

The plots of $Z^0(x^*)$ and $Z(x^*)$. 1) The Guy-Stern law ($\varkappa r_0 = 1.03$); 2) $\varkappa r_0 = 1.03$; 3) $\varkappa r_0 = 1.15$.

where $\bar{\psi}_3^{(0)}(x) = \bar{\psi}_3^{(0)}(\gamma) \exp\{-\varkappa(x-\gamma)\}$ is a potential obeying the Guy-Stern law;

$$x^* = \frac{x-\gamma}{r_0} \geqslant 0.$$

When $\varkappa r_0 = 1.03$, by the time $x^* = 3$ the function $Z(x^*)$ has declined to 0.5% of its value at $x^* = 0$ and is about one tenth as large as the corresponding value of $Z^{(0)}(x^*)$. When $\varkappa r_0 = 1.15$ the function $Z(x^*)$ oscillates weakly attaining the first zero at $x^* \sim 2$. At $x^* \sim 5$ the function returns to zero, but at the point of maximum deviation from zero in the range $2 < x^* < 5$, where $Z(x^*) < 0$, the function is only 0.7% as large as it is at $x^* = 0$; hence it can be assumed that the potential inside the diffusion layer drops off within the distance of two ionic diameters.

For the case of either infinitely large or infinitely small bulk concentrations our derivations reduce to the well known forms discussed before [1-3].

LITERATURE CITED

1. V. G. Levich, V. A. Kir'yanov, and V. S. Krylov, DAN, 135, 6 (1960).
2. V. G. Levich, V. A. Kir'yanov, and V. S. Krylov, ZhFKh, 36 (1962) (in print).
3. V. G. Levich and V. A. Kir'yanov, ZhFKh, 36 (1962) (in print).
4. N. N. Bogolyubov, The Problems of Dynamic Theory in Statistical Physics [in Russian] (1946).
5. J. G. Kirkwood and J. C. Poirier, J. Phys. Chem. 58, 591 (1964).
6. F. H. Stillinger and J. G. Kirkwood, J. Chem. Phys. 33, 1282 (1960).
7. V. A. Kir'yanov, Coll. Certain Problems in Theoretical Physics [in Russian] (1958).
8. V. G. Levich and V. A. Kir'yanov, DAN, 131, 5 (1960).

THE PROTON MAGNETIC RESONANCE OF SELENOUREA

G. M. Mikhailov, A. G. Lundin, S. P. Gabuda,

and K. S. Aleksandrov

Physics Institute, Siberian Branch of the Academy of Sciences, USSR
and The Siberian Institute of Technology
(Presented by Academician V. N. Kondrat'ev, July 24, 1961)
Translated from Doklady Akademii Nauk SSSR, Vol. 141, No. 6,
pp. 1406-1408, December, 1961
Original article submitted July 18, 1961

Selenourea belongs to a series of compounds of the type $(NH_2)_2CE$, where E = O, S and Se. A structural formula of the molecule is shown in Fig. 1. The nuclear magnetic resonance of both urea $(NH_2)_2CO$ [1, 2] and thiourea $(NH_2)_2CS$ [3, 4] have been analyzed. Intramolecular reorientation (internal rotation) was observed above 300°K in the case of urea and above 200°K in the case of thiourea.

We examined the proton magnetic resonance of polycrystalline selenourea in the range from 77°K to room temperature. We also determined the second moment of the proton resonance absorption line as a function of temperature (see Fig. 2).

From the low-temperature value of the second moment (in our case 18.2 oersted) we determined the distance between the two protons in the NH_2 group. Assuming that the N – H distance in compounds of this type is about 1 A (the assumption is borne out by a number of determinations [5, 6]), and using the Van Vleck equation [7] we find that the proton-nitrogen interaction contributes 2 oersteds to the second moment. The contribution of protons on adjacent NH_2 groups is much harder to determine since the crystal structure of selenourea is not known. It is safe to assume, however, that it is similar to that in thiourea. In that case protons of adjacent groups would contribute about 0.15 oersted to the second moment. The remaining 15.85 oersted come from the proton-proton interactions in each NH_2 group. On the basis of Van Vleck's equation this would correspond to a 1.75 A separation between the two protons in an NH_2 group, which is quite close to the corresponding distance in urea [8] and thiourea [6].

The decrease of the second moment from 18.2 to 6.9 oersted observed when the temperature is raised from 130 to 180°K may either result from the rotation of the NH_2 groups about the C – N bond or the rotation of the entire molecules about the Se – C axis. As is well known the reorientation of any atomic group decreases the second moment by a factor

$$k = {}^1/_4 (3\cos^2\theta - 1)^2, \tag{1}$$

where θ is the angle that the proton-proton vector makes with the axis of rotation. It can be readily shown that if $\theta = 30°$ the second moment is reduced from 18.2 to 6.9 oersted. Only the rotation of the molecule about the Se = C axis satisfies this requirement (see Fig. 1), since in the alternate rotation of an NH_2 group about the C – N bond the angle between the p – p vector and the rotation axis is 90°. We would also like to point out that the observed decline in the second moment could also be explained by assuming that the NH_2 groups oscillate about the C – N bond through ± 40° angle. However, we can reject this possibility as rather unlikely since Das has shown [10] that the probability of such large vibrational amplitudes is extremely small.

From the temperature dependence of the second moment one can calculate the potential barrier hindering rotation in the $(NH_2)_2CSe$ molecule. Gutowsky and Pake [11] have shown that the relationship between temperature and the second moment can be expressed by the equation

$$S_2(T) = S_2^{\text{rig}} + (S_2^{\text{rot}} - S_2^{\text{rig}}) \frac{\pi}{2} \operatorname{arc\,tg}\left(\frac{\gamma S_2^{1/2}(T)}{2\pi\nu_c}\right), \tag{2}$$

where S^{rig}_2, S^{rot}_2, and S_2 (T) are the second moments at low temperatures (rigid), high temperature (rotating), and temperature T respectively; ν_C is the reorientation correlation frequency given by [10, 11]

$$\nu_C = \nu_0 \exp\left(-\frac{V_0}{kT}\right) = \frac{1}{2\pi}\left(\frac{2V_0}{I}\right)^{1/2} \exp\left(-\frac{V_0}{kT}\right), \tag{3}$$

where ν_0 is the hindered rotation frequency of a molecule with a moment of inertia I over a barrier of height V_0; k is the Boltzmann constant; T is the absolute temperature.

The moment of inertia of a selenourea molecule rotating about the Se = C bond, calculated on the assumption that the C – N and N – H bond-lengths are close to the corresponding interatomic distances in urea and thiourea, comes out $I = 70.5 \cdot 10^{-40}$ g · cm^2.

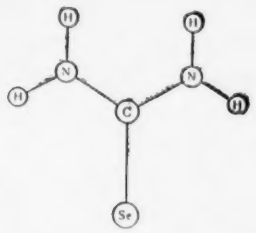

Fig. 1. A structural formula of selenourea.

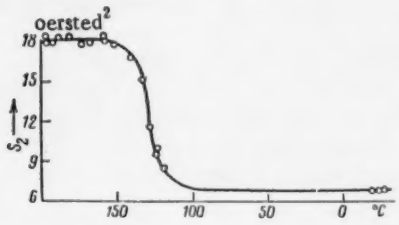

Fig. 2. The second moment of the proton magnetic resonance line of polycrystalline $(NH_2)_2CSe$ as a function of temperature.

Using Equation (2) and the experimentally determined temperature dependence of the second moment we can get the correlation frequency ν_C as a function of temperature. Equating the resulting expression with Equation (3) we evaluate the height of the potential barrier V_0 for any given moment of inertia. In Fig. 3 we have plotted the theoretical ν_C(T) functions (based on Equation (3)) for various V_0 values and the experimental functions derived from Equation (2). One can see that the experimental data agrees well with the theoretical function when $V_0 = 6.0 \pm 0.4$ kcal/mole.

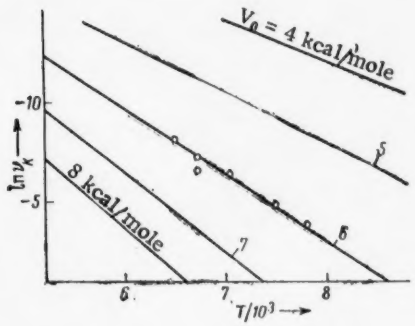

Fig. 3. The temperature dependence of the reorientation frequency of $(NH_2)_2CSe$ molecules.

One can therefore state conclusively that at temperatures above 130°K the $(NH_2)_2CSe$ molecules in crystalline selenourea undergo reorientation (rotation) about the C = Se axis. It should be pointed out though that the "rotation" is not a continuous process. As one can see from Equation (3) a selenourea molecule with an energy greater than V_0 would have a hindered rotation frequency $\nu_0 \approx 10^{12}$ cps. The reorientation apparently consists of frequent and very rapid molecular rotations through a 180° angle and less frequent rotations through angles 360° or greater. The correlation frequency ν_C actually represents a rotation averaged over all the molecules involved on the assumption that the rotation is even and proceeds with a frequency ν_C.

The experimental data yield a correlation frequency of about 10^4 cps at 150°K and 10^{10} cps at room temperature. Thus even at room temperature the lifetime of a molecule at rest exceeds by about 100 times the time a molecule spends rotating, while at 150° K the ratio between the two is 10^8.

The nature of the potential barrier hindering free rotation of selenourea is in itself of some interest. Even though in general the nature of such barriers is not too well understood in this particular case one might assume that the rotation of $(NH_2)_2CSe$ molecules is hindered by intermolecular hydrogen bonding, NH . . . Se. In favor of this assumption we can cite the fact that the calculated barriers for the rotation of thiourea and urea [2, 3] are 9 and

12.7 kcal/mole respectively. At the same time the NH . . . S hydrogen bonds in thiourea are known [8] to be weaker than the NH . . . O bonds in urea. In our opinion the observations are quite consistent, since one would expect strong NH . . . E, hydrogen bonds to be associated with high potential barriers hindering rotation in $(NH_2)_2CE$ molecules. Hence the potential barriers against rotation of selenourea determined by us, $V_0 = 6$ kcal/mole, indicates that NH...Se hydrogen bonds are weaker than the NH . . . S and NH . . . O bonds in thiourea and urea.

The author would like to thank V. F. Dvoryankin for providing the selenourea.

LITERATURE CITED

1. E. R. Andrew and D. Hyndman, Discuss. Farad. Soc. 19, 195 (1955).
2. R. Kromhout and W. Moulton, J. Chem. Phys. 23, 1673 (1955).
3. J. W. Emsley and J. A. Smith, Proc. Chem. Soc. II, 53 (1958).
4. J. W. Emsley and J. A. Smith, Arch. Sci. 12a, 122 (1959).
5. L. Pauling, The Nature of the Chemical Bond [Russian translation] IL, 1947).
6. V. F. Dvoryankin and B. K. Vainshtein, Kristallografiya, 5, 589 (1960).
7. J. H. Van Vleck, Phys. Rev. 74, 1168 (1948).
8. A. N. Lobachev and B. K. Vainshtein, Kristallografiya, 6, 395 (1961).
9. E. R. Andrew, Nuclear Magnetic Resonance [Russian translation] (IL, 1957).
10. T. P. Das, J. Chem. Phys. 27, 673 (1957).
11. H. S. Gutowsky and G. E. Pake, J. Chem. Phys. 18, 162 (1950).

All abbreviations of periodicals in the above bibliography are letter-by-letter transliterations of the abbreviations as given in the original Russian journal. *Some or all of this periodical literature may well be available in English translation.* A complete list of the cover-to-cover English translations appears at the back of this issue.

THE ABSORPTION OF WATER VAPOR ON SULFONIC AND CARBOXYLIC CATION EXCHANGE RESINS

Corresponding Member, Academy of Sciences, USSR

B. P. Nikol'skii and N. F. Bogatova

A. A. Zhdanov Leningrad State University

Translated from Doklady Akademii Nauk SSSR, Vol. 141, No. 6,
pp. 1409-1412, December, 1961
Original article submitted September 8, 1961

The absorption of water vapor on ion exchange resins has been under investigation for a number of years. Sulfonic acid cation exchange resins and strongly basic anion exchange resins have been most thoroughly examined [1-11]. However, relatively little work has been done on the adsorption of water vapor on weakly acidic carboxylic cation exchange resins [1, 11]; besides the hydrogen form only the Na^+, K^+, and NH_4^+ forms have been investigated. Yet even the little data that is available in the literature indicate that the adsorption of water vapor on carboxylic cation exchange resins seems to differ from adsorption on sulfonic acid resins; the concepts normally invoked in explaining the adsorption of water vapor on sulfonic resins [1, 2, 12, 13] fail to provide a satisfactory explanation for the absorption on carboxylic resins.

We have carried out an investigation of water vapor adsorption on two monofunctional cation exchange resins, a sulfonic acid KU-2 and a carboxylic KFU resins, in order to compare the two. Water vapor adsorption isotherms were determined by the isopiestic method [1, 14, 11]. There are two great advantages in using a vacuum apparatus with a MacBane quartz spring balance: 1) the adsorption equilibrium is attained much sooner, and 2) one can work with small amounts of material. That is why we have used this particular method in our determination of adsorption isotherms.

The vacuum apparatus was surrounded by an air-cooled thermostat with automatically regulated temperature. The isotherms of seven samples ranging in weight from 0.1 to 0.2 g were recorded simultaneously at 25°. The measurements were begun after all the water was removed from air-dried samples at ~40° in a vacuum apparatus evacuated to 10^{-5} mm. Depending on the nature and the ionic form of the resin the pumping took from 1 to 3 days. The completeness of water removal was tested in several cases by noting how much more water was lost when the resin was dried in a desiccator at $t \simeq 100$-110° (KU-2) or was left for 3-4 weeks over P_2O_5 (KU-2 and KFU). All three methods yielded compatible results.

The exchange capacity of ion exchange resins in the hydrogen form was determined potentiometrically. KU-2 resins containing 2, 10-12, and 24% of divinyl benzene (DVB) have capacities of 4.90, 4.80, and 5.10 meq/g of dry resin respectively. The hydrogen forms of the two KFU resins, one with a swelling coefficient K_s of 4.5, the other 3.8 (in 1 N NaOH), and a capacity of 5.70 meq/g of dry resin. The capacities of other ionic forms were calculated from these data.

Under our experimental conditions the adsorption equilibrium could be attained within 4 hours if p/p_s* was less than ~8, but it took 24 hrs or more to reach equilibrium at $p/p_s = 1$.

The relative experimental errors in the central portion of the isotherms ($0.4 \leq p/p_s \leq 0.6$) did not exceed ± 0.5%; as the measured quantities became larger the errors declined even further; at low p/p_s ratios the errors never exceeded ± 5%. We obtained the adsorption isotherms of water vapor on three samples of the KU-2 sulfonic acid resin in the H^+ form differing in their DVB content (2, 10-12, and 24%) and also on KU-2 samples (containing 10-12% DVB) with different H^+/Na^+ ratios.

* p is the saturated vapor pressure; p_s is the water vapor pressure over the ion exchange resin.

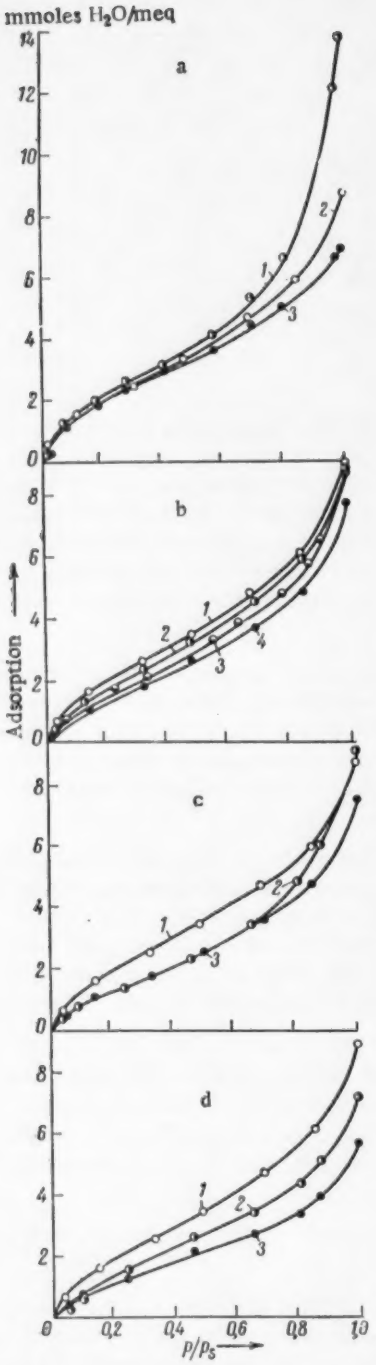

Fig. 1. Water vapor adsorption isotherms on the sulfonic acid cation exchange resin KU-2. a) The H^+ form with a DVB content of: 1) 2%; 2) 10-12%; 3) 24%. b) Isotherms on partially neutralized resins: 1) H^+ form; 2) 65% H^+ + 35% Na^+; 3) 30% H^+ + 70% Na^+; 4) Na^+ form. c) Various ionic forms: 1) H^+ form; 2) Li^+ form; 3) Na^+ form. d) 1) H^+ form; 2) Mg^{++} form; 3) Ba^{++} form.

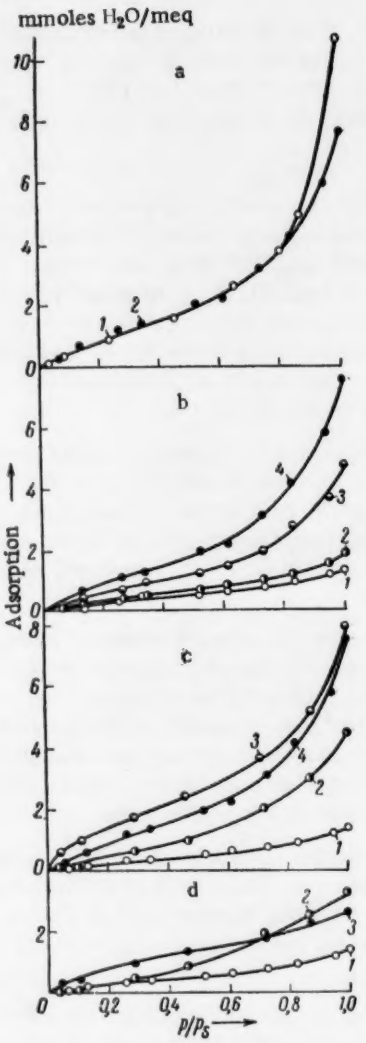

Fig. 2. Water vapor adsorption isotherms on KFU carboxylic cation exchange resins. a) The Na^+ form: 1) K_s = 4.5; 2) 3.8. b) Isotherms on partially neutralized resins: 1) H^+ form; 2) 72% H^+ + 28% Na^+; 3) 37% H^+ + 63% Na^+; 4) Na^+ form. c) Isotherms on various ionic forms: 1) H^+ form; 2) Li^+ form; 3) Cs^+ form; 4) Na^+ form. d) same as c: 1) H^+ form; 2) Mg^{++} form; 3) Ba^{++} form.

On the KFU carboxylic resin we determined the adsorption isotherms of two Na^+ forms with different swelling coefficients, 4.5 and 3.8 respectively in 1 N NaOH. On the KFU resin with a $K_s = 3.8$ we also obtained isotherms of the H^+, Li^+, Cs^+, Mg^{++}, and Ba^{++} forms. In addition to this isotherms were also determined on samples of this resin with different H^+/Na^+ ratios.

The H^+ forms of our resins were prepared by washing the commercial products with 2 N HCl until the washings gave a negative test for Fe^{+++} and removing excess acid with distilled water.

All the other forms, except the magnesium, were prepared by treating the H^+ form with 1 N solutions of the appropriate chlorides and subsequently neutralizing the displaced H^+ with hydroxide of corresponding metals. To convert either resin into its Mg^{++} form we washed the hydrogen form repeatedly with 1 N $MgCl_2$ until the pH of the equilibrium and the original solutions became the same. To prepare samples of the KU-2 resin with some of the H^+ replaced by Na^+ we treated weighed samples of the H^+ form with solutions of 0.1 N HCl + 0.1 NaCl mixed in different proportions. The percent of H^+ substituted by Na^+ was determined analytically from the change in the H^+ and Na^+ concentrations in solution. To get a partially neutralized KFU resin we treated a weighed amount of the resin with a known volume of 1 N solutions containing various amounts of NaOH. The amount of H^+ replaced by Na^+ was determined potentiometrically. After filtering off the equilibrium solutions we dried the resins on filter paper and removed the salt film retained on the surface by briefly washing the resin with distilled water. Samples prepared in this manner were dried in air.

The experimental results shown in Figs. 1 and 2 include only the adsorption branches of the isotherms. We would like to point out, however, that all the investigated samples yielded distinct either broad or narrow hysteresis loops (see also [2, 8, 11]). In contrast with adsorption on ordinary porous materials, such as silica gel, the desorption portions of our samples do not coincide with the adsorption branches until very small p/p_s ratios are reached.

One can see in Fig. 1 that all the isotherms on KU-2 are S-shaped. At first the water is adsorbed rapidly, then the isotherm becomes practically linear, and finally at $p/p_s > 0.6$ the absorption rapidly rises to its maximum. Figure 1 shows that, as has previously been reported [1, 2, 4, 9], the more DVB in the resin the lower lies the corresponding isotherm. The isotherms on partially neutralized resins show that the higher the Na^+/H^+ ratio the less water is adsorbed at a given p/p_s. The isotherms on various ionic forms of KU-2 fall in the following relative orders:

$$H^+ > Li^+ > Na^+ \text{ and } H^+ > Mg^{2+} > Ba^{2+}.$$

The order is similar to the hydration series of these ions in solutions of ordinary electrolytes [14]. This would indicate that a resin containing an ion which is most extensively hydrated in aqueous solutions will also adsorb the most water. This observation is in full accord with the results reported by other workers [1, 2, 4, 9]. Differences in the amount of water adsorbed by various forms of a resin are usually explained [1] by drawing an analogy between the hydration of cations in solution and in the resin phase. It was also assumed that in these systems the exchanging monovalent ions do not interact with the resin matrix. However, this assumption has been disputed by other workers [4, 5]. In the case of the Ba^{++} form the possibility of ion-pair formation was considered [1] so as to explain the fact that the amount of water adsorbed by the Ba^{++} forms is much smaller than one would expect from the hydration series.

Thus despite a few minor discrepancies the adsorption of water vapor on sulfonic acid cation exchange resins finds a satisfactory explanation in the assumption [1] of a simple hydration of completely free cations in the resin phase. However, things look quite different in the case of carboxylic resins.

Figure 2 shows that the KFU resin with a greater swelling coefficient adsorbs more water at high p/p_s ratios. Here the similarity between KU-2 and KFU ends. The isotherms on carboxylic resins in which the H^+ ions are replaced by various amounts of Na^+ reveal that in contrast with the KU-2 resin the greater the Na^+/H^+ ratio the more water is adsorbed by the resin. The KFU isotherms also fail to exhibit the sharp initial rise observed on the KU-2 resins.

The adsorption isotherms of water vapor on various ionic forms of KFU fall in an order exactly reverse to that observed on KU-2. The isotherm of the weakly dissociated H^+ form falls lower than any other. As far as the other forms of KFU resin are concerned differences in the amount of water adsorbed can be attributed to different degrees of interaction between the exchanging cations and the matrix anion, since the carboxyls will be polarized quite differently in the field of the cations.

Strong acids such as H_2SO_4 are known to form hard to polarize "rigid" anions. Hence in the case of the KU-2 sulfonic acid resin, where the formation of ion pairs is unlikely, the experimental adsorption data can be explained, as has been done before [1], by differences in the hydration of cations. But in the case of the KFU resin things are somewhat different. The carboxyl anion is apparently much more readily polarized in the cationic field. A Li^+ ion, for instance, which has a smaller ionic radius than Cs^+ should polarize the anionic resin much more extensively. As a result the resin should have fewer "free" cations in the Li^+ form than it would in the Cs^+ form and the amount of water adsorbed by the two forms of the KFU resin should be different. Our experimental results are in complete agreement with this argument. One might also assume that in this case changes in the number of "free" ions exert a greater influence on the adsorption of water by ion exchange resins than do differences in the degree of hydration of each ion.

The argument can also be extended to the two divalent ions, Ba^{++} and Mg^{++}, and be used to explain the relative position of the corresponding isotherms up to $p/p_s > 0.7$. At larger p/p_s ratios the Ba^{++} curve falls below the Mg^{++} curve. The reason for this is not clear.

The experimental results and their analysis thus indicate that simple ideas on the hydration of completely free cations in the resin phase [1] can not account for all the observations, particularly in the case of carboxylic resins, unless one takes into consideration the possibility of ion-pair formation involving the matrix anion and the exchanging cations. By showing how different cations interact with the resin one can account for all the results reported in this paper.

LITERATURE CITED

1. H. P. Gregor, B. R. Sundheim, K. M. Held, and M. H. Waxman, J. Coll. Sci. 7, 511 (1952).
2. B. R. Sundheim, M. H. Waxman, and H. P. Gregor, J. Phys. Chem. 57, 974 (1953).
3. K. W. Pepper, J. Appl. Chem. 1, 124 (1951).
4. G. E. Boyd and B. A. Soldano, Zs. Elektrochem. 57, 162 (1953).
5. E. Gluckauf, Proc. Roy. Soc. Ser. 214A, 207 (1952).
6. J. F. Duncan, Proc. Roy. Soc. Ser. 214A, 344 (1955).
7. E. Gluckauf and G. P. Kitt, Proc. Roy. Soc. 68, 671 (1956).
8. E. Blasius, H. Pittack, and M. Negwer, Angew. Chem. 68, 671 (1956).
9. G. Dickel, Chem. Techn. 10, 449 (1958).
10. G. Dickel, H. Degenhart, K. Haas, and J. W. Hartman, Zs. Phys. Chem. 20, 121 (1959).
11. G. Dickel and J. W. Hartman, Zs. Phys. Chem. 23, 1 (1960).
12. H. P. Gregor, J. Am. Chem. Soc. 70, 1293 (1948).
13. H. P. Gregor, J. Am. Chem. Soc. 75, 642 (1951).
14. R. H. Stockes and R. A. Robinson, J. Am. Chem. Soc. 70, 1870 (1948).

All abbreviations of periodicals in the above bibliography are letter-by-letter transliterations of the abbreviations as given in the original Russian journal. *Some or all of this periodical literature may well be available in English translation.* A complete list of the cover-to-cover English translations appears at the back of this issue.

THE INFLUENCE OF ADSORBED HYDROGEN AND OXYGEN ON THE ADSORPTIVE DISPLACEMENTS OF POTENTIAL AT A PLATINIZED ELECTRODE

A. D. Obrucheva

M. V. Lomonosov Moscow State University
(Presented by Academician A. N. Frumkin, July 24, 1961)
Translated from Doklady Akademii Nauk SSSR, Vol. 141, No. 6,
pp. 1413-1415, December, 1961
Original article submitted July 12, 1961

It has previously been shown [1, 2] that the displacements of the potential of a platinum electrode, observed in the absence of oxidizing agents and reducing agents when an electrolyte without surface-active properties, for example 1 N H_2SO_4, is replaced by an electrolyte containing surface-active ions, indicate that adsorption of the latter takes place. The observed displacements of the potential can be interpreted with a certain degree of approximation as adsorption potentials, if the surface is free from adsorbed hydrogen and oxygen, whose ionization distorts the results obtained [1]. In this connection the initial values of the potentials φ were chosen in the potential range lying approximately between 0.3 and 0.7 v. In the case of the adsorption of anions, however, the final value of the potentials falls in the hydrogen region, while the adsorption of cations displaces the potential into the region of the start of oxidation.

In the present work we have studied the influence of adsorbed hydrogen and oxygen on the displacement of the potential, brought about by the specific adsorption of ions. The conditions under which the experiments were carried out differed slightly from those described earlier, as follows: the volume of the solution was brought to 1.2 cm^3, and the purification of the initial solution and of the solution containing the ion to be adsorbed was carried out for a longer period. These precautions resulted in certain changes in the observed adsorption displacements of the potential. Thus in the case of 10^{-1} N KI for an initial value of 0.6 v, $\Delta\varphi$ amounted to between -0.49 and 0.51 v, instead of the value -0.46 v obtained under the earlier experimental conditions, and for 10^{-1} N KBr the value was -0.38 v instead of -0.35 v. The difference in the case of thallium sulfate was more marked. For an initial value of φ = = 0.3 v, $\Delta\varphi$ was equal to 0.465 v instead of 0.6 v in the earlier experiments. It is possible that complete reduction of the impurities – trivalent thallium or other oxidizing agents, which might increase slightly the displacement of the potential in the anodic direction – was reached only during the more prolonged purification on the platinized electrode.

The first series of experiments was devoted to a study of the influence of the addition of surface-active ions to the solution on the potential of a hydrogen electrode. The test electrode in 1 N H_2SO_4 solution was brought by polarization to the value of the reversible hydrogen potential. The same solution, containing a surface-active ion and saturated with hydrogen, was transferred by hydrogen pressure to the vessel containing the test electrode, after which the displacement of the potential with time was observed as hydrogen was passed through the solution. Figure 1a gives the results for 0.01 N KI. All the potentials are given relative to the normal hydrogen electrode. It can be seen that in the presence of KI the potential was displaced in the cathodic direction by 0.018 v, but after 15-20 minutes it returned to the original value of the reversible hydrogen potential. Analogous phenomena were previously observed in the case of a Pd electrode [3]. The observed displacement may to some extent be brought about directly by the adsorption of the I^- ion, which displaces the potential to more negative values, but part of the displacement is undoubtedly related to the desorption, under the influence of the adsorbed I^-, of the hydrogen adsorbed on the platinum. The desorbing action of I^- on hydrogen adsorbed on platinum follows from the decrease in the length of the hydrogen arrest on the charging curves in KI solutions [1]. When desorbed, the hydrogen atoms are converted to molecular hydrogen and partly to H^+ ions, leading to a displacement of the potential in the cathodic direction. After some time the increase in the concentration of dissolved hydrogen in the layer next to the electrode is smoothed out and the electrode potential returns to the equilibrium normal hydrogen potential for this system as a

result of the discharge of hydrogen ions from the solution. In the case of iodide the effects related to the desorption of hydrogen and to the direct effect of the adsorption of the I^- ion are of the same sign. From this viewpoint it was of interest to examine the case of the Tl^+ ion. The charging curves previously obtained in a solution of thallium sulfate indicate desorption of hydrogen when Tl^+ is adsorbed, as in the case where I^- is adsorbed, but the sign of the adsorption potential of Tl^+ is the opposite of that of the adsorption potential of I^-. Experiment shows (Fig. 1, b) that at the reversible hydrogen potential, Tl^+ ions, like I^- ions, first displace the hydrogen electrode potential in the cathodic direction, after which, in 15-20 min, the potential returns to the initial value. Since the specific adsorption of Tl^+ should increase the potential, the observed displacement can be attributed only to the desorption of hydrogen from the platinum surface; this desorption is consequently of predominating importance under the experimental conditions.

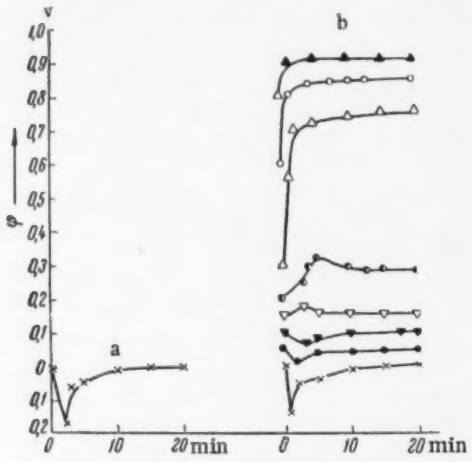

Fig. 1. a) Displacement of the potential with time under the influence of the iodide ion at the reversible hydrogen potential; b) the same under the influence of the thallium ion at different initial potentials.

By varying the values of the initial potential in the range between the reversible hydrogen potential and 0.8 v, we obtain a series of curves for the change in potential with time after replacement of 1 N H_2SO_4 by 1 N H_2SO_4 + 10^{-1} N Tl_2SO_4. In the case of positive initial potentials (Fig. 1, b) thoroughly purified nitrogen was passed through the cell while the measurement in the cathodic direction was first observed, after which the potential returned to more positive values. The decrease in the energy of adsorption of atomic hydrogen as a result of the adsorption of Tl^+ must evidently lead to its partial ionization, and also (so long as the original positive values of φ are not too high) to desorption in the form of H_2. The adsorption displacement of potential of the Tl^+ ion, which is of opposite sign is superimposed on the displacement of φ in the cathodic direction as a result of the ionization of the adsorbed hydrogen; moreover, the H_2 evolved is removed by the nitrogen. These two factors cause the potential to return gradually to more anodic values.

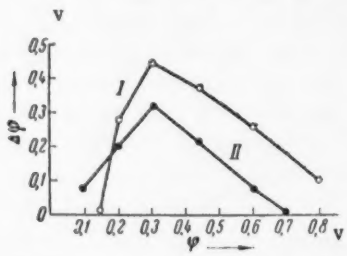

Fig. 2. The relationship between $-\Delta\varphi$ and the initial value of φ for the Tl^+ ion (I) and the Cd^{2+} ion (II).

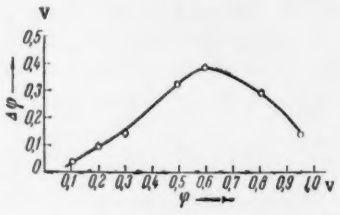

Fig. 3. The relationship between $|\Delta\varphi|$ and the initial value of φ for the Br^- ion.

From an initial potential of 0.2 v, a displacement of φ in the anodic direction is observed; in other words, the adsorption displacement of the potential exceeds the effect related to the desorption of hydrogen, which can be neglected. When a value of φ = 0.3 v is reached, a maximum value of $\Delta\varphi$ = 0.48 v is observed, and this reflects directly the change in the structure of the double layer under the influence of the specific adsorption of the Tl^+ ion. With further increase in the initial values of φ, the magnitude of $\Delta\varphi$ decreases, as a result of the decrease in the adsorption of the cation at more positive values of φ, and, more particularly, as a result of the fact that the final values of φ in this case lie in the region of potentials corresponding to considerable oxidation of the electrode surface; this is facilitated in the presence of the surface-active cations Tl^+ and Cd^{2+} [2]. The appearance of OH groups or O atoms on the surface is accompanied by the transfer of electrons to the platinum and the displacement

of the potential towards more positive values stops. As a result of this, the curve giving the relationship between $\Delta\varphi$ and the original potential φ with increase in φ (Fig. 2, I) passes through a maximum. Analogous curves are obtained for cadmium ions (Fig. 2, II) and bromide ions (Fig. 3). For Tl^+ the maximum lies at 0.36 v, for Cd^{2+} at 0.32 v, and for Br^- at 0.7 v.

In the interpretation of the nature of the observed $|\Delta\varphi|, \varphi$ curves, the following point must be remembered. If the platinum surface were free from adsorbed hydrogen and oxygen, the value of $|\Delta\varphi|$ should have increased monotonously with increase in φ in the case of surface-active anions and decreased monotonously in the case of cations. When the influence of adsorbed hydrogen and oxygen are taken into account, slightly different conclusions are obtained for two different assumptions.

1. The adsorption of the surface-active ion has no influence on the adsorption of hydrogen at constant potential. As has been shown in [1] for the case of the I^- ion, if this assumption is correct the presence of adsorbed hydrogen should decrease the absolute value of $\Delta\varphi$. It can readily be seen that this conclusion is equally applicable to the adsorption of cations in the hydrogen range.

2. The adsorption of the surface-active ion decreases the adsorption of hydrogen at constant potential. As was shown at the start of the present article, such desorption should increase the value of $|\Delta\varphi|$ compared with that which would be expected in the first case for anions and should decrease even more the expected effect for cations. This explains the extremely sharp drop in the $|\Delta\varphi|, \varphi$ curve in the case of Tl^+ as the hydrogen potential is approached. In the case of the Cd^{2+} ion, which does not decrease the hydrogen arrest on the charging curve [2] and hence does not desorb hydrogen, this drop takes place much more slowly. The same reasoning explains the relatively slow drop in $|\Delta\varphi|$ as the hydrogen potential is approached in the case of the Br^- ion. Analogous conclusions can also be reached with respect to the action of adsorbed oxygen.

The peculiar features of the process at the very low initial values of φ at which the hydrogen concentration in the bulk of the electrolyte becomes comparable with or exceeds its concentration at the surface were considered at the start of the present communication.

I wish to thank Academician A. N. Frumkin for valuable advice during this work.

LITERATURE CITED

1. A. D. Obrucheva, ZhFKh, 32, 2155 (1958).
2. A. D. Obrucheva, DAN, 120, 1072 (1958).
3. L. T. Shanina, DAN, 134, 141 (1960).

THE INFLUENCE OF CATIONS ON OXYGEN OVERVOLTAGE

Academician A. N. Frumkin, R. I. Kaganovich,

E. V. Yakovleva, and V. V. Sobol'

M. V. Lomonosov Moscow State University
Translated from Doklady Akademii Nauk SSSR, Vol. 141, No. 6,
pp. 1416-1419, December, 1961
Original article submitted September 23, 1961

The influence of the nature of cations on anodic reactions has been observed for a number of electrochemical processes taking place at high anodic potentials.

N. A. Izgaryshev et al. [1] studied the relationship between the yield of persulfates and perchlorates and the nature of the cations. In these works the influence of the cations was attributed to their dehydrating action on the anions, which depended on the radius and hydration energy of the cations. K. L. Il'in [2] attributed the influence of cations on the results of the electrolysis of chlorides in neutral media (without diaphragm) to the different solubilities of the electrolysis products. The adsorptive nature of the influence of cations on oxygen overvoltage was first pointed out by T. Erdei-Gruz and I. Shafarik [3]. They suggested that the cations are attracted by the adsorbed SO_4^{2-} anions and influence the discharge of water molecules by deforming them on the surface of the electrode. Ts'u Yung-Ts'ao and Mi T'ien-Ying [4] drew attention to the relationship between the kinetics of persulfate formation and the rate of evolution of oxygen and showed the range of potentials in which cations have the most marked influence on the oxygen overvoltage.

M. Ya. Fioshin, Yu. B. Vasil'ev, and E. G. Gaginkina [5] found that in the electrolysis of acetate solutions, cations have an influence similar to that observed during the liberation of oxygen on platinum.

The present work gives the results of a study of the influence of some cations on oxygen overvoltage in solutions of sulfuric and perchloric acids. Of particular interest is the study of the liberation of oxygen from perchloric acid solutions; this reaction is not complicated by side processes over a wide range of potentials.

The polarization curves were recorded in a cell with anodic and cathodic compartments separated by means of a glass filter. The anode consisted of a platinum wire with diameter 95 μ and area 10^{-2} cm^2. A platinum wire in the form of a spiral was used as cathode. The potentials were measured relative to a hydrogen electrode in the same solution. The hydrogen electrode was connected to the anode by a salt bridge, one end of which formed a capillary sealed into the anodic compartment. In addition to the usual polarization curves, we also recorded $I - \varphi$ curves by the method described in [6], together with curves for the potential drop after the current was broken.

Before the curves were recorded the anode was treated with dilute nitric and concentrated sulfuric acids, washed with water, and then subjected to anodic polarization for 30 minutes by a current of $6 \cdot 10^{-6}$ amp in 1 N H_2SO_4. When the polarization curves were recorded, each point was held for 2 minutes until a constant potential was reached. The acids and water used were purified beforehand by double distillation and the salts by recrystallization.

In the case of perchloric acid solutions, the influence of the addition of Cs^+, K^+, and Ba^{2+} perchlorates was studied. Figure 1 gives the polarization curves recorded in 1.34 N $HClO_4$ with the addition of Cs^+ and K^+ in different concentrations. The curves in Fig. 1 show that the effect of these ions is shown predominantly in the region of the sudden increase in potential; only a very weak effect is observed at higher polarizations. In the presence of the cations, the potential jump is displaced towards lower current density values, the activity of cesium being greater than that of potassium by almost a whole order of magnitude. With increase in the cation concentration, the transition from the lower to the upper branch of the polarization curve takes place more gradually; thus in a solution containing K^+ at a concentration of 10^{-2} N it becomes possible to measure the intermediate points on the rising section of the curve.

Figure 2 gives the $I - \varphi$ curves recorded by applying to the electrodes, through a low-resistance potentiometer, a voltage which increases linearly with time at a rate of 8 mv/sec, in pure 1.34 N $HClO_4$ solution (1) and solution containing Cs^+ and K^+ (2 and 3). The curves in Fig. 2 show that in the potential range 2.5-2.9 v a drop in the current is observed in the test solutions, indicating retardation of the evolution of oxygen. The effect of the cations is shown by a decrease in the current strength at a given potential; it is shown most strongly at the potential of the current maximum and disappears almost completely at considerable distances from the latter. When the curves are recorded from high current densities to lower values (curves 1', 2', 3'), a hysteresis loop is observed; the curve for the "reverse direction" has a plateau in the region of the potentials of the drop in current.

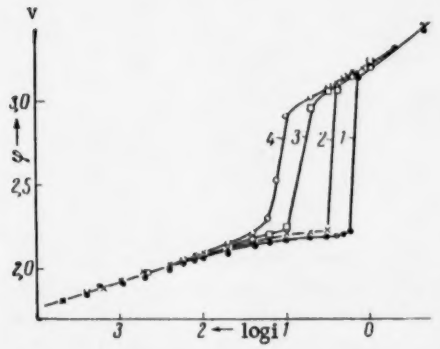

Fig. 1. Anodic polarization curves for a platinum electrode in solutions of: 1) 1.34 N $HClO_4$; 2) 1.34 N $HClO_4 + 8 \cdot 10^{-3}$ N $KClO_4$ and 1.34 N $HClO_4 + 10^{-3}$ $CsClO_4$; 3) 1.34 N $HClO_4 + 2.5 \cdot 10^{-3}$ N $CsClO_4$; 4) 1.34 N $HClO_4 +$ $+ 10^{-2}$ N $KClO_4$.

The polarization curves recorded in 1.34 N $HClO_4$ solutions containing different concentrations of added barium perchlorate are analogous to the curves obtained in the presence of Cs^+ and K^+ ions. Like these cations, the Ba^{2+} ion shows the greatest influence in the region of rapid change in potential. If, however, we compare the concentrations of cations producing a displacement of the start of the potential jump to $i = 10^{-1}$ amp/cm^2, for example, it is found that Cs^+ produces this displacement at a concentration of $2.5 \cdot 10^{-3}$ N, K^+ at 10^{-2} N, and Ba^{2+} at $4 \cdot 10^{-1}$ N, i.e., cesium is almost 200 times more active than barium.

The effect of cations on the oxygen overvoltage decreases with increase in the perchloric acid concentration. Thus in 3 N $HClO_4$ a displacement of the anodic potential is observed when Cs^+ is added at a concentration of 10^{-2} N. The K^+ ion has no effect at the same concentration. In 5.8 N $HClO_4$, even Cs^+ cations have no effect.

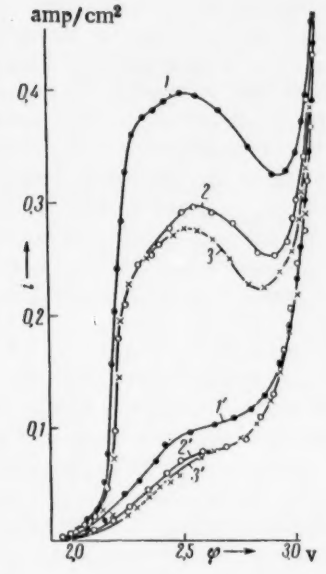

Fig. 2. Anodic polarization curves for a platinum electrode, recorded with continuous change in the applied potential in solutions of: 1) 1.34 N $HClO_4$; 2) 1.34 N $HClO_4 + 2.5 \cdot 10^{-3}$ N $CsClO_4$; 3) 1.34 N $HClO_4 + 10^{-2}$ N $KClO_4$. Curves 1', 2', and 3' were obtained in the same solutions with polarization in the reverse direction.

In the case of sulfuric acid solution, polarization curves were recorded with the addition of Cs^+, K^+, Na^+, and Li^+ sulfates in concentrations from 1 to 10^{-2} N. Figure 3 gives the polarization curves recorded in 5 N sulfuric acid in the presence of cesium sulfate. The polarization curve for pure 5 N H_2SO_4 is given for comparison.

Figure 3 shows that the general picture of the phenomenon in the case of sulfuric acid is the same as that for $HClO_4$. The relationship between the magnitude of the cationic effect and the current density is much less marked, however, and the actual changes in the slope of the polarization curve are also less marked.

The curves obtained in the presence of K^+, Na^+, and Li^+ sulfates are analogous to the curves shown in Fig. 3. The cations studied can be arranged in the following order of decreasing influence on the anode potential: $Cs^+ > K^+ > Na^+ > Li^+$. As an example table gives values of the change in the anode potential at a current density of $2 \cdot 10^{-1}$ amp/cm^2 when the cations under study are added to a solution of 5 N H_2SO_4 in different concentrations.

By measuring the curves for the potential drop after the current is broken [7], it was found that the capacity of a platinum electrode C in 1.34 N $HClO_4$ changes from 80-100 to 20 μf on going from potentials corresponding

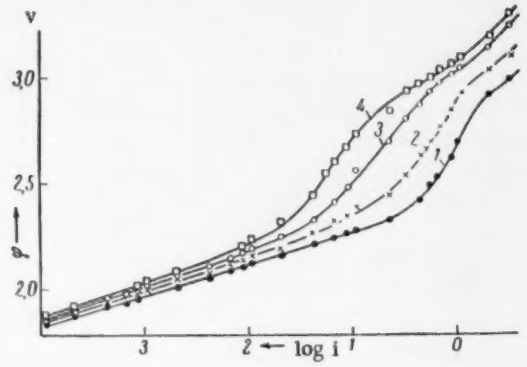

Fig. 3. Anodic polarization curves for a platinum electrode in solutions of: 1) 5 N H_2SO_4; 2) 5 N H_2SO_4 + 10^{-2} N Cs_2SO_4; 3) 5 N H_2SO_4 + 10^{-1} N Cs_2SO_4; 4) 5 N H_2SO_4 + + 1 N Cs_2SO_4.

Cation concn. N	Δφ, V			
	Cs^+	K^+	Na^+	Li^+
1	0,53	0,39	0,18	0,06
0,1	0,37	0,22	0,09	0,04
0,01	0,13	0,11	0,05	—

to the lower branch of the polarization curve to potentials lying on the upper boundary of the jump. The experimental procedure and the calculation are described in detail in [7]. The measurements which we carried out in the presence of Cs^+ and K^+ cations in a solution of 1.34 N $HClO_4$ showed that the changes in the capacity are parallel to the changes in the polarization curves; as shown in Fig. 4, the more active the cation, i.e., the more strongly the cation influence the oxygen overvoltage, the lower the values of the capacity at which drop on the C – log i curves is observed.

On the basis of the accumulated data which have been obtained, it is possible to put forward the following explanation of the influence of cations, based on the theories of the nature of the potential jump given in [7]. The appearance, on the surface, of adsorbed oxygen atoms and chemisorbed anions, forming dipoles with their negative ends turned towards the solution, makes possible the local adsorption of cations, in spite of the high positive potential of the electrode. In acid solutions the negative groups present on the platinum surface attract hydrogen ions; we may say that they acquire acidic character. When cesium, potassium, or barium cations are introduced into the solution, they replace the hydrogen ions partly or completely. The degree of replacement evidently increases with increase in the adsorbability and concentration of the cations and decreases with increase in the activity of the hydrogen ions of the acid. Since the effect of cesium is shown in the presence of such a large excess of hydrogen ions, the difference in their adsorbability in this case is evidently greater than in the case of adsorption on a negatively charged mercury surface. The replacement of the hydrogen ion by specifically adsorbed cations should increase the energy of adsorption of the anionic groups in the same way as the presence of cesium increases the strength of adsorption of iodide on a mercury surface. The increase in the adsorption energy apparently leads to an increase in the strength of the surface chemisorbed layer and to a decrease in the rate of its breakdown with the evolution of oxygen. As a result, the covering of the surface is completed at lower current densities; at the same time the repulsion between the adsorbed cations causes the covering to take place slightly more slowly in the presence of alkali metal cations than in pure acid solutions. The influence of the change in the bond energy should be shown most strongly under conditions where the covering is approaching completion. The influence of the cation is therefore revealed primarily on the current density at which the potential jump takes place, while maximum covering of the surface by anionic groups creates the most favorable conditions for the adsorption of cations. Further increase in the potential on the upper branch of the polarization curve should decrease the adsorption of cations. This adsorption should also be slightly less clearly defined on the lower branch of the curve before the potential jump takes place, in view of the lower concentration of anionic groups on the electrode surface.

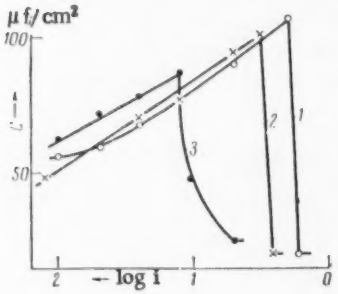

Fig. 4. Curves showing the change in the capacity with current density for solutions of: 1) 1.34 N $HClO_4$; 2) 1.34 N $HClO_4$ + 10^{-2} N $KClO_4$; 3) 1.34 N $HClO_4$ + 2.5 · 10^{-3} N $CsClO_4$.

LITERATURE CITED

1. N. Isgarischev and S. Berkman, Zs. Elektrochem. 28, 40 (1922); N. A. Izgaryshev and M. G. Khachaturyan, DAN, 59, 1125 (1948); N. A. Izgaryshev and A. A. Petrova, ZhFKh, 5, 881 (1950); N. A. Izgaryshev, Izv. AN SSSR, OKhN, 15 (1950).
2. K. L. Il'in, Tr. Novocherkassk. Politekhn. Inst. 34, 33 (1956).
3. T. Erdei-Gruz and I. Shafarik, Proceedings of the IVth Conference on Electrochemistry [in Russian] (Moscow, 1959), p. 263.
4. Ts'u Yung-Ts'ao and Mi T'ien-Ying, DAN, 125, 1069 (1959).
5. M. Ya. Fioshin, Yu. B. Vasil'ev, and E. G. Gaginkina, DAN, 135, 909 (1960).
6. R. I. Kaganovich and M. A. Gerovich, ZhFKh, 32, 956 (1958).
7. A. N. Frumkin and V. V. Sokol', DAN, 141, 4 (1961).

All abbreviations of periodicals in the above bibliography are letter-by-letter transliterations of the abbreviations as given in the original Russian journal. *Some or all of this periodical literature may well be available in English translation.* A complete list of the cover-to-cover English translations appears at the back of this issue.

THE INFLUENCE OF THE SURFACE ON THE FORM AND BEHAVIOR OF MOLECULAR PICTURES

V. A. Shishkin

Physical Chemistry Institute, Academy of Sciences, USSR
(Presented by Academician M. M. Dubinin, July 24, 1961)
Translated from Doklady Akademii Nauk SSSR, Vol. 141, No. 6,
pp. 1420-1422, December, 1961
Original article submitted July 8, 1961

The nature of molecular pictures (m.p.), i.e., the emission images produced on the screen of an electronic projector when small quantities of gases or vapor are condensed on points, is not yet clear. None of the hypotheses which have been put forward explain all the experimental data which have accumulated [1-4]. In order to understand the nature of molecular pictures it is necessary to know at least the following: the nature of the bond between the molecules responsible for the observed m.p. and the surface, and their geometrical position on the latter; the mechanism of the transfer of electrons from the emitter to the molecule; the magnitude and nature of the change in the symmetry of the electron clouds of the molecules and the individual bonds in fields of $\sim 1 \cdot 10^8$ v/cm; and the nature of the interaction of the electron beam with the distribution of charge within the molecule.

For obvious reasons it is at present impossible to obtain an answer to all these problems by carrying out direct or model experiments. We have chosen an indirect method of studying the influence of the electrical properties of the molecules, the influence of external factors (the temperature of the field and the pressure), and the influence of the nature of the surface on the form and behavior of the m.p. of an extensive range of materials.

This article is devoted to the last problem, i.e., to an experimental study of the influence of the electronic type of the solid (metal, semiconductor, dielectric), crystallographic nonuniformity, and surface relief on the form and behavior of the m.p. The other problems will be examined in latter publications.

The influence of the electronic type of the emitter. In the study of the adsorption of CO_2, divinyl, and ferrocene on Si and Ge points, a control tube with tungsten point was sealed on in parallel. The experiments showed that the forms of the observed molecular pictures on these semiconductors were the same as those observed on the metallic tungsten point and showed the same behavior. In the case of Ge and Si, however, the number of m.p. and their contrast with the surrounding background were lower than on W (see Fig. 1).

In another series of experiments the tungsten point was kept in an atmosphere of N_2 or O_2 before C_3F_6 was applied. It is known that this treatment leads to the formation of a strongly-held chemisorbed layer which saturates completely the free bonds of the surface atoms. It was found that the form of the m.p. is independent of whether the underlying adsorption layers are formed by C_3F_6 molecules or by the molecules of the residual gases. At the same time the contrast of the m.p. is a maximum in this case. This indicates that the contrast depends on the work function of the emitter. Finally, the action of heat on a tungsten point in an atmosphere of O_2 in an applied anodic field leads to the formation of a surface covered with crystallites. These crystallites collect in the light regions around 100 and 110. The forms of the m.p. on these projections* are identical with those observed on a clean tungsten surface.

The influence of crystallographic nonuniformity. In experiments on the adsorption of different gases on W and H_2 and divinyl on Ge, no difference was observed in the behavior or forms of the m.p. on faces with different densities of packing or with different work functions.** At first, certainly, the m.p. are most frequently observed around 111 and 100 (=), where the frequency of their appearance is higher. This tendency, however, is more prob-

* According to Gomer [5], these crystallites are oxides (WO_3). In the absence of a field, WO_3 is a dielectric.
** Melmed and Muller recently confirmed this for 10 metals [1].

ably related to the higher emission power of these regions and the lower local radii of curvature, which, according to the ionograms obtained [6], are shown by these faces. As covering proceeds (particularly in a strong field), re-

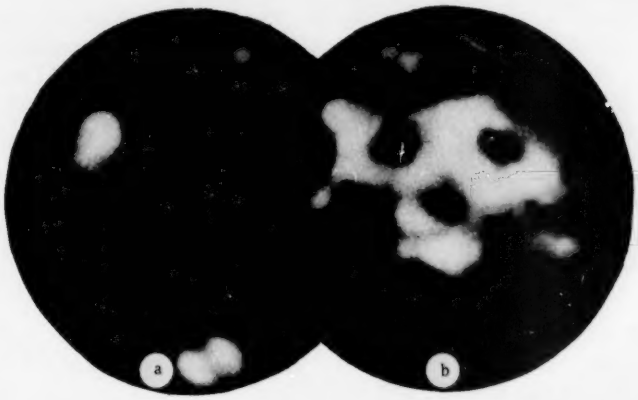

Fig. 1. a) H_2 on Ge. Only simple discs are observed. The contrast between the m.p. and the background is weak; b) ferrocene on an Si emitter from which the oxide film had not been removed.

distribution of the adsorbed layer takes place and judging by the emission picture, the surface is uniformly covered with m.p.

The influence of surface microrelief. Experiments on the adsorption of O_2, N_2, H_2 and C_2F_4 on tungsten points reformed in the field confirm that the m.p. appear predominantly on the regions with smaller radii of curvature. On these projections, which according to [7] have a height of up to 12 A, the course of the adsorption differs from that described for atomically smooth planes. The m.p. may appear even at $p < 1 \cdot 10^{-7}$ mm Hg. The m.p. themselves are larger and their concentration is so high that the m.p. from two neighboring molecules are often not resolved.

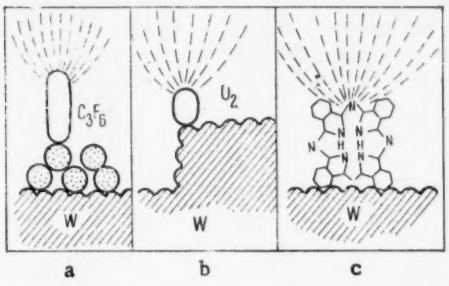

Fig. 2. Possible cases of submicroprojection formation on the surface of an emitter: a) C_3F_6 molecule adsorbed above layers strongly held to the surface; b) O_2 molecule adsorbed on a lattice projection; c) large phthalocyanine molecule (14.5 A) adsorbed "upright" on a clean surface.

Analogous results were observed for adsorption on the above-mentioned ridges, formed when the point is reformed in an atmosphere of oxygen or with heating in hydrocarbon vapors. In the study of many complex or easily-decomposed organic compounds (for example CS_2), it was found that parasitic projections are themselves formed during the observations. The low temperature at which these projections disappear (< 800°K) evidently shows that they are formed by decomposition products. The behavior of the m.p. on the parasitic projections, particularly in the case of the adsorption of large linear molecules, is more complex, and the frequency of disappearance of the interconversions of the m.p. for a given pressure is here much higher than on the flat regions. The images fit into one another and their shapes are often considerably distorted. Sometimes very complex shapes are observed, but the low life-time makes it difficult to determine exactly their shapes and interconversions. In the case of the adsorption of benzene it was observed that the number of "rosettes" on this projection was higher than on the flat regions. In the experiment with toluene the voltage necessary to maintain a constant current decreased with the growth of one parasitic projection. At the end of the experiment the anodic voltage amounted to only 1.1 kv ($I = 5 \cdot 10^{-7}$ amp) compared with 14.5 kv at the start. The m.p. became less sharp with the growth of the projection and at 1.1 kv separation of the lobes of the "two-leaved pattern" could no longer be observed.

Thus the crystallogeometric nonuniformity of the surface and the electronic type of the emitter were found to have no influence on the form and behavior of the m.p., whose contrast relative to the background increases with the work function of the emitter. Only the surface microrelief has a significant influence on the shape and behavior of the m.p. It is most natural to relate this influence to the local intensification of the field close to the microprojections, and also to the change in its symmetry. The high brightness of the m.p. can in fact be attributed either to the lower local work function at the point of adsorption of the molecule or to the presence of a a stronger local field. Since active gases increase the work function, the first explanation is inapplicable and we are left with the conclusion that a necessary condition for observing m.p. is the presence of a strong local field around the molecule. Although under the conditions of a strong field the formation of microprojections by the molecules themselves can be assumed,* the existence of lattice projections facilitates their formation. Figure 2 shows three possible cases where a strong local field is created around a molecule.

In conclusion the author wishes to thank Corresponding Member, USSR Academy of Sciences S. Z. Roginskii for valuable advice and assistance with the work.

LITERATURE CITED

1. A. J. Melmed and E. W. Müller, J. Chem. Phys. 29, 1037 (1958).
2. S. Z. Roginskii, Collection, The Structure of Matter and Spectroscopy [in Russian] (Izd. AN SSSR, 1960), No. 3.
3. S. Z. Roginskii and V. A. Shishkin, DAN, 130, 577 (1960).
4. A. P. Komar and A. A. Komar, ZhTF, 31, 2, 231 (1961).
5. R. Gomer, Adv. in Catal. 7, 93 (1955)
6. E. W. Müller, Adv. in Electronics, 8, 83 (1960).
7. E. W. Müller, Ergebn. Exakt. Naturwiss. 27, 290 (1953).

All abbreviations of periodicals in the above bibliography are letter-by-letter transliterations of the abbreviations as given in the original Russian journal. *Some or all of this periodical literature may well be available in English translation.* A complete list of the cover-to-cover English translations appears at the back of this issue.

---

* The formation of these projections will be considered in a later publication.

MISSING PAGES ARE INDEX PAGES
WHICH HAVE BEEN PHOTOGRAPHED
AT THE BEGINNING OF THE VOLUME(S)

Soviet Journals Available in Cover-to-Cover Translation

ABBREVIATION	RUSSIAN TITLE	TITLE OF TRANSLATION	PUBLISHER	TRANSLATION BEGAN Vol.	Issue	Year
AÉ	Atomnaya énergiya	Soviet Journal of Atomic Energy	Consultants Bureau	1	1	1956
Akust. zh.	Akusticheskii zhurnal	Soviet Physics – Acoustics	American Institute of Physics	1	1	1955
	Antibiotiki	Antibiotics	Consultants Bureau	4	1	1959
Astr(on). zh(urn).	Astronomicheskii zhurnal	Soviet Astronomy–AJ	American Institute of Physics	34	1	1957
Avto(mat). svarka	Avtomaticheskaya svarka	Automatic Welding	British Welding Research Association (London)		1	1959
	Avtomatika i Telemekhanika	Automation and Remote Control	Instrument Society of America	27	1	1956
	Biofizika	Biophysics	National Institutes of Health*		1	1957
	Biokhimiya	Biochemistry	Consultants Bureau	21	1	1956
Byull. éksp(erim). biol. i med.	Byulleten' éksperimental'noi biologii i meditsiny	Bulletin of Experimental Biology and Medicine	Consultants Bureau	41	1	1959
DAN (SSSR) / Dokl(ady) AN SSSR	Doklady Akademii Nauk SSSR	The translation of this journal is published in sections, as follows:				
	Life Sciences	Doklady Biochemistry Section	American Institute of Biological Sciences	106	1	1956
	Life Sciences	Doklady Biological Sciences Sections (Includes: Anatomy, biophysics, cytology, ecology, embryology, endocrinology, evolutionary morphology, genetics, histology, hydrobiology microbiology, morphology, parasitology, physiology, zoology sections)	American Institute of Biological Sciences	112	1	1957
	Life Sciences	Doklady Botanical Sciences Sections (Includes: Botany, phytopathology, plant anatomy, plant ecology, plant embryology, plant physiology, plant morphology sections)	American Institute of Biological Sciences	112	1	1957
	Chemical Sciences	Proceedings of the Academy of Sciences of the USSR, Section: Chemical Technology	Consultants Bureau	106	1	1956
	Chemical Sciences	Proceedings of the Academy of Sciences of the USSR, Section: Chemistry	Consultants Bureau	106	1	1956
	Chemical Sciences	Proceedings of the Academy of Sciences of the USSR, Section: Physical Chemistry	Consultants Bureau	112	1	1957
	Earth Sciences	Doklady Earth Sciences Sections (Includes: Geochemistry, geology, geophysics, hydrogeology, mineralogy, paleontology, petrography, permafrost sections)	American Geological Institute	124	1	1959
	Earth Sciences	Proceedings of the Academy of Sciences of the USSR, Section: Geochemistry	Consultants Bureau	106-123	1-6	1957-1958
	Earth Sciences	Proceedings of the Academy of Sciences of the USSR, Sections: Geology	Consultants Bureau	106-123	1-6	1957-1958
	Mathematics	Doklady Soviet Mathematics	The American Mathematics Society	131	1	1961
	Physics	Soviet Physics–Doklady (Includes: Aerodynamics, astronomy, crystallography, cybernetics and control theory, electrical engineering, energetics, fluid mechanics, heat engineering, hydraulics, mathematical physics, mechanics, physics, technical physics, theory of elasticity sections)	American Institute of Physics	106	1	1956
	Physics	Proceedings of the Academy of Sciences of the USSR, Applied Physics Sections (does not include mathematical physics or physics sections)	Consultants Bureau	106-117	1	1956-1957
Derevoobrabat. prom-st'.	Derevoobrabatyvayushchaya promyshlennost'	Wood Processing Industry	Timber Development Association (London)		9	1959
	Élecktrosvyaz	Telecommunications	Massachusetts Institute of Technology*		1	1957
Éntom(ol). oboz(renie)	Éntomologicheskoe obozrenie	Entomological Review	American Institute of Biological Sciences	38	1	1959
Farmakol. (i) toksikol(ogiya)	Farmakologiya i toksikologiya	Pharmacology and Toxicology	Consultants Bureau	20	1	1957
FMM	Fizika metallov i metallovedenie	Physics of Metals and Metallography	Acta Metallurgica*	5	1	1957
Fiziol. zhurn. SSSR (im. Sechenova)	Fiziologicheskii zhurnal im. I. M. Sechenova	Sechenov Physiological Journal USSR	National Institutes of Health*		1	1957
Fiziol(ogiya) rast.	Fiziologiya rastenii	Plant Physiology	American Institute of Biological Sciences	4	1	1957
	Geokhimiya	Geochemistry	The Geochemical Society		1	1958
FTT	Fizika tverdogo tela	Soviet Physics–Solid State	American Institute of Physics	1	1	1959
Izmerit. tekh(nika)	Izmeritel'naya tekhnika	Measurement Techniques	Instrument Society of America		1	1959
Izv. AN SSSR, O(td). Kh(im). N(auk)	Izvestiya Akademii Nauk SSSR: Otdelenie khimicheskikh nauk	Bulletin of the Academy of Sciences of the USSR: Division of Chemical Sciences	Consultants Bureau		1	1952

continued

Izv. AN SSSR, O(td). T(ekhn). N(auk): Met(all). i top.	(see Met. i top.)					
Izv. AN SSSR Ser. fiz(ich).	Izvestiya Akademii Nauk SSSR: Seriya fizicheskaya	Bulletin of the Academy of Sciences of the USSR: Physical Series	Columbia Technical Translations		1	1954
Izv. AN SSSR Ser. geofiz.	Izvestiya Akademii Nauk SSSR: Seriya geofizicheskaya	Bulletin (Izvestiya) of the Academy of Sciences USSR: Geophysics Series	American Geophysical Union		1	1954
Izv. AN SSSR Ser. geol.	Izvestiya Akademii Nauk SSSR: Seriya geologicheskaya	Izvestiya of the Academy of Sciences of the USSR: Geologic Series	American Geological Institute		1	1958
Kauch. i rez.	Kauchuk i rezina	Soviet Rubber Technology	Research Association of British Rubber Manufacturers	18	1	1959
	Kinetika i kataliz	Kinetics and Catalysis	Consultants Bureau	1	3	1960
	Koks i khimiya	Coke and Chemistry USSR	Coal Tar Research Association (Leeds, England)		1	1958
Kolloidn. zh(urn).	Kolloidnyi zhurnal	Colloid Journal	Consultants Bureau	14	1	1952
	Kristallografiya	Soviet Physics – Crystallography	American Institute of Physics	2	1	1957
Metalov. i term. obrabot. metal.	Metallovedenie i termicheskaya obrabotka metallov	Metal Science and Heat Treatment of Metals	Acta Metallurgica	6	1	1958
	Metallurg	Metallurgist	Acta Metallurgica		1	1957
Met. i top.	Metallurgiya i topliva	Russian Metallurgy and Fuels	Eagle Technical Publications		1	1960
Mikrobiol.	Mikrobiologiya	Microbiology	American Institute of Biological Sciences	26	1	1957
OS	Optika i spektroskopiya	Optics and Spectroscopy	American Institute of Physics		6	1959
	Pochvovedenie	Soviet Soil Science	American Institute of Biological Sciences		1	1958
	Priborostroenie	Instrument Construction	British Scientific Instrument Research Association		1	1959
Pribory i tekhn. éks(perimenta)	Pribory i tekhnika éksperimenta	Instruments and Experimental Techniques	Instrument Society of America		1	1957
Prikl. matem. i mekh.	Prikladnaya matematika i mekhanika	Applied Mathematics and Mechanics	American Society of Mechanical Engineers		1	1958
PTÉ	(see Pribory i tekhn. éks.)					
	Problemy Severa	Problems of the North	National Research Council of Canada			
Radiotekh.	Radiotekhnika	Radio Engineering	Massachusetts Institute of Technology*	12	1	1957
Radiotekh. i élektronika	Radiotekhnika i élektronika	Radio Engineering and Electronics	Massachusetts Institute of Technology*	2	1	1957
	Stanki i instrument	Machines and Tooling	Production Engineering Research Assoc.		1	1959
	Stal'	Stal (In English)	Iron and Steel Institute		1	1959
Stek. i keram.	Steklo i keramika	Glass and Ceramics	Consultants Bureau	13	1	1956
Svaroch. proiz-vo	Svarochnoe proizvodstvo	Welding Production	British Welding Research Association		4	1959
Teor. veroyat. i prim.	Teoriya veroyatnostei i ee primenenie	Theory of Probability and Its Applications	Society for Industrial and Applied Mathematics		1	1956
Tsvet. Metally	Tsvetnye metally	Nonferrous Metals	Primary Sources		1	1960
UFN	Uspekhi fizicheskikh Nauk	Soviet Physics – Uspekhi (partial translation)	American Institute of Physics	66	1	1958
UKh	Uspekhi khimii	Russian Chemical Reviews	The Chemical Society (London)		1	1960
UMN	Uspekhi matematicheskikh nauk	Russian Mathematical Surveys	London Mathematical Society	15	1	1960
Usp. fiz. nauk	(see UFN)					
Usp. khim(ii)	(see UKh)					
Usp. matem. nauk	(see UMN)					
Usp. sovr. biol.	Uspekhi sovremennoi biologii	Russian Review of Biology	Oliver and Boyd		48	1959
Vest. mashinostroeniya	Vestnik mashinostroeniya	Russian Engineering Journal	Production Engineering Research Assoc.		4	1959
Vop. gem. i per. krovi	Voprosy gematologii i perelivaniya krovi	Problems of Hematology and Blood Transfusion	National Institutes of Health*		1	1957
Vop. onk.	Voprosy onkologii	Problems of Oncology	National Institutes of Health*		1	1957
Vop. virusol.	Voprosy virusologii	Problems of Virology	National Institutes of Health*		1	1957
Zav(odsk). lab(oratoriya)	Zavodskaya laboratoriya	Industrial Laboratory	Instrument Society of America	25	1	1959
ZhAKh Zh. anal(it). khimii	Zhurnal analiticheskoi khimii	Journal of Analytical Chemistry USSR	Consultants Bureau	7	1	1952
ZhETF Zh. éksperim. i teor. fiz.	Zhurnal éksperimental'noi i teoreticheskoi fiziki	Soviet Physics–JETP	American Institute of Physics	28	1	1955
ZhFKh Zh. fiz. khimii	Zhurnal fizicheskoi khimii	Russian Journal of Physical Chemistry	The Chemical Society (London)		7	1959
ZhMÉI Zh(urn). mikrobiol. épidemiol. i immunobiol.	Zhurnal mikrobiologii, épidemiologii i immunobiologii	Journal of Microbiology, Epidemiology and Immunobiology	National Institutes of Health*		1	1957
ZhNKh Zh(urn). neorgan(ich). khim(ii)	Zhurnal neorganicheskoi khimii	The Russian Journal of Inorganic Chemistry	The Chemical Society (London)		1	1959
ZhOKh Zh(urn). obshch(el) khimii	Zhurnal obshchei khimii	Journal of General Chemistry USSR	Consultants Bureau	19	1	1949
ZhPKh Zh(urn). prikl. khimii	Zhurnal prikladnoi khimli	Journal of Applied Chemistry USSR	Consultants Bureau	23	1	1950
ZhSKh Zh(urn). strukt. khimii	Zhurnal strukturnoi khimii	Journal of Structural Chemistry	Consultants Bureau	1	1	1960
ZhTF Zh(urn). tekhn. fiz.	Zhurnal teknicheskoi fiziki	Soviet Physics–Technical Physics	American Institute of Physics	26	1	1956
Zh(urn). vyssh. nervn. deyat. (im. Pavlova)	Zhurnal vysshei nervnoi deyatel'nosti (im. I. P. Pavlova)	Pavlov Journal of Higher Nervous Activity	National Institutes of Health*		1	1958

*Sponsoring organization. Translation through 1960 issues is a publication of Pergamon Press.

SIGNIFICANCE OF ABBREVIATIONS MOST FREQUENTLY ENCOUNTERED IN SOVIET PERIODICALS

FIAN	Phys. Inst. Acad. Sci. USSR
GDI	Water Power Inst.
GITI	State Sci.-Tech. Press
GITTL	State Tech. and Theor. Lit. Press
GONTI	State United Sci.-Tech. Press
Gosenergoizdat	State Power Press
Goskhimizdat	State Chem. Press
GOST	All-Union State Standard
GTTI	State Tech. and Theor. Lit. Press
IL	Foreign Lit. Press
ISN (Izd. Sov. Nauk)	Soviet Science Press
Izd. AN SSSR	Acad. Sci. USSR Press
Izd. MGU	Moscow State Univ. Press
LEIIZhT	Leningrad Power Inst. of Railroad Engineering
LET	Leningrad Elec. Engr. School
LETI	Leningrad Electrotechnical Inst.
LETIIZhT	Leningrad Electrical Engineering Research Inst. of Railroad Engr.
Mashgiz	State Sci.-Tech. Press for Machine Construction Lit.
MEP	Ministry of Electrical Industry
MES	Ministry of Electrical Power Plants
MESEP	Ministry of Electrical Power Plants and the Electrical Industry
MGU	Moscow State Univ.
MKhTI	Moscow Inst. Chem. Tech.
MOPI	Moscow Regional Pedagogical Inst.
MSP	Ministry of Industrial Construction
NII ZVUKSZAPIOI	Scientific Research Inst. of Sound Recording
NIKFI	Sci. Inst. of Modern Motion Picture Photography
ONTI	United Sci.- Tech. Press
OTI	Division of Technical Information
OTN	Div. Tech. Sci.
Stroiizdat	Construction Press
TOE	Association of Power Engineers
TsKTI	Central Research Inst. for Boilers and Turbines
TsNIEL	Central Scientific Research Elec. Engr. Lab.
TsNIEL-MES	Central Scientific Research Elec. Engr. Lab.-Ministry of Electric Power Plants
TsVTI	Central Office of Economic Information
UF	Ural Branch
VIESKh	All-Union Inst. of Rural Elec. Power Stations
VNIIM	All-Union Scientific Research Inst. of Metrology
VNIIZhDT	All-Union Scientific Research Inst. of Railroad Engineering
VTI	All-Union Thermotech. Inst.
VZEI	All-Union Power Correspondence Inst.

NOTE: Abbreviations not on this list and not explained in the translation have been transliterated, no further information about their significance being available to us. —Publisher.